Regulation of the floral transition and inflorescence development by the bZIP transcription factor FD in *Arabidopsis thaliana*

Inaugural-Dissertation

zur

Erlangung des Doktorgrades

der Mathematisch-Naturwissenschaftlichen Fakultät

der Universität zu Köln

vorgelegt von

Chloé Marie Hélène Pocard

aus Dijon, France

Köln, August 2021

Die vorliegende Arbeit wurde am Max-Planck-Institut für Pflanzenzüchtungsforschung in Köln in der Abteilung für Entwicklungsbiologie der Pflanzen (Direktor Prof. Dr. G. Coupland), Arbeitsgruppe Prof. Dr. George Coupland durchgeführt.
The work described in this thesis was conducted at the Max Planck Institute for Plant Breeding Research in the Department of Plant Developmental Biology (Director: Prof. Dr. George Coupland) under the supervision of Prof. Dr. George Coupland.

Berichterstatter:	Prof. Dr. George Coupland
	Prof. Dr. Ute Höcker
	Prof. Dr. Maria von Korff Schmising
Prüfungsvorsitzender:	Prof. Dr. Stanislav Kopriva
Tag der Disputation:	04 November 2021

Abstract

The integration of signals in response to endogenous and exogenous stimuli at the shoot apical meristem (SAM) determines the timing of the transition from vegetative to reproductive development in Arabidopsis. Under inductive long-day (LD) photoperiods, FLOWERING LOCUS T (FT) and the bZIP transcription factor FD form the large transcriptional complex FD–(14-3-3)–FT/TSF at the SAM. Within this complex, FD is the DNA-binding component and some target genes of FD have been well characterized. The *fd* mutant is late flowering under LD conditions due to the improper regulation of its targets. Despite increased knowledge on the regulatory pathways that act through the FD–(14-3-3)–FT/TSF complex, the *cis*-regulatory elements that are required for the binding of FD to its targets remain poorly defined, and it is unclear how different targets show distinct spatiotemporal expression patterns. For example, although FD enhances *FRUITFULL* (*FUL*) transcription within the SAM, *APETALA1* (*AP1*) transcription is promoted by FD later in development and *AP1* transcripts are specific to floral primordia. Furthermore, the subset of direct targets that are involved in the floral transition before the upregulation of *FUL* and *AP1* remain uncharacterized.

During this PhD, I generated a transgenic *fd* mutant line in which the translocation of FD into the nucleus can be induced at different developmental time points. Induction of FD in this line promoted flowering, and showed that FD activity was required for several days to complete floral transition. I performed RNA-seq on apices of these plants following FD induction and identified putative additional components of the FD transcriptional network. The earliest targets of FD from this whole-transcriptome analysis could not be linked to floral transition, although *FUL* and *AP1* were upregulated at later stages, confirming that floral transition occurred following FD induction. Much evidence exists to support that *FUL* is regulated by FD and I identified two putative conserved binding sites in the proximal promoter of *FUL*. However, mutation of these *cis*-elements did not affect flowering time nor the accumulation or pattern of FUL protein at the SAM. Under non-inductive short-day (SD) conditions, the SQUAMOSA PROMOTER BINDING PROTEIN-LIKE 15 (SPL15) protein also binds to *FUL* and regulates its expression. Although FD and SPL15 regulate *FUL* through the LD and SD pathways, respectively, I hypothesise that they do not compete at the promoter level and that activation of *FUL* by FD can occur indirectly through FD-mediated activation of other transcription factors or that FD binds to redundant sites at the *FUL* locus under LDs.

Abscisic acid (ABA) regulates stress responses such as the drought-escape response, and aspects of plant development, including axillary meristem growth and meristem arrest. The

FD protein is phylogenetically closely related to bZIP transcription factors involved in ABA signalling; however, evidence for the involvement of FD in ABA signalling is weak. I disrupted ABA signalling specifically within the *FD* expression domain, which resulted in defects in plant shoot architecture under LDs. In legumes, FD paralogues mediate the floral transition but also determine inflorescence architecture. I identified *HOMEOBOX PROTEIN 21* (*HB-21*), which is involved in ABA signalling, to be a direct downstream target of FD. The level of *HB-21* mRNA was lower in *fd* than in wild-type inflorescences. The *hb21* and *fd* mutants produced taller shoots with more siliques on the main shoot compared with wild type; thus, the regulation of *HB-21* by FD links FD with inflorescence development in Arabidopsis potentially through ABA signalling.

This PhD focuses on the bZIP transcription factor FD and how it regulates flowering time and inflorescence development in Arabidopsis. Collectively, the results show that FD functions throughout the Arabidopsis life cycle, and provide insight into the temporal FD-mediated transcriptional network at the SAM.

Table of contents

Chapter 1. Introduction

1.1 Signals integrate at the shoot apical meristem of angiosperms to regulate floral transition

Photosynthetic organisms colonised terrestrial lands millions of years ago and have continuously adapted to a changing environment. Angiosperm species have evolved many mechanisms to ensure their reproductive success. Notably, the development of flowers as reproductive structures enabled angiosperms to proliferate on Earth. After fertilization of the female gametophyte, the flower produces a fruit that allows seed dispersal. During the life cycle of annual plants such as *Arabidopsis thaliana* (Arabidopsis), the whole plant slowly senesces and dies after releasing the next generation of mature seeds (reviewed in Krämer, 2015). In a given environment, an optimal growth period from germination to flowering maximises offspring number. The early vegetative phase of Arabidopsis is characterised by the continuous production of leaves at the shoot apical meristem (SAM). At later stages, genetic reprogramming within the SAM leads to the acquisition of inflorescence meristem identity, and the generation of floral primordia. The transition from vegetative to reproductive growth is referred to as the floral transition. In the model plant Arabidopsis, the floral transition is tightly regulated by endogenous and exogenous cues, which are implemented by different genetic pathways. The photoperiodic, vernalization, autonomous, gibberellin and age-related pathways have been characterized to integrate diverse environmental and internal cues to control the induction of flowering (reviewed in Kinoshita and Richter, 2020). These pathways converge to regulate the transcription of genes involved in the floral transition and the early stages of floral development at the SAM.

1.1.1 Circadian rhythm and photoperiod are major stimuli for reproduction in Arabidopsis

1.1.1.i CONSTANS and GIGANTEA promote *FLOWERING LOCUS T* transcription in leaves

Among the floral induction pathways associated with environmental cues, a favourable change in daylength promotes flowering in Arabidopsis, and long days (LD) promote faster flowering than short days (SD). The photoperiod refers to the daylength and in plants, seasonal changes in the duration of light and dark are perceived in the leaves. The transcription factor CONSTANS (CO) and the florigen FLOWERING LOCUS T (FT) are two key regulators that promote the floral transition and are expressed in leaves. The mRNAs of *CO* and *FT* accumulate in LD, supporting their role in floral induction *via* the photoperiod (Suarez-Lopez et al., 2001). Classical mutants in the photoperiodic pathway, such as *co* and *ft*, display a

longer vegetative phase in inductive environments. Thus, they are late flowering under LD, whereas they show little or no differences in flowering time under SD (Koornneef et al., 1991).

The expression of CO is influenced by light quality and daylength. The CYCLING DOF FACTOR 1 (CDF1) binds to and negatively regulates *CO* transcription (Imaizumi et al., 2005). To counteract this, the clock-regulated FLAVIN-BINDING KELCH REPEAT, F-BOX1 (FKF1) degrades CDF proteins in response to several hours of light (Imaizumi et al., 2003; Imaizumi et al., 2005). Additionally, FKF1 interacts with GIGANTEA (GI) at the *CO* genomic locus to promote its transcription (Sawa et al., 2007). The accumulation of *GI* and *FKF1* mRNA is clock dependent and peaks after 8 to 10 hours of light (Fowler et al., 1999; Imaizumi et al., 2003). This timing allows GI and FKF1 proteins to accumulate, which enables *CO* levels to peak in late afternoon under LD (Suarez-Lopez et al., 2001). The PSEUDO-RESPONSE REGULATOR (PRR) and FKF1 participate in the stabilisation of CO protein in light, whereas CONSTITUTIVELY PHOTOMORPHOGENIC (COP1) and members of the SUPPRESSOR OF PHYA-105 (SPA) protein family degrade CO during the night (Valverde et al., 2004; Laubinger et al., 2006; Jang et al., 2008; Hayama et al., 2017). Under SD, the transcription of *CO* occurs in the dark, but the CO protein is rapidly degraded by COP1 and SPA proteins (Valverde et al., 2004; Laubinger et al., 2006). Day and night cycles, as well as daylength, determine the accumulation of stable CO at the end of long days.

One predominant role of the CO protein is to physically bind to and transcriptionally activate in the leaf vasculature the gene encoding the florigen FT (Suarez-Lopez et al., 2001; Tiwari et al., 2010). Expression of either *CO* or *FT* from the *SUCROSE-PROTON SYMPORTER 2* (*SUC2*) promoter causes early flowering (An et al., 2004; Corbesier et al., 2007) and expression of *CO* from the 35S promoter leads to a higher level of *FT* in leaves (Suarez-Lopez et al., 2001). Similar to the *co* mutant, the *ft* mutant is late flowering under LD, but not under SD (Koornneef et al., 1991; Mizoguchi et al., 2005). The late flowering of *ft* plants that express *SUC2::CO* (An et al., 2004) provides evidence for the importance during floral induction of the upstream regulation of *FT* by CO. *FT* transcripts are barely detectable under SD but rapidly increase in abundance upon transfer of plants to LD, coinciding with the stable accumulation of CO in leaves (Corbesier et al., 2007). Under LD, *FT* mRNA peaks before nightfall in leaves (Suarez-Lopez et al., 2001). The CO-independent activation of *FT* occurs in natural Arabidopsis habitats (Song et al., 2018). The inclusion of far-red light in growth conditions mimics these natural conditions and strong transient upregulation of *FT* was observed shortly after dawn (Song et al., 2018). This underlies the importance of light quality in the photoperiodic pathway. Epigenetic marks are abundant at the *FT* locus, suggesting that multiple levels of gene regulation determine the correct timing of floral induction (Jiang et al., 2008; Yan et al., 2014). The closest homologue of FT in Arabidopsis is TWIN SISTER OF FT (TSF) and the

TSF gene is also controlled by CO in a circadian manner (Yamaguchi et al., 2005). No altered flowering phenotype was observed for the single *tsf* mutant, but the combination of *tsf* and *ft* mutations delays the late-flowering phenotype of *ft* even more (Yamaguchi et al., 2005).

For Arabidopsis to flower, light signals that are perceived in leaves have to be translocated to the SAM. Although a LD photoperiod acting through CO activates *FT*/*TSF* transcription in the leaves, the two encoded proteins move to the SAM to promote flowering (Corbesier et al., 2007; Jaeger and Wigge, 2007; Mathieu et al., 2007). Therefore, FT and TSF proteins are long-distance mobile signals, and are called florigens. The FT-INTERACTING PROTEIN 1 (FTIP1) and SODIUM POTASSIUM ROOT DEFECTIVE 1 (NaKR1) proteins interact with FT to facilitate its transport to the SAM (Liu et al., 2012; Zhu et al., 2016). At the SAM, FT and TSF interact with the basic leucine zipper (bZIP) transcription factor FD (Abe et al., 2005; Wigge et al., 2005). This interaction is probably indirect and is mediated by the large family of 14-3-3 proteins, as was shown in rice (Taoka et al., 2011). The large FD–14-3-3–FT/TSF complex regulates transcription of downstream target genes and leads to floral transition (Abe et al., 2005; Wigge et al., 2005; Taoka et al., 2011; Abe et al., 2019).

1.1.1.ii The bZIP transcription factors FD and FDP

Basic leucine zipper (bZIP) proteins usually contain an alpha helix with repeated leucine residues. The leucine zipper domain enables homo- and heterodimerization with other bZIP proteins. The Arabidopsis bZIP proteins have been classified into 13 groups, according to the number of leucine repeats they contain and sequence similarity (Dröge-Laser et al., 2018). Individual bZIP proteins preferentially homo-dimerize or hetero-dimerize with other members of the same bZIP family (Llorca et al., 2015); thus, bZIP transcription factors depend on protein–protein interactions for their activity at DNA. The second part of the alpha helix is a DNA-binding domain that targets an ACGT-core sequence with specific palindromic flanking nucleotides. The most commonly bound motifs are G-boxes (CACGTG), C-boxes (GACGTC) and A-boxes (TACGTA; reviewed in Dröge-Laser et al., 2018). The FD and FD PARALOGUE (FDP) proteins belong to Group A Arabidopsis bZIP proteins, which contains 11 other members. FD and FDP share protein homology with these Group A members that are associated with abscisic acid (ABA) responses (Figure 1.1; Jakoby et al., 2002; Dröge-Laser et al., 2018), which suggests that FD and FDP may also have a role in ABA-signalling. Moreover, although FT:GUS is expressed in the leaf vasculature (Yamaguchi et al., 2005), FD protein accumulates in the SAM at an earlier stage of development, 2–3 days after germination (Romera-Branchat et al., 2020). In addition, chromatin immunoprecipitation DNA-sequencing (ChIP-seq) demonstrated that FD and FDP bind *in vivo* to target genes involved in ABA-signalling (Collani et al., 2019; Romera-Branchat et al., 2020; Zhu et al., 2020). Moreover, the threonine residue of FD at the position 282 (T282) is phosphorylated by the CALCIUM

DEPENDENT PROTEIN KINASE 3 (CPK6) and CPK33 at the SAM (Abe et al., 2005; Kawamoto et al., 2015), and mutating this T residue to Alanine impairs the ability of FD to promote flowering (Collani et al., 2019). The region at the carboxyl terminus of FD and FDP containing T282 has been called the SAP motif because of the conserved amino acids present, and is also required for interaction of FD with FT (Abe et al., 2005; Taoka et al., 2011). This SAP motif is potentially recognised by 14-3-3 proteins through phosphorylation of T282 and thereby enables the FD–14-3-3–FT/TSF complex to form (Abe et al., 2005; Taoka et al., 2011). However, the *cpk33* mutant is only slightly late flowering under LD, suggesting that FD activity is not only conferred by CPK33 phosphorylation (Kawamoto et al., 2015).

The best-studied role of FD relates to the floral induction. Both FD and FDP accumulate at the SAM under LD (Abe et al., 2005; Wigge et al., 2005; Romera-Branchat et al., 2020). The late-flowering phenotype of *fd* under LD can be partially suppressed by the early-flowering phenotype caused by overexpression of *FT* (Abe *et al.*, 2005; Wigge *et al*., 2005). Mutation of *FDP* in the *fd* background leads to a slightly more severe late-flowering phenotype under LD than the single *fd* (Romera-Branchat et al., 2020). Neither *fd* nor *fdp fd* shows a late-flowering phenotype under SD, consistent with FD and FDP being involved in the photoperiodic pathway. The downregulation of *FD* transcription in young floral primordia was first observed from *in situ* hybridisation experiments (Wigge et al., 2005). Subsequently, it was demonstrated that *FD* expression increases during floral transition but is then excluded from the floral primordia, probably due to direct feedback repression by APETALA1 (AP1; Abe et al., 2019, Kaufman et al., 2010). However, this decrease in FD protein abundance in the floral primordia is transient as it is reactivated in older primordia and FD remains expressed in inflorescence meristems (Gorham et al., 2018; Romera-Branchat et al., 2020). FDP is also expressed in older floral primordia and is more strongly expressed in older inflorescence meristems than during the floral transition (Romera-Branchat et al., 2020).

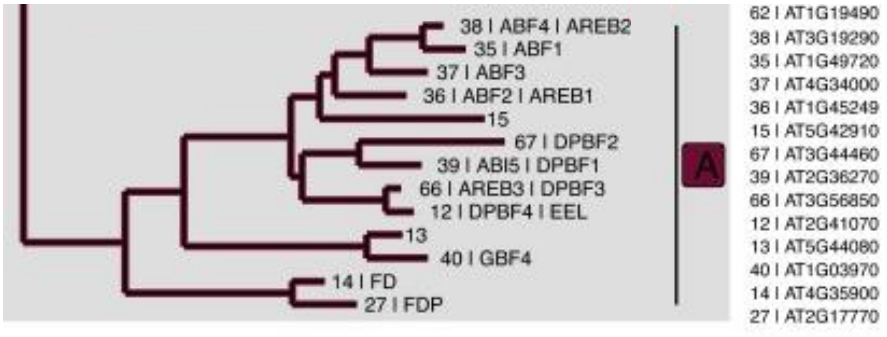

Figure 1.1 Rooted phylogenetic tree of the Group A bZIP in Arabidopsis. A branch of a phylogenetic tree from (Dröge-Laser et al., 2018) to illustrate the relationships among Arabidopsis Group A bZIP proteins. In addition to the two closely related FD and FDP proteins, many Group A bZIP proteins are involved in the ABA signalling pathway. Alignment was based on amino-acid similarities and conserved motifs.

1.1.1.iii The FD–14-3-3–FT/TSF complex promotes floral transition

Some target genes of the FD–14-3-3–FT/TSF complex are integrators that function early in the floral transition, such as *SUPPRESSOR OF OVEREXPRESSION OF CO 1* (*SOC1*) and *FRUITFULL* (*FUL*), and floral meristem identity genes such as *AP1*, *LEAFY* (*LFY*) and *SEPALLATA 3* (*SEP3*; Abe et al., 2005; Wigge et al., 2005; Yamaguchi et al., 2005; Jung et al., 2016; Collani et al., 2019; Romera-Branchat et al., 2020; Zhu et al., 2020). The earliest activated gene appears to be *SOC1* (Samach et al., 2000; Torti et al., 2012), and is followed by *FUL* mRNA accumulation at the SAM (Torti et al., 2012; Collani et al., 2019; Romera-Branchat et al., 2020). Mutation of these two genes, both of which encode MADS box transcription factors, leads to late flowering under LD photoperiods (Melzer et al., 2008) and strongly suppresses the effect of FT overexpression, supporting their importance downstream of FT (Melzer et al., 2008; Torti et al., 2012). Their expression marks commitment to the floral transition. Subsequently, the FD–14-3-3–FT/TSF complex activates the transcription of the floral meristem identity gene *LFY* and the encoded protein accumulates at the flanks of the SAM to promote the initiation of floral primordia (Weigel et al., 1992). Additionally, SOC1 binds to distal and proximal motifs in the *LFY* promoter and promotes its expression (Song et al., 2008). The FD–14-3-3–FT/TSF complex and LFY directly bind to the *AP1* genomic region and modulate *AP1* expression (William et al., 2004; Collani et al., 2019; Romera-Branchat et al., 2020; Jin et al., 2021) specifically in the floral primordia (Mandel et al., 1992; Urbanus et al., 2009). *lfy* and *ap1* mutants both display defects in floral development, but no alteration in the length of the vegetative phase (Irish and Sussex, 1990; Weigel et al., 1992). LFY requires AP1 to promote specific targets and AP1 regulates *LFY* in a positive feedback loop (Kaufmann et al., 2010; Goslin et al., 2017). Together, LFY and AP1 promote formation of the flowers.

1.1.1.iv FD is the DNA-binding component of FD–14-3-3–FT/TSF

The timing for FT to interact with FD and regulate their targets seems transient at the SAM and the complex is proposed to disappear from the inflorescence meristem (Abe et al., 2019). Notably, FT is not required for the binding of FD to its gene targets, but is crucial for the transcriptional regulation of these target genes (Collani et al., 2019). Some FD-interacting proteins may even be components of potentially larger transcriptional complexes at the targeted loci (Jung et al., 2016; Li et al., 2019). These are the SQUAMOSA PROMOTER BINDING PROTEIN-LIKE 3 (SPL3), SPL4 and SPL5 as well as the class II CINCINNATA (CIN) TCP 5, TCP13 and TCP17. FD preferentially recognises and binds to G-boxes in genome-wide assays (Collani et al., 2019; Romera-Branchat et al., 2020; Zhu et al., 2020). Controversial studies exist regarding the precise binding sites of FD to some targets and no *in planta* analysis has demonstrated functionality of these binding motifs (Abe et al., 2005; Benlloch et al., 2011; Collani et al., 2019). FD is strongly enriched in ChIP-qPCR assay to the proximal *AP1* promoter which contains one C-box (Jung et al., 2016). However, Electrophoretic

Mobility Shift Assay (EMSA) of the phosphorylated FD-C-ter form shows FD–14-3-3–FT to bind a GTCGAC fragment, 100 bp away from the previously identified C-box (Abe et al., 2005; Jung et al., 2016; Collani et al., 2019). Thus, despite increased knowledge on the regulatory role of the FD–(14-3-3)–FT/TSF complex, the binding of FD to its targets involved in the floral transition remain controversial.

In summary, a regulated cascade of signals illustrates how reproductive stimuli perceived by the leaves are necessary to initially promote floral transition, but also to subsequently maintain commitment to flowering. In particular, the activation of FT in leaves by exposure to LD results in the switch from vegetative to reproductive growth at the SAM (Figure 1.2).

1.1.2 *FLOWERING LOCUS C* integrates the vernalization and autonomous pathways

Vernalization refers to a long exposure to winter cold that promotes flowering following return to warmth, such as in spring. The two major genetic components of the vernalization pathway of Arabidopsis are FRIGIDA (FRI) and the floral repressor FLOWERING LOCUS C (FLC). The MADS-domain FLC protein physically binds to *SOC1*, *FT*, *FD* and *SEP3* chromatin and represses flowering (Helliwell et al., 2006; Searle et al., 2006; Deng et al., 2011). The Arabidopsis Col-0 summer accession does not respond to vernalization, because it carries an inactive allele of *FRI*. By contrast, some natural Arabidopsis accessions carry a functional FRI protein, which upregulates *FLC* transcription (Johanson et al., 2000). As a result of strong repression of *FT* and *SOC1* transcription, these plants display a pronounced late-flowering phenotype that can be overcome by vernalization. During vernalization, *FLC* transcript abundance is reduced and the degree of promotion of flowering is proportional to the degree to which the plant is vernalized (Michaels and Amasino, 1999; Lee et al., 2013). The regulation of *FLC* expression involves an interplay of epigenetic marks at the *FLC* locus that has been extensively studied. For example, the stable silencing of *FLC* occurs *via* the deposition of repressive nucleosome marks such as tri-methylation of lysine 27 on histone 3 by polycomb repressive complex 2 (PRC2; De Lucia et al., 2008). The transcriptional silencing of *FLC* by VIVIPAROUS1/ABI3-LIKE 1 (VAL1) is promoted by exposure to cold as VAL1 removes acetyl marks from *FLC* chromatin (Questa et al., 2016). Vernalization also promotes the transcription of two noncoding RNAs (ncRNA) at the *FLC* locus, named *COOLAIR* and *COLD ASSISTED INTRONIC NONCODING RNA* (*COLDAIR*), which both repress the *FLC* transcription (Heo and Sung, 2011; Csorba et al., 2014). Transgenic plants that lack *COLDAIR* ncRNA have a reduced response to vernalization and are late flowering compared with wild type (Heo and Sung, 2011). Following return to higher temperature after vernalization, the abundance of *FLC* transcripts decreases, which allows promotion of *FT*

and *SOC1* transcription and thus induces flowering (Corbesier et al., 2007). Notably, FT and FD coordinately repress *FLC* expression in young seedlings in a negative feedback loop (Luo et al., 2019). This is one of the many feedback loops that promote commitment to floral induction in Arabidopsis.

The repression of *FLC* mostly occurs through post-transcriptional regulation that lowers the abundance of mature *FLC* mRNA, and some of these involve *COOLAIR* (reviewed in Wu et al., 2020). Proteins that post-transcriptionally regulate *FLC* are part of the autonomous pathway and mutants in this pathway show a severe delay in flowering due to increased *FLC* levels, but flower rapidly after vernalization (Koornneef et al., 1991; He et al., 2003). The FVE and FLD proteins are components of histone deacetylase complexes and modulate epigenetic marks at *FLC* chromatin to promote silencing (He et al., 2003; Ausín et al., 2004; Liu et al., 2007). The FLOWERING CONTROL LOCUS A (FCA), FY and FPA, positively modify poly(A) sites and the splicing of *COOLAIR* transcripts (Hornyik et al., 2010; Marquardt et al., 2014).

Taken together, the vernalization pathway promotes flowering through the stable silencing of *FLC* in winter-annual accessions of Arabidopsis, and autonomous pathway components maintain *FLC* at a low level in summer annual accessions such as Col-0. The vernalization pathway ensures a rapid response and a strong induction of flowering in the presence of subsequent warmer temperatures.

1.1.3. Crosstalk between the autonomous and photoperiodic pathways promotes floral induction during elevated ambient temperatures

Environmental stimuli such as the photoperiod promote flowering, and Arabidopsis plants grown under LD transition to flowering faster than those under SD. Another important environmental stimulus is the ambient growth temperature. A slight increase in temperature strongly promotes flowering of Arabidopsis under LD (Balasubramanian et al., 2006). This response to higher temperatures can be so strong that wild-type plants display a similar flowering phenotype when grown under SD at 27°C as under LD at 23°C. Mutants of genes in the autonomous pathway do not respond to high temperatures and show similar flowering-time phenotypes at 23°C and 27°C (Blázquez et al., 2003; Balasubramanian et al., 2006). The autonomous pathway is therefore involved in floral induction in response to higher temperature. In wild type, FCA and FVE are required to reduce levels of the MADS-domain transcription factor SHORT VEGETATIVE PHASE (SVP) at elevated temperatures (Lee et al., 2007; Lee et al., 2013). In the *svp* mutant, *FT* and *SOC1* mRNA levels are increased and the *soc1 ft* double mutant is more insensitive to higher temperature than either single mutant (Lee et al., 2013). *SOC1* genomic DNA is directly regulated by SVP and FLOWERING

LOCUS M (FLM) which explains why a higher level of *SOC1* mRNA is present in *svp* and *flm* mutants (Tao et al., 2012; Lee et al., 2013). Thus, a reduction in SVP accumulation under high ambient temperature causes higher levels of *SOC1* and *FT* mRNAs to accumulate and earlier flowering. Additionally, in response to higher temperature, the chromatin of *FT* is relaxed by depletion of the H2A.Z nucleosome variant (Kumar and Wigge, 2010). Therefore, an increased level of *FT* transcription promotes flowering at warm temperatures. The transcription factor PHYTOCHROME-INTERACTING FACTOR 4 (PIF4) is also associated with the perception of light stimuli and promotes flowering under elevated temperature by increasing *FT* transcripts (Kumar et al., 2012; Fernández et al., 2016).

1.1.4 The process of ageing under long- and short-day conditions is dependent on photoperiod and the level of gibberellin

The ageing pathway promotes floral transition and is mainly regulated by the microRNA (miRNA)156/7 and SPL module. Plant miRNAs are non-coding small RNAs that consist of 21 to 24 nucleotides. They regulate gene expression by recognizing target sites in mRNAs and cause post-transcriptional effects such as transcript cleavage or inhibition of translation (Gandikota et al., 2007; Li et al., 2013). miRNA156 and miR157 are involved in the floral transition, but also regulate traits involved in the juvenile-to-adult transition, such as leaf morphology and trichome distribution (Wu and Poethig, 2006; He et al., 2018). Both miR157 and miR156 redundantly promote juvenile traits in leaves and miR156 represses to a higher degree some of their common targets (He et al., 2018). The mature miR156 is encoded by eight *MIR156* genes and miRNA156 transcripts are highly expressed in cotyledons and leaves formed early on the shoot, but their expression decreases in leaves formed later on the shoot (Wu and Poethig, 2006; Xu et al., 2016). miR156 targets the mRNAs of ten *SPL* genes, including *SPL3*, *SPL4*, *SPL5*, *SPL9* and *SPL15*, and represses their translation in seedlings by association with ARGONAUTE proteins (Schwab et al., 2005; Gandikota et al., 2007; He et al., 2018; Roussin-Leveillee et al., 2020). The increase in the level of miR156-targeted SPL proteins in older plants is concomitant with a decrease in the expression of miR156 (Wang et al., 2009; Xu et al., 2016). That expression of miR156/7 in younger plants causes the reduction in SPL expression was shown by constructing miRNA156/7 resistant *SPL* transgenes, and demonstrating that these allowed SPL expressions early in shoot development. Double mutant *spl9 spl15* plants and those that transgenically overexpress *MIR156* are very late flowering under LD (Schwarz et al., 2008; Wang et al., 2009). The *rSPL* lines are often early flowering and provide useful tools with which to study SPL functions (Wu and Poethig, 2006; Wang et al., 2009; Hyun et al., 2016). For example, the ubiquitous expression of *rSPL3* enables SPL3 to directly bind to *FUL*, *LFY* and *AP1* genomic loci and the subsequent upregulation of their transcription under LD leads to early flowering (Wang et al., 2009; Yamaguchi et al., 2009). The SPL3, SPL4 and SPL5 proteins physically interact

with FD at the *FUL* and *AP1* promoters and enhance their transcription (Jung et al., 2016). Thus, a decrease in the levels of miRNA156/157 enables the stable accumulation of SPL proteins, which in turn, activates the expression of floral integrators at the SAM. Notably, the photoperiodic and ageing pathways converge at the SAM in the formation of a larger complex containing FD–FT and SPLs under LD (Jung et al., 2016). However, the role of the miRNA/SPL module in floral induction is less important under LD, because its effect on flowering time is less pronounced when *FT* is expressed under LD than under SD when *FT* is not expressed (Schwab et al., 2005; Hyun et al., 2016).

The SPL proteins and gibberellic acid (GA) are the two major components that promote floral transition under non-inductive conditions, independently of the FD–14-3-3–FT/TSF complex. The *spl9 spl15* double mutant is late flowering under SD, but the quintuple *spl2 spl9 spl11 spl13 spl15* mutant and plants expressing *35S::MIR156A* flower even later because of the post-transcriptional downregulation of all targeted SPL proteins (Wang et al., 2009; Hyun et al., 2016; Xu et al., 2016). A low level of SPL expression inhibits the expression of their downstream targets and delays the floral transition. Mutants of *DELLA* genes, which encode repressors of gibberellic acid (GA) signalling, are extremely late flowering under SD (Dill and Sun, 2001) as are mutants with strongly reduced GA levels (Wilson et al., 1992). The degradation of DELLA proteins is induced by GA and wild-type plants supplemented with GA are early flowering under SD (reviewed in Conti, 2017). Exogenous GA application causes the upregulation of *SPL3*, *SPL4* and *SPL5* by SOC1 under SD (Jung et al., 2012). Also, SPL proteins interact with DELLAs to regulate SPL activity at the post-translational level (Yamaguchi et al., 2014; Hyun et al., 2016). Notably, flowering of the *spl15* mutant is insensitive to GA application (Hyun et al., 2016). When GA levels are low DELLAs interact with SPL15 to repress its activity, but when GA levels rise, SPL15 interacts with SOC1 at several regions of the *FUL* promoter to activate its transcription. Thus, the balance between DELLA and GA levels are important and the ageing and GA pathways converge on SPL15 to regulate floral integrators such as *SOC1*, *FUL* and *MIR172B* (Hyun et al., 2016).

1.1.5 Sugar signalling is tightly related with the photoperiodic and ageing flowering pathways

In Arabidopsis, photosynthetic activity results in the accumulation of sugars such as sucrose, glucose, maltose and trehalose in leaves and other source tissues. These sugars are transported between cells through sugar transporters or plasmodesmata, and throughout the plant in the vascular tissue. The transporters are membrane proteins that have affinity for specific sugar substrates, which probably fine-tune biological responses (Sivitz et al., 2007). A transient boost in the sucrose level occurs in leaf tissues after a shift from SD to LD (Corbesier et al., 1998). Because the floral transition occurs rapidly in Arabidopsis plants

shifted from SD to LD, the transient peak in sucrose accumulation may contribute to the photoperiodic flowering pathway (Torti et al., 2012). This transient increase might result from the relocalisation of sugar transport and altered flux. Trehalose-6-phosphate (T6P) is considered to be a signal molecule for the sucrose level in plants: sucrose positively influences the level of T6P and in shoot apices, T6P and sucrose concentrations increase as the plant ages (Wahl et al., 2013; Yadav et al., 2014). Interestingly, the concentration of T6P under LD peaks just before dark, similar to the temporal pattern of *FT* mRNA expression (Wahl et al., 2013). The activity of T6P SYNTHASE 1 (TPS1) catalyses T6P biosynthesis. Plants transgenic for *35S::amiRTPS1* display a reduction in TPS1 activity and a lower T6P concentration (Wahl et al., 2013). *TPS1* mRNA accumulates at the SAM and a reduction in TPS1 enzyme activity in *35S::amiRTPS1* plants leads to a late-flowering phenotype at least partly due to reduced *FT* mRNA levels (Wahl et al., 2013; Ponnu et al., 2020). Thus, the T6P pathway is necessary for floral transition under LD (Wahl et al., 2013). Moreover, it has been suggested that the T6P pathway acts upstream of the miR156/SPL ageing pathway (Ponnu et al., 2020). The levels of the two miRNA precursors encoded by *MIR156A* and *MIR156C* are increased in seedlings when T6P levels are reduced by *35S::amiRTPS1*. Hence, the T6P pathway promotes flowering at least partially by increasing *FT* expression and downregulating two *MIR156* genes.

1.1.6 Components of the abscisic acid pathway are integrated into the photoperiodic pathway

ABA is synthesised in leaves in response to various stresses and regulates stomatal opening in response to drought (Schroeder et al., 2001; Christmann et al., 2007). However, ABA responses are not limited to drought stress and ABA also regulates germination, seed maturation, bud dormancy and pathogen responses (reviewed in Cutler et al., 2010). Defects in development have been observed in mutants involved in the ABA pathway (Cheng et al., 2002; Fujii et al., 2009). A cascade of enzyme and transcription factor phosphorylation underlies responses to ABA. In the absence of ABA, the enzymatic activity of Snf1-RELATED KINASE 2s (SnRK2s) is inhibited by PROTEIN PHOSPHATASE 2C (PP2C) co-receptors to prevent ABA-induced gene transcription (Umezawa et al., 2009; Vlad et al., 2009). When ABA is perceived by the family of RABACTIN RESISTANCE1/PYR1-LIKE/REGULATORY COMPONENTS OF ABA RECEPTORS (PYR/PYL/RCAR) receptors, a large ABA–PYR/PYL/RCAR–PP2C complex is formed, which inactivates the PP2C and enables phosphorylation of the SnRK2s (Fujii et al., 2007; Melcher et al., 2009; Park et al., 2009; Umezawa et al., 2009; Nishimura et al., 2010). Two clade A PP2Cs named ABA INSENSITIVE 1 (ABI1) and ABI2 have been studied for their negative role in ABA signalling (Leung et al., 1997; Gosti et al., 1999; Song et al., 2018). Mutants in the catalytic domain of these genes named *abi1-1* and *abi2-1* cause dominant negative mutations that block the

interaction with the PYR/PYL/RCAR receptors in presence of ABA which prevents the phosphorylation cascade (Koornneef et al., 1984; Leung et al., 1997; Rodriguez et al., 1998; Melcher et al., 2009; Vlad et al., 2009). In the wild type, downstream transcriptions factors, such as the Group A bZIP ABSCISIC ACID RESPONSIVE ELEMENT-BINDING FACTOR (ABF) proteins, are then phosphorylated by SnRK2s, bind to ABSCISIC ACID RESPONSIVE ELEMENT (ABRE) *cis*-elements and induce ABA-responsive gene expression (Choi et al., 2000; Yoshida et al.; Yoshida et al., 2015). The ABRE-BINDING PROTEIN (AREB) proteins are also involved in ABA-responsive gene expression and similar to the ABF proteins, belong to the bZIP Group A transcription-factor family in Arabidopsis (Choi et al., 2000; Furihata et al., 2006). ABA-responsive genes include *RESPONSIVE TO DESICCATION 92 A* (*RD29A*) and *RD29B* (Yamaguchi-Shinozaki and Shinozaki, 1994). A Förster Resonance Energy Transfer (FRET)-based system composed of *PYR1* and the *ABI1* co-receptor has been developed to monitor ABA responses and shows high signal in aerial tissues of seedlings under non-stress conditions, especially in young leaf primordia (Waadt et al., 2014). However, the method lacks high-resolution imaging and to date, no other method to monitor ABA signalling in tissues has been developed.

Wild-type plants grown under low water availability (hydric stress) are early flowering (reviewed in Riboni et al., 2013; Martignago et al., 2020). Thus, components of the ABA pathway play a role in the floral transition. Moreover, water deficiency affects the flowering time of loss-of-function mutants of genes involved in the photoperiodic pathway. For instance, the *ft tsf* double mutant flowers earlier when grown under a low-water regime (Riboni et al., 2013). The mechanism by which Arabidopsis flowers more rapidly under low-water conditions is referred to as drought escape. Loss-of-function mutants in genes involved in ABA biosynthesis, such as *ABA DEFICIENT 1* (*ABA1*) and *ABA2*, are later flowering than wild-type plants under LD, but not under SD conditions (Riboni et al., 2013; Riboni et al., 2016). Mutation of *ABI1* in the L*er* background results in late flowering under SD but not under LD (Riboni et al., 2016). Moreover, the *abf3 abf4* mutant is late flowering under LD due to the downregulation of *SOC1* (Hwang et al., 2019). Although these findings highlight that ABA positively regulates the floral transition, mutation of *ABI4* leads to an early-flowering phenotype under non-stress growth conditions (Foyer et al., 2012; Shu et al., 2016).

The mediation of flowering time by ABA-signalling components is an emerging field of study, but more data are required to construct precise regulatory networks and to elucidate whether ABA biosynthesis and ABA signalling regulate flowering independently.

1.1.7 TERMINAL FLOWER 1 and other repressors of floral transition

Precocious flowering in non-optimal environments can be deleterious for plants and for their ability to produce progeny. Thus, many repressors of the floral transition are expressed in

embryonic tissues, during early stages of plant growth and in adult plants under non-inductive environments. Genes such as *FLC* or *MIR156* encode negative regulators of the floral transition, as previously reported in this chapter (Michaels and Amasino, 1999; Schwab et al., 2005). An important family of flowering-time repressors includes *APETALA2*, (*AP2*) and the *AP2*-like genes *TARGET OF EAT 1* (*TOE1*), *TOE2*, *TOE3*, *SCHLAFMÜTZE* (*SMZ*) and its paralogue *SCHNARCHZAPFEN* (*SNZ*; Aukerman and Sakai, 2003). Loss-of-function mutants of these individual genes are early flowering, and a sextuple mutant of all six genes is extremely early flowering under LD, suggesting that the genes redundantly regulate flowering time (Aukerman and Sakai, 2003; Yant et al., 2010). AP2 binds to the promoters of several genes involved in the floral transition, such as *AP1*, *SOC1* and *SEP3* and negatively regulates their transcription (Yant et al., 2010). The negative effect of AP2 on flowering time is counteracted by cleavage of its mRNA and inhibition of its translation mediated by miR172 (Chen, 2004; Ó'Maoiléidigh et al., 2021). The level of miR172 increases as the plant ages, which attenuates the level of AP2 at the SAM (Aukerman and Sakai, 2003; Ó'Maoiléidigh et al., 2021). In parallel, miR172 promotes the accumulation of *SPL3*, *SPL4* and *SPL5* (Gandikota et al., 2007). SOC1 also binds to the *AP2*-like genes and represses their transcription to overcome *SOC1* repression (Liu et al., 2012).

Expression of *FT* in the leaf vasculature promotes floral transition at the SAM (Corbesier et al., 2007) and FT integrates several flowering-time pathways, including the photoperiodic, the autonomous and T6P pathways. Therefore, the transcriptional regulation of *FT* is crucial for determining optimal flowering time and depends on positive and negative regulators. In addition to FLC, the MADS-domain transcription factor SVP integrates the GA, temperature and autonomous flowering-time pathways (Song et al., 2008; Lee et al., 2013; Andres et al., 2014). The *svp* mutant is early flowering under LD and SD, partially due to upregulation of *FT* (Hartmann et al., 2000; Jang et al., 2009). The two transcription factors TEMPRANILLO (TEM1) and TEM2 contain an AP2-related domain and prevent precocious flowering by negatively regulating *FT* transcription (Castillejo and Pelaz, 2008). Thus, FLC, SVP and the TEM transcription factors negatively regulate floral transition *via FT* repression.

In plants, scaffold 14-3-3 proteins and FD interact with TERMINAL FLOWER 1 (TFL1) and the resulting complex represses floral induction (Shalit et al., 2009; Taoka et al., 2011; Zhu et al., 2020). TFL1 is expressed at the SAM and in axillary buds and *tfl* mutants are early flowering under LD (Shannon and Meeks-Wagner, 1991; Bradley et al., 1997; Goretti et al., 2020). Notably, *FT* and *TFL1* share high DNA sequence homology and belong to a group of proteins related to phosphatidylethanolamine-binding proteins (PEBPs), which form a phosphatidylethanolamine ligand-binding pocket. However, FT lacks key residues that are

conserved among PEBPs and its enzymatic role remains unclear (Ahn et al., 2006). *FT* and *TFL1* antagonistically determine flowering time and their protein sequences mostly differ in the external loop (Hanzawa et al., 2005; Ahn et al., 2006; Ho and Weigel, 2014). Single amino-acid substitutions in FT confer TFL1-like activity (Hanzawa et al., 2005; Ho and Weigel, 2014). TFL1 and FT are mobile proteins that move between cells and their movement is required for their function (Conti and Bradley, 2007; Corbesier et al., 2007; Goretti et al., 2020). The FD-TFL1 complex binds to and negatively regulates the expression of many genes involved in the floral transition, such as *LFY* (Goretti et al., 2020; Zhu et al., 2020). By contrast, FT positively regulates *LFY*, which exemplifies the antagonistic roles of FT and TFL1. Many of the gene targets of TFL1 are shared by FD, and FD is required for the binding of TFL1 to these common DNA targets (Goretti et al., 2020; Zhu et al., 2020). Constitutive overexpression of *TFL1* from the 35S promoter leads to late flowering, whereas additional mutation of *TFL1* in the *fd* mutant background only partially rescues the late-flowering phenotype of *fd*, suggesting that TFL1 requires FD for the repression of flowering (Hanzawa et al., 2005; Hanano and Goto, 2011). TFL1 also binds to a subset of unique genes distinct from those bound by FD, indicating that both PEBP proteins also have independent functions (Goretti et al., 2020; Zhu et al., 2020). For example, in addition to regulating the floral transition, TFL1 confers meristem indeterminacy (Bradley et al., 1997). The TFL1 interacts with FD in biomolecular fluorescence complementation and Y2H assays (Hanano and Goto, 2011; Zhu et al., 2020). Phosphorylation of the SAP motif of FD is required to mediate interaction with FT, and is likely also required for the interaction with TFL1, as this also interacts with the SAP motif (Kawamoto et al., 2015; Collani et al., 2019). Because the FT–FD interaction is mediated by 14-3-3 proteins, it is reasonable to assume that FD–TFL1 interaction is also similarly mediated by 14-3-3 and/or TCP proteins (Ho and Weigel, 2014). Models suggest that TFL1 interacts with FD to repress floral integrator genes, but the arrival of FT at the SAM displaces TFL1 from the FD–4-3-3–TFL1 complex at the chromatin of target genes and TFL1 and FT antagonistically regulate the same subset of target genes (Corbesier et al., 2007; Jaeger et al., 2013; Zhu et al., 2020).

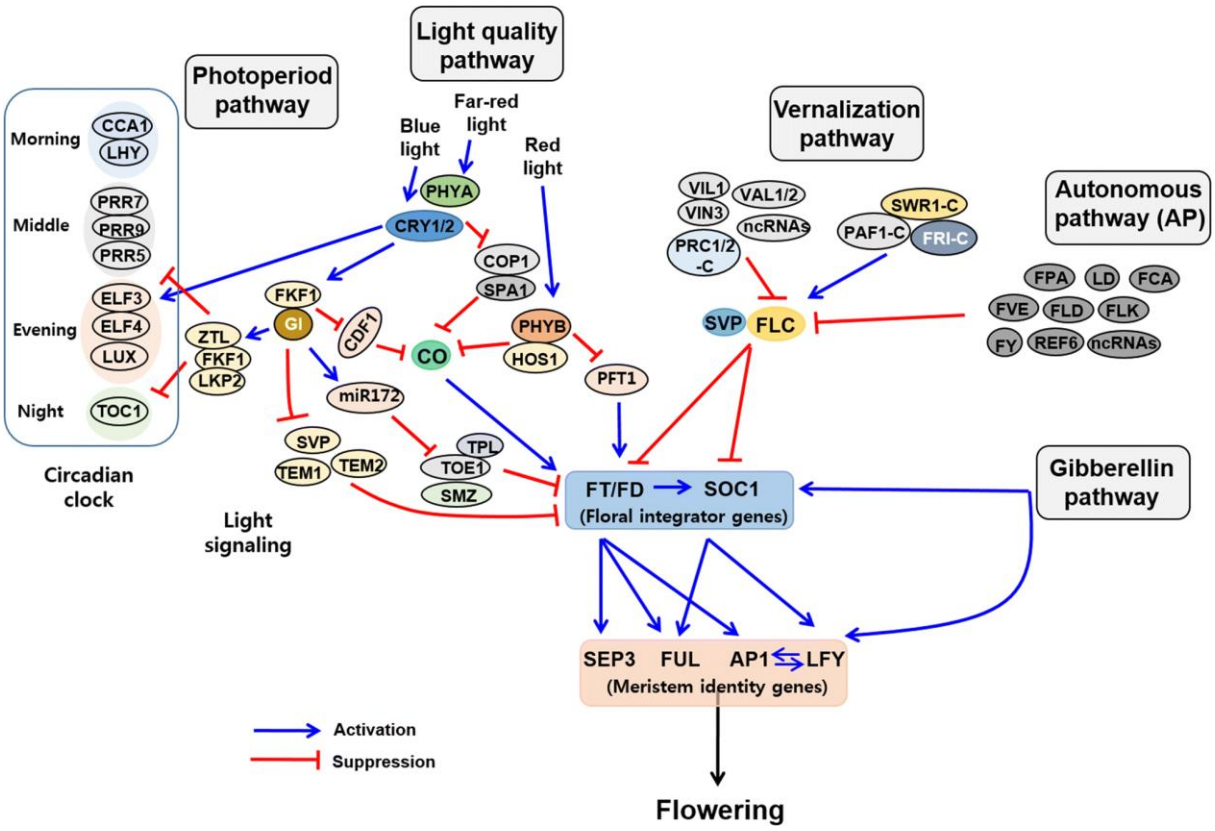

Figure 1.2 A complex genetic network regulates the floral transition in Arabidopsis. In the leaves, the perception of favourable photoperiod and light quality induces *CONSTANS* (*CO*) expression. The accumulation of CO is clock dependent and CO and GIGANTEA (GI) together activate the transcription of *FLOWERING LOCUS T* (*FT*). FT protein and its paralogue TWIN SISTER of FT (TSF) (not shown) move to the shoot apical meristem (SAM) to form a complex containing FLOWERING LOCUS D (FD) and 14-3-3 proteins, to form the FD–(14-3-3)–FT/TSF complex. In young seedlings, *FT* expression is repressed by FLOWERING LOCUS C (FLC) through the vernalization and autonomous pathways. *FT* expression is also repressed by TEMPRANILLO (TEM) proteins and proteins from the APETALA2-like family, such as APETALA2 (AP2) (not shown), TARGET OF EAT 1 (TOE1) and SCHLAFMUTZE (SMZ). At the SAM, the floral integrator SUPPRESSOR OF OVEREXPRESSSION OF CO (SOC1) promotes flowering and its expression is regulated by the FD–(14-3-3)–FT/TSF complex and GA levels (the gibberellin pathway). The SQUAMOSA PROMOTER BINDING PROTEIN LIKE 15 (SPL15) (not shown) transcription factor acts downstream of GA to promote flowering under SDs by activating *FRUITFUL* (*FUL*) and *MIR172* transcription. The different floral induction pathways converge to promote the expression of floral integrator such as *FUL* meristem identity genes such as *APETALA1* (*AP1*) and *LEAFY* (*LFY*) that lead to the formation of flower primordia. Figure from (Kim, 2020).

1.2 Structure and characteristics of the Arabidopsis shoot apical meristem

Meristems in plants maintain a continuous population of stem cells that are initially established during embryogenesis. These cells divide and are recruited for growth of the

surrounding tissues (reviewed in Gaillochet et al., 2015). The primary root apical meristem (RAM) provides cells for root elongation, whereas the primary shoot apical meristem (SAM) gives rise to all aerial organs of the plant and integrates genetic pathways and environmental signals that regulate floral transition. Secondary meristems such as axillary meristems derive from primary meristems (*e.g.* the SAM or RAM). In contrast to the RAM, the identity of the SAM changes when floral induction occurs in response to optimal environmental conditions (Kinoshita and Richter, 2020). Thus, after integration of the flowering-time pathways, the SAM undergoes morphological changes and genetic reprogramming to produce floral primordia, which initiate the reproductive organs. The floral meristem is determinate and forms four types of floral organs: sepals, petals, stamens and carpels. By contrast, the SAM is indeterminate and continuously forms lateral organs until the end of inflorescence growth.

1.2.1 Meristem structure and organ initiation

The upper first cell layer of the meristem (L1) and the first two primordia delimit the SAM. It can be separated into three zones: the central zone (CZ) which is located at the apex and contains the stem cells, the peripheral zone (PZ) which surrounds the CZ laterally and where primordia are formed, and the rib zone (RZ) that generates the stem and is located below the CZ (Figure 1.3A; reviewed in Fletcher, 2018). The depth of the CZ extends through three layers, from the L1 to the L3. The CZ contains the pluripotent stem cells and after mitosis, the daughter cells are displaced into the PZ, where they are recruited for lateral-organ initiation. The cell reservoir within the CZ is maintained by the organising centre (OC), which is located between the CZ and the RZ. The *WUSCHEL* (*WUS*) gene is expressed within the OC but the WUS protein, which is a homeodomain transcription factor, is also detected in the PZ and the CZ (Yadav et al., 2011). WUS migrates to the CZ where it activates *CLAVATA 3* (*CLV3*) transcription, and CLV3 peptide in turn moves to the OC and triggers transcriptional repression of *WUS* (Mayer et al., 1998; Brand et al., 2000; Yadav et al., 2011). Thus, an essential function of CLV3 is to restrict *WUS* expression to the OC (Brand et al., 2000; Schoof et al., 2000). The *wus* mutant has a small flat meristem whose activity terminates after the formation of a few deformed flowers (Schoof et al., 2000). A reduction in CLV3 activity leads to an enlarged CZ and SAM (Clark et al., 1995; Schoof et al., 2000; Reddy and Meyerowitz, 2005). The WUS/CLV3 feedback loop is thus necessary to maintain SAM identity, SAM size and cell division (reviewed in Fletcher, 2018). A second homeodomain transcription factor, SHOOTMERISTEMLESS (STM), is expressed at the SAM and is required for the maintenance of a pool of undifferentiated stem cells (Long et al., 1996; Su et al., 2020). In *stm-1* and *stm-5* mutants, cell divisions in the apical region of the embryo do not occur and no SAM is formed (Endrizzi et al., 1996; Long et al., 1996). In partial loss-of-function alleles of *STM*, such as *stm-2* and *stm-6*, a disorganised SAM is formed but organ phyllotaxis is affected, and leaf-like structures are produced before premature meristem

arrest (Endrizzi et al., 1996). STM prevents the differentiation of stem cells into lateral organs by negatively regulating *ASYMMETRIC LEAVES 1* (*AS1*), which encodes a MYB-domain transcriptional repressor that is broadly expressed in leaves and flowers (Byrne et al., 2000; Sun et al., 2002). STM also interacts with WUS at the *CLV3* promoter to increase its activity (Su et al., 2020).

Organogenesis at the SAM is mainly regulated by hormones and transcription factors (reviewed in Gaillochet et al., 2015), which also determine the position of the newly formed organs in a process known as phyllotaxis. In plants such as Arabidopsis that form organs in a spiral phyllotaxy, the divergence angle between successively initiated organs is about 137° following a clockwise spiral arrangement (Galvan-Ampudia et al., 2020). In large meristems, phyllotaxis on the main shoot is disrupted, so organs are formed in an irregular pattern (Landrein et al., 2015). The plastochron, which is defined as the time interval between the initiation of two successive organs at the SAM, is also tightly regulated. In Arabidopsis, the plastochron of floral primordia is about 10 to 14 hours (Galvan-Ampudia et al., 2020). The transcription factors SPL9 and SPL15 regulate the leaf plastochron and meristem size (Wang et al., 2008). Cytokinin promotes mitosis via MYB-DOMAIN PROTEIN3R-4 (MYB3R4) activity at the SAM (Zuo et al., 2021). Because cytokinin promotes cell division, the hormone is necessary for lateral organ initiation (Bartrina et al., 2011). Auxin waves and local auxin maxima via PIN-FORMED 1 (PIN1) and AUXIN RESISTANT 1 (AUX1) generate sites of accumulation of local auxin that prepattern the positions of lateral organ initiation in an appropriate phyllotaxy (Reinhardt et al., 2003; Galvan-Ampudia et al., 2020). Moreover, in addition to hormonal flux, lateral-organ phyllotaxis is affected by cell-wall composition and xyloglucan levels (Zhao et al., 2019). The plasticity of the cell cytoskeleton and the cell wall probably limit organogenesis. Changes in meristem size and shape also accompany floral transition. During this process the SAM becomes larger due to increases in cell number and size, and characteristic changes in SAM shape occur, referred to as doming (Kinoshita et al., 2020). This phenomenon is partially dependent on GA biosynthesis and signalling (Kinoshita et al., 2020). At the SAM, therefore, the combined functions of transcription factors as well as hormone synthesis and signalling tightly regulate the stem cell population, meristem size and the initiation of lateral organs with an appropriate phyllotaxis.

1.2.2 The fate of the shoot apical meristem

Summer-annual Arabidopsis has a short lifespan and flowers rapidly under LD conditions (Hensel et al., 1993). A major role of the Arabidopsis inflorescence meristem is to maximize the number of fertile flowers formed by the plant (Hensel et al., 1994). The cessation of inflorescence meristematic activity is accompanied by whole-plant senescence. This phenomenon is called global proliferative arrest (GPA) and determines plant longevity

(Hensel et al., 1993; Hensel et al., 1994; Wuest et al., 2016), because the later GPA occurs, the longer is the plant lifespan. It is proposed that maintenance of a stem cell population in the SAM is responsible for plant longevity, because the SAM of the *wus* mutant terminates prematurely (reviewed in Schoof et al., 2000; Dijkwel and Lai, 2019). GPA is characterized by a reduction in mitotic activity, programmed cell death, cell vacuolation, the production of reactive oxygen species (ROS) and ABA responses (Wuest et al., 2016; Wang et al., 2020). By four weeks after bolting, the area of the SAM decreases by up to one-third of that at 1 week after bolting (Wang et al., 2020). This reduction in meristem size is accompanied by a depletion of WUS and then CLV3 (Wang et al., 2020). Another study revealed that FUL and AP2 contribute to GPA (Balanzà et al., 2018). Indeed, meristem arrest also results from an increase in the expression of *FUL* and an associated but indirect decrease in *AP2* mRNA (Balanzà et al., 2018; Martínez-Fernández et al., 2020). In the *ful* mutant, the duration of meristem activity is extended because of prolonged WUS activity and upregulation of the *AP2*-like genes, especially *AP2* and *SNZ* (Balanzà et al., 2018). The *ful* mutant produces more flowers on the main shoot than wild type, probably because of longer meristem activity (Balanzà et al., 2018). The *pOpON:AP2m3* transgenic line expresses a modified *AP2* mRNA that is resistant to recognition and degradation by miR172, and is expressed from the chemically inducible *pOpON* promoter (Martínez-Fernández et al., 2020). After application of dexamethasone to induce expression of the resistant AP2 form in arrested meristems, the SAM is re-activated and the initiation of flowers resumes (Martínez-Fernández et al., 2020). This confirms that the AP2/FUL module regulates GPA in Arabidopsis and that AP2 function is sufficient to re-activate stem-cell activity.

The mechanisms that control Arabidopsis SAM arrest have been proposed to be related to those involved in bud dormancy/outgrowth of axillary meristems (AM; Kaufmann et al., 2010; Yao and Finlayson, 2015; Gonzalez-Grandio et al., 2017; Martínez-Fernández et al., 2020). Bud dormancy predominantly occurs in perennial plants such as poplar, in which reduced ABA sensitivity increases lateral bud outgrowth (Arend et al., 2009). During GPA at the SAM of Arabidopsis, reduced AP2 activity was proposed to induce the ABA response and reduce cytokinin signalling (Martínez-Fernández et al., 2020). Consistent with the involvement of ABA as well as other hormone signalling pathways, the exogenous application of GA or cytokinin cannot re-activate arrested meristems in Arabidopsis (Hensel et al., 1994); however, exogenous application of the synthetic auxin naphthalene acetic acid (NAA) triggers premature GPA (Ware et al., 2020). Mutation of the F-box CORONATINE INSENSITIVE 1 (COI1) jasmonic acid (JA) co-receptor results in an extreme delay of meristem arrest and the *coi1* mutant in the *Arabidopsis thaliana* Wassilewskija (Ws) ecotype produces about 300 flowers on the main shoot (Lee et al., 2013). *WUS* transcription is no longer detectable during meristem arrest in Ws, although *WUS* expression remains high at

the same age after sowing in the *coi1* mutant (Lee et al., 2013). These studies show that auxin, ABA and JA are involved in determining plant longevity.

In summary, complex genetic interactions occur at the SAM of Arabidopsis to regulate floral induction and meristem identity, up to GPA. This ensures rapid flowering and seed dispersal at an optimal time in a given environment. However, how transcription factors involved in floral transition, such as AP2 and FUL, also regulate meristem arrest remains poorly understood, and it suggests that some of these factors might act throughout inflorescence development having different roles at particular stages. It is therefore of interest to study genes associated to AP2 and FUL, such as *FD* and *FDP*, and determine whether they are involved in meristem arrest. Furthermore, ChIP-seq and transcriptomic analyses indicate that FD and FDP regulate ABA related genes (Romera-Branchat et al., 2020) suggesting a link between both bZIPs and the meristematic arrest activities.

1.3 Plant architecture and fitness

The conversion of the SAM into an inflorescence meristem is accompanied by elongation of the main shoot. Similar to the root system, Arabidopsis inflorescences are also branched and the branches arise from the axils of leaves on the primary inflorescence. The primary inflorescence, or main shoot, consists of cauline leaves that subtend the branches, flowers and, after fertilization, siliques. These structures are organised into phytomers: each phytomer consists of a node with a leaf, an axillary meristem and a segment of stem termed the internode that separates two adjacent nodes. The floral phytomer is composed of a flower that in some species is subtended by a leaf-like structure called a bract, but in other species, including Arabidopsis, the bract is suppressed (reviewed in Chandler, 2012; Wang et al., 2018). Meristematic activity zones that are formed in *Arabis alpina* during shoot development have been described in detail (Vayssières et al., 2020). Similarly, two distinct inflorescence zones can be defined in Arabidopsis. They consist in the succession of phytomers of two types. In inflorescence zone 1 (I1) at the base of the inflorescence, the lateral organs are cauline leaves, and axillary meristems are formed in the axils that give rise to inflorescence branches. Higher up on the stem, the I2 zone consists of lateral organs that are individual flowers attached to the main shoot by a pedicel. At these nodes the axillary meristem is converted to a floral meristem, and the subtending cauline leaf is suppressed (Figure 1.3B). Varying the time of transition from I1 to I2 contributes to plant architecture, and potentially has a dramatic effect on the seed yield of the plant and thereby its fitness.

1.3.1 Inflorescence and shoot growth

A huge variety of inflorescence morphologies exist among angiosperms. The Arabidopsis inflorescence is a simple raceme, in which flowers are formed directly on the main stem and

are attached to it by a short pedicel. By contrast that of *Pisum sativum* is a compound raceme in which flowers are not formed directly on the main shoot, but this produces leaves subtending lateral branches, and only the lateral branches harbour the flowers (Sussmilch et al., 2015). Grass inflorescences are more complex than those of dicots and different aerial structures are formed (reviewed in Koppolu and Schnurbusch, 2019). The increased complexity of sequential meristem transitions in certain grass species leads to a higher level of branching. The rice inflorescence is a branched panicle, which derives from a series of meristem transitions: vegetative meristems firstly transition into inflorescence meristems, but instead of producing flowers, these produce branch meristems. The branch meristems elongate and produce spikelet meristems, which in turn, initiate the floret meristems that generate the reproductive organs. The spike inflorescence of barley is not produced by branch meristems, but by several spikelet meristems that each give rise to a single floret meristem. In members of the *Solanaceae*, such as the tomato, *Solanum lycopersicum*, the inflorescence is a cyme and derives from repeated meristem branching (reviewed in Perilleux et al., 2014). After the vegetative growth phase, the tomato SAM transitions into a floral meristem and terminates, but initiates an axillary meristem that produces leaves and ultimately a new inflorescence meristem before maturing into the flower meristem. This sympodial process repeats to form the inflorescence; however, how many nodes the inflorescence meristem forms before terminating varies greatly among cultivars creating large differences in inflorescence architecture and height. In view of the diversity of inflorescence architecture, understanding the molecular-genetic basis of meristem identity changes and meristem branching mechanisms is important in maximizing seed production during the breeding of crop cultivars, and to understand how it is optimized by natural selection to maximize fitness in natural populations

In Arabidopsis, stem growth refers to primary growth that consists of the vertical elongation of the stem, and secondary growth, which causes an increase in stem width. Cell division at the RZ contributes to stem elongation (reviewed in Serrano-Mislata and Sablowski, 2018). Transversal sections of the stem show the radial pattern of the epidermis, the cortex, the endodermis, the vasculature and the pith. Understanding how the stem elongates is of particular interest in explaining inflorescence development, and it involves communication between stem tissues. The peptides EPIDERMAL PATTERNING FACTOR-LIKE (EPFL) 4 and EPFL6 function together with the membrane-located receptor protein kinase ERECTA (ER) in phloem-to-endodermis communication (Uchida et al., 2012). These molecules are necessary for stem growth, because *er* and *epfl4 epfl6* mutants have shorter stems than wild type (Uchida et al., 2012). FUL promotes stem elongation in part by repressing *SMALL AUXIN UPREGULATED RNA 10* (*SAUR10*; Bemer et al., 2017). Higher-order mutants for

genes encoding the auxin receptor F-box proteins have very short stems under LD (Dharmasiri et al., 2005), demonstrating the importance of auxin in shoot elongation. One role of auxin is to promote GA biosynthesis by upregulating *GA 2-OXIDASE* (*GA2OX*) genes (Frigerio et al., 2006). Concordantly, mutants deficient in GA synthesis or signalling show a dwarf-like phenotype. Low GA levels resulting from loss of *GIBBERELLIN ACID REQUIRING 1* (*GA1*) function or the abolition of GA perception by mutating three *GIBBERELLIN-INSENSITIVE DWARF 1* (*GID1*) GA receptors abolishes stem elongation (Griffiths et al., 2006). Furthermore, the stem phenotype of GA biosynthetic mutants, such as *ga1*, is rescued by exogenous GA_4 application and GA_4 application also increases stem elongation in wild type (Koorneef et al., 1985; Griffiths et al., 2006). GA1 participates in GA biosynthesis (Sun and Kamiya, 1994) and the GA GID1 receptors induce degradation of DELLA proteins in the presence of GA (Nakajima et al., 2006). Therefore, mutation of the *DELLA* gene *REPRESSOR OF ga1-3* (*RGA*) in the triple *gid1* background partially rescues the stem phenotype of the triple *gid1* mutant (Griffiths et al., 2006). This underlines the importance of GA in triggering the degradation of the growth-suppressing DELLA proteins to regulate plant height.

1.3.2 Floral integrators affect floral reversion and meristem identity

Some Arabidopsis mutants display floral reversion, which affects reproductive success. In these cases, the inflorescence meristem initially forms flowers and then reverts to the initiation of vegetative organs such as leaves, bracts or aerial rosettes, from which new inflorescences initiate. For example, reversion occurs on the main shoot of *ft* and *soc1 ful* double mutants under LD (Melzer et al., 2008; Liu et al., 2014). Mutation of *LFY* results in an increase in the number of cauline leaves and leaf-like structures on the main shoot, essentially extending I1, and is suggestive of partial reversion (Weigel et al., 1992). In pea, the FD orthologue, VEG2, promotes floral transition but also maintains the identity of the floral meristem, because floral reversion is observed in the *veg2* mutant (Sussmilch et al., 2015). The orthologue FDa in *Medicago truncatula* regulates inflorescence development, notably by upregulation of *MtTFL1* in inflorescence meristems, and *mtfda* produces I1-like branches instead of flowering I2 structures (Cheng et al., 2021). However, floral reversion does not occur in the Arabidopsis *fd* mutant. Interestingly, combination of the *fd* or *ft* mutations with *lfy* enhances the floral development defects of *lfy,* and this occurs at least in part through the transcriptional activation of *AP1* by FD (Ruiz-Garcia et al., 1997; Abe et al., 2005). Therefore, LFY and FD/FT potentially have at least partially redundant roles in the activation of *AP1* and probably other genes involved in floral and inflorescence development because they bind several common target genes (Collani et al., 2019; Romera-Branchat et al., 2020; Zhu et al., 2020; Jin et al., 2021). Moreover, the combination of either *fd* or *ft* with

stm enhances the inflorescence defects of weak *stm* alleles and the double mutants have an increased number of solitary cauline leaves (Smith et al., 2011).

In floral meristems, high expression levels of *LFY* and *AP1* promote floral development (Mandel et al., 1992; Weigel et al., 1992), but floral meristems are determinate and cease activity after floral organs are initiated. By contrast, the Arabidopsis primary SAM is indeterminate, continuing to form primordia and lateral organs indefinitely, but ectopic expression of *AP1* at the SAM in *tfl1* mutants causes the production of a precocious terminal flower (Bowman et al., 1993; Hanano and Goto, 2011). How the activity of the floral integrators LFY, TFL1 and AP1 and their homologues in other plant species regulate inflorescence identity has been reviewed in detail (Benlloch et al., 2007).This emphasises that a major function of TFL1 is to ensure the appropriate expression of the floral genes within floral primordia, and their exclusion from the SAM to ensure indeterminacy of the inflorescence meristem. Intriguingly, mutation of the acyl-CoA *N*-acyltransferase gene *HvMND1* in barley causes the reversion of spikelets into branch meristem-like organs, which coincides with the downregulation of *AP1* and *FUL* homologues and the upregulation of two *TFL1*-like genes in inflorescences (Walla et al., 2020).

Thus, comparative genetic analysis suggests that floral integrators of the photoperiodic pathway and homeotic genes determine meristem identity and that this role may be common to diverse angiosperm species. Whether FD in Arabidopsis continuously targets floral integrators and other genes to regulate inflorescence development and how this is related to GPA remains uncharacterised. Deciphering the downstream targets of FD which reflect flowering-independent functions of FD is therefore of interest.

1.3.3 Axillary meristems, secondary inflorescences and apical dominance

Axillary meristems (AM) initiate in the axils of leaves, including cauline leaves, and subsequently behave similarly to the SAM: an AM initiates leaf primordia and transitions into an inflorescence meristem that produces flowers. After stem elongation of Arabidopsis, the AMs from the axils of some rosette leaves give rise to secondary inflorescences (Figure 1.3B). AMs that initiate in the axils of cauline leaves on the main shoot can also develop into primary cauline-leaf branches (reviewed in Xue et al., 2020). The AMs of rosette-leaf axils are mostly dormant in Arabidopsis and their outgrowth is dependent on the genetic background, hormone level and environmental conditions (reviewed in Xue et al., 2020). Similar to the SAM, the activity of the AM depends on the WUS/CLV feedback loop and on STM (Shi et al., 2016; Xin et al., 2017). Expression of *STM* confers AM identity and is followed by *WUS* transcription. A stable OC and CZ dynamic is only reached at stage 5 of

AM development (Xin et al., 2017), which corresponds to a visible AM flanked by leaf primordia.

Some Arabidopsis mutants show defects in secondary inflorescence or primary cauline-leaf branch formation. For instance, the transcription factor LATERAL SUPPRESSOR (LAS) is a major contributor to rosette shoot branching and loss of *LAS* inhibits secondary inflorescence outgrowth (Greb et al., 2003). SPL9 and SPL15 bind to *LAS* DNA fragments in Y1H and EMSA assays and repress *LAS* transcription (Tian et al., 2014). The upregulation of *LAS* in AMs of the *spl9 spl15* double mutant might contribute to the observed increased branching phenotype (Schwarz et al., 2008). Loss-of-function of *MORE AXILLARY BRANCHES 1* (*MAX1*) and *MAX2* results in an increase in the number of secondary inflorescences (Stirnberg et al., 2002). The expression of *BRANCHED 1* (*BRC1*) is downregulated in *max1* and *max2* mutants (Aguilar-Martínez et al., 2007). More secondary inflorescences are produced in the *brc1* mutant (Aguilar-Martínez et al., 2007). Moreover, the increased branching phenotype of *max1* is suppressed by exogenous strigolactone (SL) application, suggesting that SL inhibits axillary bud outgrowth (Gomez-Roldan et al., 2008). However, the synthetic strigolactone analogue GR24 does not reduce the number of secondary inflorescences of Arabidopsis wild-type plants (Gomez-Roldan et al., 2008). It has been suggested that instead of directly inhibiting branching, SL inhibits auxin transport via PIN1 and its modulation by MAX proteins, which reduces auxin levels in the bud and thus promotes dormancy (Shinohara et al., 2013). More bud outgrowth is observed in the ABA-biosynthesis mutant *aba2-1* than in wild type under low and high R:FR light (Yao and Finlayson, 2015). The growth rate of axillary branches has been linked to several plant hormones, including auxin and ABA (Chatfield et al., 2000). Interestingly, lateral branches of *ft tsf* show slower growth under LD than those of wild type (Hiraoka et al., 2013); however, the mechanism that underlies how FT regulates branch growth remains unknown. In summary, the balance between plant hormone transport and signalling determines the dormancy or outgrowth state of the AMs.

Lateral bud outgrowth is strongly promoted by decapitation of the main shoot (Ongaro and Leyser, 2008), suggesting that the SAM of the main shoot inhibits outgrowth of the axillary meristems, which is termed apical dominance. After decapitation, lower buds show a decrease in *BRC1* expression and more rapid lateral branch outgrowth (Seale et al., 2017). Thus, mutants with defects in apical dominance show reduced stem height and more secondary inflorescences. For instance, *tfl1* shows an increase in branching and a reduction in the height of the main shoot height (Alvarez et al., 1992). Similarly, more secondary inflorescences arise from the rosettes of *max1* and *max2* mutants and the height of the main stem is reduced (Stirnberg et al., 2002). Apical dominance relates to source–sink

communication and the involvement of sugars, auxin, SL and cytokinins, several models have been proposed to explain its precise regulation (reviewed in Kebrom, 2017).

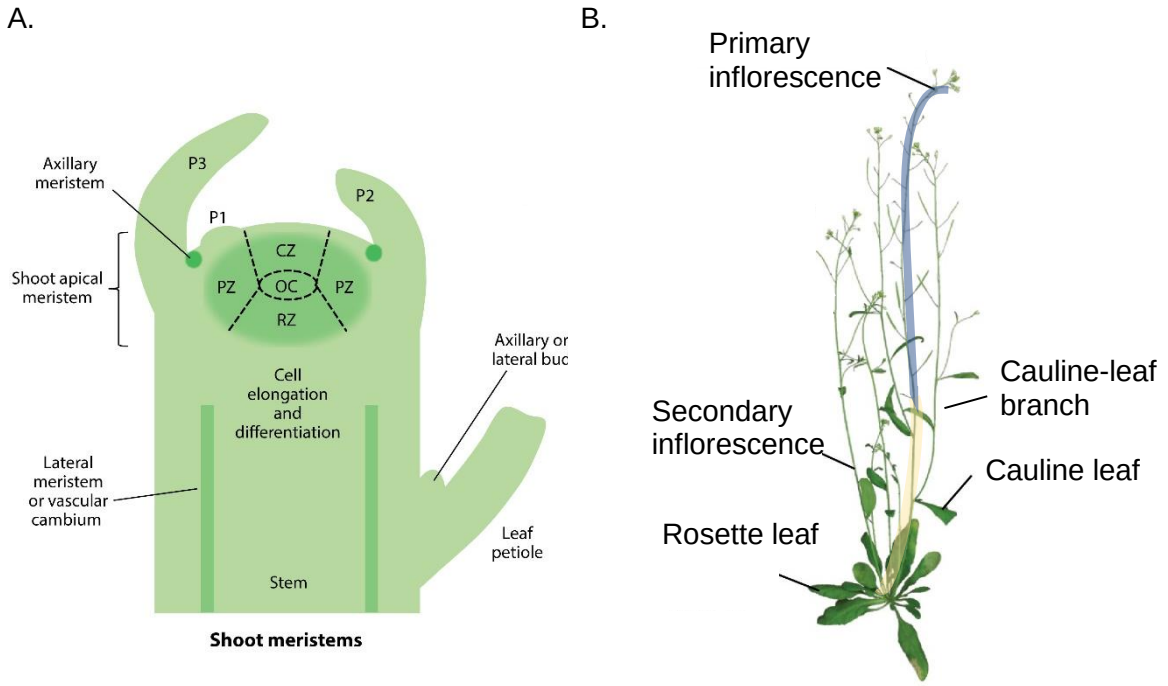

Figure 1.3 The organisation of the Arabidopsis shoot apex and inflorescence. **A**, Schematic representation of the Arabidopsis shoot apex. A regulatory feedback loop between WUSCHEL (WUS) in the organising centre (OC) and CLAVATA3 (CLV3) in the central zone (CZ) maintains the population of stem cells within the CZ. In the peripheral zone (PZ), undifferentiated cells that are displaced from the OC are recruited for the initiation of lateral organs, such as leaves or flowers. Cell divisions in the rib zone (RZ) contribute to stem elongation and provide cells that differentiate into the vasculature. **B**, Representation of Arabidopsis inflorescence architecture. The SAM produces rosette leaves as lateral organs during vegetative growth. After floral transition, the stem elongates and the inflorescence meristem produces two types of phytomers: 1) internodes subtending cauline leaves that initiate axillary meristems in their axils to create inflorescence zone 1 (I1; in yellow); and subsequently during development, 2) internodes that contain flowers supported on pedicels without subtending bracts to form inflorescence zone 2 (I2; in blue). The main shoot formed by the activity of the SAM is called the primary inflorescence. The rosette leaves have the potential to initiate axillary meristems in their axils that produce rosette-leaf branches also known as secondary inflorescences. The axillary meristems from the axils of cauline leaves become cauline-leaf branches that also produce flowers and further branches. Illustrations modified from (Wang et al., 2018).

1.3.4 Silique production

As plants age, the main shoot elongates and during the inflorescence phase the number of nodes containing flowers and siliques progressively increases (Wang et al., 2020). There is evidence that the number of siliques present on the main stem influences the duration of inflorescence growth. Mutations that impair flower fertility increase the number of nodes, measured as fruits, formed on the main shoot (Hensel et al., 1994; Balanzà et al., 2019).

Fruit production terminates first on the main shoot and the cauline branches, whereas secondary inflorescences continue to produce fruits for slightly longer times (Ware et al., 2020). Fruit removal delays meristem arrest causing the inflorescence to form more nodes, and this effect is proposed to be related to source–sink connections between the SAM and the fruits (Balanzà et al., 2018; Ware et al., 2020). Mutants such as *tfl1* and *ga1* have shorter main shoots and produce fewer siliques on the main shoot than wild type (Koornneef and van der Veen, 1980; Shannon and Meeks-Wagner, 1991; Hensel et al., 1993; Hensel et al.; Hanano and Goto, 2011). Notably, mutation of *FD* in L*er* accession leads to an increased production of fruit on the main shoot, although each flower is fully fertile (Hensel et al., 1994; Gorham et al., 2018). Mutation of the *FD* orthologue in *Medicago truncatula MtFDa1* results in fewer flowers on the axillary branches (Cheng et al., 2021; Zhang et al., 2021). C*YTOKININ OXIDASE 3* (*CKX3*) and *CKX5* are expressed at the shoot apex and encode enzymes involved in cytokinin degradation (Bartrina et al., 2011). A double *ckx3 ckx5* mutant has a larger SAM, more fruits and larger floral organs than those of wild type (Bartrina et al., 2011). An increase in fruit number in accessions of *Brassica napus* was associated with increases in biomass, photosynthesis and auxin-related processes (Li et al., 2020). Furthermore, during the initial stage of inflorescence meristem development, the vegetative SAMs of these *Brassica napus* accessions were similar in size, regardless of the number of fruits produced. However, a difference in SAM size was visible at later stages of IM development, after the production of several buds (Li et al., 2020). This suggests that fruit number does not necessarily correlate with meristem size.

There is therefore communication between the siliques and the inflorescence meristem that underlies a feed-back mechanism controlling the number of flowers and ultimately fruits and seeds formed on each shoot. The role of transcription factors such as FD that have been implicated in floral transition and shoot determinacy in this process remains unclear.

1.4 Aims of the project: The multiple roles of the bZIP transcription factor FD in plant development

The complex genetic and signalling networks that regulate floral transition in Arabidopsis are well understood, especially the photoperiodic pathway. For example, direct downstream targets of the FD–(14-3-3)–FT/TSF complex include *FUL*, *SEP3* and *AP1* (Collani et al., 2019; Romera-Branchat et al., 2020; Zhu et al., 2020). FD is expressed at the SAM at the floral transition and spatiotemporally regulates *FUL* and *AP1* transcription (Jung et al., 2016; Romera-Branchat et al., 2020). However, in addition to its function in regulating flowering time at the SAM, FD is also expressed in the SAM during the early stages of seedling development (Romera-Branchat et al., 2020). Thus, FD binds to many DNA loci, but which of

its direct targets are regulated by FD at specific stages in shoot development and what their functions are at these times remain unclear. Thus, the first objective of this project is to identify a subset of FD targets specifically during floral transition by performing RNA-seq followed by FD induction and to assess the function of these targets.

Transcription of *FUL* is increased by FD and SPL15, under LD and SD conditions, respectively, but it is unknown how the activities of these transcription factors are prioritized or how they converge on the regulation of *FUL* expression. Moreover, the *cis*-regulatory motif(s) to which FD binds in the *FUL* promoter to activate its transcription are also unknown. Thus, the second goal is to identify these motifs and investigate how they relate to regulation by FD and SPL15.

Thirdly, Arabidopsis FD orthologues in other species affect inflorescence development and fruit number (Hensel et al., 1994; Gorham et al., 2018; Cheng et al., 2021; Zhang et al., 2021). Therefore, I aim to perform a detailed phenotypic analysis of the Arabidopsis *fd* inflorescence, to characterise whether FD regulates inflorescence development in Arabidopsis after floral induction. Inflorescence architecture and meristem activity are largely regulated by plant hormones. Therefore, as FD is closely related to a clade of bZIPs involved in ABA signalling, an additional aim is to study whether FD and the ABA signalling pathway interact at the SAM to regulate flowering and inflorescence development.

The overall aim of this PhD thesis is to understand better how the FD bZIP transcription factor affects floral transition via the photoperiodic pathway, notably by regulating *FUL*, and how FD regulates inflorescence architecture, which has not been characterised in Arabidopsis.

Chapter 2. Temporal role of FD at the shoot apical meristem of *Arabidopsis thaliana* during the floral transition

2.1 Introduction

The floral transition of *Arabidopsis thaliana* is promoted by long daylengths. The protein FT and its partner FD are components of the photoperiodic flowering pathway. Together with the stabilizing 14-3-3 proteins, they form a large transcriptional complex that promotes flowering in diverse plant species, including Arabidopsis and rice (Abe et al., 2005; Wigge et al., 2005; Lifschitz et al., 2006; Taoka et al., 2011). FD physically binds to and regulates genes involved in the floral transition, such as *SOC1* and *FUL*, or those in the formation of floral primordia, such as *SEP3* and *AP1* (Schmid et al., 2003; Abe et al., 2005; Wigge et al., 2005; Collani et al., 2019; Romera-Branchat et al., 2020). The temporal activation of gene expression can be observed in wild-type plants transferred from short days (SDs), where they remain vegetative, to LDs, where flowering is induced. The *SOC1* and *FD* transcripts rapidly increase in abundance at the meristem within 1–3 days following transfer (Torti et al., 2012). Although a recent RNA-seq experiment using the *fd-2* and an *fd-2* mutant transgenic for *pFD::GFP:FD* showed no difference in *SOC1* expression after transfer to LDs, an increase in *FUL* expression was first detected in the complemented line (Collani et al., 2019). As plants underwent floral transition, *AP1* transcripts increased on the fifth day, when floral primordia begin to be formed (Collani et al., 2019). Similar results were observed by *in situ* hybridization using wild-type plants growing under continuous LDs. Transversal sections of the SAM showed accumulation of *FUL* mRNA at 14 LD, followed by *AP1* mRNA only at 17 LD in floral primordia (Romera-Branchat et al., 2020). In addition, this temporal regulation was supported by ChIP-qPCR assays, where GFP:FD protein was highly enriched at the *FUL* promoter before the *AP1* promoter (Jung et al., 2016). Therefore, FD binds to and activates direct targets in temporally distinct patterns during the floral transition.

The *fd* mutant is late flowering under LD conditions and can partially suppress the early-flowering phenotype caused by overexpression of *FT* (Abe et al., 2005; Wigge et al., 2005). Both *FD* mRNA and protein are localized at the SAM under LD (Abe et al., 2005; Wigge et al., 2005; Romera-Branchat et al., 2020). The *FT* mRNA is transcribed in the leaf vasculature (Yamaguchi et al., 2005; Corbesier et al., 2007) and FT protein moves to the SAM, where it displaces the repressor protein TFL1 from a complex with FD (Ahn et al., 2006; Jaeger et al., 2013). Prior to the translocation of FT, the FD–TFL1 complex is proposed to repress floral transition. The FD expression pattern becomes broader during floral transition but is then excluded from the floral primordia, which is proposed to be due to direct feedback repression by AP1 (Kaufmann et al., 2010; Romera-Branchat et al., 2020).

Floral transition is considered to be a dynamic balance of FD interactors with several feedback loops of regulation to prevent early flowering or premature termination of the SAM (Ahn et al., 2006; Jaeger et al., 2013). Moreover, FD protein accumulates at the SAM at an earlier stage, only 2–3 days after germination (Romera-Branchat et al., 2020). These observations emphasise the spatiotemporal action of FD, which is modulated by potential interactors before, during, and after the floral transition. The precise timing in which FD is needed to promote the floral transition is so far unknown. In this chapter, I aim to detect the first target genes activated by FD in vegetative *fd* SAMs by using inducible transgenic lines, and to study how these genes relate to the floral transition.

2.2 Results

2.2.1 Characteristics of the late-flowering *fd-3* mutant grown under long-day photoperiods

FD is a floral integrator that promotes the floral transition under LD conditions (Abe et al., 2005; Wigge et al., 2005). To summarize the role of FD in Arabidopsis, I compared phenotypic and molecular traits shown by Col-0 and *fd-3* (Figure 2.1). The total leaf number at bolting can be used as a proxy to measure the floral transition. Under LD-conditions, the bolting of *fd-3* was delayed and the total number of leaves produced was statistically significantly greater than that of wild-type Col-0 plants (Figure 2.1A, B). Under SD conditions, no differences between the flowering phenotype of wild-type Col-0 and *fd-3* were observed (Figure 2.1A, B). These results confirm that FD promotes the floral transition under inductive LD conditions. To compare the development of the shoot apical meristem of Arabidopsis with and without FD, I analysed the morphology of wild-type and *fd-3* meristems using confocal microscopy. In LD cabinets, the floral transition of Col-0 occurred at about 12 LD according to the doming of the SAM, and was followed by the formation of the first floral primordia at about 14 LD (Figure 2.1C). The doming of the SAM in *fd-3* was visible significantly later, from 17 LD, and the first floral primordia were detected around 20 LD. Therefore, the developmental transition in *fd-3* was delayed compared with that in Col-0 by approximatively one week. The *fd-3* mutant had a longer vegetative phase, which is consistent with more leaves being produced by the vegetative meristem (Figure 2.1B). The accumulation of VENUS:FD protein at the SAM was imaged in *fd-3* complemented with *FD::VENUS:FD* (Romera-Branchat et al., 2020). The fusion protein was detected in the nuclei of cells of the upper part of the shoot apical meristem as well as those on the abaxial side of the leaf primordia (Figure 2.1D). In this transgenic line, doming of the SAM occurred at about 11 LD and flower primordia were formed by day 14. The pattern of VENUS:FD expression coincided with *FD* mRNA expression patterns detected by *in situ* hybridization (Romera-

Branchat et al., 2020) and the protein was continuously present at the SAM from 7 LD to 14 LD, that is, from the vegetative to the reproductive stages.

This analysis of *fd-3* is consistent with published data (reviewed in Kinoshita and Richter, 2020) and demonstrates a clear role for FD in promoting floral transition under LD at the SAM.

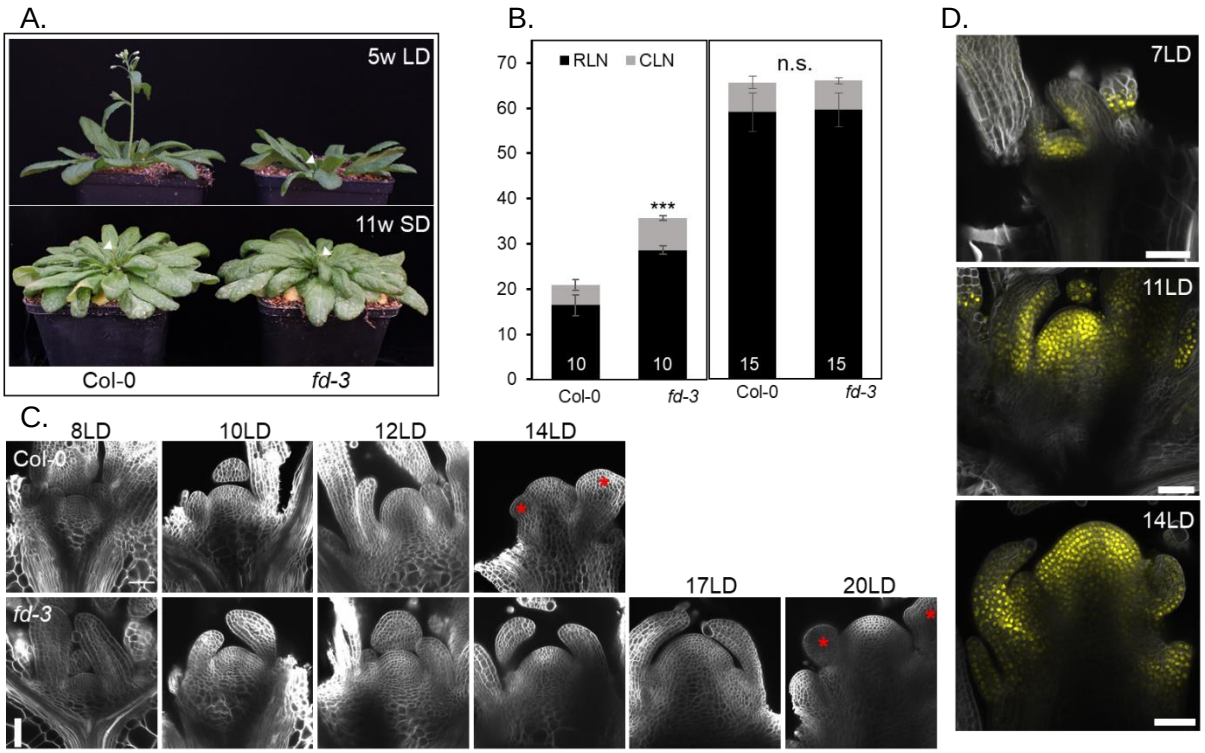

Figure 2.1. Characteristics of the late-flowering *fd-3* mutant under long-day photoperiod. **A**, Photographic image showing the late-flowering phenotype of *fd-3* compared with Col-0 after 5 weeks under long days (LD) and 11 weeks under short days (SD). **B**, Flowering time presented as total leaf number under LD (left panel) and SD (right panel) conditions. The number of plants used for each measurement is shown in white text. Error bars represent ±SD (two-tailed Student's *t*-test ***$p < 0.01$). **C**, Morphological changes of Col-0 and *fd-3* mutant apices during the floral transition at the indicated time points. Red asterisks indicate floral primordia. Samples were fixed in 4% PFA, soaked in Clearsee for one week and Renaissance staining was added one day before imaging by confocal microscopy. **D**, Accumulation of VENUS:FD protein expressed from the *FD::VENUS:FD* construct in *fd-3* mutant plants under LDs at the indicated time points. Scale bars represent 50 µm.

2.2.2 An inducible FD transgene complements the *fd-3* mutation

Complementation lines carrying the genomic locus of *FD* have been described to suppress the late-flowering phenotype of *fd* mutants (Collani et al., 2019; Romera-Branchat et al., 2020). To test whether the induction of FD complements the *fd-3* late-flowering phenotype, a chimeric open reading frame was constructed that encodes the ligand binding domain of the human glucocorticoid receptor (GR) inserted at the N-terminus of FD in the context of the genomic locus of *FD*. This construct was transformed into the *fd-3* mutant background using *A. tumefaciens*. The fusion protein, named GR:FD, is expected to be sequestered in the

cytoplasm in the absence of steroid ligand, and the transgenic *FD::GR:FD fd-3* plants should therefore behave like the *fd-3* mutant under LD conditions. Induction of GR:FD by application of the steroid dexamethasone (DEX) should trigger the floral transition through enabling translocation of GR:FD to the nucleus, thereby inducing FD function and the transcriptional activation of its target genes (Figure 2.2A).

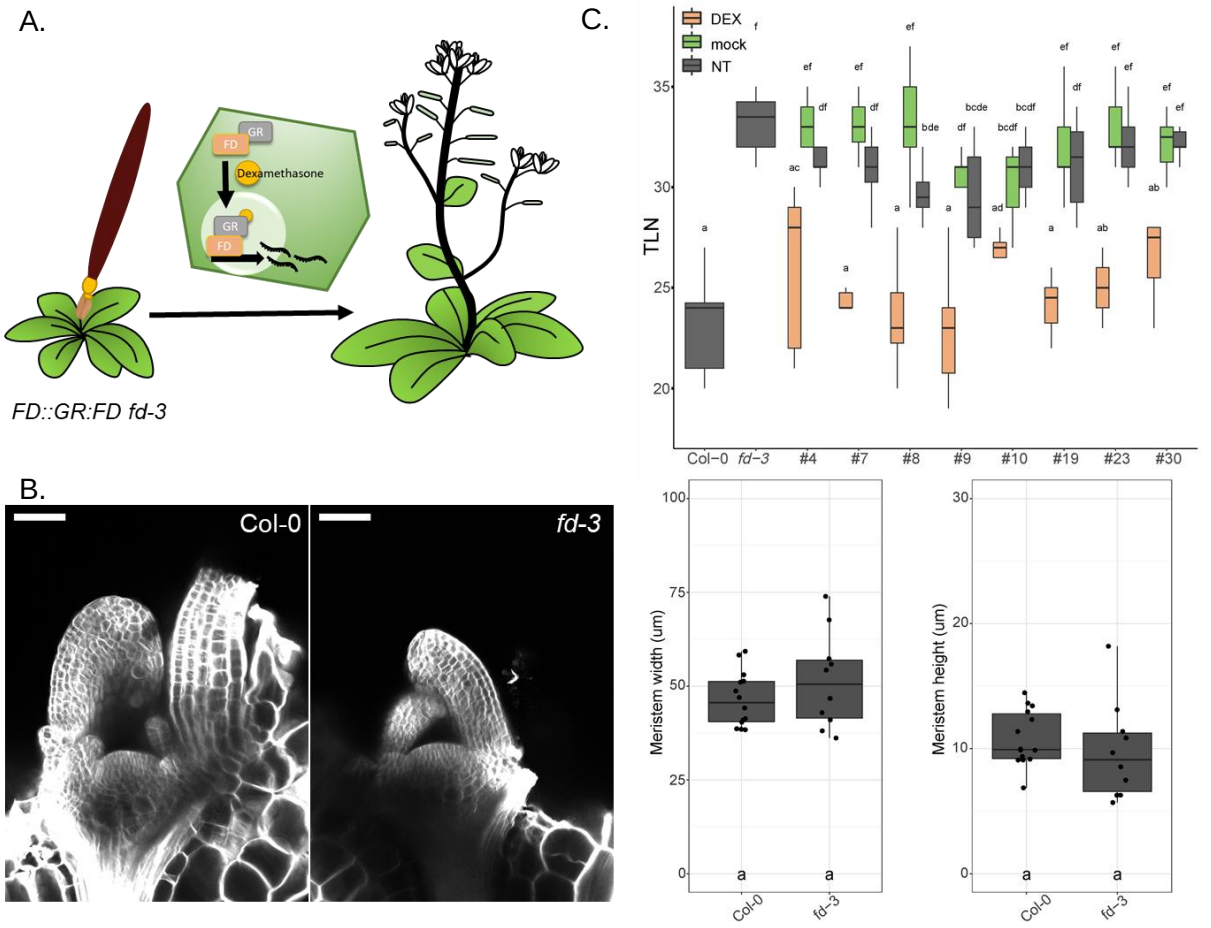

Figure 2.2 Continuous DEX treatment from day 7 onwards partially complements *FD::GR:FD fd-3* transgenic mutant plants.
A, Schematic diagram of the mechanism of induction of the inducible *FD::GR:FD fd-3* line. After DEX application, the GR:FD protein moves to the nucleus to activate its targets. This promotes floral transition and the rescue of the late-flowering phenotype of *fd-3* plants. **B**, Morphology of 7-day-old wild-type and *fd-3* mutant plants assessed by confocal microscopy and measurements of width and height from 2D images (n = 14 and 10, respectively, for each genotype). Measurements were performed using Fiji software. The width was defined as the length between two emerging primordia and the height was measured from the middle of the width to the top of the apex. **C**, Total leaf number (TLN) of eight *FD::GR:FD fd-3* transgenic T3 lines under long days. Plants were subjected to no treatment (NT), DEX (10 µM) or mock (EtOH) solutions. For Col-0, *n* = 12; for *fd-3*, *n* = 12; for *FD::GR:FD fd-3*, *n* = 2-10. Values for genotypes with the same letter do not differ significantly from each other (ANOVA, Tukey's HSD test).

Because evidence points to an early regulatory role for FD (Romera-Branchat et al., 2020), confocal microscopy was used to assess the meristem shape of wild type and *fd-3* at early time points (7 LD; Figure 2.2B, left panel). The meristem width and height of both genotypes were similar (Figure 2.2B, right panel). Therefore, I tested eight stable homozygous *FD::GR:FD* lines for complementation of the *fd-3* mutation under LD in the greenhouse. The plants were treated every three days with mock (EtOH 10 µM) or DEX (diluted in EtOH, 10 µM) from day 7 until the appearance of a visible floral bud. In the absence of DEX treatment, most of the lines flowered similarly to *fd-3*, with the exception of lines *#8* and *#9* (Figure 2.2C). This indicates no leakiness of the construct for the majority of the transgenic lines. The total leaf number of all *FD::GR:FD fd-3* lines treated with DEX was similar to that of wild-type Col-0, confirming the complementation of the lines and functional FD:GR activity. Line *#4* was not a suitable candidate for further study because of a high variability in total leaf number of the DEX-treated individuals. Complementation of the *fd-3* mutant phenotype of DEX-treated plants of lines *#10* and *#30* was not as effective as that for the lines *#7*, *#19* and *#23*. The lines *#19* and *#23* were therefore selected for further experiments.

A flowering-time experiment was performed with the lines *#19* and *#23* in a LD cabinet (Figure 2.3A). The centre of the plant was brushed every three days with either a mock or DEX solution from the seventh day after sowing onwards until the inflorescence buds emerged (Figure 2.3A). Flowering time, defined as time to bolting or total leaf number, was not significantly different between mock-treated *FD::GR:FD* plants (lines *#19* and *#23*) and mock- or DEX-treated *fd-3*. However, continuous DEX treatment of the transgenic lines caused them to flower earlier, and led to partial complementation of the *fd-3* phenotype in terms of number of days to bolting and total leaf number (Figure 2.3A and B). The response to DEX in the transgenic line *#19* appeared stronger than in the line *#23,* which showed higher variation within the population. Thus, the transgenic line *FD::GR:FD #19* was selected for future experiments. RT-qPCR analysis using tissues enriched for 17-LD apices revealed that the lines *#19* and *#23* expressed higher levels of *FD* mRNA than wild type and *fd-3*, indicating the presence of exogenous *FD* mRNA in the transgenic lines (Figure 2.3C). Analysis showed that the levels of *FUL* and *AP1* were lower in the *FD::GR:FD fd-3 #19* and *#23* genotypes compared with the wild type, supporting no leakiness of the GR:FD protein. The higher mRNA levels in the wild-type plants indicates that the floral transition as well as the formation of the flower primordia occurred. In conclusion, *FD::GR:FD fd-3 #19* is a suitable genetic background in which to study the effects of induction of FD function by the application of DEX.

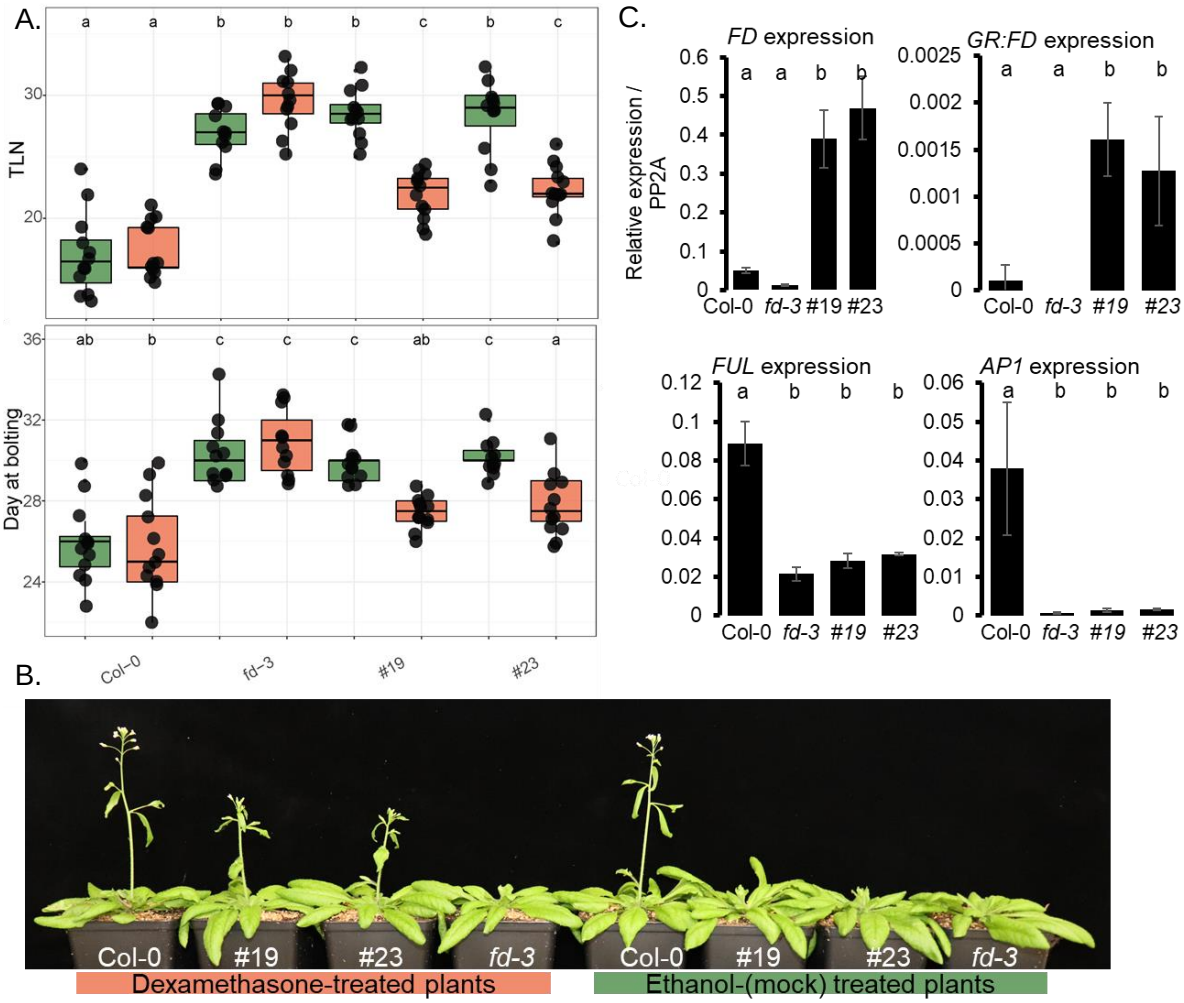

Figure 2.3. Induction of GR:FD promotes flowering of *fd-3* mutants.
A, Flowering time of Col-0, *fd-3* and *FD::GR:FD fd-3 #19* and *#23* under long days (LDs). Continuous 10 µM DEX treatment rescued the *fd-3* late-flowering mutant and partially the total leaf number (TLN). Mock- and DEX-treated genotypes are represented by green and orange boxes, respectively. Each dot represents one individual plant; *n* = 11–12. Values for genotypes with the same letter do not differ significantly from each other (ANOVA, Tukey's HSD test). **B**, Photographic image of the plants after continuous DEX treatment after 30 LDs. The flowering time of *FD::GR:FD* transgenic lines *#19* and #23 treated with DEX were similar to Col-0, whereas mock-treated plants were phenotypically similar to the *fd-3* mutant plants. **C**, Real time qPCR on 17-day old apices of Col-0, *fd-3* and the two transgenic *FD::GR:FD* lines *#19* and *#23*. Similar *FRUITFULL* (*FUL*) and *APETALA1* (*AP1*) expression levels in the *FD::GR:FD* and *fd-3* lines suggest no leakiness of the *GR:FD* construct. The data are means for biological triplicates ±SD and statistics were performed with one-way ANOVA and post-hoc Tukey's HSD test ($p < 0.05$).

2.2.3 The *GR:FD fd-3* meristems continuously treated with DEX solution undergo floral transition earlier than those only treated once

The FT–FD–14-3-3 complex promotes floral transition at the SAM when the active repressive role of TFL1 is overcome (Kobayashi et al., 1999; Abe et al., 2005; Wigge et al., 2005; Hanano and Goto, 2011; Zhu et al., 2020). The *fd* mutation partially suppresses the early-

flowering phenotype of 35S::*FT* plants (Abe et al., 2005; Wigge et al., 2005). Furthermore, introducing the *fd* mutation into the *ft* mutant delays even more the floral transition (Jang et al., 2009). Although FT is referred to as the co-activator of FD, the binding of FD to its DNA target is apparently independent of this partner (Collani et al., 2019). Although FD has redundant functions with FT, the bZIP transcription factor also acts independently of FT. To investigate whether FD protein is necessary and sufficient to induce the floral transition in *fd-3*, the effect of a single induction of GR:FD was compared with the effect of multiple inductions. Previously, I showed that multiple DEX applications restore the flowering phenotype of *fd-3* due to induction of FD activity (Figures 2.2C and 3A). To test whether FD activity is needed either transiently or for an extended period, transgenic plants were treated at different developmental stages and with different frequencies. In all treatment conditions, the *fd-3* and mock-treated *FD::GR:FD* plants displayed a late-flowering phenotype compared with the wild type (Figure 2.4).

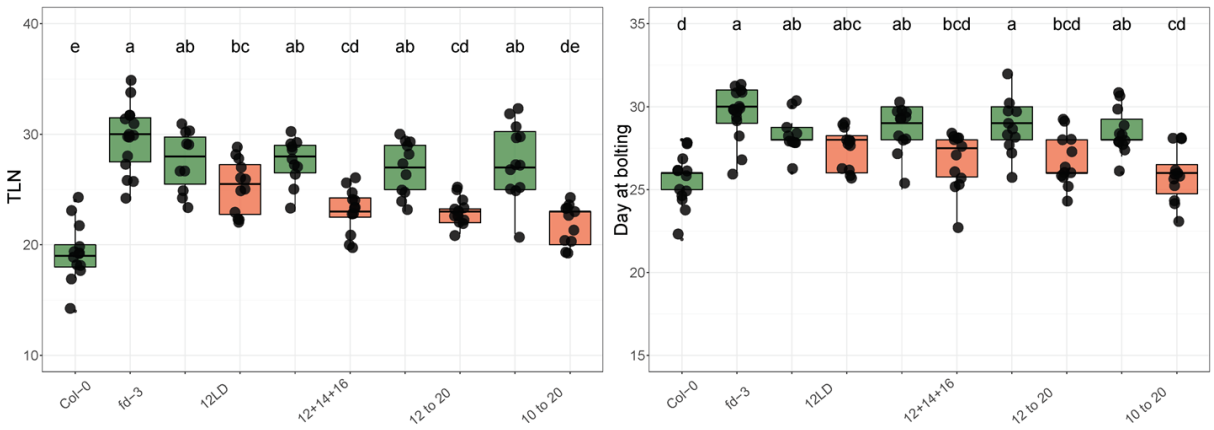

Figure 2.4. The rescue of the *fd-3* late-flowering phenotype by GR:FD depends on the DEX treatment frequency.
Flowering time of Col-0 and *fd-3* compared with that of the *FD::GR:FD fd-3 #19*. Total leaf number (TLN) and day at 1-cm bolting were scored under LD. Plants were treated with either mock (EtOH, green) or DEX (10 µM, orange) at the indicated time points (12LD, 14LD, 16LD, 18LD and 20LD); *n* = 11–15. Values for genotypes with the same letter do not differ significantly from each other (ANOVA, Tukey's HSD test).

A single DEX treatment at 12 LD caused a reduction of three leaves on average, compared with the mock-treated plants, but no statistically significant differences in days to bolt or total leaf number were detected. Partial rescue of the late-flowering phenotype (measured as leaf number) of *fd-3* was observed in the DEX-treated plants at 12 LD+14 LD+16 LD as well as in the 12 LD to 20 LD treated plants (Figure 2.4). Because DEX-treated plants at 12, 14 and 16 LD had similar leaf numbers as the DEX-treated plants from 12 LD to 20 LD, I hypothesize little contribution of FD to floral induction at days 18 and 20. Furthermore, only the plants treated with DEX every two days from 10 LD to 20 LD displayed a leaf-number phenotype

comparable to that of the wild-type, suggesting that FD activity promotes flowering between 10 LD and 12 LD. Remarkably, the date for 1-cm bolting of DEX-treated plants at 12+14+16 LD and from 12 LD to 20 LD was similar to that of the wild type (Figure 2.4), suggesting that the contribution of FD to this bolting phase can occur before day 16.

To confirm that early application of DEX affects floral transition, the SAM morphology was documented by confocal microscopy. The inflorescence meristem of 17-day-old Col-0 plants harboured flower primordia, whereas *fd-3* meristems at this time point did not (Figure 2.5A). In all treatment regimes, mock-treated *FD::GR:FD* plants displayed vegetative meristems at day 17 (Figure 2.5B). Inflorescence meristems were observed at 17 LD in *FD::GR:FD* plants DEX-treated at 12 LD, 10+12 LD and 10+12+14+16 LD with visible flower primordia. No flower primordia were visible on 17-day-old plants after a single DEX treatment at 10 LD, but the meristem was highly domed, suggesting that floral induction was well advanced. The meristem width of 17-day-old *FD::GR:FD* plants was reduced by two DEX treatments at days 10 to 12, four treatments from days 10 to 16, and two treatments at 12 and 14 LD (Figure 2.5C). Meristems of *FD::GR:FD* and Col-0 plants after treatment at days 10 to 12 and days 10 to 16 were morphologically similar. These results suggest that FD activity around days 10 to 12 has an important role in regulating SAM width. The height of the SAM of DEX-induced plants did not differ significantly from that of Col-0 after four treatments from 10 LD to 16 LD, but did with either of the other treatments (Figure 2.5C). Taken together, the results indicate that repeated DEX treatment from day 10 onwards is required for most effective complementation of the *FD::GR:FD fd-3* transgenic lines, suggesting a continuous role for FD in the floral transition throughout this period. One single induction of FD is sufficient to initiate the floral transition but not enough to rescue the late-flowering phenotype of *fd-3* compared with the wild type. The continuous requirement for FD is consistent with its expression pattern, and suggests that it might directly activate different targets at several stages of the floral transition, or that continuous activation of the same targets might be required.

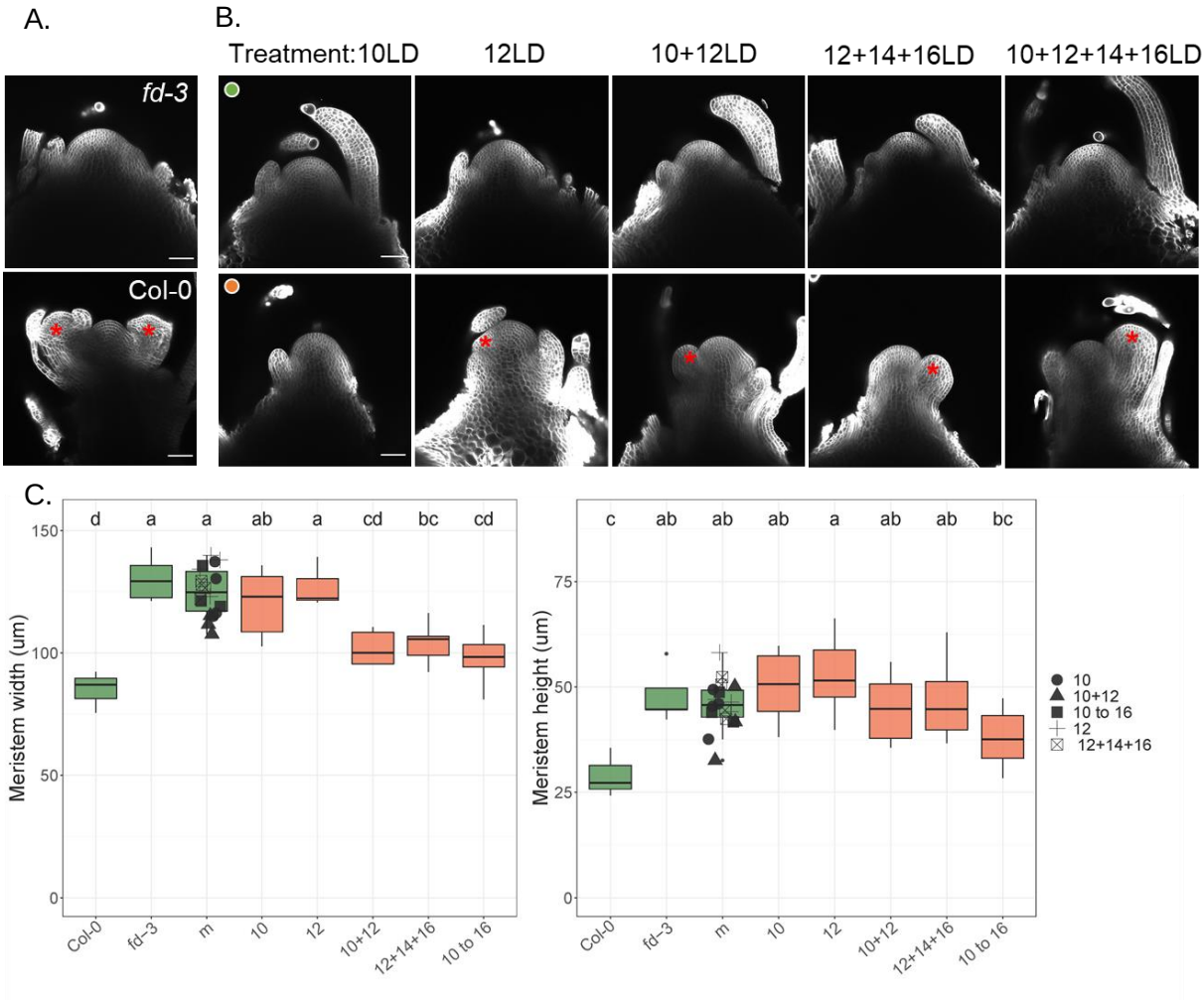

Figure 2.5. Higher frequency of GR:FD induction restores SAM morphology.
A, A 17-day-old meristem of *fd-3* and Col-0 (upper and lower panel, respectively). **B**, 17-day-old meristems of *FD::GR:FD fd-3 #19*. The plants were treated with either mock (EtOH, upper panel) or DEX (10 µM, lower panel) at the indicated time points. Red asterisks indicate floral primordia and scale bars represent 50 µm. **C**, Width and height of 17-day-old meristems. The Col-0 and *fd-3* plants received no treatment, whereas the transgenic *FD::GR:FD #19* plants were treated at the indicated time points with mock ("m"; green boxes) or DEX (orange boxes). The mock-treated *FD::GR:FD #19* meristems were clustered into "m" for visual comparison and each dot represent an individual meristem; the legend on the right refers to mock-treatment time points. Measurements of 2D images were performed with Fiji as described in Figure 2. Values for genotypes with the same letter do not differ significantly from each other (ANOVA, Tukey's HSD test). Represented meristems are shown in the images in **A**, and **B**.

2.2.4 Single induction of FD leads to changes in floral gene expression

The early floral integrators such as FUL and SOC1 initiate floral transition (Torti et al., 2012). Development of flower primordia coincides with an increase in expression of floral meristem identity genes such as *AP1*, which is expressed in stage 1 primordia, and *SEP3*, which first appears in late stage 2 primordia (Mandel and Yanofsky, 1998; Wigge et al., 2005). One induction of GR:FD at 12 LD led to the formation of flower primordia after 5 days, and a

reduction in rosette leaf number compared with that of *fd-3* (Figures 2.4 and 2.5B). The effect of this single DEX application on floral integrator and floral meristem identity gene expression was also tested. The *FD::GR:FD fd-3* line *#19* was treated once during the vegetative stage, at day 12. After five days, floral primordia were observed in most of the dissected meristems of DEX-treated plants but not in those of mock-treated plants (Figure 2.5A). To investigate further the effect of FD induction, RT-qPCR was conducted on RNA extracted from tissues harvested 6 and 8 h after single DEX or mock treatment of 12 LD plants. No consistent differences were found for *SOC1*, *FUL*, *SEP3* and *AP1* mRNA levels between DEX- and mock-treated samples (Figure 2.6A). Only the mRNA level of *FUL* was significantly higher in the DEX-treated samples, but could not be repeated (independent experiments not shown). RT-qPCR analysis following two consecutive DEX treatments at day 10 and 12 revealed similar levels of *AP1* and *FUL* between the mock and DEX samples, 20 h after treatment (Supplementary Figure 2.1A). Because the floral transition is a continuous process rather than a sudden switch, gene expression was monitored for several days after treatment. Five days after single DEX treatment, the levels of *SOC1* and *FUL* mRNAs were greater in the DEX samples compared with the mock, by 1.5- and 2.3-fold, respectively (Figure 2.6B). Similarly, *SEP3* and *AP1* expression increased five days after DEX treatment. This result correlates with the confocal images and the timing of initiation of the floral primordia in Figure 2.5A. In addition to flowering-time data and confocal microscopy images, inflorescences formed by these plants were photographed. The inflorescence of *FD::GR:FD fd-3* plants resembled that of *fd-3* with one treatment and several DEX treatments led to rapid development of the inflorescence compared with the mock-treated plants (Supplementary Figure 2.2A and B; Figure 2.3). The morphology of the inflorescence of the single-treated *FD::GR:FD fd-3* plants was not presented in these images (Supplementary Figure 2.2A).

Several days of treatment are therefore required to detect changes in floral integrator gene expression after GR:FD induction, which are required for the initiation of floral primordia.

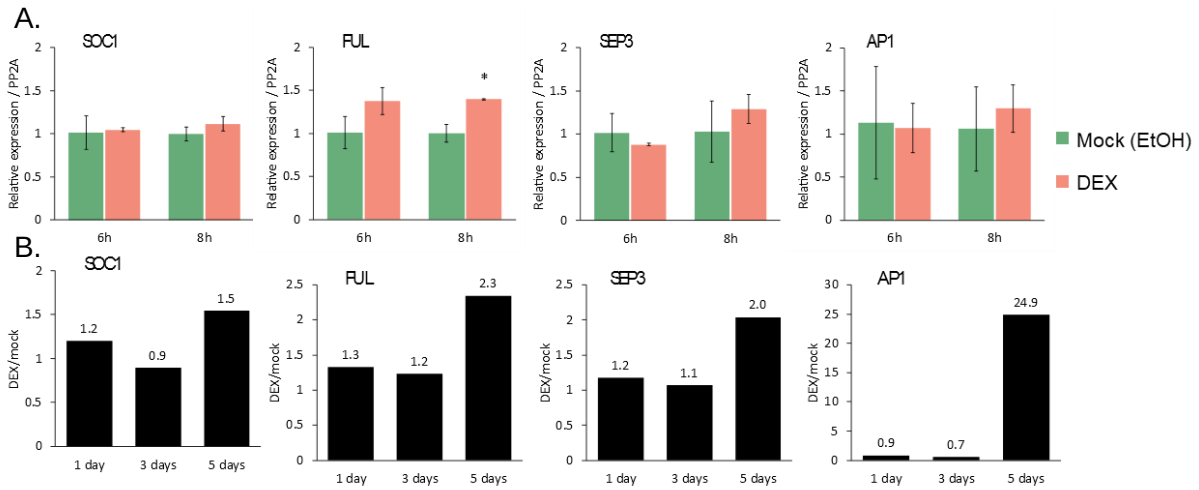

Figure 2.6. Induction of GR:FD causes transcriptional changes in flowering-time genes at the shoot apical meristem.
A, RT-qPCR on 12-day-old apices of *FD::GR:FD fd-3 #19* transgenic plants. Tissues enriched for apices were dissected 6 and 8 h after DEX (10 µM) or mock treatments. Levels of *SUPPRESSOR OF OVEREXPRESSION OF CO 1* (*SOC1*), *FRUITFULL* (*FUL*), *SEPALLATA 3* (*SEP3*) and *APETALA1* (*AP1*) are shown. The data are means for three biological replicates ±SD and statistics were performed using the Student's *t*-test. Mock and DEX of each time point were compared (*$p < 0.05$). Green and orange correspond to mock- and DEX-treated plants, respectively. **B**, RT-qPCR on *FD::GR:FD fd-3 #19* transgenic plants. Treatments were performed at day 12 and tissues enriched for apices were dissected 1, 3 and 5 days after DEX (10 µM) or mock treatments. Data represent fold changes in expression between the DEX and mock samples. The data are means ±SD for three technical replicates of one biological replicate.

2.2.5 Genome-wide transcriptomic analysis of *GR:FD* confirms temporal activity

FD physically binds to target genes, mostly at their promoter regions (Collani et al., 2019; Romera-Branchat et al., 2020; Zhu et al., 2020). The activation of some FD targets is dependent on the spatiotemporal activity of FD (Jung et al., 2016; Romera-Branchat et al., 2020). To identify early targets of FD necessary for the floral induction, I harvested samples to study genome-wide transcriptomic changes at the SAM after DEX application in *FD::GR:FD #19*. Biological triplicates of 12-day-old samples enriched for meristems were harvested before treatment as a control (Figure 2.7A; referred to as time 0). The centre of the apex of each individual treatment plant was then brushed with either mock or DEX solutions and meristem-enriched tissues were harvested 8 h after the treatment and then every 24 h for 5 days. Although morphological changes at the SAM were detected between DEX- and mock-treated samples, a PCA plot showed little difference between the transcriptomes of mock- and DEX-treated samples at the same time point (Supplementary Figure 2.3, Figure 2.7B). Analysis of the RNA-seq data comparing DEX and mock for a single time point identified almost no differentially expressed genes (DEGs). However, the samples diverged over the time course (colour gradient in Figure 2.7B) compared with the untreated time 0 (t0). This is presumably due to the growth and development of the plants over the five days, because the mock- and DEX-treated plants behaved similarly. In this study, all the data sets were compared with t0 for mock- and DEX-treated sample, and DEGs specific to the DEX samples were selected (Figure 2.7A). Cut-offs of a $\log_2$(fold change) of 1.5 and a *p*-value of 0.05 were applied. The DEGs were compared with the list of 306 genes involved in the floral transition compiled from the literature (Kinoshita and Richter, 2020). Several genes involved in the floral transition and flower development were found (Figure 2.7C). For instance, *FUL* mRNA levels were higher in the DEX samples 3 days after treatment compared with at t0, and this was not true for the mock-treated samples at day 3 (Figure 2.7C-D). Consistent with floral induction, *MIR157A* levels were downregulated after DEX application (Wang et al., 2009). Increase of *TFL1* after FD induction suggests previous hypothesis that the FD– TFL1

is required to repress genes and maintain the reproductive meristematic identity (Benlloch et al., 2007; Hanano and Goto, 2011). The levels of *AP1* and *FPF1* mRNAs were higher specifically in the DEX samples 4 days after the treatment, and *LFY* and *SPL4* were more highly expressed at day 5. Interestingly, the temporal activation of *FUL* and *AP1* observed in this analysis is consistent with previous reports (Figure 2.7C-D; Collani et al., 2019; Romera-Branchat et al., 2020).

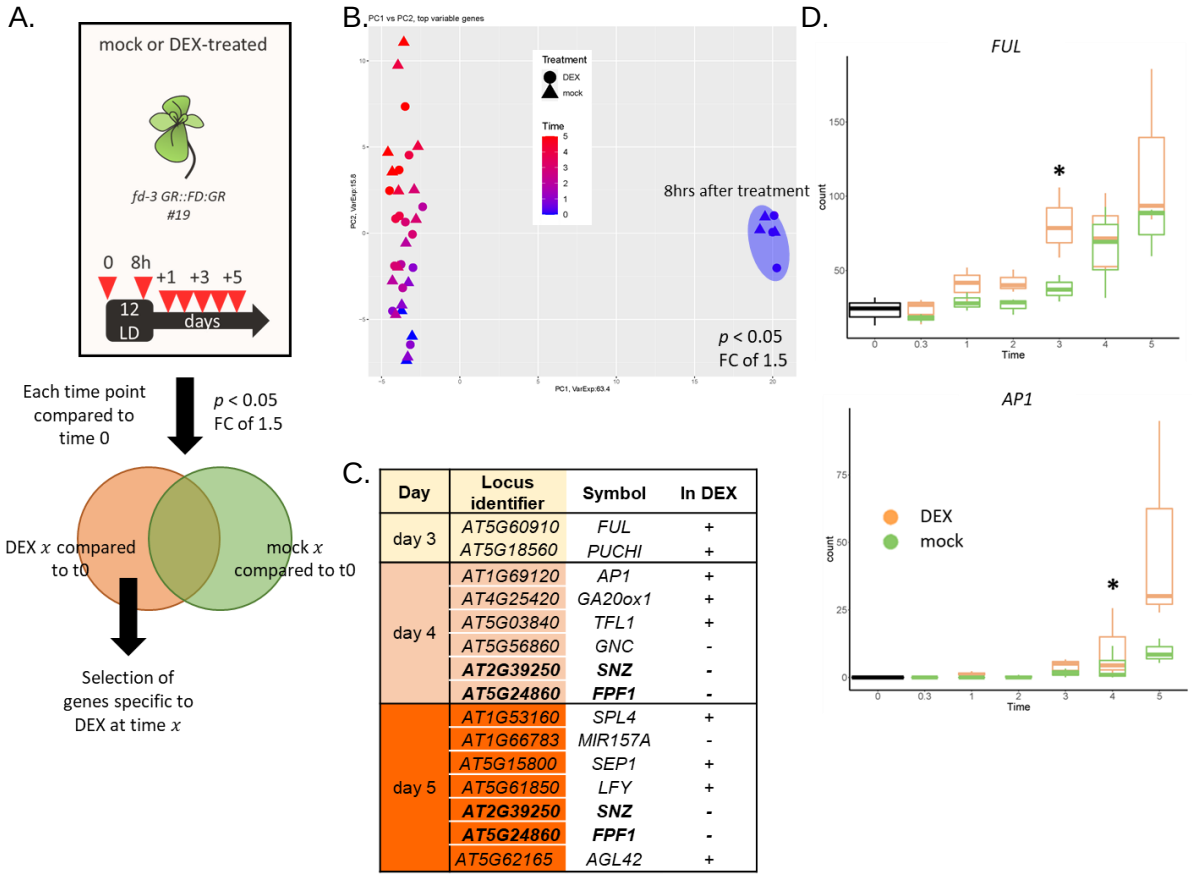

C.

Day	Locus identifier	Symbol	In DEX
day 3	*AT5G60910*	*FUL*	+
	AT5G18560	*PUCHI*	+
day 4	*AT1G69120*	*AP1*	+
	AT4G25420	*GA20ox1*	+
	AT5G03840	*TFL1*	+
	AT5G56860	*GNC*	-
	AT2G39250	***SNZ***	-
	AT5G24860	***FPF1***	-
day 5	*AT1G53160*	*SPL4*	+
	AT1G66783	*MIR157A*	-
	AT5G15800	*SEP1*	+
	AT5G61850	*LFY*	+
	AT2G39250	***SNZ***	-
	AT5G24860	***FPF1***	-
	AT5G62165	*AGL42*	+

Figure 2.7. Transcriptome analysis of 12-day old *FD::GR:FD* transgenic plants after DEX treatment.

A, Design of the RNA-seq experiment with enriched apices of *FD::GR:FD #19* under long days (LD). The apices of the plants were brushed with either DEX (10 μM) or ethanol (mock) at 12 LD. Time 0 corresponds to the time point at which the samples were harvested prior to treatment. Tissues enriched for apices were harvested 8 h after treatment and every 24 h for 5 days. **B**, Principal component analysis plot of all RNA-seq time-course samples. **C**, Table of the genes involved in floral transition and flower development that were differentially expressed specifically in the DEX samples compared with those at time 0. Genes in bold were differentially expressed for two consecutive days. **D**, Gene count comparisons by DESeq2's median of ratios. Normalisation was shown for *FRUITFULL* (*FUL*) and *APETALA1* (*AP1*). Asterisks indicate significant differences in gene expression specifically in the DEX samples ($p < 0.05$) compared with those at time 0. Boxplots were calculated from the three biological replicates of the mock (green) and DEX (orange) samples.

Next, all the DEGs were compared with published ChIP-seq lists of FD (Collani et al., 2019; Romera-Branchat et al., 2020; Zhu et al., 2020). The RNA-seq supports a direct regulatory role of FD at the loci of *FUL*, *FPF1*, *AGAMOUS-LIKE 42 (AGL42)*, *MIR157A* in floral induction and *LFY, PUCHI*, *SEP1* and *AP1* in floral development (Supplementary Table 1). These genes are temporally regulated by FD. Moreover, transcriptomic analysis revealed targets that are so far not associated with the floral transition. Some of these genes are *MYB DOMAIN PROTEIN 47* (*MYB47*)*, MYB8, AITR1* and *HOMEOBOX PROTEIN 53* (*HB53*) (Supplementary Table 1). For example. AITR1 and HB53 are known to be involved in the ABA-signalling pathway (Gonzalez-Grandio et al., 2017; Tian et al., 2017). These genes can be new components of the FD genetic pathway, independent of the floral transition.

2.2.6 Transcriptomic analysis of *GR:FD* reveals genetic control of *DREB2A* by FD

To analyse specifically the first targets of FD, I focused the analysis on the time point 0.3 (8 h after treatment, 12 LD plants). GO-term analysis of the 621 in total genes from the DEX list showed a greater representation of stress-related genes (Figure 2.8A). Among these 621 genes, about 13.8 % (97 genes) were specific to the DEX treatment (Figure 2.8B, in orange). From these, 27 genes were bound by FD in ChIP-seq assays (Figure 2.8C, Table 2.1; (Collani et al., 2019; Romera-Branchat et al., 2020; Zhu et al., 2020). These genes are mainly involved in the regulation of biological processes but also in response to stress and stimuli (Figure 2.8D). Brushing plants with solution containing Silwet L-77 stressed the plant and most likely contributed to such responses, even if the genes selected were specific to the DEX treatment. Next, to study the differences in expression between the mock- and DEX-treated samples, volcano plots of the 27 selected genes bound by FD were displayed (Figure 2.9A). *GALACTINOL SYNTHASE 2* (*GolS2*) and *HECATE 1* (*HEC1*) were preferentially bound by FD and had a $\log_2$(fold change) of about 2 (Table 2.1). By contrast, *DEHYDRATION-RESPONSIVE ELEMENT-BINDING PROTEIN2A* (*DREB2A*) and *AT4G28290* were found in one of the ChIP-seq lists with a $\log_2$(fold change) approaching the cut-off. The normalised count of these genes was displayed (Figure 2.9B) and to test their regulation by FD, the overexpression line *35S::HA:FD* was used (Romera-Branchat et al., 2020). Analysis by RT-qPCR using RNA extracted from 10-day-old seedlings showed an increase in *DREB2A* expression compared with that of Col-0 (Figure 2.9C). The other three selected genes did not show a difference at this seedling stage, even if *GolS2*, for instance, was preferentially bound by FD. To test the effect of multiple FD induction on *DREB2A* expression, RT-qPCR was performed with samples treated at day 10 and day 12. However, this analysis revealed no differences in gene expression 20 h after the treatment (Supplementary Figure 2.1B). The *dreb2a-2* showed no flowering phenotype under LD compared with that of the Col-0, suggesting little role for DREB2A in flowering (Figure 2.9D).

C.

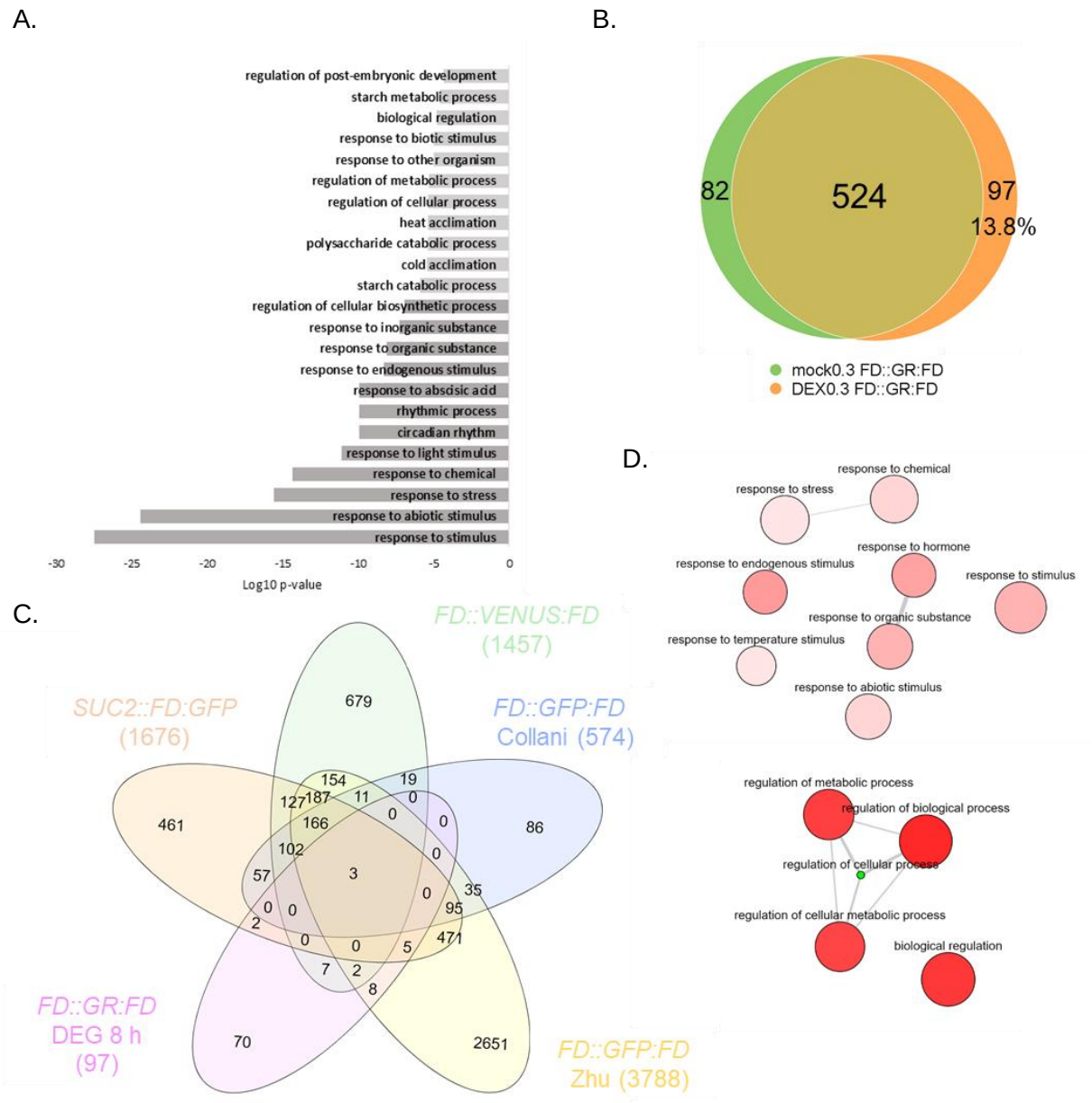

Figure 2.8. Selection of differentially induced genes for the inducible *FD::GR:FD #19* line after 8 h of treatment and GO-term enrichment analysis.

A, Bar graph illustrating the GO-terms of the 621 genes that were significantly more highly expressed in the DEX samples at 8 h compared with at time 0 (p-value < 0.05, $\log_2$(fold change) ≥ 1.5). **B**, A Venn diagram displaying the number of upregulated and downregulated genes from mock (green) and DEX (orange) treatments at time 8 h compared with at time 0 in 12-day-old tissues enriched for apices. A cut-off p-value < 0.05 and the $\log_2$(old change) ≥ 1.5 were used. The percentage represents the specific proportion of differentially expressed genes in the DEX samples. **C**, A Venn diagram comparing the overlap of genes bound and regulated by FD in the *FD::GR:FD fd-3 #19* inducible line at time 8 h with four ChIP-seq lists (Collani et al., 2019; Romera-Branchat et al., 2020; Zhu et al., 2020). **D**, Representation of two clusters from the GO-term analysis of all differentially expressed genes in the DEX samples 8 h after treatment. For each circle, the more intense the red, the higher the *P*-value. The agriGO (reference TAIR9) and REVIGO online tools were used with default parameters.

Locus Identifier	Symbol	Gene Description - Araport11	log2FC	padj	Bound
AT4G38550	*AT4G38550*	phospholipase-like protein (PEARLI 4) family protein	1.6171	0.0000	Z
AT1G16850	*AT1G16850*	transmembrane protein	1.5714	0.0008	Z
AT4G33985	*AT4G33985*	membrane insertase, putative (DUF1685)	1.7303	0.0000	Z
AT4G16140	*AT4G16140*	proline-rich family protein	-1.5060	0.0000	Z
AT1G07135	*AT1G07135*	glycine-rich protein	2.0480	0.0129	Z
AT3G48360	*BTB AND TAZ DOMAIN PROTEIN 2 (bt2)*	Encodes a protein (BT2) that is an essential component of the TAC1-mediated telomerase activation pathway	1.5514	0.0001	Z
AT2G26150	*HEAT SHOCK TRANSCRIPTION FACTOR A2 (HSFA2)*	member of Heat Stress Transcription Factor (Hsf) family	-2.0553	0.0007	Z
AT3G03450	*RGA-LIKE 2 (RGL2)*	Encodes a DELLA protein, a member of the GRAS superfamily of putative transcription factors	-1.6231	0.0000	Z
AT1G72760	*AT1G72760*	Protein kinase superfamily protein	-1.9110	0.0023	R
AT1G75800	*AT1G75800*	Pathogenesis-related thaumatin superfamily protein	1.5040	0.0000	R
AT4G27530	*AT4G27530*	hypothetical protein	-2.1332	0.0345	R
AT5G05320	*AT5G05320*	FAD/NAD(P)-binding oxidoreductase family protein	1.6246	0.0033	R
AT1G67855	*AT1G67855*	hypothetical protein	-2.4901	0.0067	R
AT1G20440	*COLD-REGULATED 47 (COR47)*	Belongs to the dehydrin protein family	1.5914	0.0000	R, Z, C
AT1G69570	*CYCLING DOF FACTOR 5 (CDF5)*	CDF5 is a circadian regulated transcript that is antiphasic with respect to its natural antisense transcript (NAT) *FLORE* (*AT1G69572*)	-1.5429	0.0023	R, Z, C
AT5G05410	*DRE-BINDING PROTEIN 2A (DREB2A)*	Encodes a transcription factor that specifically binds to DRE/CRT cis elements	1.5579	0.0014	R
AT1G56600	*GALACTINOL SYNTHASE 2 (GolS2)*	GolS2 is a galactinol synthase that catalyzes the formation of galactinol from UDP-galactose and myo-inositol	-2.3171	0.0020	C, R, Z
AT3G24500	*MULTIPROTEIN BRIDGING FACTOR 1C (MBF1C)*	One of three genes in *A. thaliana* encoding multiprotein bridging factor 1, a highly conserved transcriptional coactivator	-1.7102	0.0000	R
AT3G57520	*SEED IMBIBITION 2 (SIP2)*	SIP2 encodes a raffinose-specific alpha-galactosidase that catalyzes the breakdown of raffinose into alpha-galatose and sucrose	1.5127	0.0000	R, Z
AT3G15360	*THIOREDOXIN M-TYPE 4 (TRX-M4)*	Encodes a prokaryotic thioredoxin The mRNA is cell-to-cell mobile	1.5222	0.0000	R, Z
AT1G06570	*PHYTOENE DESATURATION 1 (PDS1)*	Mutation of the PDS1 locus disrupts the activity of p-hydroxyphenylpyruvate dioxygenase (HPPDase)	-1.6099	0.0000	C,Z
AT2G34430	*LIGHT-HARVESTING CHLOROPHYLL-PROTEIN COMPLEX II SUBUNIT B1 (LHB1B1)*	Photosystem II type I chlorophyll a/b-binding protein	1.6950	0.0000	C, Z
AT2G47780	*LD-ASSOCIATED PROTEIN 2 (LDAP2)*	Encodes a small rubber particle protein homolog	-1.7380	0.0000	C, Z
AT4G11370	*RING-H2 FINGER A1A (RHA1A)*	Encodes a putative RING-H2 finger protein RHA1a	1.6062	0.0011	C, Z
AT4G28290	*AT4G28290*	hypothetical protein	-1.8217	0.0001	C
AT5G15970	*KIN2*	Encodes a gene that can be induced by cold and abscisic acid and may be involved in cold acclimation and salt tolerance. The mRNA is cell-to-cell mobile	1.6496	0.0017	C,Z
AT5G67060	*HECATE 1 (HEC1)*	Encodes a bHLH transcription factor that is involved in transmitting tract and stigma development	1.9383	0.0384	C,Z

Table 2.1 Transcriptome analysis of the *FD::GR:FD fd-3* inducible line reveals new putative FD targets.

A list of 27 genes selected from all time points of the RNA-seq time course. Each gene was significantly differentially expressed in the DEX samples compared with time 0. Genes were selected with a cut-off *p*-value ≤ 0.05 and a $\log_2$(foldchange) ≥ 1.5. ChIP-seq identified genes bound by VENUS:FD (Romera Branchat et al., 2020; referred to as “R” in the legend),

GFP:FD (Collani et al., 2019; annotated “C”) and GFP:FD from the *FD* promoter (Zhu et al., 2020; annotated “Z”).

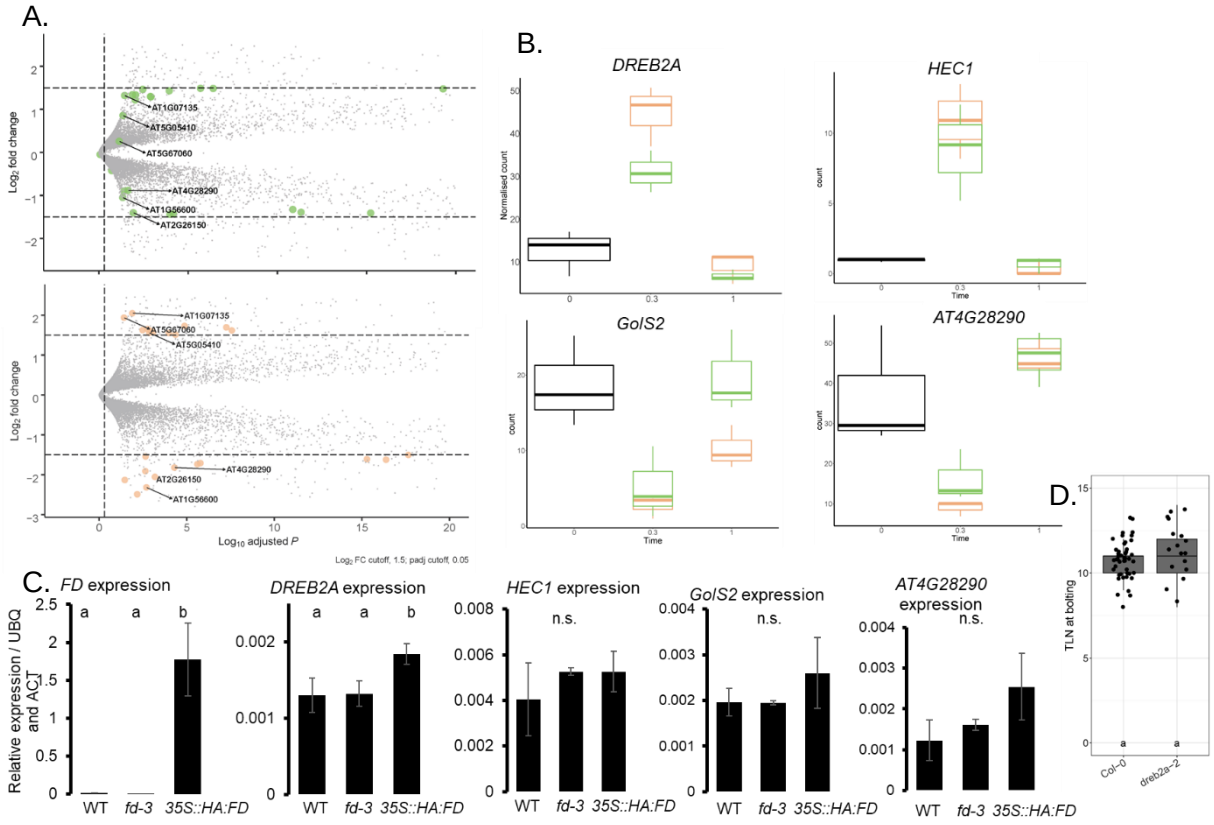

Figure 2.9. FD regulates *DREB2A* expression in *Arabidopsis thaliana.*
A, Volcano plots showing the $\log_2$(fold change) in gene expression after mock (upper panel) or DEX (lower panel) treatment after 0.3 days compared with time 0. The y-axis represents the statistical significance ($\log_{10}$-adjusted *p*-value). The selected 19 deltaDEX genes with at least a 2.8-fold increase in expression are annotated and displayed with larger dots. **B**, Gene count comparisons by DESeq2’s median of ratios. Normalisation counts were shown for *DEHYDRATION-RESPONSIVE ELEMENT BINDING PROTEIN 2* (*DREB2A*; *AT5G05410*), *HECATA 1* (*HEC1*, *AT5G67060*), *Galactinol synthase 2* (*GolS2*; *AT1G56600*) and *AT4G28290* genes. **C**, Validation of FD target genes in *35S::HA:FD* and *fd-3* mutants by real-time qPCR in 10-day-old samples. The data are means for biological triplicates ±SD and were statistically analysed using ANOVA followed by Tukey’s HSD test ($p < 0.05$). **D**, Flowering time of Col-0 and *dreb2a-2*. Total leaf number (TLN) was scored under LD; for Col-0, $n = 46$; for *dreb2a-2*, $n = 16$. Values for genotypes with the same letter do not differ significantly from each other (ANOVA, Tukey’s HSD test).

Stringent cut-offs and RNA-seq at an early time point after DEX induction strongly suggested *DREB2A* to be a target of FD. However, *DREB2A* loss-of-function mutant could not be linked to the floral induction. These results suggest a role for FD and DREB2A at different developmental stages such as during stress responses.

2.2.7 Removal of *TFL1* does not promote gene expression after FD induction

The effect of FD on the timing of the floral transition depends on interaction with its partner proteins TFL1 and FT. The presence of FT at the SAM overcomes the negative role of TFL1–FD under LD (Jaeger et al., 2013; Zhu et al., 2020). The weak differences in gene expression observed after GR:FD induction in the *fd-3* background by RNA-seq (Figure 2.7B) might be due to repression by TFL1. To test the regulatory role of FD in the absence of its repressor, the *FD::GR:FD fd-3 #19* line was crossed to *tfl1-18 fd-3* (Dr. A. Pajoro). First, RT-qPCR was performed to assess the expression of specific genes involved in the floral transition. At day 12, *tfl1-18 fd-3 FD::GR:FD #19* plants were brushed once with either mock or DEX solution. Tissues enriched for apices were harvested 20 h and 3 days after treatment. No differences in gene expression were detected for *AP1*, *FUL*, *SEP3* or *DREB2A* (Figure 2.10). This indicates that repression by TFL1 did not prevent detection of gene expression changes in the previous experiments (Figures 2.6, 2.7 and Supplementary Figure 2.1).

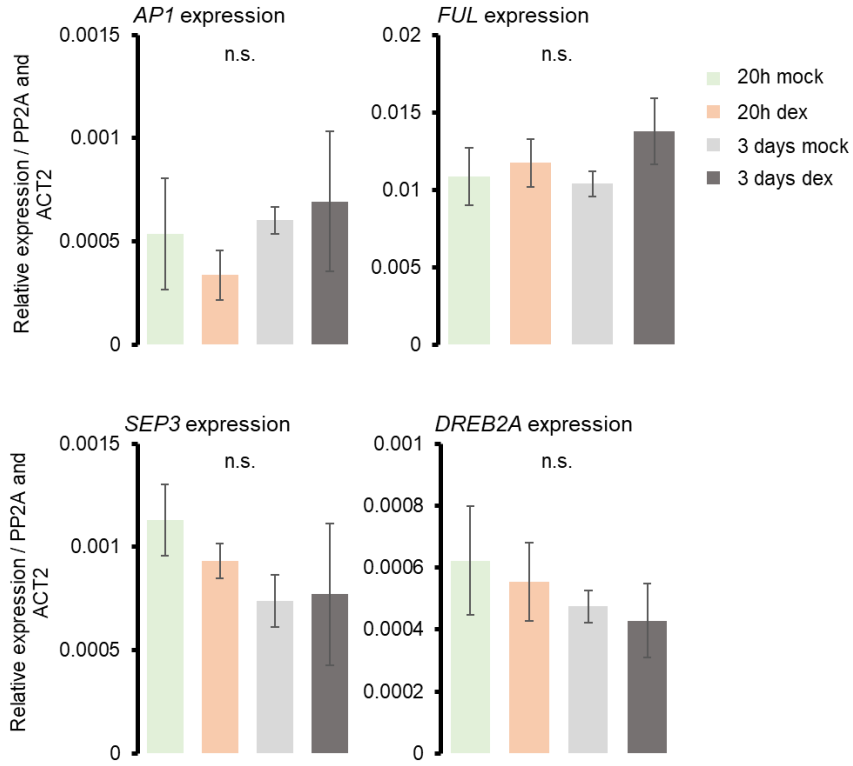

Figure 2.10. Suppression of TFL1 does not change the expression of selected genes after FD induction in the *tfl1-18 fd-3 FD::GR:FD* background. Expression of FD target genes in *tfl1-18 fd-3 FD::GR:FD #19*. Analysis was conducted on *APETALA1* (*AP1*), *FRUITFULL* (*FUL*), *SEPALLATA 3* (*SEP3*) and *DEHYDRATION-RESPONSIVE ELEMENT BINDING PROTEIN 2* (*DREB2A*) mRNA. Plants were treated with either mock or DEX solution at day 12 and tissues enriched for apices were harvested at the indicated time points (either 20 h after treatment or 3 days after treatment). The data are means for biological triplicates ±SD and were statistically analysed using ANOVA followed by Tukey's HSD test ($p < 0.05$).

2.3 Discussion

2.3.1 Induction of FD in the *fd-3* vegetative meristem

Induction of the activity of transcription factors using exogenously applied chemicals is a powerful means to identify their downstream targets and determine their role in controlling developmental responses. Induction systems with dexamethasone have been implemented in Arabidopsis and are widely used to study biological processes such as root development (Santuari et al., 2016), floral transition and flower development (Simon et al., 1996; Wagner et al., 1999; William et al., 2004; Ecker et al., 2006; Gunl et al., 2009) and genome-wide analysis of inflorescence transcriptome (Goslin et al., 2017). The system relies on fusion of the protein of interest, usually a transcription factor, and the ligand-binding domain of the glucocorticoid receptor (GR) from mammals. The receptor is held in the cytoplasm in the absence of its steroid ligand and can be released to the nucleus on the application of DEX (Yamaguchi et al., 2015). Therefore, after DEX application the fusion proteins move to the nucleus and the transcription factor regulates target genes. This system allows rapid induction of protein activity, because the fusion protein is already present in the cytoplasm of the cells prior to DEX application. Direct target genes can therefore be identified by identifying genes that are induced on application of DEX in the presence of a translational inhibitor, such as cycloheximide. A disadvantage of this method is that the GR fusion might affect the activity of the transcription factor, and it is not straightforward to determine when DEX has activated the activity of the transcription factor, as this depends on shuttling from the cytoplasm to the nucleus. A second strategy depends on the activation of a synthetic transcription factor, such as LhG (Craft et al., 2005), by DEX application, and this then activates transcription of the gene of interest via the LhG target promoter. This system has the advantage that the expression of the gene of interest in response to DEX application can be followed by real-time qPCR, but has the disadvantage that it is slower, because the gene of interest must be transcribed and translated after DEX application.

In this chapter, inducible *FD::GR:FD fd-3* transgenic lines were generated to understand better the role of FD at the floral transition. A low DEX concentration was used in this study to better mimic endogenous processes. Single induction of FD did not fully complement the *fd-3* late-flowering phenotype (Figure 2.4, Supplementary Figure 2.2A). However, single induction of FD at day 12 did promote early flower primordium initiation as detected by microscopy (Figure 2.5B, Supplementary Figure 2.3). These morphological changes were followed by transcriptional activity related to the floral transition, particularly 4 and 5 days after DEX application (Figures 2.6C and 2.7C). Indeed, although rapid gene effects are usually detected after DEX induction (Yamaguchi et al., 2015), rapid transcriptional changes of known FD-regulated, target genes (*e.g*. *FUL* and *AP1)* were not detected after DEX

induction (Figure 2.6B). Three to five days were required to observe upregulation of *FUL* and *AP1* compared with the mock samples (Figures 2.6C and 2.7C, D). The more the transgenic plants were treated with DEX solution, the stronger was the observed complementation of the *fd-3* flowering phenotype (Figures 2.3A and 2.4). But even two consecutive DEX treatments at day 10 and 12 did not promote a rapid response in *FUL* and *AP1* expression (Supplementary Figure 2.1). This indicates that FD regulates targets before *FUL*. Some transcription factors require the activation of their own cofactors to regulate downstream genes (Yamaguchi et al., 2015). Because FD is continuously present at the SAM, even before floral induction, it is also possible that FD cofactors are required before the floral induction, discussed in more details in section 2.3.3. Another possibility is that 12-day-old meristems of *fd-3* mutants are qualitatively different to those of the wild type, and therefore respond to FD activity less effectively. Similarly, in the absence of FD, floral repressors may accumulate to high levels, and antagonize FD activity on its target genes. A related possibility was tested for TFL1 by introducing GR:FD into the *tfl1* mutant background, but this did not enable more rapid induction of target genes (Figure 2.10). Other floral repressors such as SVP or AP2 may antagonize FD function. Lastly, it is not known how much FD is required within the meristematic tissues to trigger floral transition, and whether functions in different tissues are required. For instance, it would be interesting to study the flowering phenotype of *the SUC2::FD fd* and the *fd* compared with the wild type.

In Arabidopsis, meristem width and area increase towards the floral transition, and decrease when flower primordia are formed (Figure 2.1C; Kinoshita and Richter, 2020; Wang et al., 2020). In *ft tsf* mutant plants, the area of the meristem is bigger than that in Col-0 (Kinoshita et al., 2020), and *fd* meristem area is bigger than that in Col-0 (Figure 2.1C; personal communication from Dr. M. Cerise). Early induction of FD at day 7 followed by multiple DEX applications are necessary to trigger floral induction and to restore the wild-type flowering phenotype (Figures 2.3A and 2.4). The 17-day-old inflorescence meristem of Col-0 was smaller than that of *fd-3*, and coincided with the presence of inflorescence primordia (Figure 2.5). Four DEX treatments (day 10 to 16) led to the developmentally most advanced inflorescence meristems compared with those after three, two or single treatments (Figure 2.5). The most-induced meristem had the smallest size, which is consistent with a reduction in meristematic size due to flower production (Wang et al., 2020). Because early DEX treatments are needed to restore the *fd-3* phenotype, I hypothesize that: 1) the floral transition is a gradual process that involves a cascade of steps initiated by FD to result in the formation of flower primordia, and the presence of FD coactivators may partially determine the timing of different steps; and 2) the timing of FT arrival at the SAM is likely crucial to

regulate gene expression by the FAC, and has not been thoroughly described (Abe et al., 2019).

2.3.2 Identification of the early targets of FD

To identify the earliest targets regulated by FD after induction, I performed transcriptomic analysis on samples enriched for apices in a time course from day 12. No differences in gene expression were detected between mock and DEX by direct comparison of the same time points (Figure 2.7B). The harvested samples were enriched for apices, but contained part of the stem, vasculature and leaf primordia. Therefore, the induction of gene expression by FD may have been diluted by tissues lacking FD expression. One other possibility concerns whether the DEX concentration used in this assay was sufficient, but 10 µM DEX has widely been used in successful transcriptomic analyses (Yamaguchi et al., 2015). Nevertheless, by comparing each time point to the t0 sample and selecting DEGs specific to the DEX samples with stringent cut-offs to reduce false discoveries, I was able to identify genes specific to FD induction. The DEGs identified 8 h after treatment were compared with available ChIP-seq lists and 27 genes were selected (Table 2.1). These genes may be bind and regulated by FD before that of *FUL*. An important part of these genes has not been characterised or has not been linked to the floral transition. For instance, the *GALACTINOL SYNTHASE 2* (*GolS2*) encodes for an enzyme responsible of higher galactinol levels during drought-stress conditions (Taji et al., 2002) and seems to be the strongest FD target from the RNA-seq. It displays a negative fold change of -2.3 and the locus of *GolS2* is bound by FD in three independent ChIP-seq assays (Collani et al., 2019; Romera-Branchat et al., 2020; Zhu et al., 2020). However, the level of *GolS2* in over-expression line of FD were similar to that of Col-0 (Figure 2.9C). The *CYCLING DOF FACTOR 5* (*CDF5*) was downregulated after FD induction. Mutation of *CDF5* triggers early flowering under LD and SD conditions (Fornara et al., 2009), suggesting a direct role for FD in *CDF5* downregulation to promote flowering. It would be interesting to cross *cdf5* with *fd* and assess the flowering time. It is known that mutations at *HECATE 1* (*HEC1*) and *HEC3* genes in the *hec1 hec3* mutant led to an early-flowering phenotype (Gaillochet et al., 2018). Although *HEC1* transcription was slightly upregulated after 8 h of induction (Figure 2.9B, Table 2.1), the increase could not be confirmed in the overexpression line of FD (Figure 2.9C). However, upregulation of the *DREB2A* gene was confirmed in the FD overexpression line and appears the best candidate as a novel FD target (Figure 2.9C). Overexpression of the constitutively active form of DREB2A led to a late-flowering phenotype (Qin et al., 2008). The floral repressor encoded by the *EARLY FLOWERING3* (*ELF3*) gene indirectly regulates the expression of *DREB2A* in stress conditions (Sakuraba et al., 2017). But *dreb2a-2* did not altered floral transition under LD (Figure 2.9D), suggesting that DREB2A function may be restricted to ABA-stress related conditions as it recognizes specific *cis*-regulatory elements of genes involved in dehydration

and biotic stresses (Kim et al., 2011). DREB2A may act by promoting drought-escape responses for instance (Conti, 2019). Members of the Group A bZIP proteins in Arabidopsis are involved in responses to abiotic stress and some have been linked to promoting flowering in drought by regulating *SOC1* (Dröge-Laser et al., 2018; Hwang et al., 2019). It would thus be interesting to test the ability of *fd-3* to flower under drought-stress conditions. Lastly, FD is expressed throughout development at the SAM and its positive role in *DREB2A* activation may be indicative of a pleiotropic function for FD, such as its role in the seedling (Romera-Branchat et al., 2020).

2.3.3 Temporal activity: what are the cofactors of FD?

Interestingly, ABA-mediated phosphorylation of ABF3 promotes the interaction with 14-3-3 proteins (Sirichandra et al., 2010). This finding supports that other bZIP proteins involved in floral transition interact with 14-3-3 proteins in Arabidopsis (Hwang et al., 2019). In plants, 14-3-3 proteins stabilise the interactions between FT and TFL1 or FD orthologues at the chromatin to regulate floral transition (Taoka et al., 2011; Kaneko-Suzuki et al., 2018; Zuo et al., 2021). However, due to the predominance and versatile role of 14-3-3 proteins in plant development, their relevance has been questioned (Jaspert et al., 2011). The FT and TSF proteins are not required for binding of FD to the majority of its targets, but are crucial for the transcriptional activation of its target genes (Collani et al., 2019). Some FD-interacting proteins have been identified and may contribute to potentially even larger transcriptional complexes at the TSS (Transcription Start Site; Jung et al., 2016; Li et al., 2019). Pull-down assays followed by mass spectrometry analysis of FD would be a powerful method to identify partners of FD and potential cofactors involved in the floral transition.

From the DEG list, I found two genes rapidly regulated after FD induction that encode potential cofactors in the FD–(14-3-3)–FT/TSF or TFL1 complexes (Table 2.1). FD potentially regulate their transcription prior to forming a large complex at the DNA to regulate genes involved in floral transition. The *BT2* mRNA levels increased after FD induction. The *BT2* gene encodes a transcription factor containing a TAZ-domain (Transcriptional Adaptor Zinc finger) that localizes to the cell nucleus. The protein acts in auxin responses and gametophyte development, and the *bt2* mutant suppresses the delayed-flowering phenotype of the *yucca* mutant (Mandadi et al., 2009; Robert et al., 2009). BT2 is involved in regulating the chromatin environment of telomeric regions (Ren et al., 2007). Speculatively, BT2 may modify the chromatin environment of FD targets and indirectly act as a cofactor of FD to modulate expression at the promoters of target genes. Furthermore, the *Multiprotein Bridging Factor 1C* (*MBF1*) gene is downregulated after FD induction (Table 2.1) and is known to be a cofactor of the transcription of genes in several developmental and stress-related pathways, such as thermotolerance in Arabidopsis (Suzuki et al., 2008). The MBF1 protein might also function together with FD in a larger complex to repress gene expression, with TFL1 for

instance. Expression of MBF1 and BT2 under *FD* promoter or the constitutive 35S promoter would be interesting to know whether these two proteins limit FD action at the SAM and thus, determine whether they affect flowering.

2.3.4 Concluding summary of chapter 2

To improve our understanding of the role of FD in floral transition, an inducible FD system was generated. This chapter demonstrates the efficiency of the *FD::GR:FD* construct in inducing floral induction in the *fd-3* mutant background. Both flowering-time scoring and confocal microscopy of the SAM showed early flowering of the DEX-treated plants compared with the mock-treated plants, indicating that FD activity is required over several days from day 7 or 10 onwards to induce flowering. The complementation of the flowering phenotype and the meristem shape in the transgenic line indicate that the GR:FD fusion protein provides functional FD activity. Although induction of GR:FD with DEX induced the expression of genes required for floral transition in temporal manner, the effect was surprisingly slow and weak, suggesting that FD induction at the SAM is not sufficient to strongly induce the transcription of genes. *FUL* expression was expected to increase within hours after FD induction but was detected three days after the DEX treatment. This delay may be due to the difficulty to detect small changes in gene expression in hand dissected tissues, but also because of the vegetative stage of *fd-3* at day 12 and the absence of requisite cofactors for FD. Interestingly, induction of GR:FD regulates the expression of *FUL, FPF1*, *AGL42* and *MIR157A*, which have roles in floral induction and are bound by FD (Kania et al., 1997; Collani et al., 2019; Kinoshita and Richter, 2020; Romera-Branchat et al., 2020; Zhu et al., 2020). This indicates early floral transition after FD induction in the *fd-3* background compared with the mock. Next, changes in the expression of floral meristem identity genes such as *AP1, LFY, PUCHI* and *SEP1* were observed and usually coincided with the initiation of floral primordia. These results confirm the temporal promotion of flowering by FD. Furthermore, the data reveal a novel role for FD in the regulation of genes such as *MYB47, MYB8, AITR1* and *HB53*. The regulation of these genes and binding to their promoters by FD could be confirmed by RT-qPCR and ChIP-qPCR, respectively.

2.4 Supplementary figures

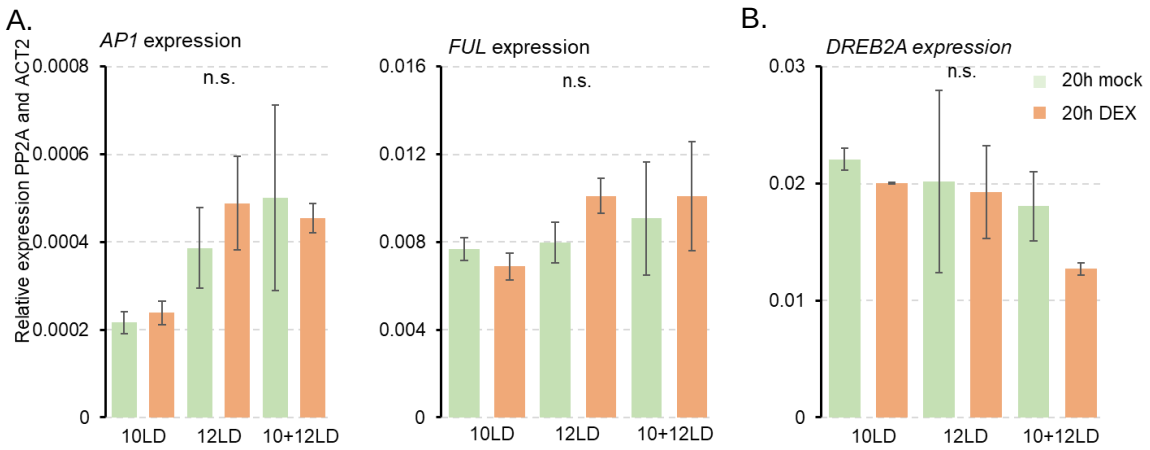

Supplementary Figure 2.1. Analysis of gene expression after DEX treatment at day 10 and 12.

A, and **B**, RT-qPCR on *FD::GR:FD #19* apices to detect *APETALA1* (*AP1*), *FRUITFULL* (*FUL*) and *DEHYDRATION-RESPONSIVE ELEMENT BINDING PROTEIN 2* (*DREB2A*) expression levels. Tissues enriched for apices were dissected 20 h after DEX (10 µM) or mock treatments at the indicated time points. The data are means for two biological replicates ±SD and were statistically analysed using ANOVA followed by the Tukey's HSD test. Green and orange correspond to mock- and DEX-treated plants, respectively.

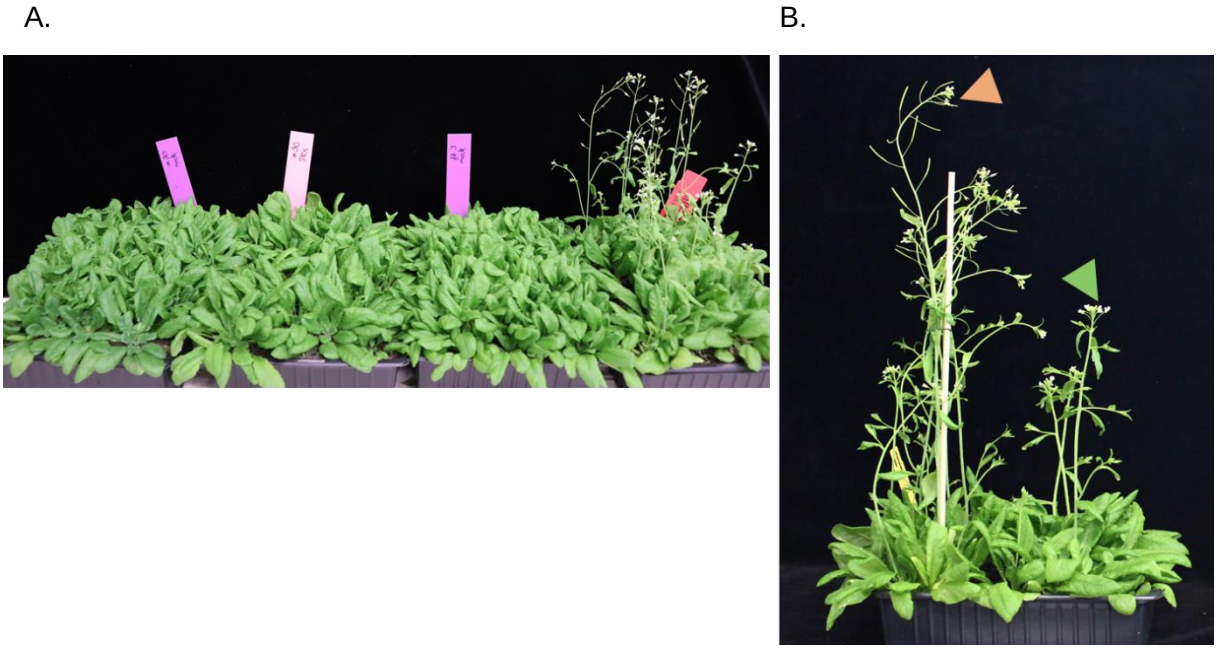

Supplementary Figure 2.2. Several DEX treatments are required to rescue the *fd-3* late-flowering phenotype under long days.

A, Photographic image of 4-week-old plants after a single DEX treated plants at day 14 in long days. From left to right: *FD::GR:FD #30* mock, *#30* DEX (10 µM), *fd-3* mock and Col-0 mock. **B**, Photographic image of 5-week-old *FD::GR:FD #19* plants after continuous DEX treatment from day 7 up to the appearance of buds. The plant on the left was treated with DEX (10 µM) and the plant on the right was mock-treated.

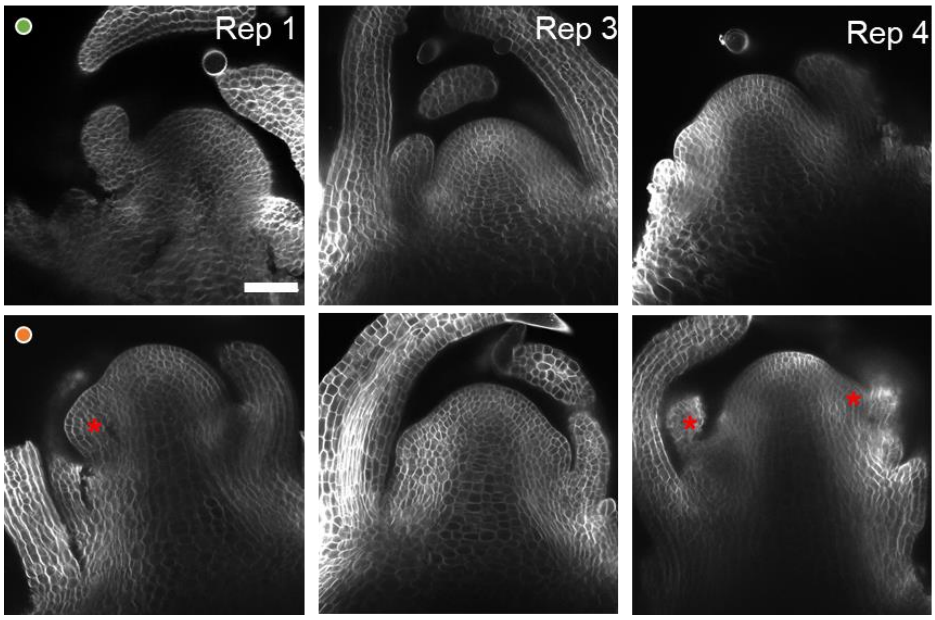

Supplementary Figure 2.3. Induction of GR:FD at day 12 triggers the early formation of floral primordia, from the RNA-seq experiment.
Morphology of representative 17 LD meristems 5 days after mock (upper panel) or DEX treatment (lower panel) of *FD::GR:FD #19* plants. The replicate 1, 3 and 4 correspond to the batch of plants harvested for RNA sequencing. Samples were fixed in 4% PFA, soaked in Clearsee for one week and Renaissance staining was added one day before imaging by confocal microscopy. The scale bar represents 50 µM.

Day	Locus Identifier	Symbol	Gene Description - Araport11	Bound
1	AT4G36040	DNAJ11 (J11)	Chaperone DnaJ-domain superfamily protein	Z
	AT2G20670		sugar phosphate exchanger, putative (DUF506)	Z, SUC2
	AT4G32480		sugar phosphate exchanger, putative (DUF506)	Z, SUC2
	AT3G07350		sulfate/thiosulfate import ATP-binding protein, putative (DUF506)	Z
2	AT1G23390	KELCH DOMAIN-CONTAINING F-BOX PROTEIN (KFB)	A kelch domain-containing F-box protein	Z
	AT4G36040	DNAJ11 (J11)	Chaperone DnaJ-domain superfamily protein	Z
	AT2G25900	ATCTH	Encodes a protein with two tandem-arrayed CCCH-type zinc fingers that binds RNA and is involved in RNA turnover. The mRNA is cell-to-cell mobile	Z
	AT1G80920	J8	A nuclear encoded soluble protein found in the chloroplast stroma. Negatively regulated by light and has rapid turnover in darkness.	SUC2
	AT4G32480		sugar phosphate exchanger, putative (DUF506)	Z, SUC2
	AT3G07350		sulfate/thiosulfate import ATP-binding protein, putative (DUF506)	Z
3	AT2G19590	ACC OXIDASE 1 (ACO1)	encodes a protein whose sequence is similar to 1-aminocyclopropane-1-carboxylate oxidase	R
	AT1G01520	ALTERED SEED GERMINATION 4 (ASG4)	RVE3 is one of eleven homologous MYB-like transcription factors in Arabidopsis and a member of the RVE8 clade. Plays a minor role in clock regulation	SUC2
	AT5G60910	AGAMOUS-LIKE 8 (AGL8) / FUL	MADS box gene negatively regulated by APETALA1	SUC2, C, Z
	AT4G33070	PYRUVATE DECARBOXYLASE 1 (PDC1)	Thiamine pyrophosphate dependent pyruvate decarboxylase family protein	Z
	AT1G19630	CYTOCHROME P450, FAMILY 722, SUBFAMILY A, POLYPEPTIDE 1 (CYP722A1)	cytochrome P450, family 722, subfamily A, polypeptide 1	Z
	AT5G59490		Haloacid dehalogenase-like hydrolase (HAD) superfamily protein	R
	AT4G37780	MYB DOMAIN PROTEIN 87 (MYB87)	encoded by the Myb-like transcription factor MYB87, regulates axillary meristem formation, expressed throughout the plant. Member of the R2R3 factor gene family	Z
	AT5G18560	PUCHI	Encodes PUCHI, a member of the ERF (ethylene response factor) subfamily B-1 of ERF/AP2 transcription factor family. Expressed in early floral meristem (stage 1 to 2). Required for early floral meristem growth and for bract suppression	SUC2, Z
	AT1G67810	SULFUR E2 (SUFE2)	Encodes a protein capable of stimulating the cysteine desulfurase activity of CpNifS (AT1G08490) in vitro. Transcript levels for this gene are high in the pollen. The mRNA is cell-to-cell mobile.	Z
	AT1G63820		CCT motif family protein	Z
4	AT4G01950	GLYCEROL-3-PHOSPHATE SN-2-ACYLTRANSFERASE 3 (GPAT3)	putative sn-glycerol-3-phosphate 2-O-acyltransferase	Z
	AT3G07340	CRY2-INTERACTING BHLH 3 (CIB3)	basic helix-loop-helix (bHLH) DNA-binding superfamily protein	Z
	AT3G29670	PHENOLIC GLUCOSIDE MALONYLTRANSFERASE 2 (PMAT2)	Encodes a malonyltransferase that may play a role in phenolic xenobiotic detoxification. The mRNA is cell-to-cell mobile	Z
	AT2G46720	3-KETOACYL-COA SYNTHASE 13 (KCS13)	Encodes KCS13, a member of the 3-ketoacyl-CoA synthase family involved in the biosynthesis of VLCFA (very long chain fatty acids)	Z
	AT1G09350	GALACTINOL SYNTHASE 3 (GolS3)	Predicted to encode a galactinol synthase	Z
	AT2G01918	PSBQ-LIKE 3 (PQL3)	Encode a protein homologous to each PQL protein. Mutational analysis indicates that PQL3 is also required for NDH activity	Z
	AT5G24210		alpha/beta-Hydrolases superfamily protein	SUC2
	AT1G18710	MYB DOMAIN PROTEIN 47 (MYB47)	Member of the R2R3 factor gene family. Promotes seed longevity (viability of seed over time.) Expressed in the chalazal seed coat. Overexpresion enhances resistance of seed to deterioration	Z
	AT1G69120	APETALA1 (AP1)	Floral homeotic gene encoding a MADS domain protein homologous to SRF transcription factors. Specifies floral meristem and sepal identity.	SUC2, C , Z, R
	AT1G67810	SULFUR E2 (SUFE2)	Encodes a protein capable of stimulating the cysteine desulfurase activity of CpNifS (AT1G08490) in vitro. Transcript levels for this gene are high in the pollen. The mRNA is cell-to-cell mobile.	Z
	AT5G06090	GLYCEROL-3-PHOSPHATE SN-2-ACYLTRANSFERASE 7 (GPAT7)	putative sn-glycerol-3-phosphate 2-O-acyltransferase	SUC2
	AT5G62480	GLUTATHIONE S-TRANSFERASE TAU 9 (GSTU9)	Encodes glutathione transferase belonging to the tau class of GSTs. Naming convention according to Wagner et al. (2002).	SUC2
	AT5G24860	FLOWERING PROMOTING FACTOR 1 (FPF1)	encodes a small protein of 12.6 kDa that regulates flowering and is involved in gibberellin signalling pathway. It is expressed in apical meristems immediately after the photoperiodic induction of flowering.	C
	AT5G45630		senescence regulator (Protein of unknown function, DUF584)	SUC2, Z, R

Day	Locus Identifier	Symbol	Gene Description - Araport11	Bound
5	AT5G15120	PLANT CYSTEINE OXIDASE 1 (PCO1)	2-aminoethanethiol dioxygenase, putative (DUF1637)	Z
	AT1G29660		GDSL-motif esterase/acyltransferase/lipase. Enzyme group with broad substrate specificity that may catalyze acyltransfer or hydrolase reactions with lipid and non-lipid substrates	SUC2
	AT5G61850	LEAFY (LFY)	Encodes transcriptional regulator that promotes the transition to flowering.Involved in floral meristem development.	SUC2, R, Z
	AT4G35030		Protein kinase superfamily protein	C
	AT3G07340	CRY2-INTERACTING BHLH 3 (CIB3)	basic helix-loop-helix (bHLH) DNA-binding superfamily protein	Z
	AT5G62165	AGAMOUS-LIKE 42 (AGL42)	Encodes a MADS box transcription factor. Expressed in quiescent center. Involved in floral transition.	R, Z
	AT3G21870	cyclin p2	CYCLIN P2;1 (CYCP2;1)	SUC2, R, Z
	AT1G66783	MICRORNA157A (MIR157A)	Encodes a microRNA that targets several SPL family members, including SPL3,4, and 5. By regulating the expression of SPL3 (and probably also SPL4 and SPL5), this microRNA regulates vegetative phase change.	Z
	AT3G56290		potassium transporter	Z
	AT1G07180	ALTERNATIVE NAD(P)H DEHYDROGENASE 1 (NDA1)	nternal NAD(P)H dehydrogenase in mitochondria.	Z
	AT1G10070	BRANCHED-CHAIN AMINO ACID TRANSAMINASE 2 (BCAT-2)	Encodes a chloroplast branched-chain amino acid aminotransferase. Complements the yeast leu/iso-leu/val auxotrophy mutant. Involved in cell wall development.	R
	AT4G11370	RING-H2 FINGER A1A (RHA1A)	Encodes a putative RING-H2 finger protein RHA1a	SUC2, Z
	AT3G27250	(AITR1)	ABA-induced transcription repressor that acts as feedback regulator in ABA signalling	SUC2, Z
	AT5G64780		holocarboxylase synthetase	Z
	AT3G12833		hypothetical protein	Z
	AT5G24860	FLOWERING PROMOTING FACTOR 1 (FPF1)	encodes a small protein of 12.6 kDa that regulates flowering and is involved in gibberellin signalling pathway. It is expressed in apical meristems immediately after the photoperiodic induction of flowering.	C
	AT5G15800	SEPALLATA1 (SEP1)	Encodes a MADS box transcription factor involved flower and ovule development. Functionally redundant with SEP2 and SEP3	SUC2, C, R
	AT5G66700	HOMEOBOX 53 (HB53)	Encodes a homeodomain protein. Member of HD-ZIP 1 family, most closely related to HB5. AtHB53 is auxin-inducible and its induction is inhibited by cytokinin, especially in roots therefore may be involved in root development	SUC2, C, R, Z
	AT5G45630		senescence regulator (Protein of unknown function, DUF584)	SUC2, R, Z
	AT4G04330	HOMOLOGUE OF CYANOBACTERIAL RBCX 1 (RbcX1)	Encodes a chloroplast thylakoid localized RbcX protein that acts as a chaperone in the folding of Rubisco	SUC2

Supplementary Table 2.1. List of genes specifically altered in expression in response to DEX treatment in *FD::GR:FD #19* plants.

Summary of selected genes after FD induction at day 12. The list includes genes from day 1 to day 5 after the DEX treatment. Locus identifiers shaded in light orange are of interest. ChIP-seq identified genes bound by VENUS:FD (Romera Branchat et al., 2020; referred to as “R” in the legend), GFP:FD from the *FD* promoter or *SUC2* promoter (Collani et al., 2019; annotated “C” and “SUC2”, respectively) and GFP:FD from the *FD* promoter (Zhu et al., 2020; annotated “Z”).

Chapter 3. Transcriptional regulation of *FRUITFULL* by FD and SPL15 transcription factors

3.1 Introduction

In the annual Arabidopsis plant, the vegetative-to-reproductive transition is promoted by long day lengths. To ensure the production of seeds, parallel pathways promote flowering in different daylength conditions. The photoperiodic pathway involving FT/FD promotes flowering in LD, whereas delayed flowering under SD is notably promoted by the ageing pathway and SPL15 accumulation at the SAM (Abe et al., 2005; Wigge et al., 2005; Hyun et al., 2016). Although the genetic strategy for flowering differs, common targets are similarly regulated before the floral transition. For instance, the increase in *FUL* mRNA observed in wild-type towards the floral transition is delayed in both *fd* and *spl15* mutants under LD and SD, respectively. Hence, the late-flowering phenotype of the *fd* and *spl15* mutants is similar but more severe than that of the *ful* mutant, which is slightly late flowering under LD and SD conditions (Ferrandiz et al., 2000; Melzer et al., 2008). The *FUL* gene encodes a MADS-domain transcription factor that is not only involved in the floral transition but also in branch and stem architecture, cauline leaf shape, silique size, and meristem arrest after fruit production (Gu et al., 1998; Ferrandiz et al., 2000; Bemer et al., 2017; Balanzà et al., 2018). In Arabidopsis, *FUL* is transcribed and translated at the SAM under LD and SD conditions (Mandel and Yanofsky, 1995; Gu et al., 1998; Urbanus et al., 2009; Hyun et al., 2016). The transcription factors SPL15 and FD are observed in the nuclei of cells in the SAM (Hyun et al., 2016; Romera-Branchat et al., 2020) in similar places and times as the FUL protein, which suggests that they potentially transcriptionally regulate *FUL*.

Initial evidence that FD might directly regulate *FUL* transcription came from the demonstration of binding of FD to the *FUL* genomic region in the *35S::FD* line, in which the heterologous promoter from cauliflower mosaic virus (*CaMV 35S*) is fused to the CDS of *FD* (Jung et al., 2012; Jung et al., 2016). Binding to *FUL* in this line was detected based on enrichment by ChIP-qPCR. Recently, genome-wide analysis by ChIP-seq data from the transgenic lines *SUC2::GFP:FD* in Col-0 and *ft tsf* genetic backgrounds and *FD::GFP:FD* in *fd* confirmed the binding of FD to the *FUL* promoter (Collani et al., 2019; Zhu et al., 2020). However, the precise motif(s) that are bound by FD to promote *FUL* transcription are unknown. In parallel, the SPL15 transcription factor is a major activator of *FUL* transcription under SD conditions by directly binding to the DNA promoter (Hyun et al., 2016). Four SPL-bound motifs at two loci are probably bound by SPL15 to regulate the *FUL* promoter.

Thus, the control of *FUL* expression is considered to be a point of intersection between the LD and SD pathways via direct regulation by FD and SPL15, respectively, and

FUL a relevant gene to understand how these pathways interact. In this chapter, I aim to identify the binding sites of FD at the *FUL* promoter and how they relate functionally to the SPL15-binding sites involved in the floral transition.

3.2 Results

3.2.1 Floral transition coincides with an increase in *FUL* mRNA and FUL protein

The *FUL* mRNA level increases in the SAM of plants transferred from SD to LD (Torti et al., 2012), which coincides with induction of the floral transition. To confirm the expression pattern of *FUL* mRNA in continuous LD, I first conducted RT-qPCR analysis. Expression of *FUL* increases in the wild-type between day 11 and 14 (Figure 3.1A). These time points represent the approximate timing of the floral transition in these conditions. The maximum of *FUL* expression is reached at day 20 in both wild-type and transgenic *35S::FD* plants (Romera-Branchat et al., 2020). No increase in *FUL* expression was detected in the *fd-3* mutant in this time-course analysis. The result underlies the role of FD in *FUL* transcriptional activation under LD. Next, to observe FUL protein at the SAM, I used a transgenic line generated by Dr. A. van Driel and Dr. R. Martinez Gallego (A. van Driel PhD thesis, 2020). The DNA construct *FUL::FUL:9AVENUS* contains the entire *FUL* locus fused to the VENUS fluorophore. The exogenous DNA was transformed into *ful-2* and was then crossed to *fd-3* (A. van Driel PhD thesis, 2020). The selected rescue line *FUL::FUL:9AVENUS F9.1 ful-2* (referred to as *F9.1*) over-complemented the *ful-2* late-flowering phenotype and under LD flowered slightly earlier than wild type (A. van Driel PhD thesis, 2020).

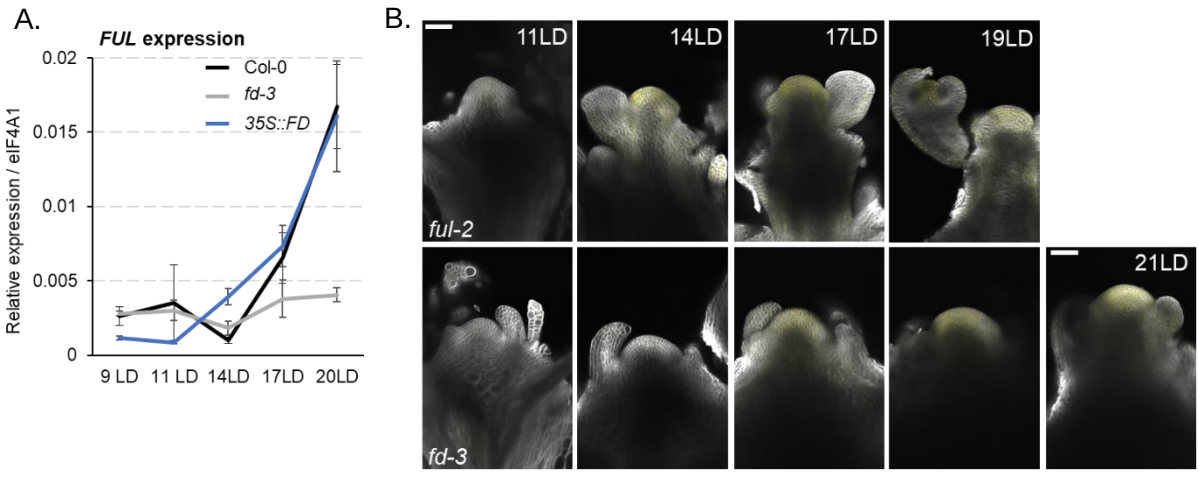

Figure 3.1. FD promotes the accumulation of *FUL* transcripts and FUL protein at the SAM under LD.

A, *FUL* transcript accumulation in tissues enriched for apices. Expression levels were normalized to that of *EIF4A1*. Data represent the mean of three technical replicates from a single biological replicate under LD conditions at the indicated time points. **B**, Apices of *FUL::FUL:9AVENUS* grown under LD to detect VENUS fluorescence in the *ful-2* or *fd-3*

backgrounds (upper and lower panel, respectively). The scalebar in the 11 LD *ful-2* panel represents 50 µm and applies to all other images if not indicated differently.

In this experiment, the rescue line *F9.1* initiates floral primordium formation between 11 and 14 LD (Figure 3.1B). This timing coincides well with the transition observed with the increase in *FUL* mRNA in wild-type from day 11 (Figure 3.1A). At day 14, FUL:VENUS first accumulates at the SAM of *ful-2*. The fluorescent VENUS signal seems stronger in the apical region of the meristem. The signal rather spreads evenly across cells with some presence in few nuclei of meristem cells at this stage, although in flowers and mature inflorescence meristems at 19 LD it is clearly nuclear. FUL:VENUS is also visible in the stem vasculature as previously described for the *FUL* mRNA (Mandel and Yanofsky, 1995; Hyun et al., 2016). The FUL:VENUS signal is absent from the young flower primordia but reappears at approximately stage 4 (in 19 LD sample) as previously described (Mandel and Yanofsky, 1995). The accumulation of FUL:VENUS protein in *fd-3* is delayed at the SAM by around 3-5 days (Figure 3.1B). The first flower primordia are detected at day 21 and this coincides with the *fd-3* late-flowering phenotype. FUL:VENUS may be present at the SAM for longer prior to floral development in *fd-3* than in Col-0, it first appears in *fd-3* at day 17 whereas the first floral bud appears at day 21, while in *ful-2* it appears after day 11 and the first floral bud is present at day 14. Therefore, the *fd-3* mutation may both delay *FUL* expression and delay events after *FUL* expression but before floral development. The FUL:VENUS protein accumulates at the apical region of the mature inflorescence meristem at day 21 as well as in the vasculature, which is similar to the pattern of protein expression in the inflorescence meristem of *ful-2* mutant.

Taken together, the results underlie the importance of FD to promote the increase in *FUL* mRNA and FUL protein at the SAM under LD conditions for proper floral induction.

3.2.2 Conservation of *FUL* among *Brassicaceae* species and physical evidence of FD binding at the *FUL* proximal promoter

FD belongs to the bZIP transcription factor family and binds to G-boxes (CACGTG), C-boxes (GACGTC) and A-boxes (TACGTA; Jakoby et al., 2002; Dröge-Laser et al., 2018). Genome-wide datasets confirmed a high preference for FD protein to recognize G- boxes *in vivo* (Collani et al., 2019; Romera-Branchat et al., 2020; Zhu et al., 2020). Previous studies have proposed *in vivo* and *in vitro* assays to elucidate the precise binding of FD to its targets involved in floral primordium identity, such as *AP1* and *SEP3* (Benlloch et al., 2011; Jung et al., 2016; Collani et al., 2019). Furthermore, phosphorylation of the FD protein may lead to the recognition of different *cis*-regulatory motifs within a single promoter (Kawamoto et al., 2015; Collani et al., 2019). However, these assays failed to confirm FD binding to specific

sites by mutagenesis *in planta* (Benlloch et al., 2011). Thus, there is a lack of information concerning the significance of binding of FD to its targets involved in the floral transition. In the previous section, I used a fluorescent protein marker to demonstrate the role of FD in the transcription of *FUL* at early stages of the floral transition (Figure 3.1). To identify FD binding site(s) at the *FUL* promoter, I first carried out *in silico* analysis of the promoter locus. Genome-wide analysis of VENUS:FD by ChIP-seq suggested that FD binds to its DNA targets by recognising one or two closely spaced motifs within each enrichment peak (Figure 3.2A; Romera-Branchat et al., 2020). One ChIP-seq replicate of this published data identified *FUL* as a target of VENUS:FD in inflorescence tissues, consistent with other ChIP-seq experiments (Collani et al., 2019; Zhu et al., 2020). Using this information, the reads from VENUS:FD were displayed with the IGB view to demonstrate the enrichment peak at the *FUL* promoter (Figure 3.2B). The peak maximum is 115 bp upstream of the TSS. Because bZIP transcription factors such as FD recognise A-, C- or G-boxes, I searched for these motifs, but none were present within the peak region. However, two ACGT cores that are non-canonical bZIP binding sites were detected within the *FUL* enrichment peak (Figure 3.2C). These cores are known as ACGT-containing elements (ACE; Hartmann et al., 2005). The two ACEs are located about 200 bp upstream of the *FUL* TSS and were named *B1* and *B2*. Consistent with this, ChIP-seq of FD:GFP expressed from *SUC2* and *FD* promoters display peak centres at 240 and 220 bp upstream of *FUL* TSS, respectively (Collani et al., 2019). Next, the *AtFUL* locus was aligned with that of a diverse group of nine *Brassicaceae* species to detect highly conserved regulatory regions (Figure 3.3). The genomic locus of *FUL* in *Arabis lyrata* is most similar to that of *AtFUL*, and *A. lyrata* is also the closest relative species to *Arabidopsis thaliana* from this list (Kiefer et al., 2019). The 5′ UTR, as well as the first and last exons, are highly similar among the nine species. In addition, five conserved blocks were present in the *FUL* promoter (Figure 3.3). The second and the fifth conserved blocks contain the well-characterised G-box and the two ACEs *B1* and *B2*, respectively.

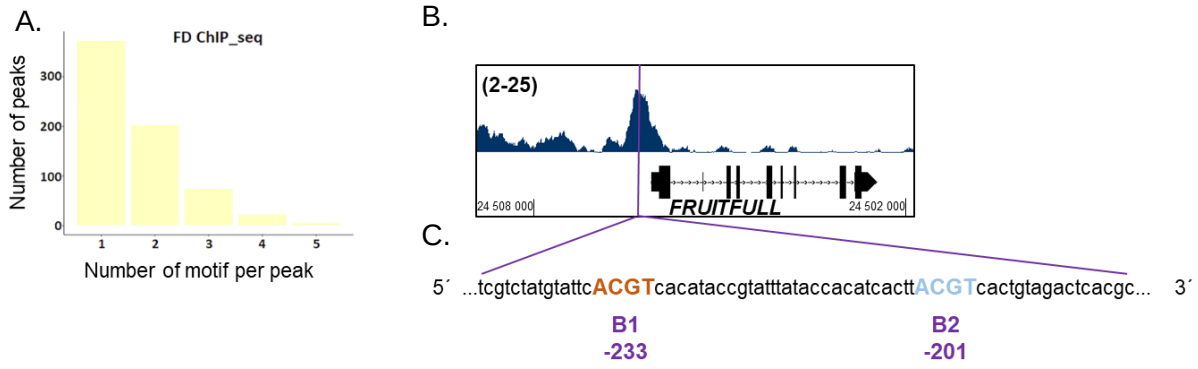

Figure 3.2. FD potentially binds two motifs near the transcription start site of *FUL*. **A**, Number of predicted FD-binding motifs for each peak from genome-wide ChIP-seq data for *FD::VENUS:FD* inflorescences. **B**, ChIP-seq of *FD::V:FD* in the *fd-3* background shows an enrichment of sequence reads at the *FUL* promoter, visualized by the Integrated Genome

Browser (IGB). The vertical purple line indicates the centre of the enriched VENUS:FD peak at 115 bp upstream of the *FUL* start codon. **C**, Partial sequence from 5′ to 3′ of the *FUL* promoter to illustrate the identified *B1* and *B2* motifs. The sequence is located about 200 bp upstream of the transcription start site of *FUL*.

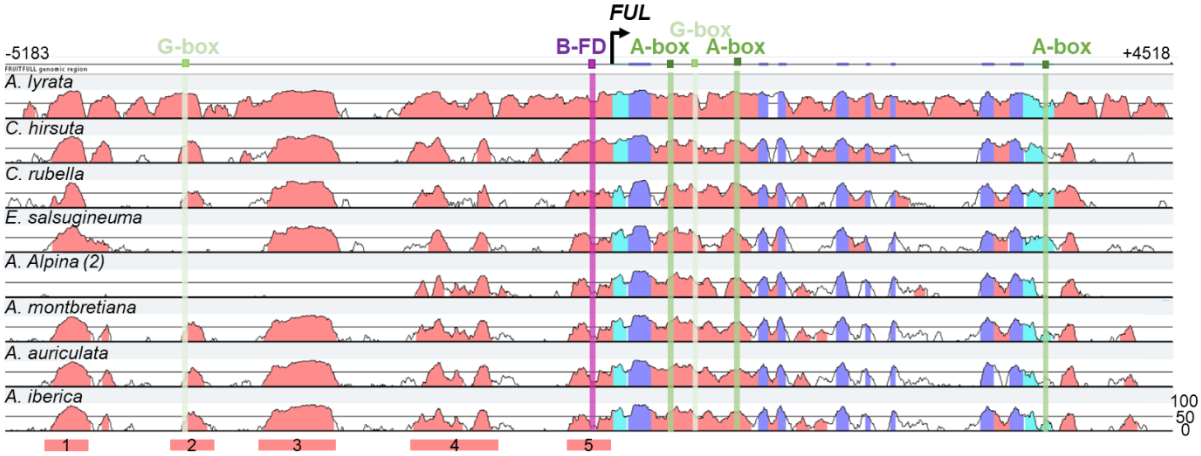

Figure 3.3 The *FUL* genomic locus is conserved within the *Brassicaceae* family.
An mVISTA alignment of the *Arabidopsis thaliana FUL* genomic locus with that from nine *Brassicaceae* species. The black arrow represents the transcription start site of the *FUL* coding sequence (CDS). The cyan-coloured peaks represent untranslated regions, the purple-coloured peaks represent introns within the CDS. The salmon-coloured peaks indicate greater than 50% sequence identity to the *AtFUL* locus for each species. 50% identity is also represented by the central light-grey horizontal lines. The bottom line for each species indicates no identity and the upper grey line indicates 100% identity. Canonical G- and A-boxes are indicated in light green and green, respectively. The putative FD-binding sites covered by the ChIP-seq peak are highlighted in purple (*B-FD*). The five highly conserved regions of the *FUL* promoter among the *Brassicaceae* species are indicated by horizontal salmon-coloured bars beneath the alignment, and were added manually.

For better resolution, nucleotide alignment using Fast Fourier Transform (MAFFT) with Multiple Alignment of the *B1* and *B2* region revealed complete conservation of the core of the *B2* site among the nine species (Figure 3.4A). The five least-related species do not contain *B1*, but have a 14-nucleotide indel between *B1* and *B2* sites, which is absent in *Arabidopsis thaliana*. This short sequence includes a duplication of the *B2* site (Figure 3.4A). This alignment suggests that *B2* and a second motif, either *B1* or the duplicated version of *B2*, are evolutionarily important for *FUL* regulation.

A previous report showed a high binding of FD when expressed from the *35S* promoter to the beginning of the first exon of *FUL* and also before the TSS (Jung et al., 2016). This latter site does not contain the *B1* and *B2* motifs; therefore, the ability of FD to bind *in vivo* at *B1* and *B2* sites was tested by ChIP-qPCR. For this experiment, I used the complemented *FD::VENUS:FD* line in *fd-3* that was used for ChIP-seq experiments (Romera-Branchat et al., 2020). The *B-FD* amplicon includes the *B1* and *B2* motifs. Tissues enriched for 16-day-old

apices revealed a higher percentage of input of VENUS:FD associated with the putative *B-FD* binding site compared with the internal *ACTIN2* (*ACT2*) control. No differences in percentage of input of VENUS:FD to *B-FD* were detected in the *35S::GFP:YFP* control line or in the inflorescence tissues (Figure 3.4B). This supports that FD binds to the *FUL* promoter at the *B-FD* site through the *B1* and *B2* motifs, and is consistent with the other ChiP-seqs (Collani et al., 2019).

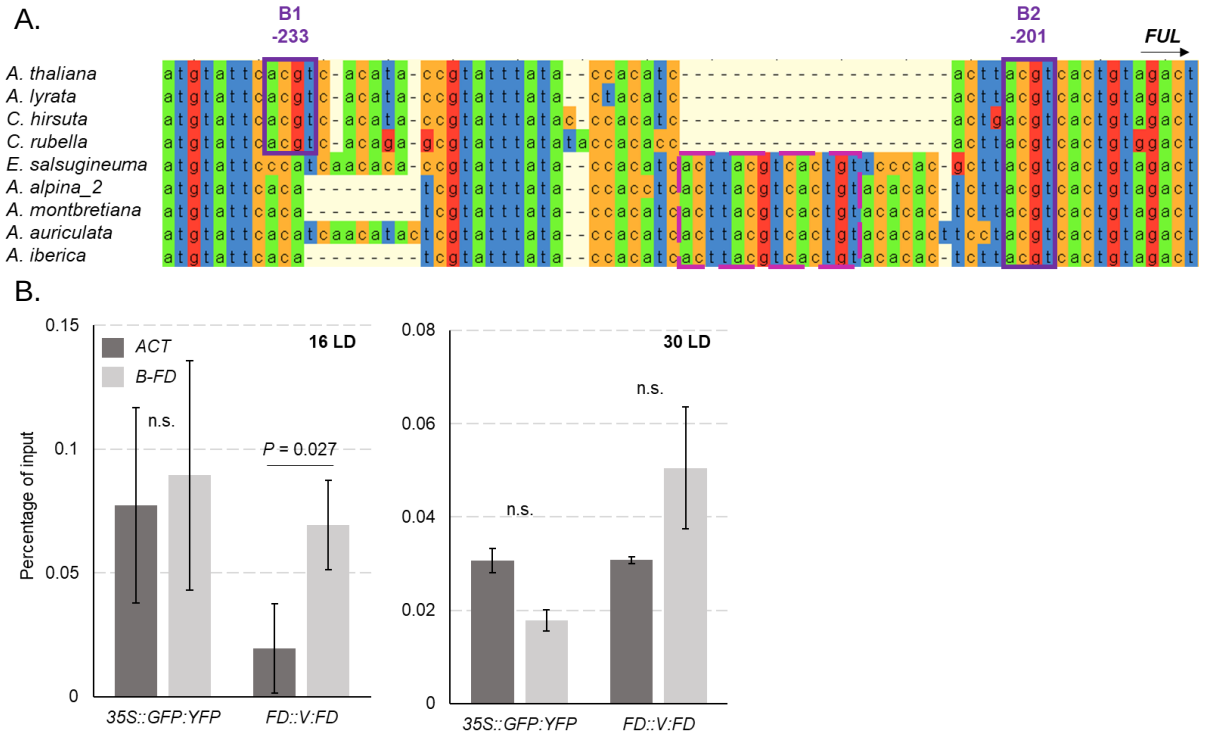

Figure 3.4. The bZIP transcription factor FD binds to the *B-FD* region within the *FUL* promoter.

A, Nucleotide sequences of the *FUL* promoter in nine Brassicaceae species show two ACGT-containing element motifs (*B1* and *B2*) that are potentially bound by FD upstream of the transcription start site. **B**, ChIP-qPCR of *FD::VENUS:FD* and *35S::GFP:YFP* transgenic lines. The percentage of the input is based on three biological replicates for VENUS:FD and four biological replicates for GFP:YFP at 16 LD, and two biological replicates for 30-day old inflorescence tissues. The anti-GFP antibody from abcam (ab290) was used to detect GFP and VENUS. *ACTIN2* was used as an internal control. Amplicon *B-FD* covers the two putative FD-binding sites. Percentage of input is represented by the mean ±SD (two-tailed Student's *t*-test).

Taken together, *in silico* and *in vivo* analysis strongly support the binding of FD at this newly identified and conserved region in the *FUL* promoter. Therefore, the *B1* and *B2* motifs are putative binding sites for the bZIP FD transcription factor.

3.2.3 Mutation of *cis*-regulatory elements to study the effect of FD in *FUL* regulation

Two putative FD-binding sites in the *FUL* promoter were detected by ChIP-seq and sequence comparisons, and the region containing these ACEs was confirmed to bind FD by

ChIP-qPCR assays (Figure 3.4B). To test the regulatory role of these sites in the floral transition, the two ACEs were modified for *in planta* experiments. The DNA construct *FUL::FUL:9AVENUS* containing the entire *FUL* locus was used as a template (A. van Driel PhD thesis, 2020). The *B1* and *B2* motifs were mutated by PIPE-cloning (Klock and Lesley, 2009), resulting in *m1* and *m2*, respectively (Figure 3.5A). The *FULm1m2::FUL:9AVENUS* construct was transformed into *ful-2* (Figure 3.5B, referred as *m1m2*). The four putative binding sites for SPL were mutated by Dr. A. van Driel to create the *FULmGTAC::FUL:9AVENUS* transgenic lines. One representative transformant was selected and used for this thesis (Figure 3.5B, referred as *mGTAC* lines and transformant *S2.5*). Mutation of the two putative FD binding sites in the existing *mGTAC* DNA construct resulted in the *FULm1m2+mGTAC::FUL:9AVENUS* transgenic lines (Figure 3.5B, referred to as *m1m2+mGTAC*). After three generations and on the basis of transgene segregation, I selected four homozygous *FULm1m2::FUL:9AVENUS* and six *FULm1m2+mGTAC::FUL:9AVENUS* transgenic lines in the *ful-2* background.

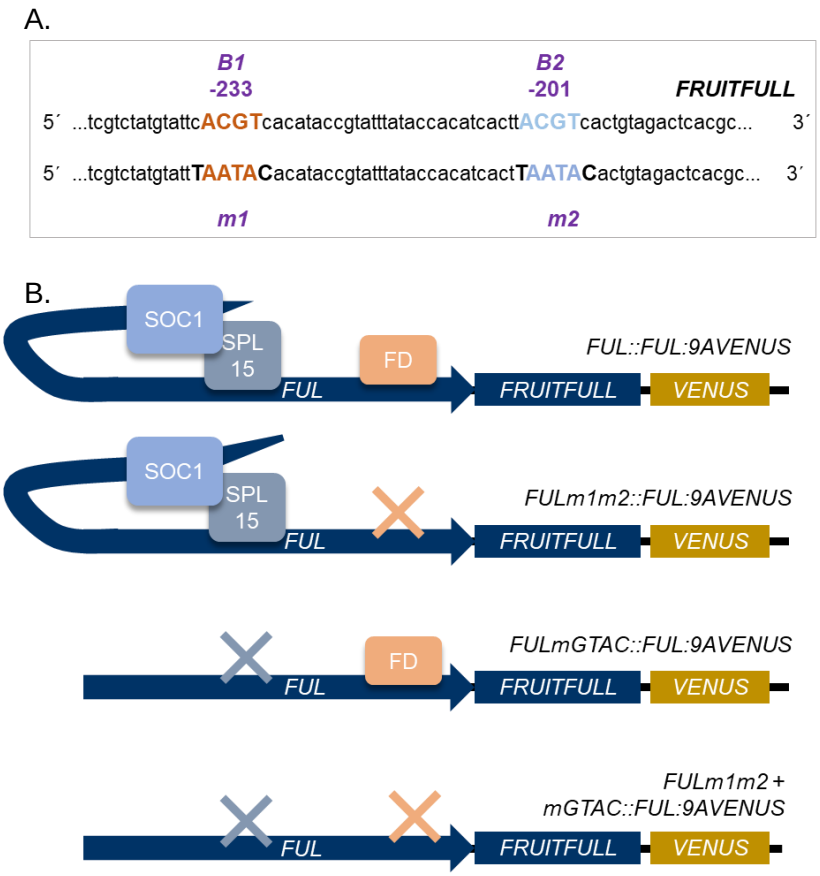

Figure 3.5. Mutagenesis of putative FD-binding sites and SPL-binding sites in the *FUL* promoter by PIPE-cloning.
A, The *B1* and *B2* sites were mutated together with their flanking nucleotides and is predicted to abolish FD recognition and binding. The PIPE-cloning technique was used to modify the nucleotide sequences of the *FUL::FUL:9AVENUS* construct. **B**, Schematic representation of the four transgenic constructs transformed into the *ful-2* background. Constructs two and four were generated in this study.

To describe bias in the level of gene expression caused by random insertion of the T-DNA, *FUL* expression was analysed in the flowers at anthesis-stages, where the FD binding sites are not expected to affect gene expression. As previously described, the complementation line *F9.1* and the *S2.5* transgenic plants had a similar level of *FUL* mRNA in these flowers to that of the wild-type (A. van Driel PhD thesis, 2020, Figure 3.6A). The lines *m1m2 #25*, *#40*

and *m1m2+mGTAC #10* and *#20* exhibited a high level of *FUL* mRNA, whereas *m1m2 #3*, *#27* and *m1m2+mGTAC #1, 2, 13* and *#23* had a similar level of *FUL* mRNA to that of the complementation line *F9.1* and the Col-0. The *ful-2* mutant exhibits round cauline leaves and short siliques compared with the wild-type (Gu et al., 1998; Ferrandiz et al., 2000). To our knowledge, neither mutation of *SPL15* nor *FD* leads to this phenotype. To further select the candidate lines, phenotypic analyses of cauline leaf shape and silique length were performed. Photographs of the first cauline leaf showed that *F9.1*, as well as *m1m2 #27* and *#40* and *m1m2+mGTAC #1*, *2* and *20* rescued the leaf phenotype (Supplementary Figure 3.1). Next, siliques of these plants were measured with a ruler (Figure 3.6B). All the lines rescued the silique length phenotype of the *ful-2* mutant. The *m1m2 #25* line showed the longest mean silique length, and had a high expression of *FUL* in the flowers (Figure 3.6A). On the basis of these results, I selected *m1m2 #3* and *#27* and *m1m2+mGTAC #1*, *2* and *13* for further experiments.

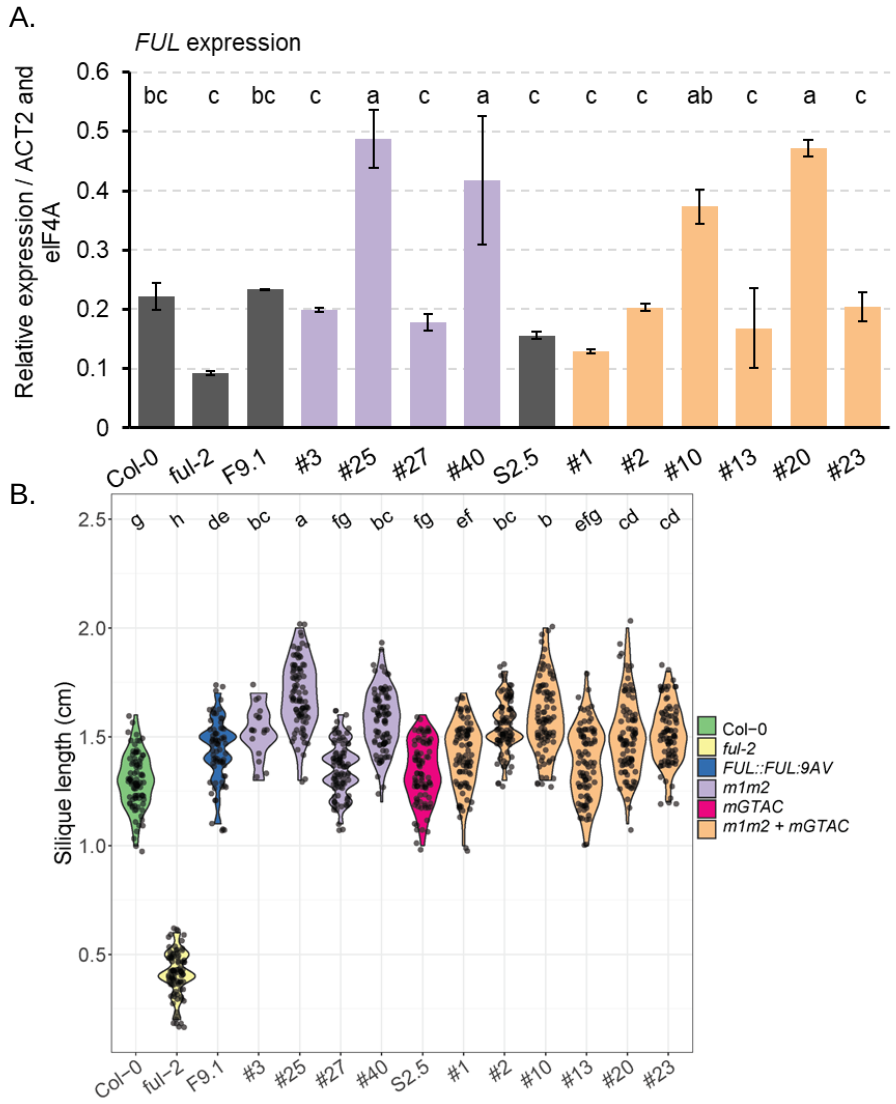

Figure 3.6. Complementation of the *FUL* mutagenesis lines.
A, Real-time qPCR to quantify *FUL* mRNA levels in apices of plants grown under LD at two weeks after bolting. Two biological replicates of flowers at the anthesis-stage were harvested

for analysis. Relative expression is represented by the mean ±SD (ANOVA, Tukey's HSD test). **B**, Silique lengths of plants grown under LD. Width is proportional to the number of individuals for the same values and extremities represent minimum and maximum values for each genotype; *n* = 15 - 80 (ANOVA, Tukey's HSD test).

Detailed analysis of the generated *FULm* transgenic lines allowed the selection of representative homozygous individual lines with which to further study flowering traits in the absence of the two ACE motifs in the *FUL* promoter.

3.2.4 Assessing the function of FD-binding sites within the *FUL* promoter during the floral transition under LD

Mutation of two identified ACE motifs in the *FUL* genomic promoter may prevent the binding of FD to these sites and further delay FUL accumulation. To test the regulatory function of FD, the *FULm* lines were first scored for flowering time under LD. The *F9.1* control line overcomplemented the *ful-2* mutation and had fewer leaves at bolting than the wild type, despite a similar *FUL* expression in flowers (A. van Driel PhD thesis, 2020). Although variation was observed, the four *m1m2* lines displayed no consistent or statistically significant differences in flowering time as measured by total leaf number compared with that of the *F9.1* control line (Figure 3.7A). Previously, the disruption of SPL-binding sites (*i.e. mGTAC* lines) was shown to lead to an early-flowering phenotype (A. van Driel PhD thesis, 2020; Supplementary Figure 3.2). In this experiment, no significant early-flowering phenotype was detected. The *m1m2+mGTAC* transgenic lines showed a similar flowering-time phenotype to that of the *S2.5* line. Four out of six transgenic *m1m2+GTAC* lines were statistically significantly earlier flowering than the *F9.1* line. The *ful-2* mutant produces more cauline leaves than Col-0, and all transgenic lines complemented this phenotype (Figure 3.7B). Disruption of FD binding to *B-FD* sites had little effect on the flowering time under LD, irrespective of exogenous *FUL* mRNA levels in flowers (Figure 3.6A). To test whether the disruption of FD binding affects FUL protein accumulation, confocal microscopy was used to image the floral transition of the *FULm* transgenic lines. The VENUS signal was first detected in *S2.5* and the two *m1m2+mGTAC* lines from day 11 (Figure 3.7C). The pattern and timing of FUL:VENUS accumulation in the two *m1m2* lines was similar to that of *F9.1*, with visible signal only appearing at day 14. Floral primordia were observed in *F9.1* at day 14, consistent with previous observations (Figure 3.1B). Although no statistically significant differences were observed in flowering time (Figure 3.7A), the *S2.5* and *mGTAC+m1m2* lines were clearly advanced in development in this time-course series. Elongation of the stem was visible below the SAM in these lines at day 14, indicating slightly earlier bolting than the *F9.1* line (Figure 3.7C).

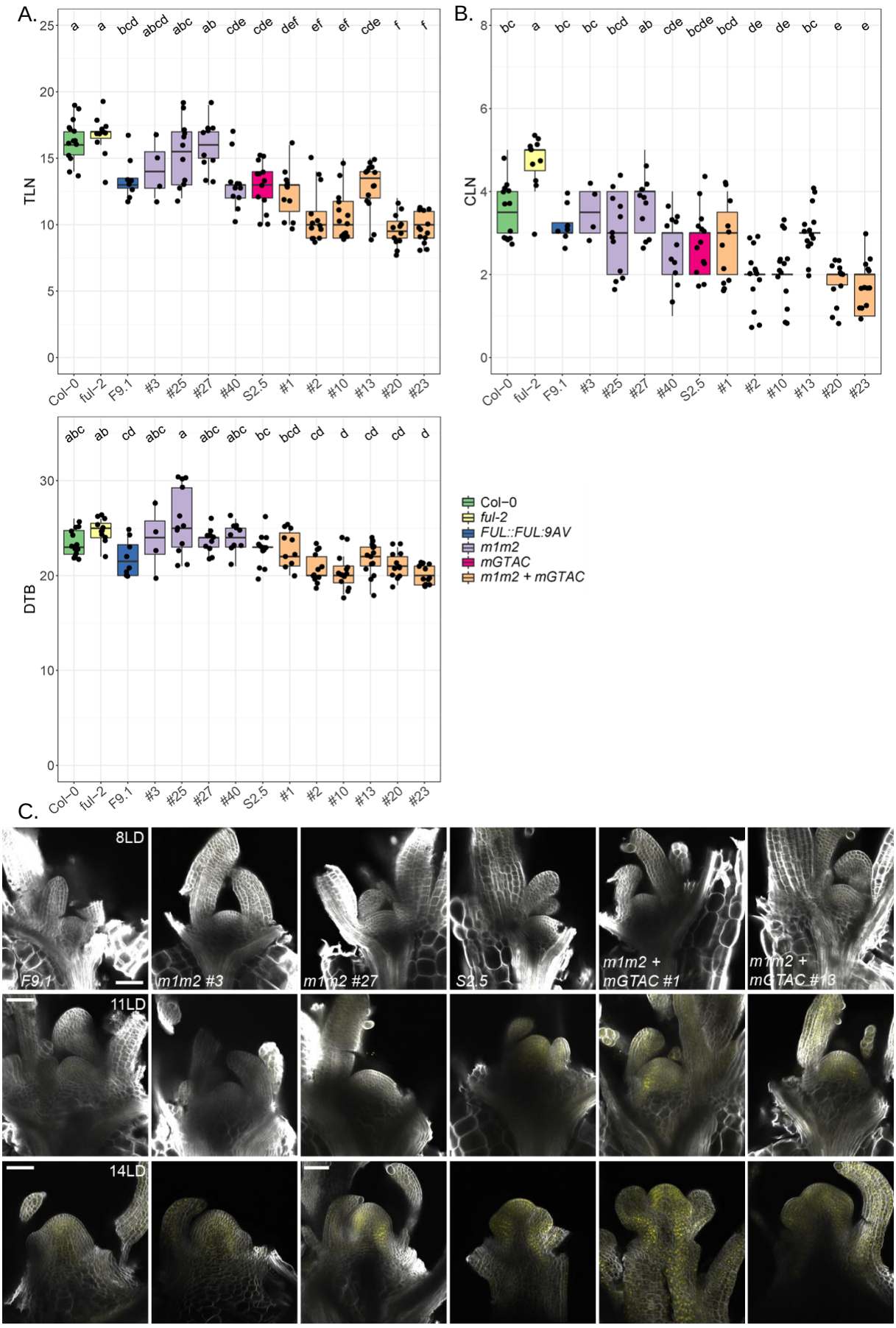

Figure 3.7. Disruption of FD binding sites *B1* and *B2* does not affect flowering time under LD.

A, Flowering time of *FUL::FUL:VENUS* transgenic lines under LD represented as total leaf number (TLN), or days to 1 cm bolting (DTB) and **B**, cauline leaf number (CLN) on the main shoot. Box-plot medians is indicated by the centre line and were used for ANOVA followed by Tukey's HSD test. **C**, Analysis of the *FUL::FUL:VENUS* along a time course in LD conditions. FUL:VENUS was expressed from wild-type and mutant promoters to test the role of *cis*-regulatory elements. The meristem samples were fixed in PFA and cleared with Clearsee. The scalebar on the left represents 50 µm and applies to all other images or the row if not indicated otherwise.

The combination of flowering time and confocal imaging data showed that the loss of the putative FD binding sites had no detectable effect on expression of FUL:VENUS, and therefore a much weaker effect than the loss of FD function in the *fd-3* mutant (Figure 3.1). Similarly, mutation of the SPL-binding sites in the *mGTAC* line caused earlier expression of FUL:VENUS, as previously described (A. van Driel PhD thesis, 2020), but no compensation effect on flowering or FUL:VENUS expression was detected by the loss of the putative FD binding sites in the same promoter. Taken together these results suggest that FD mainly activates *FUL* expression indirectly during floral transition, or that it can also bind to additional sites in the *FUL* gene that are still present in the mutant promoter.

3.2.5 The putative FD-binding sites do not contribute to *FUL* regulation under non-inductive conditions

Mutation of *FUL* in *Arabidopsis thaliana* leads to a late-flowering phenotype under SD conditions (Torti et al., 2012). The late flowering of *spl15* is partially caused by a delay in *FUL* accumulation (Hyun et al., 2016). Although *FD* mRNA is present at the SAM under SD, no flowering-time phenotype was observed in the *fd* mutant under these conditions (Wigge et al., 2005; Jang et al., 2009). A flowering-time experiment was conducted to test whether the disruption of either or both of the proposed FD and SPL binding sites affected *FUL* regulation under SD and thus the floral transition. Under non-inductive conditions, the line *F9.1* and Col-0 bolted at the same time, whereas the bolting of *ful-2* was delayed (Figure 3.8A). No difference in leaf number or bolting time was observed between the *S2.5* and the *F9.1* plants. The two *m1m2* lines were slightly late flowering under SD, but much earlier flowering than the *ful-2* control. Only the line *#27* showed a statistically significant difference in flowering time compared with the *F9.1* line, with a total of 55 and 49 leaves, respectively. The line *#27* was also the strongest late flowering under LD (Figure 3.7A). The *m1m2+mGTAC* lines show similar flowering behaviour compared with the *S2.5* control line (Figure 3.8A). Bolting and total leaf number of *m1m2+mGTAC #13* was lower than that of the two other *m1m2+mGTAC* lines and most closely resembled values for *S2.5* (Figure 3.8A and C). The *ful-2* has the greatest number of cauline leaves among all the genotypes (Figure 3.8B). Although most of

the transgenic lines had similar numbers of cauline leaves to that of the *F9.1* control line, only the *m1m2+mGTAC #2* had more cauline leaves than its control *S2.5* (Figure 3.8B).

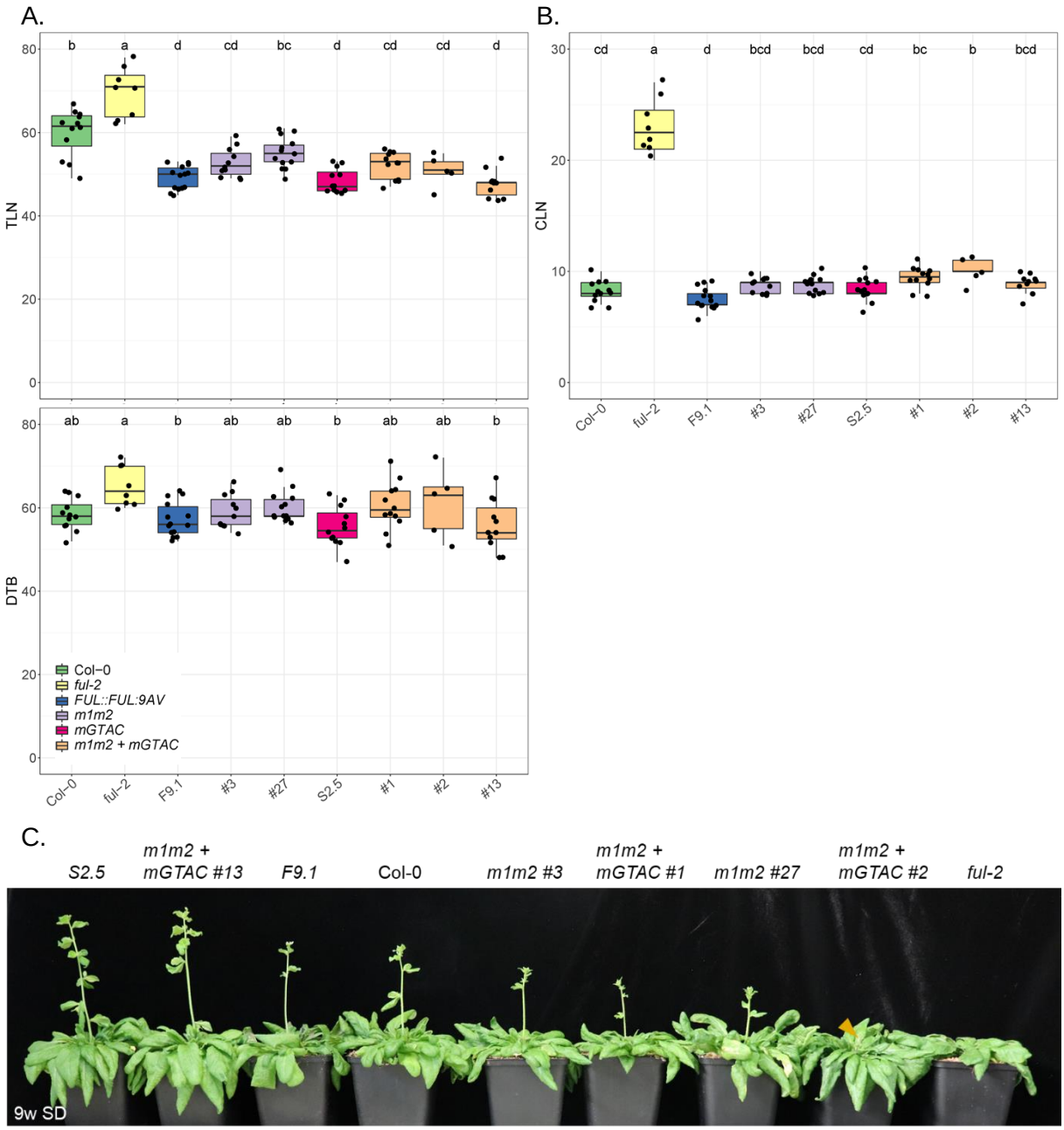

Figure 3.8. Mutation of *B1* and *B2* sites within the *FUL* promoter has a minor effect on flowering time under SD.

A, Flowering time of *FUL::FUL:VENUS* transgenic lines under SD represented by total leaf number (TLN) or days to 1 cm bolting (DTB) and **B**, cauline leaf number (CLN) on the main shoot. Box-plot medians is indicated by the centre line and were used for ANOVA followed by Tukey's HSD test. n = 5 – 14 individuals. **C**, The phenotype of one representative plant from each genotype grown for 9 weeks under SD.

To understand how the FUL protein accumulates at the SAM under SD, I imaged meristems along a time-course using confocal microscopy. In general, only few cells expressed FUL:VENUS from 3wSD and this expression might represent background fluorescence

(Figure 3.9). Clear accumulation of FUL:VENUS was visible from 5wSD at the SAM as well as in the leaf primordia of *mGTAC S2.5* and *m1m2+mGTAC #1.* At 6wSD, FUL:VENUS was visible in all transgenic lines. The pattern of accumulation was similar to that in the SAM under LD (Figure 3.7). At 6wSD, the lines *S2.5*, *FULm1m2+mGTAC #1* and *#13* developed flower primordia. Floral primordia were observed one week later in lines *F9.1* and *m1m2 #1.* In this image series, the meristems of *m1m2+mGTAC #1* plants were developmentally more advanced than those of *m1m2+mGTAC #13* and were more similar to those of *S2.5*. This differs from the flowering-time data (Figure 3.8) and potentially represents variation among independent experiments or individual plants. Moreover, *FUL* is transcribed earlier in the *mGTAC* transgenic lines, but the flowering time of these lines was not different to that of the *F9.1* or *m1m2* transgenic lines. This indicates that the accumulation of FUL protein at the SAM at an earlier time point under SD is not sufficient to promote the floral transition.

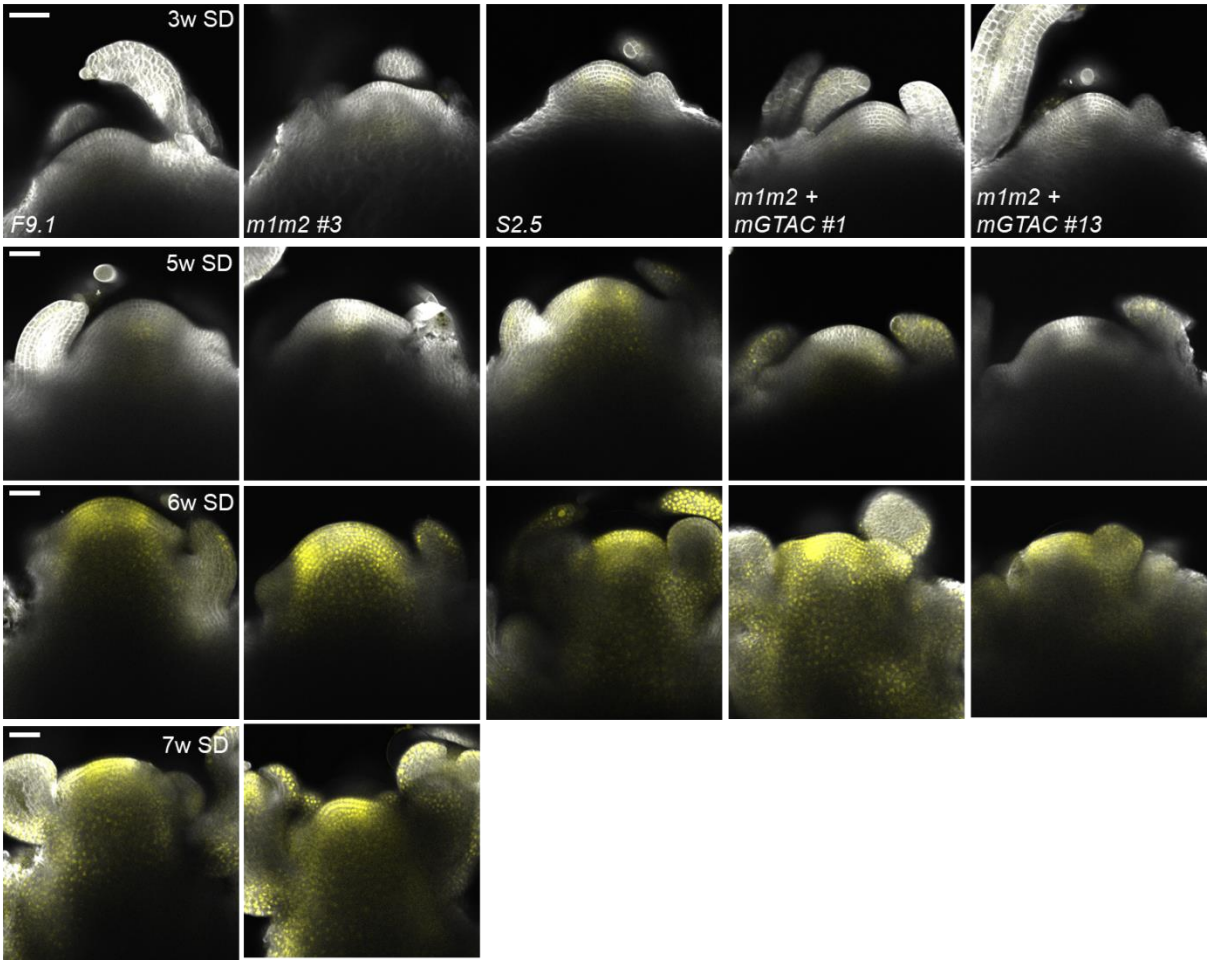

Figure 3.9. Disruption of GTAC binding sites within the *FUL* promoter leads to the early accumulation of FUL:V under SD.
Time course of apices of *FUL::FUL:VENUS* under SD conditions. FUL:VENUS was expressed from different promoters to test the role of *cis*-regulatory elements. The scalebars on the left represents 50 µm and applies to all images in the same row.

Taken together, analysis of the flowering time of the transgenic lines under SD showed no or few effects of the disruption of the putative SPL and FD binding sites in the *FUL* promoter. I suggest that FD and SPL15 do not compete at the *FUL* promoter level. As in LDs, the main effect appeared to be that mutation of the putative SPL binding site caused earlier expression of FUL:VENUS. Potentially, other *cis*-regulatory elements are bound by both transcription factors, or these sites make little contribution to *FUL* transcription, perhaps due to redundancy with the action of transcription factors binding to other sites.

3.3 Discussion

3.3.1 Binding of FD and SPLs and their interaction at the *FUL* promoter in Arabidopsis

The aim of this chapter was to test the possible FD and SPL15 direct binding to *FUL* during the floral transition, and thereby contribute to understanding *cis*-regulatory mechanisms at the *FUL* promoter. The FUL:VENUS accumulation at the SAM is delayed in the absence of FD, suggesting that FD is required for proper *FUL* activation (Figure 3.1). The *FUL* genomic locus is well conserved within the *Brassicaceae* family and my initial hypothesis based on ChIP-seq data and sequence comparisons was that FD binds to the *B-FD* region, which was confirmed by ChIP-qPCR assays (Figure 3.4B). The *B-FD* region near the TSS corresponds to a highly accessible DNA environment, and similar regions in other promoters contribute to the control of transcriptional activity (Leaf DNase-seq Score, plantdhs.org; *AT5G60910*). Within this region, the identified *B1* and *B2* sites have not been previously described and differ from the canonical A-, C- or G-boxes that are bound by bZIPs. The regions to which FD binds in the genome wide ChIP-seq analysis often contain two binding sites, suggesting that this is a common feature of FD binding (Romera-Branchat et al., 2020). However, it has been difficult to link the function of these sites to the floral transition (Figures 3.7 and 3.8). Other bZIP transcription factors may bind to these sites and promote *FUL* transcription in the absence of FD binding. Moreover, other motifs within the *FUL* promoter might act redundantly with *B1* and *B2*. In wild-type plants, weaker binding to these sites might not have been detected by ChIP-seq or ChIP-qPCR assays on FD. Because Jung et al. (2016) identified and proposed two other sites for FD binding in the *FUL* promoter and CDS, it would have been interesting to also mutate these sites to study their effect on floral transition. Moreover, the distal and conserved G-box that did not appear as a binding site based on *in vivo* ChIP data may nevertheless be crucial for promoting *FUL* transcription in a loop-fashion, as was demonstrated for SOC1 at the *FUL* promoter (Hyun et al., 2016). However, to my knowledge, no evidence exists for loop formation by FD. Detailed analysis of FD binding to *AP1* promoter was performed *in vitro* using EMSA (Collani et al., 2019). The C-box at *AP1* promoter as well as three other sites were bound by the phosphomimic version of FD. In all

these sites, FD is able to form a complex with TFL1. The super-shift formed by the binding of phosphomimic FD together with FT and 14-3-3 proteins was observed at one site, 92 bp downstream of the C-box. This site is not a canonical ACGT box but contains the nucletodies GTCGAC (Collani et al., 2019). These six nucleotides are also present in the *SEP3* promoter, but not in the *FUL* promoter. This suggests that multiple binding sites for FD exist within its target genes and that only certain loci allow formation of complexes with certain protein partners, but it is unknown which sites functionnaly regulate gene activity.
It is widely acknowledged that FD directly binds to DNA because of the presence of its bZIP domain, but a single *in vivo* study suggested that FD is recruited to the *AP1* promoter by the SPL3, 4 and 5 proteins (Jung et al., 2016). Indeed, disruption of the SPL-binding sites, but not the FD-binding site, unable transcriptional activity of *AP1* in protoplast, suggesting that FD protein alone does not promote *FUL* transcription. However, according to this logic, the disruption of SPL binding in the *mGTAC S2.5* line would prevent the recruitment of FD to DNA and probably result in late-flowering plants under LD. This phenotype was not observed in my experiments. In addition, such a scenario from Jung et al. (2016) is facilitated by the proximity of a SPL-binding motif near a bZIP-binding motif in *AP1*. Indeed, the *AP1* promoter has a *GTAC* motif to which SPL binds that is associated with a C-box, which presumably facilitates the binding of FD to DNA. The SPL3, 4 and 5 proteins interact with FD in *in vitro* pull-down assays (Jung et al., 2016), but no evidence of interaction with SPL15 has been reported. The binding region of VENUS:SPL15 identified by ChIP-qPCR is located about 450 bp upstream of the *FUL* TSS (Hyun et al., 2016). More than 200 bp separate the *B-FD* site from the two GTAC motifs, which is a much larger distance than the spacing observed in the *AP1* promoter. Thus, it is unlikely that SPL15 facilitate FD binding around the *B-FD* site.

Overall, I hypothesis either that 1) direct binding of FD at *B-FD* is not necessary for *FUL* expression and FD requires protein partners, such as SOC1, to indirectly activate *FUL* or 2) FD binds to other sites on the *FUL* promoter, or a combination of both hypotheses and 3) the *B1* and *B2* sites are not involved in the early activation of *FUL* when the SPL15 sites are mutated, suggesting no evidences for SPL15 and FD competition at the *FUL* promoter.

3.3.2 Regulatory role of the identified *cis*-regulatory elements at the *FUL* promoter under different environmental conditions

Expression of *FUL* is delayed in *spl15*, resulting in a strong late-flowering phenotype under SD and a slight delay in flowering under LD (Hyun et al., 2016). In the same study, the authors reported two potential SPL15-binding sites in the *FUL* promoter. For this reason, the *GTAC* elements recognised by SPL15 were mutated in the *FUL* promoter and the generated *mGTAC* lines revealed an early-flowering phenotype under LD compared to the control rescue line (A. van Driel PhD thesis, 2020; Supplementary Figure 3.2). This result is contrary

to the initial expectation that SPL15 binds to promote *FUL* transcription and flowering. There are 16 SPL transcription factors in Arabidopsis and all potentially bind to the same sites in the *FUL* promoter as SPL15 (Cardon et al., 1999). The early flowering caused by the *mGTAC* constructs may not be caused by the disruption of specific SPL15 binding sites, but suggests that *FUL* might be regulated by other SPLs. These proteins would have a negative regulatory role on *FUL* and flowering at early stages of development. Under SD conditions, the *mGTAC* line did not undergo floral transition earlier than the *F9.1* control line, although FUL:VENUS accumulated earlier. In addition, the morphology of the *mGTAC* and *m1m2+mGTAC* was more advanced than that of the *F9.1* and *m1m2* lines (Figure 3.9). This suggests that the early accumulation of FUL is not sufficient to promote the floral transition under SD.

An early study showed no signal of *FUL* mRNA in young flowers and is consistent with the FUL:VENUS pattern at the SAM under LD (Mandel and Yanofsky, 1995). However, FUL:VENUS was observed in older floral primordia, from about stage 4 or 5 under LD (Supplementary Figure 3.3). Signal appears to accumulate in floral primordia under SD conditions as well (Figure 3.9). Strikingly, the pattern of FUL:VENUS expression in flowers is similar to that of VENUS:FD accumulation (unpublished data). It would be interesting to test the effect of *fd-3* on the timing and pattern of expression of *FUL* in flowers, and to compare their precise temporal and spatial patterns using complementary fluorescent markers. But mutation of the proposed FD binding sites in *FUL* does not seem to alter its pattern of expression based on comparing *F9.1* to *m1m2* lines (data not shown). It would be interesting to decipher the mechanisms behind the negative regulation of *FUL*, a positive floral integrator, at early stages of flower formation under LD.

3.3.3 FUL function as a transcription factor

Little is known about the targets of FUL and the mechanisms by which it promotes the floral transition at the SAM. The FUL MADS-box protein was used in ChIP-seq experiments using siliques (Bemer et al., 2017). According to the ChIP-seq list of candidate gene targets, several *SPL* and *ERF/AP2*-family genes were bound by FUL. It would be interesting to study the impact of these downstream genes of FUL and how their function relates to the floral transition. A decrease in expression of the negative flowering-time regulator *AP2* coincides with the increase in *FUL* expression in the SAM towards meristem arrest (Balanzà et al., 2019). It is not known whether *FUL* mediates this regulation directly or indirectly. VENUS-tagged AP2 disappears from the SAM during the floral transition, which coincides with the increase in *FUL* expression under LD (Q. Sang PhD thesis, 2018). Interestingly, AP2 binds to the *FUL* promoter and most likely represses its transcription before floral transition (Yant et al., 2010). Hence, I hypothesise a model in which *FUL* is first promoted by FD–(14-3-3)–

FT/TSF and in turn, the FUL protein leads directly or indirectly to a decrease in the accumulation of its negative regulator AP2 to promote the floral transition. However, this hypothesis does not correlate with the *m1m2* lines in which accumulation of FUL:VENUS occurs in the same pattern as to the control line.

3.3.4 Limitations of this study

In vitro experiments would have been helpful to confirm the binding of FD to the *B1* and *B2* motifs and to address whether their mutation disrupts binding, and such assays were initially considered. The literature describes many assays to study protein–DNA interactions *in vitro*. For this project, an initial approach was to use the Microscale Thermophoresis assay (Jerabek-Willemsen et al., 2011). This determines whether a fluorescently labelled molecule interacts with a partner, such as DNA or proteins. Measuring the fluorescence signal in the buffer estimates the binding affinity between the two partners by calculating the dissociation constant, K_D. Such quantitative data is a major advantage that is often overlooked in other routine assays such as the Electrophoretic Mobility Shift Assay (EMSA). The coding sequence of FD was fused to GFP in a system induced by IPTG in *Escherichia coli* SoluB21. However, protein aggregation was detected, which was confirmed by a low solubility of the GFP:FD protein. Moreover, FD functions as a homo- or heterodimer and oligomerisation precedes the recognition of the motif and thus, binding. Generate functional FD proteins is thus primordial. Another approach was to investigate the transcriptional activity of *FUL*. For this, different reporters and effectors were designed for protoplast *trans*-activation assays. The *FUL*, *FULm1m2* and *FULm1m2+mGTAC* promoters were cloned into the vector pGreenII-LUC (Hellens et al., 2005). In this assay, the promoter of interest is cloned with the CDS of the *Luciferase firefly*, and the CDS of the *Renilla firefly* is cloned under the *35S CaMV* promoter and acts as a transfection control. The assay allows FD to be co-expressed with different partners, such as FT or SPL15, to measure the level of luciferase activity in the cells. However, because of difficulties in the amount of plasmid required for protoplast transfection, such experiments were not pursued.

All experiments performed under LD conditions did not indicate that *ful-2* was late flowering compared with wild-type, as previously described (Ferrandiz et al., 2000). Such a phenotype may have been observed in different light conditions in which the light bulb emits a different light intensity and spectrum. In my experiment, if the flowering phenotype of *ful-2* were different from the wild-type, it would be interesting to study the behaviour of the *FULm* as the effect of FD and SPL15 on *FUL* expression may be hidden by the growth conditions.

Furthermore, slight differences in flowering time under LD were observed along this study and reinforce this hypothesis.

The *fd* and *ft fd* mutants ultimately undergo floral transition under LD, and *FUL* mRNA is upregulated. As it was demonstrated in tomato, profiling wild type and florigen mutant shows similar transcriptomic profiles around the time of their transition (Meir et al., 2021). This suggests the presence of independent pathway(s) that promotes *FUL* transcription and that may not rely on the *B1* and *B2* motifs and to some extent, the photoperiod pathway. This pathway may not include SPL15. For example, it was shown that auxin signaling regulates *FUL* through a possible direct binding of the ARF4 in strawberry (Dong et al., 2021). It is reasonable to ask whether the over-expression or the induction of ARF4 in the *ft fd* double mutant triggers the floral transition. Analysis of such scenario in *Arabidopsis thaliana* would be an asset to understand the important of flowering through the hormonal pathway.

3.4 Supplementary figures

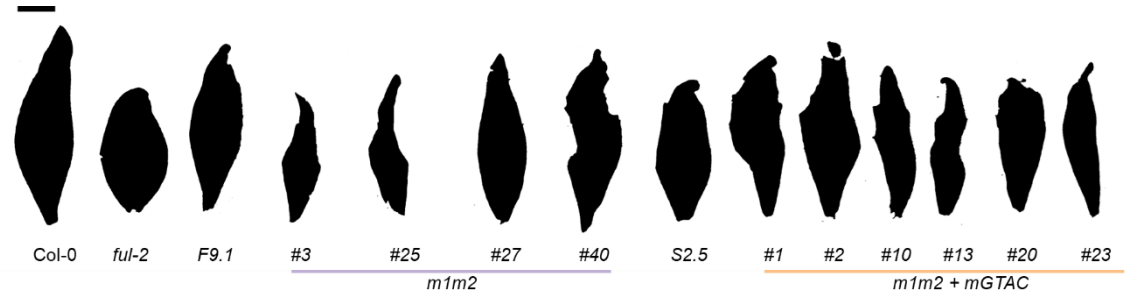

Supplementary Figure 3.1. Complementation of the leaf *ful-2* phenotype under LD. Photographic projections of the first cauline leaf of *FUL::FUL:V* transgenic lines at day 42 together with that of Col-0 and *ful-2* mutant plants. The scalebar represents 1 cm.

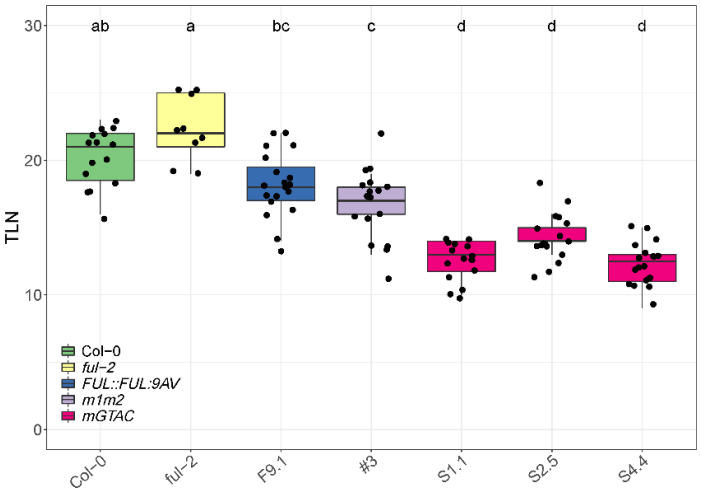

Supplementary Figure 3.2. The *mGTAC* transgenic lines are early flowering.
Flowering time is expressed as the total leaf number (TLN) of plants grown under LD. n = 9 -18 individuals.

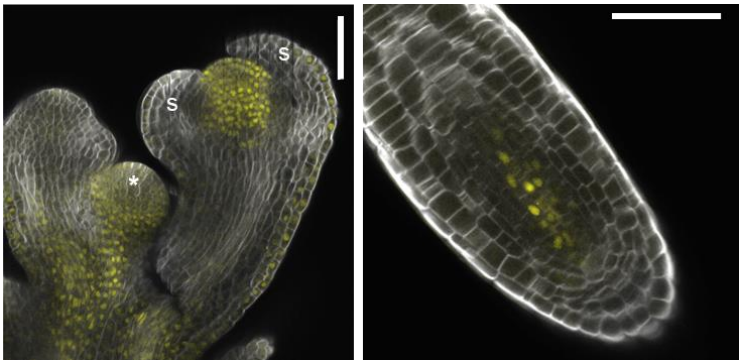

Supplementary Figure 3.3. FUL protein accumulates in diverse tissues of Arabidopsis plants under LD.
Expression of *FUL::FUL:VENUS* in inflorescence and root meristems of 14 day-old plants. VENUS signal is visible in the SAM and the flower primordia at stage 5 but not at stage 3. VENUS signal accumulates at the root tip. An asterisk indicates the shoot apical meristem; s, sepal. Scale bars indicate 50 µm.

Chapter 4. ABA signalling in the FD domain affects flowering time and inflorescence development

4.1 Introduction

FD and the FD paralogue, named FDP, belong to Group A of the Arabidopsis bZIP transcription factor family and are closely related to a clade of bZIPs involved in abscisic acid (ABA) signalling (Dröge-Laser et al., 2018; Romera-Branchat et al., 2020). Furthermore, among the targets of FD identified by ChIP-seq are several genes previously shown to be regulated by ABA (Romera-Branchat et al., 2020). These observations suggest that FD and FDP may regulate ABA-related processes. The ABA signalling cascade is well described (Umezawa et al., 2010; Dong et al., 2015), but little is known concerning the molecular mechanisms and tissues that underlie the role of ABA in flowering.

Hormonal pathways affect many aspects of plant growth, including stem and inflorescence development. For example, dwarf phenotypes have been observed in mutants deficient in gibberellin (GA; Koorneef et al., 1985; Dill and Sun, 2001) and lateral shoot growth is partially regulated by ABA (Yao and Finlayson, 2015; Gonzalez-Grandio et al., 2017). *ABI1* and *ABI2* encode protein phosphatases that function within the ABA signalling pathway and mutation of these genes leads to increased silique number (Hensel et al., 1994). Furthermore, application of exogenous GA strongly promotes flowering, whereas mutations or transgenes that reduce GA levels strongly delay flowering under SDs and weakly delay flowering under LDs (Wilson et al., 1992; Dill and Sun, 2001; Porri et al., 2012). The degradation of DELLA proteins in response to GA accumulation allows SPL15 to directly activate *FUL* transcription (Hyun et al., 2016). Recently, a role for the ABA pathway in the regulation of flowering has also emerged (reviewed in Conti, 2017; Hwang et al., 2019) and Arabidopsis plants supplemented with ABA applied directly to the soil flowered earlier than control plants (Riboni et al., 2016).

Defects in plant architecture are also observed in mutants of genes involved in the floral transition (*e.g.* mutation of *TFL1* leads to reduced stature and a determinate inflorescence; (Hanano and Goto, 2011). In particular, a negative correlation between total leaf number and global morphological phenotypes has been described (Pouteau et al., 2004). The photoperiodic pathway affects meristematic growth (Kinoshita et al., 2020) and alterations in the size of the meristem can disrupt organ formation and thus affect silique phyllotaxy at the stem (Landrein et al., 2015). The late-flowering *spl15 spl9* mutant displays a dwarfism-like phenotype, with reduced stem height and increased branching, similar to that observed for mutation of their orthologue, *GmSPL9,* in soybean (Schwarz et al., 2008; Bao et al., 2019). Interestingly, orthologues of the bZIP FD affect plant architecture in two *Fabaceae* species

(Sussmilch et al., 2015; Cheng et al., 2021; Zhang et al., 2021). Variation in fruit number on the main shoot of *fd* has been observed in Arabidopsis (Hensel et al., 1994; Gorham et al., 2018). However, how activity of the photoperiodic pathway through FD affects fruit number remains unknown.

In this chapter, the first addressed aim concerns how FD, and to some extent FD and FDP, are related to fruit production on the main shoot. Secondly, I asked whether ABA-signalling regulates floral transition *via* a relationship with FD at the SAM. For this, a transgenic line expressing the dominant-negative form of *ABI2* in the *FD* transcriptional domain was generated. Lastly, the generated material was used to identify potential aspects of inflorescence morphology through FD and the ABA-signalling pathway.

4.2 Results

4.2.1 Plant fitness in *fd, fdp* and *fd fdp* double mutants is related to meristematic arrest

To understand the role of FD and FDP in silique production, I first characterized the spatio-temporal accumulation of the proteins under LD conditions and asked whether both proteins co-localised. The *FDP::VENUS:FDP* transgenic line (Romera-Branchat et al., 2020) was crossed to the transgenic line *FD::mCherry:FD fd-3* generated by Dr. H. Gao (MPIPZ). Confocal microscopy was used to visualize the VENUS:FDP and mCherry:FD fusion proteins (See Materials and Methods). Accumulation of the two fluorophores was visible at day 8 (Figure 4.1A). Both signals localised to the nucleus in cells of the SAM, as previously described (Romera-Branchat et al., 2020). Notably, FDP fluorescent signal was visible at the base of the shoot apex, whereas FD signal was more apical. At day 8, both signals were observed in distinct cells. As the plants aged, both signals extended in opposite vertical directions; strong FDP:VENUS expression was observed in the vasculature in the centre of the stem, whereas mCherry:FD was expressed broadly in the SAM and the flower primordia at day 14 (Figure 4.1A). Central cells at the SAM showed co-localisation of FD and FDP from day 10 until day 21 (Figure 4.1B) and even up to day 42 (not shown). At 42 LD, the two fluorophores were still accumulating at the SAM but were also present in the flowers (Figure 4.1C). In these conditions, floral transition occurred between day 12 and 14, because flower primordia were formed at 14 days. To assess the expression level of *FD* and *FDP* in the wild type, tissues enriched for apices were harvested at comparable time points to those used for confocal imaging. Analysis of transcript levels RT-qPCR showed that *FD* expression peaked at day 21, whereas *FDP* expression continuously increased and reached a maximum at day 42 (Figure 4.1D). Although the floral transition likely occurred around day 14, there was a 6-fold increase in *FD* expression from day 14 to day 21. However, it was impossible by this

method to distinguish expression of *FD* and *FDP* mRNAs at the SAM from that in leaf and flower primordia.

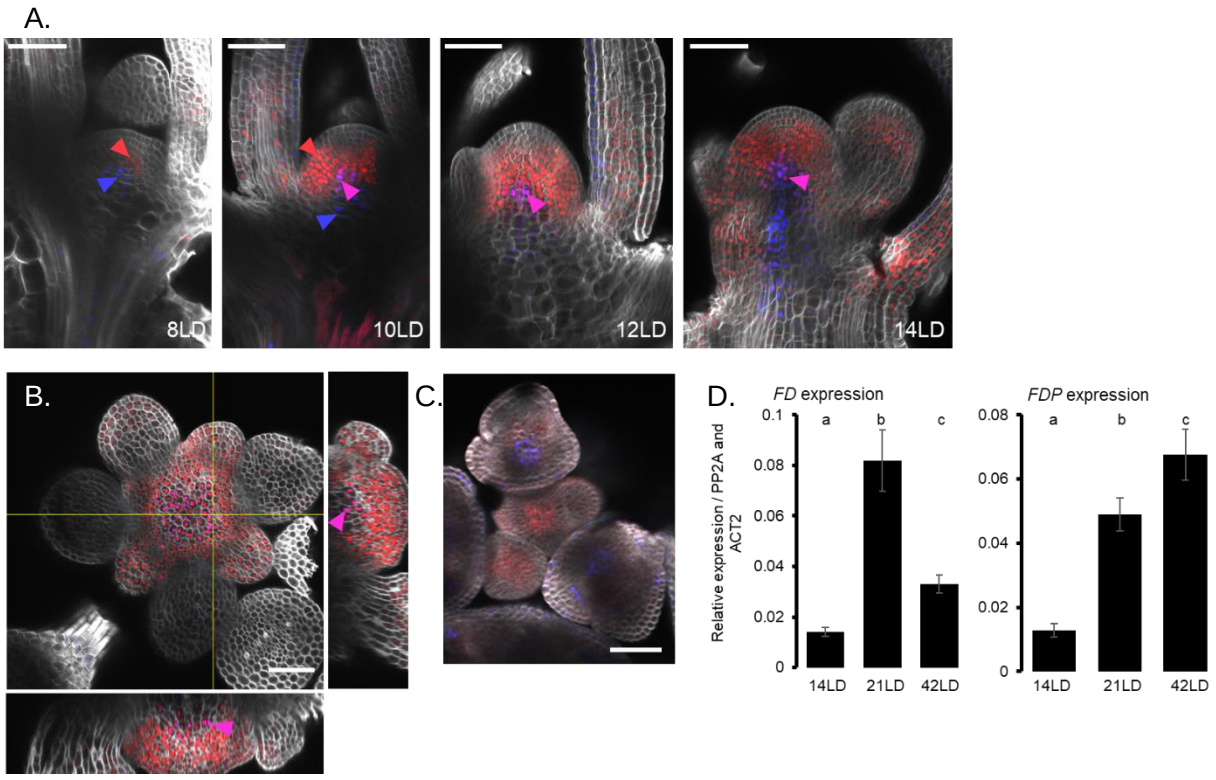

Figure 4.1. FD and FDP are expressed in the SAM throughout the life cycle of *Arabidopsis thaliana*.
Confocal images of SAM of the *FD::mCherry:FD FDP::VENUS:FDP* line under LD conditions in **A**, a time-course series and **B**, 21 LD inflorescence of mCherry:FD VENUS:FDP and the corresponding longitudinal sections as well as **C**, 42 LD around the GPA phase. Red and blue nuclei of cells represent fluorescence signals of mCherry:FD and VENUS:FDP, respectively. Co-localisation of the fluorophores leads to purple colours represented by the pink arrows. Plants were grown in controlled conditions in growth cabinets. The meristem samples were fixed in PFA and cleared with Clearsee. The scale bar represents 50 µm. **D**, *FD* and *FDP* transcript accumulation in wild-type Col-0 tissues enriched for apices. Expression levels were normalized to those of *PP2A* and *ACT2*. Data represent the mean of three biological replicates ±SD under LD conditions at the indicated time points. (ANOVA, Tukey's HSD test).

The *fd* mutant produces more fruits than wild-type plants, suggesting that *FD* function limits fruit production (Hensel et al., 1994; Gorham et al., 2018). Because FD and FDP both contribute to floral transition, I asked whether their function in regulating fruit production is conserved. Under LD conditions in the greenhouse, plant height was measured at final stages of growth before senescence, referred to as the global proliferation arrest (GPA) stage. Surprisingly, *fd-3* plants reached GPA after the wild type and produced a taller main shoot bearing a greater number of fruits than wild type (Figure 4.2A). Introduction of the CRISPR-Cas9-*FDP* mutation into the *fd-3* mutant led to an enhancement of the *fd* phenotype, and GPA of *fd-3 fdp-CRP2* plants occurred two weeks after that in wild type and

one week after that in *fd-3* (Figure 4.2A). Compared with the wild-type, *fd-3* and *fd-3 fdp-CRP2* plants produced on average 10 and 31 more fruits on the main shoot, respectively. In addition to flower number, the aerial biomass, silique length and seed number were greater for *fd-3* and *fd-3 fdp-CRP2* than for wild type (Supplementary Figure 4.1). Interestingly, the longest siliques of Col-0 and *fd-3 fdp-CRP2* are displayed in acropetal and basipetal orders, respectively. This suggests evolutionary strategy in Arabidopsis. The observed greater number of fruits in the *AP2::rAP2* transgenic line resulted from a faster production of flowers at the SAM (Q. Sang PhD thesis, 2020; Sang and Vayssières, *in preparation*). By contrast, the increased fruit number in *ful* was due to an extended GPA and not to an increased flower production rate (Balanzà et al., 2018). To understand the mechanisms behind the increased fruit number in the *fd-3 fdp-CRP2* mutant, flower production rate and main shoot elongation were measured in LD growth conditions in the greenhouse. No differences in these parameters were detected in the mutants (Figure 4.2C). These results suggest that the greater stem height and flower number of *fd* and *fdp* mutants is due to delayed GPA, similar to that of to *ful* (Figure 4.2B and C).

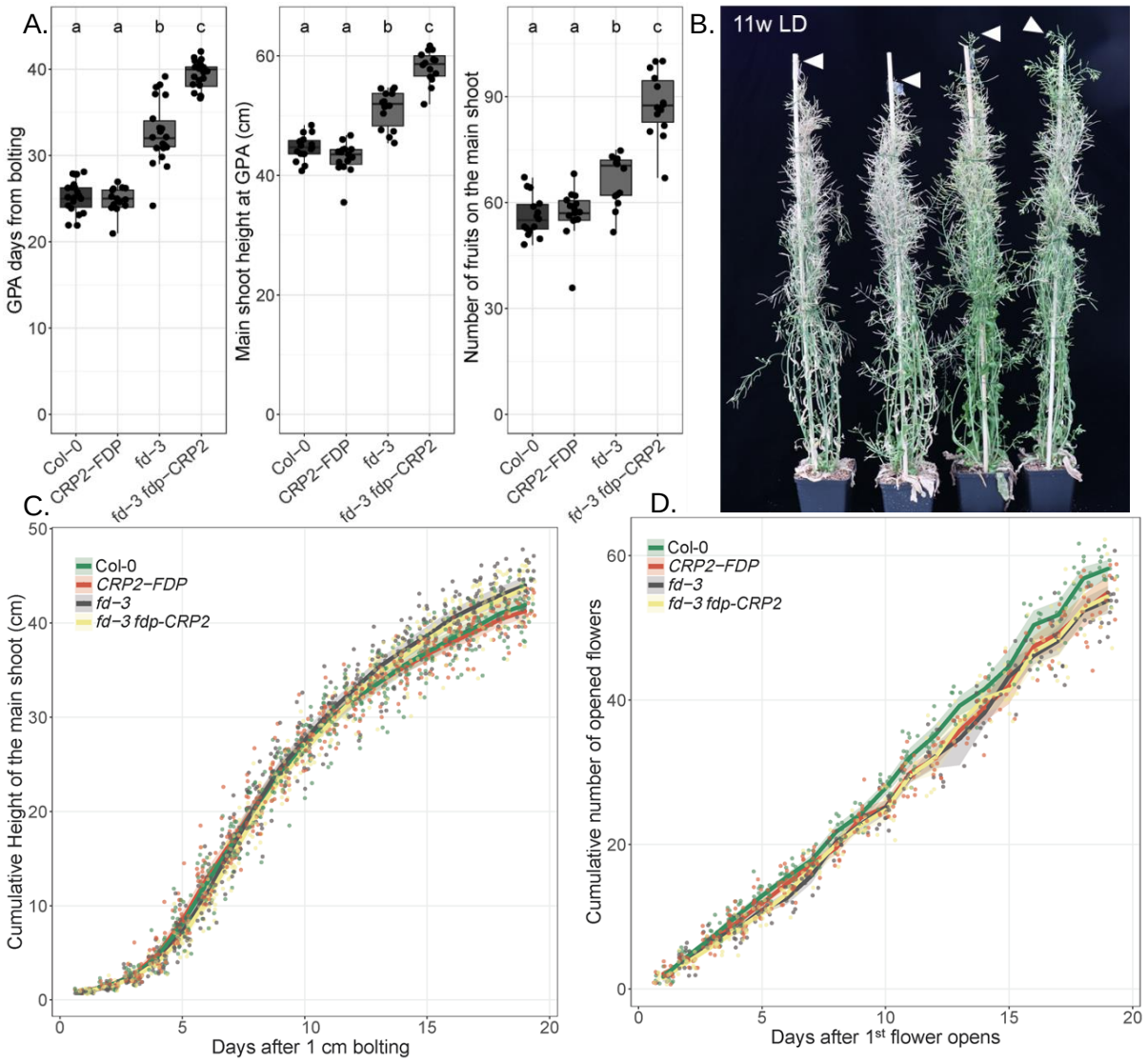

Figure 4.2. The CRISPR-Cas9 mutant of *FDP* enhances the *fd-3* phenotype at GPA. Phenotypic analysis of the main shoot of *fdp-CRP2* and *fd-3* mutants under LD: **A**, the days from bolting to GPA, the height of the main shoot and the number of fruits at the main shoot; *n* = 14–15. Statistical tests were performed using ANOVA followed by the Tukey's HSD test. **B**, Photographic image of 11-week-old representative wild-type plants compared with *fdp-CRP2* and *fd-3* mutants. The apex of the main shoot is represented by a white arrowhead. **C**, growth rate of the main shoot after 1 cm bolting and **D**, flower production after the opening of the first flower; *n* = 24.

Extended GPA in *ful-2* led to reduced levels of *BEL1-LIKE HOMEODOMAIN* (*BLH1*) and *HOMEOBOX PROTEIN 21* (*HB-21*) mRNA (Martínez-Fernández et al., 2020). To test whether the expression of these genes was affected by the transcription factors FD and FDP, RT-qPCR analysis was conducted using 3-week-old inflorescence tissues. Levels of *BLH1* and *HB-21* were reduced in *fd-3* and *fd-3 fdp-CRP2* compared with those in the wild-type control (Figure 4.3A). However, no changes in *AP2* or *FUL* expression were observed at that time point, in contrast to the known effect of AP2 on GPA (Martínez-Fernández et al., 2020). The genomic region of *HB-21* was pulled down in ChIP-seq assays of FD (Collani et al., 2019; Romera-Branchat et al., 2020; Zhu et al., 2020), suggesting a direct regulation by FD. The expression of *HB-21* peaked at day 21, similar to that of FD under LD (Supplementary Figure 4.1; Figure 4.1D).

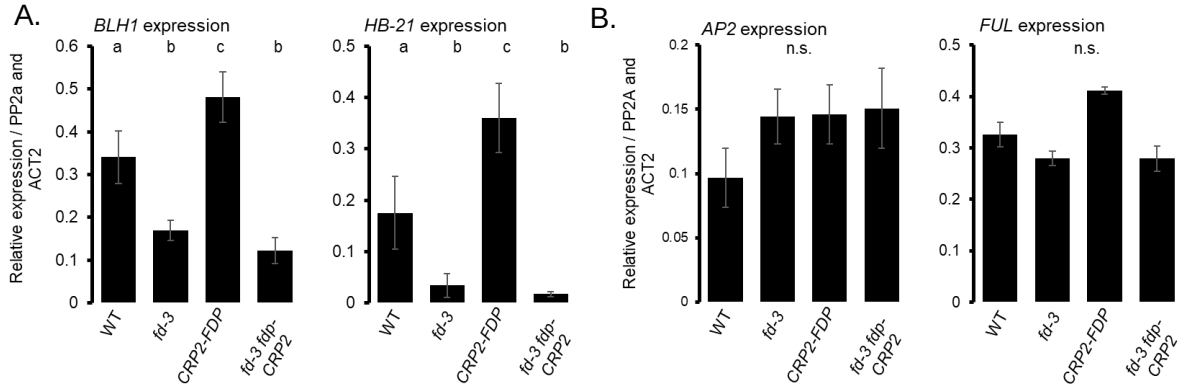

Figure 4.3. FD increases the expression of genes involved in the GPA pathway. **A**, Quantification of the expression of *BLH1* and *HB-21* mRNAs and **B**, *AP2* and *FUL* mRNAs by RT-qPCR in the four genotypes at 3 weeks after bolting under LD. Data represent the mean of three biological replicates ±SD and statistics were performed using ANOVA followed by Tukey's HSD test.

These results indicate that FD and FDP promote proliferative arrest, and that the greater number of fruits on the main shoot of *fd* and *fdp fd* is the result of an extended meristematic activity at the SAM. The molecular and genetic mechanisms are poorly understood, but FD is likely involved in meristematic activity, notably by regulating *HB-21*.

4.2.2 Confirmation of novel *fd* phenotypes by complementation analysis

To confirm whether FD is responsible for an increased silique number and a taller main shoot, I performed complementation analysis of *fd* for plant shoot architectural traits. I first

selected another allelic mutant of *FD*. The *fd-3* and *fd-4* allelic mutants in Col-0 background contain a T-DNA insertion in the first exon of the CDS (SALK T-DNA assembly). The two lines *FD::VENUS:FD* and *FD::mCherry:FD* complement the *fd-3* late-flowering phenotype and were chosen for this experiment (Romera-Branchat et al., 2020; Dr. H. Gao). As expected, floral transition under LD conditions was significantly delayed in *fd-3* and *fd-4* compared with that in wild-type Col-0 (Figure 4.4A). The delay was reflected by an increased total number of leaves and days to bolting. The delayed flowering time of *fd-3* was complemented in the two transgenic lines and their flowering times resembled that of wild-type plants. Similarly, the greater height of the main shoot and the extended I1 phase in *fd-3* plants were rescued in the two transgenic lines (Figure 4.4B). Moreover, total fruit number on the main shoot, as well as the number of secondary inflorescences, were rescued in the two transgenic lines (Figure 4.4C). Expression of *FD::VENUS:FD* in *fd-3* over-complemented the total number of leaves at bolting and the total height of the main shoot but not the length of the I1 phase or number of fruits produced on the main shoot (Figure 4.4). Strikingly, *fd-4* had an extended I1 zone compared with that of the *fd-3*, but the number of fruits did not differ from that of wild-type Col-0. Overall, the greater total height of the main shoot in *fd* mutants was mostly caused by an extended I1 length (Figure 4.4B). Flower number rather than date to GPA was used as an indicator of meristematic activity at the SAM.

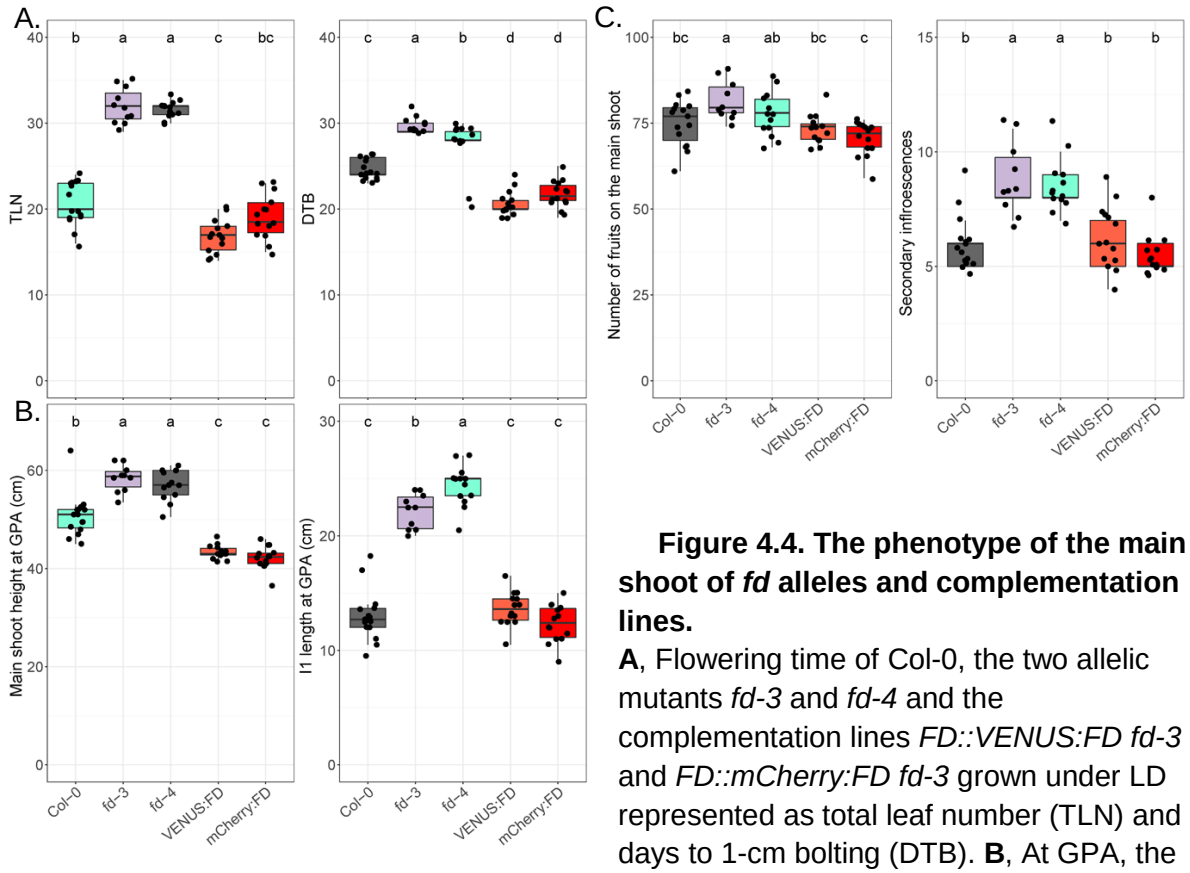

Figure 4.4. The phenotype of the main shoot of *fd* alleles and complementation lines.

A, Flowering time of Col-0, the two allelic mutants *fd-3* and *fd-4* and the complementation lines *FD::VENUS:FD fd-3* and *FD::mCherry:FD fd-3* grown under LD represented as total leaf number (TLN) and days to 1-cm bolting (DTB). **B**, At GPA, the height of the main shoot and I1 length were measured with a ruler and **C**, the number of fruits on the main shoot as well as the secondary inflorescences (rosette branches) were scored at

GPA. Box-plot medians are indicated by the centre line and were used for ANOVA followed by Tukey's HSD test; *n* = 10–15.

In conclusion, the defects in flowering and plant architecture described for *fd-3* are somehow similar to those of *fd-4* and are rescued by *FD* genomic DNA.

4.2.3 Inducible *GR:FD* demonstrates that the regulation of floral induction and inflorescence development are two distinct functions of FD

The GR:FD protein promotes floral transition most effectively when induced at early stages of development (Chapter 2, Figure 2.4), but FD continuously accumulates at the SAM from soon after germination until GPA (Figure 4.1). The number of fruits produced by the SAM is controlled by a complex combination of mechanisms, because exogenous signals, genetic pathways and hormone levels affect fruit number during development (Ware et al., 2020). To some extent, the increased fruit number observed in *fd* resulted from longer meristematic activity at the SAM (Figure 4.2). It is unclear when FD regulates fruit number or meristematic activity, and I therefore investigated whether these are affected by FD function at the time of the floral transition or later. Wild-type Col-0 and *fd-3* controls were grown together with *FD::GR:FD fd-3 #19* plants in LD in the greenhouse (Figure 4.5; Chapter 2; referred as to *GR:FD*). For this experiment, all genotypes were treated every three days with either mock or DEX solutions from day 7 to day 21 or from day 21 to day 63. Previously, I detected no flowering-time defects of Col-0 and *fd-3* plants treated with mock and DEX solutions (Chapter 2, Figure 2.3). Thus, data for Col-0 mock-treated plants from day 7 to day 21 were presented together with Col-0 mock-treated plants from day 21 to day 63 in Figure 4.5. This was also the case for Col-0 plants treated with DEX and *fd-3* plants treated with mock and DEX. A delay in flowering of *fd-3* compared to Col-0 was observed, similar to that of mock-treated *GR:FD* (Figure 4.5A). *GR:FD* plants treated with DEX from day 6 to day 21 were early flowering compared with the respective mock-treated plants. By contrast, *GR:FD* treated with DEX from day 21 showed a flowering-time phenotype not significantly different from that of the *fd-3* mutant (Figure 4.5A). This was expected because the 21-day-old *GR:FD* meristems had already produced flower primordia indicating that floral induction had already ended (Chapter 2, Figure 2.1C). Next, plant architectural traits were scored after GPA. Induction of GR:FD by DEX led to a reduction in fruit number and a shorter I1 length compared with the mock-treated plants, irrespective of the timing of FD induction (Figure 4.5B and C). The shortest I1 length was observed when *GR:FD* plants were treated at early developmental stages. This suggests an important role for FD in regulating the length of I1 at early time points up to day 21. Although the I1 length of DEX-treated plants from day 7 to 21 LD was decreased, the total height was not statistically significantly affected by DEX treatment. This was due to an extended I2 zone of the plants in these conditions. As I1 length, fruit number and height at GPA but not flowering time were reduced by DEX application from 21 LD, FD

must regulate these inflorescence traits at least partly independently of its role in regulating floral induction.

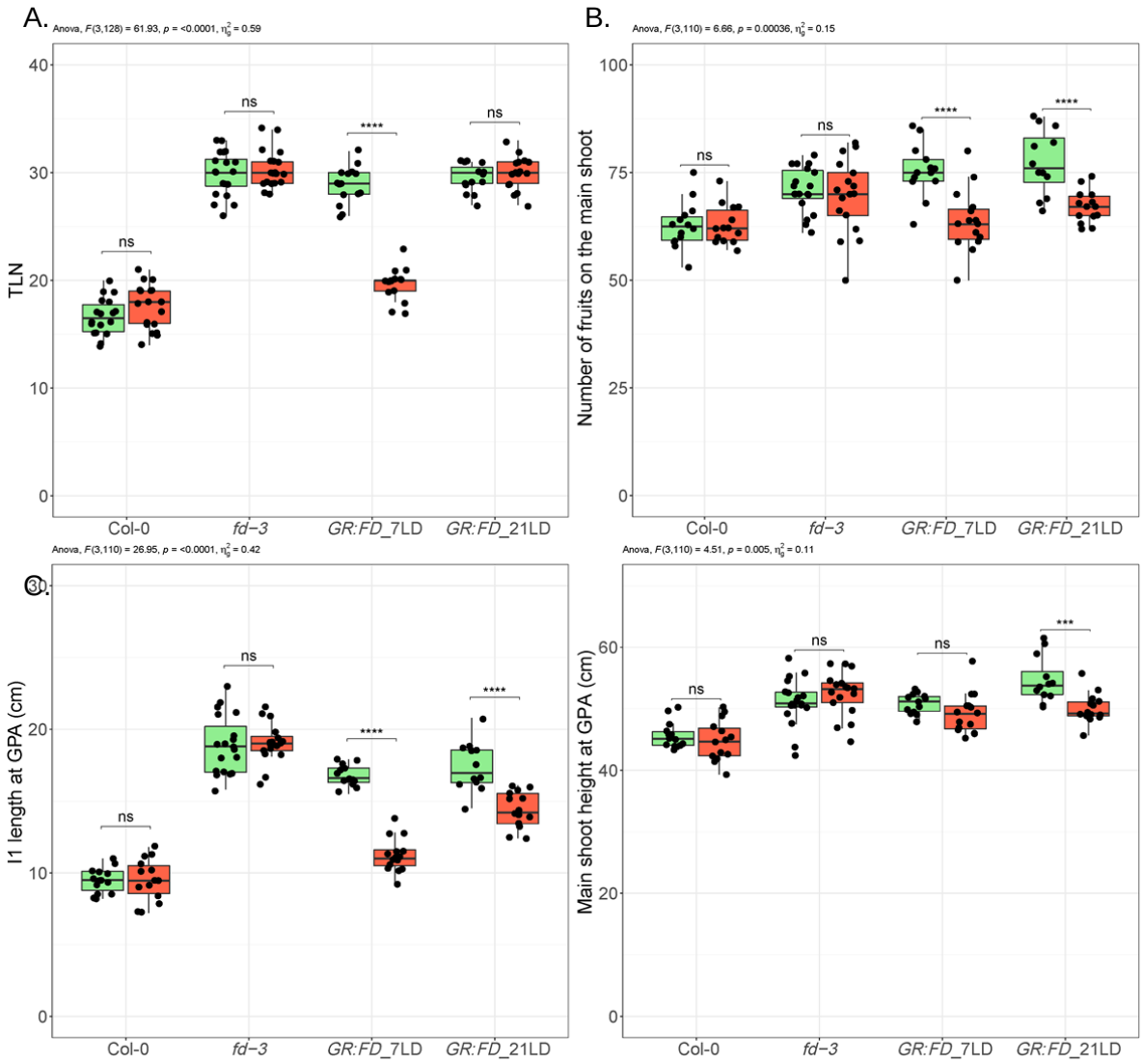

Figure 4.5. Induction of GR:FD in the *fd* background leads to early-flowering plants with a reduction of fruit number and I1 length.
A, Flowering time scored under LD as total leaf number (TLN) for Col-0, *fd-3* and the *FD::GR:FD #19* treated with either mock or DEX solution (green and orange coloured-boxes, respectively). **B**, Fruit numbers were scored at GPA along the I2 zone for each genotype. **C**, Height of the I1 length and total height of the main shoot were measured with a ruler at GPA. Box-plot medians are indicated by the centre line and were used for two-way ANOVA adjusted with the Bonferroni correction. Each genotype was tested for differences between the effect of treatment between mock and DEX solutions. ns, non-significant, for *** *P*-value < 0.01 and for **** *P*-value < 0.001. The *GR:FD* plants were treated every three days from day 7 to day 21 (*GR:FD_7LD*) or from day 21 to day 63 (*GR:FD_21LD*). For each single treatment, Col-0 and *fd-3* n = 18–20 and for the transgenic *GR:FD* line, n = 15–16.

FD negatively affects the I1 length and the number of fruits produced during plant development. DEX application to *FD::GR:FD fd-3* plants demonstrates the functional activity

of GR:FD in complementing shoot architectural traits. Moreover, it suggests that FD partially regulates these phenotypes after the floral transition and thus, independently of its function in regulating flowering time.

4.2.4 Mutation of *FD* and *FDP* led to mild flowering but optimal fruit production when compared to multiple flowering mutants under LD

In addition to FD and FDP, many positive regulators of the floral transition stably accumulate after the formation of the first flower primordium. For instance, SOC1 (Immink et al., 2012) and FUL (Chapter 3), SPL15 and *MIR172D* (Hyun et al., 2016; Ó'Maoiléidigh et al., 2021) are present in the inflorescence meristem under LD. The TFL1 floral repressor is present in the inflorescence meristem but not in floral primordia (Zhu et al., 2020; Dr. A. Pajoro, Dr. M. Cerise). *fd-3, ft-10* and higher-order mutants with *tsf* show a late-flowering phenotype compared with that of wild-type Col-0 (Abe et al., 2005; Yamaguchi et al., 2005; Jang et al., 2009). Mutation of *FUL* or *SOC1* delays flowering and the double *ful-2 soc1-2* mutant has the strongest late-flowering phenotype compared with the wild-type and respective single mutants (Melzer et al., 2008). Mutation of *SPL15* or *SPL9* slightly delays floral transition under LD (Schwarz et al., 2008; Hyun et al., 2016; A. van Driel PhD thesis, 2020). Phenotypic analysis of double *spl15-1 spl9-1* mutant plants revealed a decrease in plant inflorescence height by half compared with that of the wild type (Schwarz et al., 2008). Mutation of *TFL1* leads to an early-flowering phenotype (Shannon and Meeks-Wagner, 1991; Hanano and Goto, 2011) and introgression of *fd* into the *tfl1* background suppresses the early-flowering phenotype of *tfl1* (Hanano and Goto, 2011; Jaeger et al., 2013). Mutation of *SVP* leads to a slightly earlier flowering under LD and greater stem height than wild type (Jang et al., 2009; Andres et al., 2014). To understand whether the morphological traits of *fd-3 fdp-CRP2* are shared among mutants of genes involved in the photoperiodic pathway, we characterised 22 genotypes for plant shoot architecture during development. First, flowering time was scored to confirm the phenotypes of the mutants under LD (Supplementary Figure 4.3) and the resulting rosette leaf number from four independent experiments was plotted. The double *fd-3 ft-10* mutant had a shorter vegetative phase compared with that of ft-*10 tsf-1* and *ft-10 fd-3 tsf-1*. The double *soc1 ful* plants were late flowering and the rosette leaf number was comparable with that of the *fd-3 fdp-CRP2* plants. Next, ten traits were compared for each individual of the genotype data set (Figure 4.6A, $P < 0.01$).

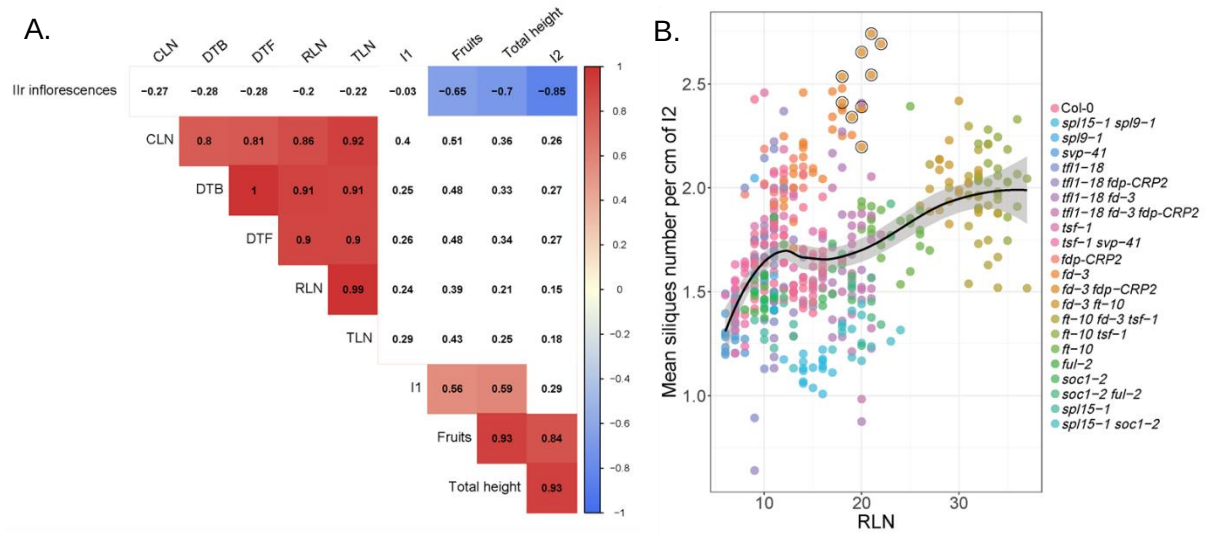

Figure 4.6. No correlation was found between flowering time and the number of siliques produced on the main shoot.
A, Correlation plot of ten phenotypic traits across the 24 genotypes grown under LD in the greenhouse. The linear correlation value *r* is indicated for each box and absolute values higher than 40 correspond to strong to very strong relationships. Coloured boxes indicate correlated traits with a *P*-value < 0.01 and were selected for interpretation. Blue boxes represent negative correlations and red boxes represent positive correlations. **B**, The correlation between mean silique number in the inflorescence (I2) zone and RLN of the 24 genotypes. The double mutant *fd-3 fdp-CRP2* produced a high number of siliques on the main shoot compared with the other genotypes and are considered as outliers (orange circles bordered with black). The data for four experiments are depicted together, because the wild-type plants behaved similarly across the datasets. Each dot represents one individual. The black line represents the calculated polynomial for the dataset.

Remarkably, the matrix clustered the flowering traits together with a highly positive correlation. For instance, cauline leaf number strongly correlated with the time to bolting (*r* = 1.00), indicating that the later that flowering occurred, the more cauline leaves were produced. This increase in the number of cauline leaves was previously observed for the late-flowering *fd* mutant (Abe et al., 2005) as well as for the mutant in the *FD* orthologue of pea, *veg2* (Chapter 2, Figure 2.1B, Sussmilch et al., 2015). A second cluster indicated a negative correlation between the number of secondary inflorescences and total primary inflorescence height (*r* = -0.70), fruit number (*r* = -0.65) and I2 length (*r* = -0.85) of the primary inflorescence. This is consistent with previous findings for shoot-branching mutants in which apical dominance is affected (reviewed in Kebrom, 2017). Lastly, the third correlation group clustered I1, I2, total height and the number of fruits. This result is expected, given that the total height of the main shoot is the sum of I1 and I2. Total fruit number was then strongly associated with the height of the stem (*r* = 0.93). To compensate for the variation in I2 length among the genotypes, the mean density of fruits within I2 was compared with the number of rosette leaves (Figure 4.6B). The resulting correlation showed

a large variation for plants with a low number of rosette leaves (6–12 leaves), but less variation for late-flowering genotypes such as *fd-3 ft-10*. This indicates that *fd-3 fdp-CRP2* had an increased silique density on the main shoot compared with genotypes with a similar number of rosette leaves.

This dataset does not support a straightforward relationship between the length of the vegetative phase and the plant shoot architectural traits scored. Floral transition controlled by the photoperiod pathway is uncoupled from the number of fruits produced. These results support a distinct regulatory role for FD and FDP in determining the extent of fruit production in Arabidopsis.

4.2.5 Generation of *FD::abi2-1*: a new genetic tool to block ABA signalling at the SAM in Arabidopsis

The group A protein phosphatase type 2Cs (PP2Cs) negatively regulate ABA signalling by dephosphorylating the T-loop in SnRK2 protein kinases (Leung et al., 1997; Merlot et al., 2001; Yoshida et al., 2006; Umezawa et al., 2009; Vlad et al., 2009; Soon et al., 2012). In the presence of ABA, the PP2Cs are repressed by the ABA receptor allowing SnRK2 phosphorylation and activation of downstream transcription factors. The SnRK2 protein kinases therefore provide resistance to a variety of stresses by promoting ABA-signalling. The ABA-insensitive *abi1* and *abi2* mutants are dominant mutations in the PP2Cs rendering them insensitive to the ABA receptor, so that the SnRK2s are constitutively dephosphorylated impairing ABA signalling. These mutants display an enhancement in the number of fruits produced on the main shoot (Hensel et al., 1994). In poplar, ectopic expression of *abi1* leads to increased internode growth but smaller leaves (Arend et al., 2009). The Arabidopsis *abi1-1* mutant is early flowering in SDs (Riboni et al., 2016). In Aspen, expression of *abi1* bypasses bud dormancy (Tylewicz et al., 2018). Staining of the *ABI1:GUS* transgenic line revealed a high accumulation of *ABI1* at the shoot apical region of Arabidopsis (Riboni et al., 2016). The SAM dataset from the BAR eFP Browser (www.bar.utoronto.ca) indicates a high level of *ABI1* and *ABI2* mRNA. Although ABI1 and ABI2 are homologous, they potentially have non-overlapping functions (Zhang et al., 2004; Yoshida et al., 2006). Studies have mostly focused on the ABI1 protein and there is a lack of knowledge on the function of *ABI2* in plant development. Moreover, *abi2* produces a greater number of fruits than *abi1* (Hensel et al., 1994). Thus, I decided to study the role of ABI2 in floral transition and plant shoot architecture, and thereby the role of ABA-signalling in development. Because FD belongs to the bZIP group A together with other bZIPs that regulate abiotic and ABA-stress-related processes, I asked whether FD and ABI2 have redundant or partially redundant roles in plant development. To test this, I amplified *ABI2* and *abi2-1* coding sequences from L*er* DNA and expressed them from the *FD* promoter (Dr. D.

Ó'Maoiléidigh). The resulting *FD::ABI2* and *FD::abi2-1* transgenes were introduced into Col-0 plants by *Agrobacterium tumefaciens*-mediated transformation.

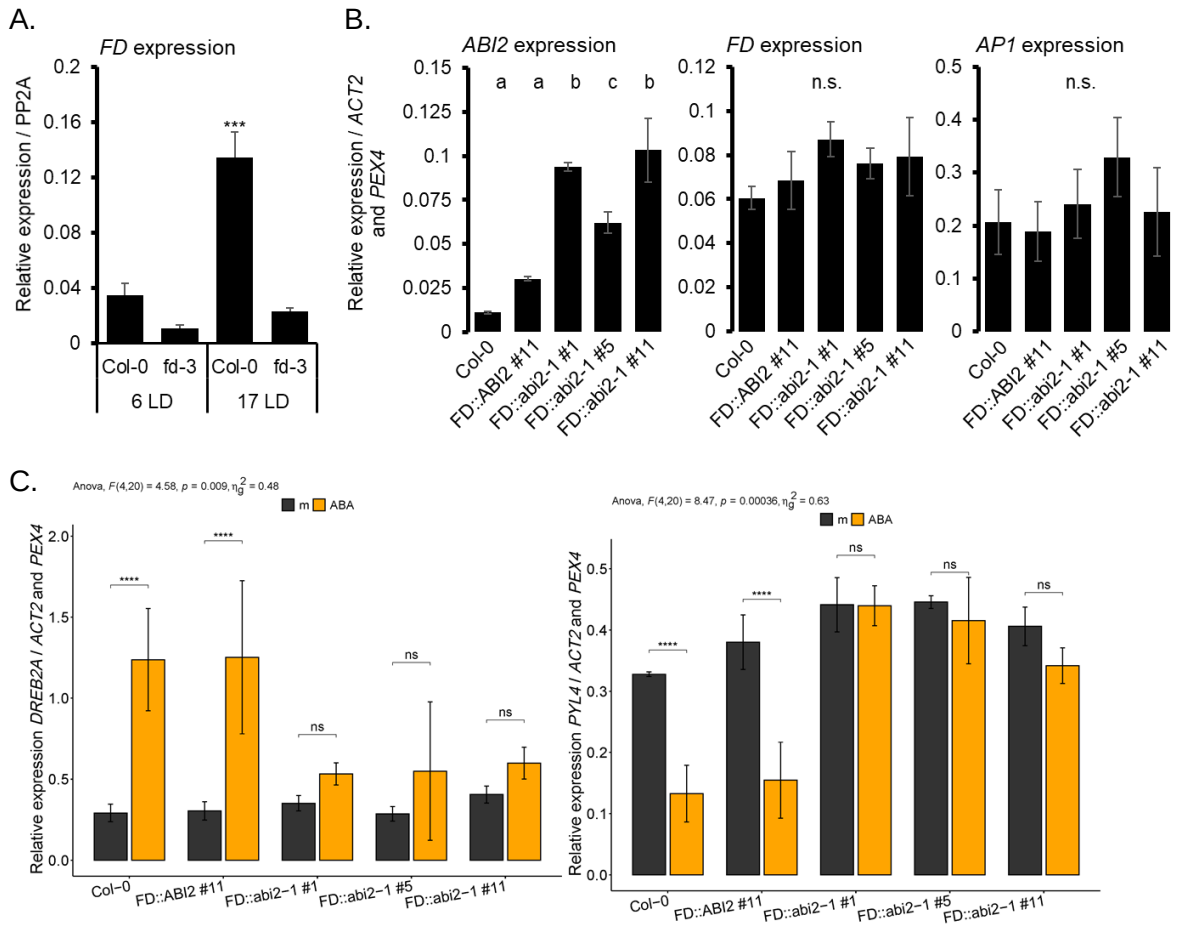

Figure 4.7. Blocking ABA signalling in the SAM by generating *FD::abi2-1* transgenic lines.
A, Transcript levels of *FD* in the wild-type Col-0 and *fd-3* mutant before floral transition (6 LD) and after floral transition (17 LD). The data represent the mean of three biological replicates ± SD and the statistics at day 6 compared to day 17 were analysed using the Student's *t*-test (*$P < 0.05$). **B**, Transcript levels of *ABI2*, *FD* and *AP1* in wild-type and the transgenic lines *FD::ABI2* and *FD::abi2-1*. Samples enriched for 17-day-old apices were harvested for RT-qPCR. Data represent the mean of three biological replicates ± SD and were statistically analysed using ANOVA followed by Tukey's HSD test. **C**, Expression level of *DREB2A* and *PYL4* after ABA treatment. The central region containing the SAM of 17LD plants were brushed with either mock or 40 µM ABA. Tissues enriched for apices were harvested 4 hours after induction in biological replicates. Statistics were analysed with two-way ANOVA adjusted with the Bonferroni correction; ns, non-significant; **** represents a *P*-value < 0.01.

Higher levels of *FD* mRNA were detected by RT-qPCR at day 17 compared with day 6 in Col-0 (Figure 4.7A). The level of *ABI2* mRNA was quantified in 17-LD tissues enriched for apices for one *FD::ABI2* and three *FD::abi2-1* lines (Figure 4.7B). The *FD::abi2-1* lines expressed *ABI2* mRNA at a higher level than wild-type Col-0 and lines *#1* and *#11* showed the greatest level of expression. Neither the level of *FD* nor *AP1* expression was affected in the transgenic lines, suggesting there was no effect of the constructs on floral transition under LD (Figure 4.7B). To test the efficiency of the construct to attenuate ABA signalling, I

first quantified ABA-related gene expression by RT-qPCR after ABA application. The ABA-signalling mediator *PYRABACTIN RESISTANCE 1-LIKE 4* (*PYL4*) and the regulator of ABA-gene expression *DEHYDRATION-RESPONSIVE ELEMENT-BINDING PROTEIN 2A* (*DREB2A*) promote ABA stress-related responses in Arabidopsis and are transcriptionally repressed or induced by ABA respectively (Park et al., 2009; Kim et al., 2011). Tissue enriched for apices treated with ABA or mock treated was harvested at 17 LD when *FD* mRNA levels were high (Figure 4.7A). In Col-0, *DREB2A* mRNA levels were increased by ABA treatment, while *PYL4* mRNA was reduced by ABA treatment. Both of these responses to ABA treatment were attenuated in the *FD::abi2-1* lines compared with the controls *FD::ABI2 #11* and Col-0 (Figure 4.7C). This demonstrates that ABA signalling is disrupted in *FD::abi2-1* within the FD expression domain.

4.2.6 *FD::abi2-1* leads to defects in plant shoot architecture but not in flowering time under LD

To test the effect of continuous disruption of ABA signalling specifically at the SAM, flowering time was first monitored under LD. Some of the *FD::ABI2* and *FD::abi2-1* transgenic lines displayed statistically significant differences in flowering time compared with the wild-type as measured by rosette leaf number and bolting time, but these differences were not consistently observed in all lines (Figures 4.7B, 4.8A and B). Next, the total number of fruits produced by the shoot apical meristem was scored at GPA. Compared with the wild-type, plants of the *FD::abi2-1* line *#1* produced an increased number of fruits (Figure 4.9C), as observed previously for *abi2-1* in L*er* accession (Hensel et al., 1994). In addition, the transgenic line displayed a greater main shoot length due to an elongated I2 zone (Figure 4.8D and E).

Under non-stress conditions, in LD, expression of *abi2-1* from the *FD* promoter has no consistent effect on the timing of floral transition. However, fruit number was increased, consistent with the phenotype described for *abi2-1* in L*er*, and therefore impairment of the ABA pathway at the SAM in the *FD* expression pattern increases fruit number.

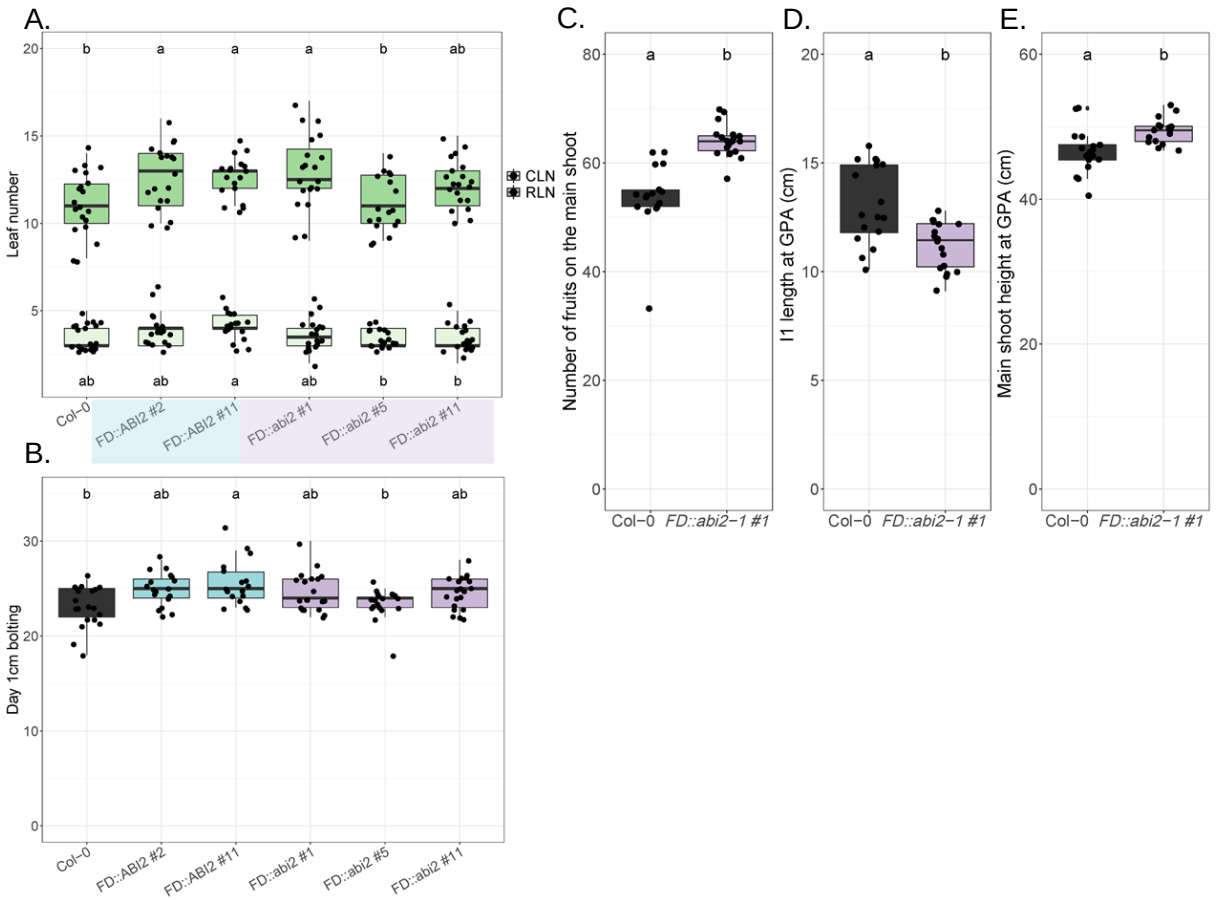

Figure 4.8. The *FD::abi2-1* transgenic lines affect shoot length and fruit numbers under LD.

The transgenic control line *FD::ABI2* was grown together with wild-type Col-0 and *FD::abi2-1* transgenic lines. The *FD::ABI2* lines are depicted in light blue and the *FD::abi2-1* lines in purple. **A**, Total leaf number (TLN) was scored under LD. **B**, Days to bolting of the different genotypes under LD; *n* = 23–34. **C**, Number of flowers produced on the main shoot at GPA. **D**, Height of the I1 zone on the main shoot at GPA. **E**, Height of the main shoot at GPA; *n* = 17–18. Values for genotypes with the same letter do not differ significantly from each other (ANOVA, Tukey's HSD test).

4.2.7 The impairment of ABA signalling in *FD::abi2-1* promotes floral transition under SD

The *abi1-1* mutant flowers early in SD compared with wild-type L*er* (Riboni et al., 2016). To study the effect of *ABI2* mutation on ABA signalling at the SAM, I first used confocal microscopy to establish whether FD is expressed in the SAM under SD. The VENUS:FD protein was present from an early developmental stage up to the formation of flower primordia (Figure 4.9). After 1 week in SD, the signal was rather not in the meristem, but rather in the leaf stipules. At later times, the accumulation pattern resembled that in LD-grown meristems (Chapter 2, Figure 2.1D). At each time point, the signal was localised to the cell nucleus. Therefore, VENUS:FD was present throughout development under SD but no flowering-time phenotype has been reported for *fd* mutants in these conditions (Jang et al., 2009). The signal appeared to be depleted in the upper central region of the apex at 6 weeks

in SD, which was confirmed by the top view at 9 weeks in SD (Figure 4.9). Because FD is expressed in the SAM under SD, *abi2-1* was expected to be actively transcribed in the *FD::abi2-1* transgenic line.

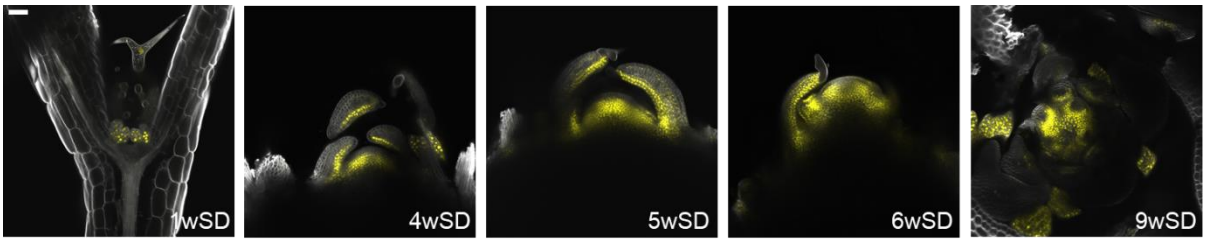

Figure 4.9. VENUS:FD accumulates in the nuclei of meristematic cells under SD.
Confocal images of shoot apical meristem of *FD::VENUS:FD fd-3* under SD conditions at the indicated time points. Floral primordia are visible in 6-week-old plants. The scale bar represents 50 µm and applies to all images.

To test the effect of the transgenic line, the plants were grown under SD and scored for flowering time. The wild-type plants and the *FD::ABI2* transgenic lines bolted on average 53 days after sowing and with 57 total leaves, whereas the *FD::abi2-1* lines bolted on average after 49 days with 50 total leaves (Figure 4.10A–C). Therefore, *FD::abi2-1* lines were earlier flowering than wild type under SD.

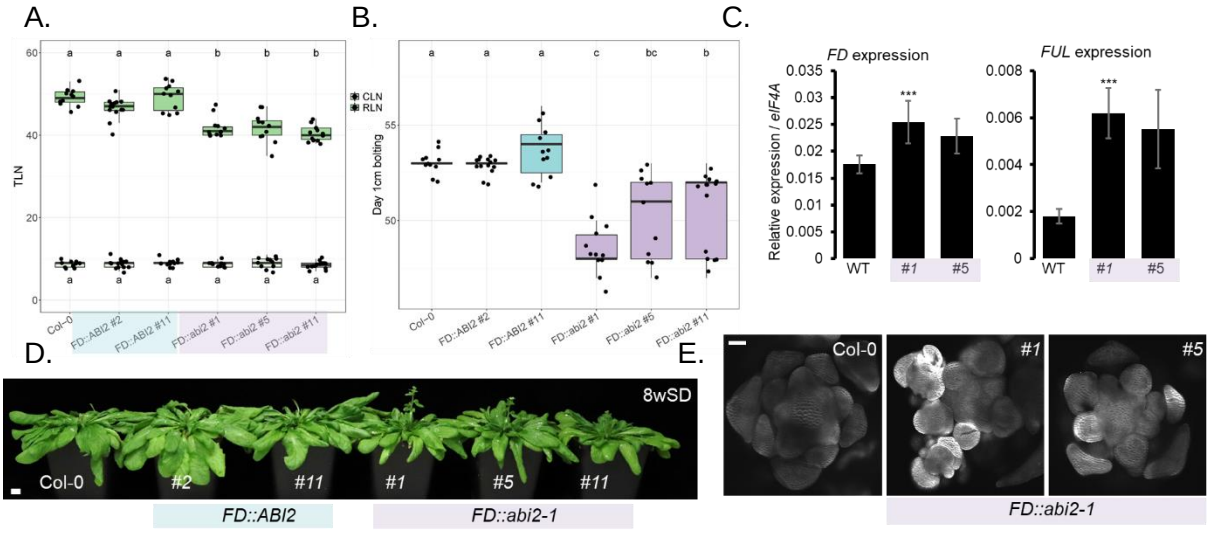

Figure 4.10. Disruption of ABA signalling at the SAM accelerates flowering time under SD conditions.
The transgenic control lines *FD::ABI2* (coloured in light blue) were grown under SD together with Col-0 and *FD::abi2-1* transgenic lines (coloured in purple). **A**, Total leaf number (TLN) and **B**, days to bolting; *n* = 11–14. Values for genotypes with the same letter are not statistically significantly different from each other (ANOVA, Tukey's HSD test). **C**, Photographic images of the different genotypes at 8 weeks under SD; #1, #5 and #11 refers to the *FD::abi2-1* lines. The scale bar represents 1 cm. **D**, Real-time PCR for expression of *FD* and *FUL* in wild-type and *FD::abi2-1* transgenic lines. Tissues enriched for meristems were harvested from of 6-week-old plants. Error bars represent ±SD (two-tailed Student's *t*-test ***$p < 0.01$ compared to the wild-type, WT). **E**, Morphology of apices of Col-0 and the two *FD::abi2-1* transgenic lines #1 and #5 at 6 weeks after sowing. Meristematic samples

were fixed in PFA and cleared with Clearsee. The scale bar represents 50 µm and applies to all images.

Similarly, I tested the flowering time of the *abi2-1* mutant and L*er* under SD. Scoring of total leaf number and days at bolting confirmed an early flowering phenotype of *abi2-1*, which supports a biological role for *FD::abi2-1* (Supplementary Figure 4.4A). At 6 weeks in SD, *FD* and *FUL* expression was higher in the *FD::abi2-1 #1* line (Figure 4.10D). This correlates with their early flowering and the flower primordia visible by confocal microscopy in the transgenic lines (Figure 4.10E). Although line *#5* displayed an early-flowering phenotype, expression of the floral integrator *FUL* was lower and the developmental stage was less advanced at 6 weeks (Figure 4.10). This may be explained by the higher expression of *ABI2* mRNA in line *#1* than in line *#5* (Figure 4.7C).

Overall, confocal microscopy, gene expression and flowering-time experiments showed an early-flowering phenotype for the *FD::abi2-1* transgenic lines under SD.

4.2.8 Plant shoot architecture is strongly affected in *FD::abi2-1* lines under SD

To test further the effect of disrupting ABA signalling at the SAM, the plant architecture of *FD::abi2-1* lines was studied after flowering in SD growth cabinets. Because of space constraints, the height of the main shoot was measured 20 days after bolting for each individual. All *FD::abi2-1* lines had a short main shoot and a high number of secondary inflorescences (Figure 4.11A, B, C and D). The main shoot of the *FD::abi2-1* line failed to elongate and the plant was rather compact (Figure 4.11C). The secondary inflorescences and cauline-leaf branches are much longer than the main shoot (Figure 4.11D). This phenotype resembled that of the *abi2-1* mutant in L*er* (Supplementary Figure 4.4B). The reduction in shoot height and the increase in the number of secondary inflorescences from the rosette leaf axils suggest a loss of apical dominance in the *FD::abi2-1* lines. The reduction in stem elongation was concomitant with reductions in the expression of genes affecting growth, such as *SPL9* and *AtHB-12* (Figure 4.11E; Schwarz et al., 2008; Son et al., 2010). Moreover, the *FD::abi2-1* plant had more leaves at each node of the main shoot (Supplementary Figure 4.5). This is consistent with the aerial-rosette phenotype previously described for other mutants (Teotia and Lamb, 2009).

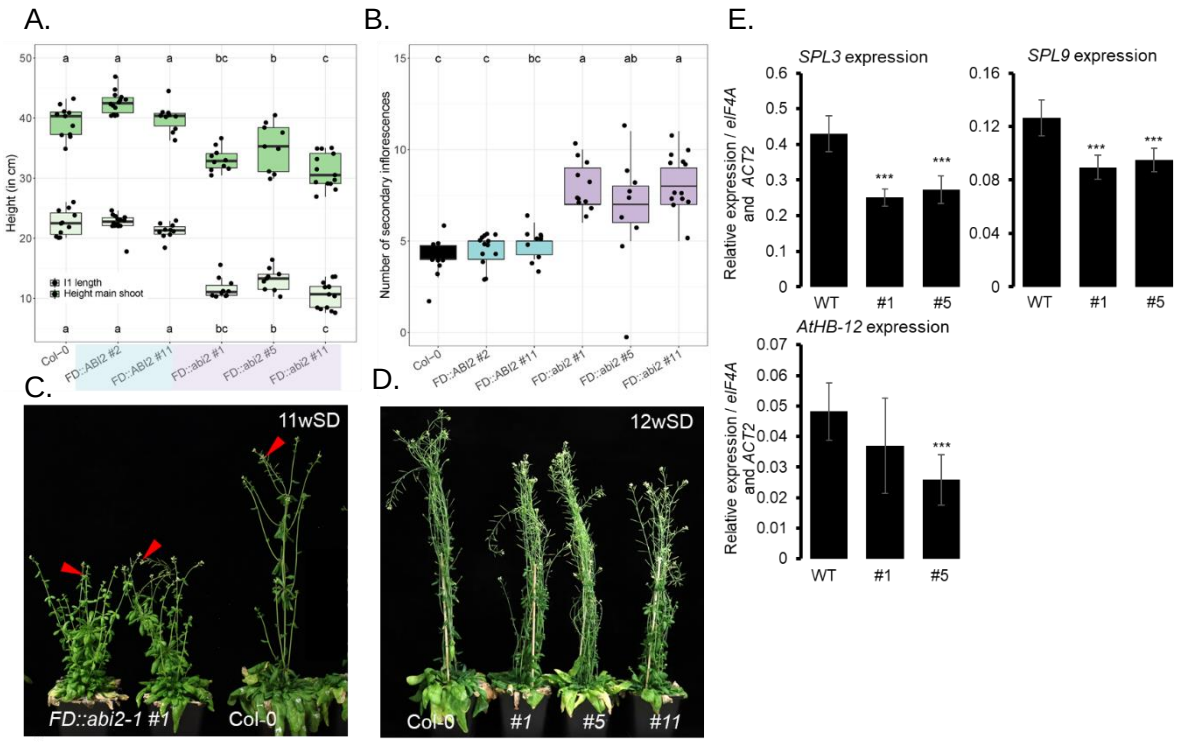

Figure 4.11. The *FD::abi2-1* lines affect plant architecture under SD conditions.
A, Box plot showing the height to the first silique (I1 length; light green) and total height of the main shoot (dark green) scored 20 days after flowering; *n* = 9–14. **B**, Number of primary inflorescences (rosette branches) at 20 days after flowering for the indicated genotypes; *n* = 9–13. Box-plot medians is indicated by the centre line and were used for ANOVA followed by Tukey's HSD test. **C**, Photographic image of two *FD::abi2 #1* individuals compared with the wild type at the indicated time points. The red arrowhead indicates the primary inflorescence of the plant which is shorter in the *FD::abi2-1*. The scale bar represents 1 cm. **D**, Photographic image of three individuals from the *FD::abi2-1* lines number *#1*, *#5* and *#11* grown for 12 weeks under SD. The main shoot stops elongating and axillary inflorescence take over in the *FD::abi2-1* lines. **E**, Expression levels of *SPL3*, *SPL9* and *AtHB-12* in the wild type and *FD::abi2-1 #1* and *#5*. Samples are enriched for 6-week-old meristems of plants grown under SD. Data represent the mean of three biological replicates ±SD and statistical analysis was performed using the Student's *t*-test (**P* < 0.05) and each transgenic line was compared with the wild type.

4.2.9 Demonstration of the role of FD and ABA signalling at the SAM

The *FD::abi2-1* line displayed defects in plant architecture under LD and SD conditions, but flowering time was affected only under non-inductive SD conditions. A greater stem height and increased fruit number were observed for *fd*, similar to those for *FD::abi2-1.* The I1 length of *FD::abi2-1* was smaller whereas the I2 length was extended, and *fd* mostly displayed a greater I1 length (Figures 4.4B and 4.8D). To test the relationship between ABA and FD at the SAM in regulating plant architecture, *FD::abi2-1* was crossed to *fd-3.* Because FT and ABA co-regulate bud-growth in Aspen (Tylewicz et al., 2018), I also crossed the *FD::abi2-1* transgenic line to *ft-10.* Using this material, I aimed to understand the joint role of

ABI2, FT and FD at the SAM in floral induction and inflorescence development. Although introducing ectopic *abi2-1* into *fd-3* did not affect total leaf number, a slight significant reduction in rosette leaf number was observed for *ft-10 FD::abi2-1* compared with that of the single *ft-10* mutant (Figure 4.12A). This suggests an opposing role for ABI2 and FT in promoting floral transition. Surprisingly, a stronger reduction in total leaf number and rosette leaf number was observed for *fd-3 ft-10 FD::abi2-1* compared with *fd-3 ft-10*. Indeed, *fd-3 ft-10 FD::abi2-1* transitioned earlier than *ft-10 FD::abi2-1* (Figure 4.12B). Next, the plants were scored at GPA. Unexpectedly, many plants underwent premature GPA, possibly because of insufficient watering. Therefore, plants were only scored for I1 length, which is stable before GPA. The I1 length was greater in *fd-3* and lower in *FD::abi2-1 #1*, as previously observed (Figures 4.4B, 4.8D and 4.12C). *fd-3 FD::abi2-1 #1* resembled the wild-type and *FD::abi2-1 #1* (Figure 4.12C). This indicates that the lack of *FD* weakly supressed the *FD::abi2-1* phenotype. *fd-3* and *ft-10* had a similar I1 length, but the length was reduced in the *fd-3 ft-10* double mutant. The I1 length of *fd-3 ft-10 FD::abi2-1 #1* was similar to that of the transgenic *FD::abi2-1 #1* line.

These data show that late flowering and plant height of *ft fd* are slightly supressed by disrupting ABA signalling at the SAM in the *FD::abi2-1* lines under LD.

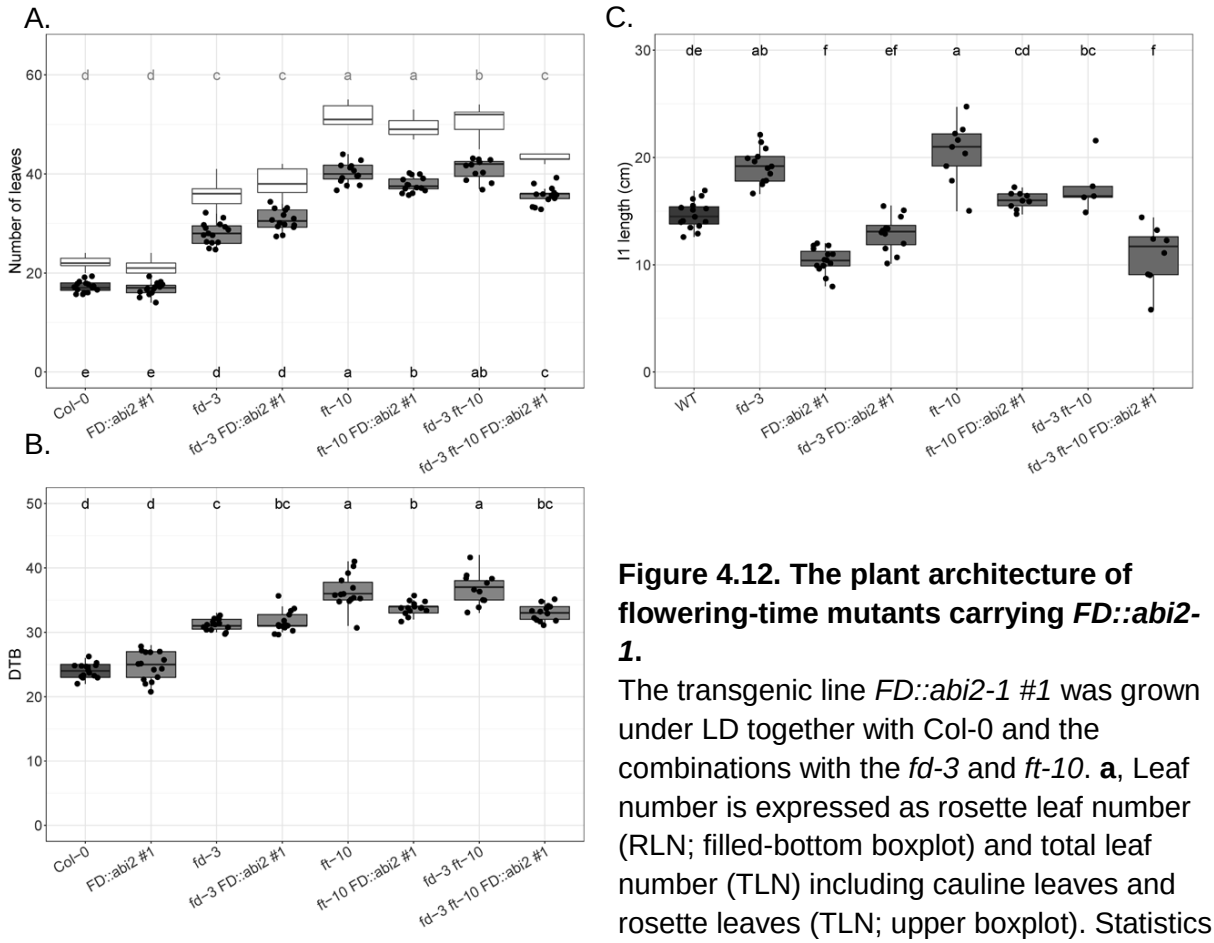

Figure 4.12. The plant architecture of flowering-time mutants carrying *FD::abi2-1*.

The transgenic line *FD::abi2-1 #1* was grown under LD together with Col-0 and the combinations with the *fd-3* and *ft-10*. **a**, Leaf number is expressed as rosette leaf number (RLN; filled-bottom boxplot) and total leaf number (TLN) including cauline leaves and rosette leaves (TLN; upper boxplot). Statistics for TLN and RLN are displayed on top and bottom, respectively. **b**, Days to bolting is

presented for each genotype; *n* = 11–15. **c**, The length of the I1 zone was scored at GPA for *FD::abi2-1 #1* and *fd-3* to understand the role of ABA and FD at the SAM in I1 elongation; *n* = 5–15. Data for genotypes with the same letter are not statistically significantly different from each other (ANOVA, Tukey's HSD test).

4.3 Discussion

The role of FD after the floral transition has not been extensively addressed in Arabidopsis. In this chapter, protein localisation and shoot phenotypes of *fd, fdp fd* and the inducible *FD::GR:FD* line were studied. Flowering time and shoot architectural traits were also measured for the generated *FD::abi2-1* transgenic line in which ABA signalling is impaired in the domain of expression of *FD*.

4.3.1 Regulatory functions of FD and FDP in shoot apical meristem arrest

The transcription factors FD and FDP are involved in the floral transition and bind to common target genes involved in the ABA-signalling pathway, such as *ABI FIVE BINDING PROTEIN 4* (*ABF4*; Romera-Branchat et al., 2020). In addition to these common functions, FD and FDP have independent functions, because they bound 540 and 79 unique regions in the Arabidopsis genome, respectively (Romera-Branchat et al., 2020). FD plays a greater role in regulating the floral transition than FDP, because it binds specifically to the genes of many floral integrators (Collani et al., 2019; Romera-Branchat et al., 2020; Zhu et al., 2020). However, introduction of *fdp-CRP2* into *fd-3* delays the floral transition slightly more than that of *fd-3* alone, which indicates that FDP promotes floral induction in the *fd* background (Romera-Branchat et al., 2020). To define the interaction between FD and FDP after floral induction, architectural traits of the *fd-3 fdp-CRP2* inflorescence shoot were measured at GPA. The *fd-3 fdp-CRP2* plants grew for a longer period, were taller, and bore more fruits on the main shoot than single *fd-3* plants, demonstrating positive additive effects between FD and FDP after the floral transition (Figure 4.2). By contrast, *fdp-CRP2* mutation alone had no detectable effect on shoot growth after floral transition. It would be interesting to detect *WUS* and *CLV3* mRNA by *in situ* hybridisation assays on Col-0 and *fd-3 fdp-CRP2* inflorescence to confirm the GPA phenotype (Schoof et al., 2000; Dijkwel and Lai, 2019). A correlation matrix for shoot architectural traits of mutants involved in photoperiodic flowering responses showed that shoot height and fruit number were not correlated with the length of the vegetative phase, suggesting a novel negative role for FD and FDP in plant shoot architecture (Figure 4.6A). However, the mechanisms by which the two bZIP transcription factors synergistically constrain shoot length and promote meristematic arrest is unknown. Laser-assisted microdissection performed on arrested meristems and reactivated meristems after fruit removal shows that *FD* and *FUL* are differentially expressed, suggesting their expression is regulated during meristem arrest (Wuest et al., 2016). Also, the *FUL* promoter is targeted by

FD during the vegetative growth and its activity is reduced in *fd* mutants (Collani et al., 2019; Zhu et al., 2020). Interestingly, the *ful* mutant has a delayed GPA and a greater number of fruits on the main shoot than wild type, similar to *fd* (Balanzà et al., 2018), suggesting that FD might be an upstream regulator of *FUL* during GPA. This can be tested directly using the *fd-3 FUL::FUL:9AVENUS* line generated in this thesis. Notably, *FD* transcripts accumulate during the lifespan of the plant but slowly decrease in abundance as the plant ages (Supplementary Figure 4.2; Figure 4.1D). Combination of the *ful-2* mutation with *fd-3* and *fdp-CRP2 fd-3* and measurement of the time to GPA and fruit number on the main shoot would confirm the existence of genetic interactions. The *ful-2* and *fd-3* mutants were crossed by Dr. A. van Driel and the homozygous double mutant was selected for this thesis. However, in LD conditions, neither a late-flowering phenotype nor increased silique number was observed in *ful-2* compared with Col-0 (Chapter 3, data not shown), in contrast to the report of Balanzà et al (2018). During the experiment, the late-flowering *fd-3* and *fd-3 ful-2* plants experienced insufficient watering, which affected the time at which they reached GPA. Because of time constraints, the experiment was not repeated, and therefore it remains untested whether the double mutant shows a further delay in GPA compared to either single mutant.

The AP2/FUL module regulates GPA in Arabidopsis (Martínez-Fernández et al., 2020); however, the level of *AP2* transcripts was similar in 3-week-old meristems of Col-0 and *fd* after their respective bolting (Figure 4.3B). Col-0 reaches GPA before *fd* and differential *FUL* levels were expected. Quantification of *FUL* expression in meristem-enriched apices of Col-0 by RT-qPCR showed that the level of *FUL* transcripts was four-fold greater at day 42 than at day 21, but *AP2* was expressed at a similar level at both time points (Supplementary Figure 4.2). These results contrast with the postulated repression of *AP2* by FUL to promote GPA (Gonzalez-Grandio et al., 2017). Nevertheless, the expression of both proteins may overlap temporally before *AP2* is repressed or *AP2* downregulation may occur after the time points used for these RT-qPCR experiments. No difference in the level of *AP2* and *FUL* expression was observed among any of the late-flowering genotypes and Col-0 at 3 weeks after bolting (Figure 4.3B). Therefore, the downregulation of *HB-21* and *BLH1* observed in *fd* and *fd fdp-CRP2* 3 weeks after bolting may be independent of the described FUL/AP2 pathway (Gonzalez-Grandio et al., 2017). It also suggests that FD may regulate *HB-21* expression before the decrease in *AP2* expression. However, using RT-qPCR it is difficult to distinguish expression of *FUL* and *AP2* in the meristem from that in young floral primordia, and it would be interesting to analyse the expression of these genes in *fd* mutants and Col-0 during GPA using fluorescent protein fusions and confocal microscopy.

FDP, but not *FD*, was downregulated after the AP2-mediated re-activation of arrested shoot apical meristems, which suggests that *FDP* plays a positive role in GPA (Martínez-Fernández et al., 2020). AP2 was reported to bind the *FDP* promoter (Yant, 2010), but reanalysis of the data demonstrated no significant enrichment at *FDP* genomic locus (Dr. E. Severing). The *AP2* genomic locus is enriched in ChIP-seq assays by GFP:FD expressed from the *SUC2* promoter and the native *FD* promoter, but no differences in the level of *AP2* transcripts was observed in *fd* mutant compared with wild type (this chapter; Collani et al., 2019; Zhu et al., 2020). Thus, I propose that FD and FDP regulate GPA independently of AP2/FUL. Nevertheless, the functions of AP2, FD and FDP converge to regulate GPA, and it is expected that all three proteins regulate common downstream targets. For instance, AP2 and FD both bind to *HB-21* (Yant et al., 2010; Collani et al., 2019; Romera-Branchat et al., 2020; Zhu et al., 2020; Dr. E. Severing). In axillary buds, the expression of *HB-21* is upregulated by BRANCHED 1 (BRC1) to promote ABA synthesis in light with a low red: far-red ratio or in SD and thereby inhibit axillary bud growth (Gonzalez-Grandio et al., 2017). The *hb-21* mutant produces more fruits on the main shoot than wild type (Martínez-Fernández et al., 2020). Because genes involved in ABA responses are upregulated in meristems towards GPA, *HB-21* appears to be a major regulator of GPA (Wuest et al., 2016), where it might have similar roles as in axillary meristems by inducing meristem arrest through increasing ABA levels. Moreover, AP2, FD and FDP all bind to the promoter of *AUXIN RESPONSE FACTOR 2* (*ARF2*) in inflorescence tissues (Yant et al., 2010; Romera-Branchat et al., 2020). Mutation of *ARF2* leads to a late-flowering phenotype and confers increased longevity, similar to the *fd-3* phenotype (Ellis et al., 2005; Lim et al., 2010). Although, the loss-of-function *arf2* mutant has fewer siliques on the main shoot than wild type (Van Daele et al., 2012), *HB-21* and *ARF2* are two candidate genes with which to study GPA, and specifically the roles of FD and FDP, in Arabidopsis.

Delayed GPA and taller shoot phenotypes of *fd-3 fdp-CRP2* are stronger than that of single *fd-3* mutants but *BLH1* and *HB-21* are equally downregulated in both genotypes, suggesting that mutation of *FD* only affects the expression of both genes (Figures 4.2A and 4.3A). A more detailed temporal analysis could be performed to test whether the mRNAs of these genes remain at low levels for longer in *fd-3 fdp-CRP2* compared to *fd-3*. However, it is more likely that other genes change in expression in *fd-3 fdp-CRP2* but not in *fd-3* to confer longer GPA and the shoot-architecture phenotype. An important experiment to identify differentially expressed genes that are regulated by FD and FDP would be to perform RNA-seq of meristem-enriched tissues of *fd*, *fdp* and *fd fdp* compared with Col-0 at 21 LD, and 2, 3 and 4 weeks after bolting. In addition to the phenotypic analysis of these genotypes, this approach would extend knowledge about the regulation of GPA by FD and FDP.

4.3.2 The vegetative phase of photoperiodic flowering-time mutants does not correlate with the number of fruits produced on the main shoot

I aimed to identify interactions between the traits of flowering time and shoot architecture among mutants involved in the photoperiod pathway. The phenotypes of plants of twenty-two genotypes were analysed in LD in the greenhouse. The numbers of rosette and cauline leaves were used as a proxy for the length of the vegetative phase, and the number of siliques on the main shoot was used as a proxy for yield-related traits. A correlation matrix showed no interaction between the regulation of the length of the vegetative phase and number of siliques among the selected genotypes (Figure 4.6A). In this experiment, plants received 16 h of natural light supplemented by light bulbs whenever the light intensity was insufficient and continuous nutrition via watering. These growth conditions are optimal for plant growth but do not mimic native environmental conditions. As an analogous example, the yield of maize plants with a longer vegetative phase is lower in the natural environment, because reproductive development is not completed before the end of the growing season (Parent et al., 2018). Plotting yield and leaf number in maize resembles a bell-shape curve, whereas for late-flowering Arabidopsis plants, the interaction curve tended towards a plateau (Figure 4.6B). This can be explained by the constant growth conditions used for the Arabidopsis experiments here; for example, the growth temperature was maintained at 21°C in the greenhouse. Higher temperatures affect shoot morphology and yield in Arabidopsis (Ibanez et al., 2017), which makes it difficult to predict the yield-related traits of Arabidopsis late-flowering mutants in natural environments and to establish whether flowering time and yield would be correlated in native growth conditions. In the growth conditions of the experiments described here, several plants failed to reach GPA and many dormant buds remained unopened. In these experiments, *ful* mutant plants produced a similar number of fruits on the main shoot to Col-0, which is contrary to the findings of other studies (Balanzà et al., 2018; data not shown). The number of secondary inflorescences depends on the genetic background and the available nitrogen content in the soil (de Jong et al., 2019). The phenotypes under consideration are greatly influenced by environmental parameters and stricter control of plant growth conditions will be necessary to compare the GPA and yield phenotypes obtained here with those described in other studies.

The lengths of the I1 and I2 phases as well as the number of fruits varied for all photoperiodic flowering-time mutants (data not shown). This suggests that some genes involved in the photoperiod pathway affect shoot architecture of Arabidopsis, without correlating with the length of their vegetative phase (Figure 4.6). More inflorescence traits should be scored to confirm this. Arabidopsis hybrids between Col/L*er* and Ws/L*er* show increased plant height and yield-related traits (Wang et al., 2020). In these plants, the

expression level of genes that promote the floral transition, such as *FT*, *SOC1* and *FUL*, is lower in leaves, suggesting that these genes are part of the plant architecture organisation. The choice of the photoperiodic mutants for this study can be controversial. For instance, *tfl1* strongly affects floral transition and the SAM terminates quickly (Shannon and Meeks-Wagner, 1991; Hanano and Goto, 2011). To confront this, I removed *tfl1* as well as *tfl1* higher order mutants from the dataset. It did not modify the relationship of the correlation plot (data not shown). The *ful-2* mutant has short siliques (Mandel and Yanofsky, 1995; Gu et al., 1998). Reduced number of fruits per silique influences source–sink connection and the fate of the inflorescence meristem and may create unbalance within the other photoperiodic mutants (Hensel et al., 1994; Balanzà et al., 2018; Ware et al., 2020).

4.3.3 The effect of FD on ABA signalling

The *abi2-1* mutation in the L*er* background leads to a reduced sensitivity to ABA, due to loss of the interaction of ABI2 with the ABA receptor PYL/PYR/RCAR. The *abi2* mutant harbours a missense mutation that causes a substitution of a glycine^{168} residue in wild type with asparagine (Rodriguez et al., 1998). The *abi2-3* mutation in the Col-0 background was identified from a genetic screen (Cai et al., 2014) and is also insensitive to ABA because it contains the same mutation as *abi2-1* in L*er.* The *ABI2::abi2-1* transgenic mutant line was generated to study ABA and brassinosteroid signalling (Wang et al., 2018). However, the localization of ABI2 protein is unknown and little is known about the role of ABA signalling downstream of ABI2 at the shoot apical meristem in the absence of stress. To address this, I generated an *FD::abi2-1* transgenic line using the L*er abi2-1* CDS to transform Col-0. *FD::abi2-1* attenuates ABA-mediated gene responses in tissues enriched for apices (Figure 4.7C). Under LD conditions, the flowering time of *FD::abi2-1* resembled that of wild type, whereas *fd-3* was late flowering. Plants of the *fd-3 FD::abi2-1* line produced two more leaves at bolting on average compared with the *fd-3* mutant (Figure 4.12), suggesting that disruption of ABA signalling has little effect of the flowering-time phenotype of *fd-3*. The length of the vegetative phase under SD was reduced when *abi2-1* was expressed within the FD expression domain from the *FD* promoter (Figure 4.10). The *abi2-1* mutant in the *Ler* background modulated flowering time in a similar way (Supplementary Figure 4.4), suggesting that the ABA signalling pathway is active under SD and negatively regulates the floral transition within the *FD* domain. The total leaf number at bolting of *ft-10 FD::abi2-1* was statistically significantly lower than that of *ft-10* under LD and *fd-3 ft-10 FD::abi2-1* was the earliest-flowering genotype among the *ft fd* mutant combinations (Figure 4.12). Because the photoperiodic flowering pathway is impaired in the *ft* mutant, the ABA signalling pathway appears to be either downstream of FT or acting in parallel to it, and can partially explain the SD flowering-time phenotype of the *FD::abi2-1* line. Moreover, the early-flowering-phenotype of *abi1-1* under SD is rescued by downregulation of *SOC1* transcription in the *abi1 soc1*

double mutant (Riboni et al., 2016). Transcript levels of *FUL* and *FD* are upregulated in *FD::abi2-1* lines but the expression levels of *SOC1* and *FT* were not quantified (Figure 4.10).

Accumulating evidence suggests that the ABA pathway regulates GPA at the SAM (Wuest et al., 2016; Martínez-Fernández et al., 2020). *BLH1* and *ABI2* are involved in ABA signalling and both were shown to be direct targets of AP2 and FD by ChIP-seq (Yant et al., 2010; Zhu et al., 2020). Both genes are downregulated in apical meristems that are reactivated by AP2 (Martínez-Fernández et al., 2020). However, little is known about the molecular mechanism by which ABA promotes GPA. Greater yield was observed for the *abi2-1* mutant in L*er* and for *FD::abi2-1*, suggesting that these genotypes have a delayed GPA (Figure 4.8C; Hensel et al., 1994). ABI2 appears to act at the SAM to regulate early meristematic arrest and thus, limits the number of fruits produced on the main shoot. To understand the genetic interaction between ABI2 and FD at the SAM, it will be necessary to score the number of flowers and the timing of GPA for *fd-3 FD::abi2-1* plants, to determine if they have additive or epistatic effects. If the *fd* GPA phenotypes are due to differences in ABA-gene expression, I hypothesize that *fd FD::abi2-1* plants should produce a similar number of fruits to *FD::abi2-1*.

Extensive crosstalk among plant hormones challenges the characterization of individual hormones in specific tissues (Golldack et al., 2013). Hormones such as GA and ABA have antagonistic effects and it would be interesting to apply GA in the *FD::abi2-1* lines to test whether it restores shoot phenotypes such as the length of the I1 phase.

4.3.4 Breeding opportunities?

Orthologues of Arabidopsis genes involved in the photoperiodic flowering pathway have been studied for their role in crops (Blumel et al., 2015). FD orthologues are found in several cultivated vegetables and fruit trees (Tsuji et al., 2013). The late-flowering phenotype of *fd fdp* is less severe than that of *ft tsf* and shoot architectural traits as well as yield are particularly improved in the *fd fdp* double mutant. In tomato, mutants in the *TFL1* and *FT* orthologues are early and late flowering, respectively, but both produce low yield (Park et al., 2014). The yield of the mutant in the *FD* orthologue is similar to that of the *TFL1* and *FT* orthologue mutants. This is not what I observed in *Arabidopsis*, as *tfl1* produces a reduced number of fruits compared with that of the *ft* and *fd* mutants (Figure 4.6B). Median flowering time and optimal yield is found in the *tfl1 fd/+ ft/-* orthologue mutants of tomato (Park et al., 2014). These mutations influence the dose-dependent action of the florigen activation complex on the transcription of its targets and thereby the determinacy of the inflorescence meristem and ultimately the number of flowers and fruits formed. The relationship between flowering time and yield obtained by Park et al. is similar to what I observed with the photoperiodic mutant analysis in Arabidopsis, in that the relatively mild late flowering of *fd fdp*

produced the highest seed yield (Figure 4.6B). Testing heterozygotes for mutations in *FD*, *FDP*, *FT* and *TFL1* would allow a more direct comparison between the Arabidopsis and tomato results.

To assess the breeding applications of plants that lack FD and FDP orthologues, several phenotypic aspects should be considered. At GPA in Arabidopsis, which is analogous to the developmental stage of harvesting of crop plants, the number of siliques on the main shoot was 18% greater than that of wild type for *fd-3* plants and 56% greater for *fd-3 fdp-CRP2* plants (Figure 2). In particular, silique length and seed number per silique were greater in *fd-3* and *fd-3 fdp-CRP2* than in wild type (Supplementary Figure 4.1). No defect in cotyledon greening was observed for either genotype (Romera-Branchat et al., 2020). Each of the cauline leaves of *fd-3* plants subtends an inflorescence branch and the number of secondary inflorescences was greater in these genotypes (Chapter 2, Figure 2.1, and Figure 4.4 of this chapter). Although the total number of seeds produced by *fd-3* plants was not quantified, yield-related traits were improved by mutation of *FD* and *FDP*: The aerial dry weight of *fd-3* and *fd-3 fdp-CRP2* at 3 weeks after bolting was about twice heavier that of wild type (Supplementary Figure 4.1). However, the main shoots of *fd-3* and *fd-3 fdp-CRP2* plants were 14% longer or 30% longer, respectively, than those of wild-type. This trait may represent a limitation to the agricultural use of lines that lack *FD* and *FDP* orthologues. However, a positive agricultural trait is that the stem diameter of *fd* plants is greater than that of wild type, which confers increased strength to the overall plant shoot (A. Pajoro, *in preparation*). The bolting of *fd-3* and *fd-3 fdp-CRP2* was delayed by about 18% and 27%, respectively, compared with that of the control Col-0 (Figure 4.2). GPA was also extremely delayed in FD and FDP mutants. Although an extension of the growth period before harvesting is not a trait that is usually selected for by breeding, identifying the genes that regulate yield and biomass in *fd* and *fd fdp* would be highly relevant for breeding strategies.

4.4 Supplementary figures

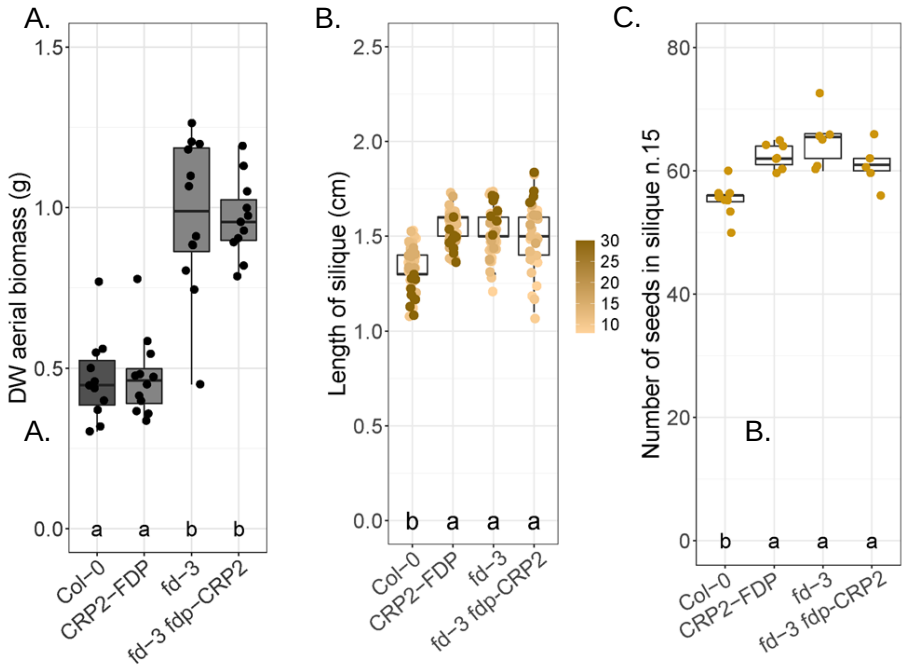

Supplementary Figure 4.1. Biomass and seed production are positively affected in *fdp-CRP2* and *fd-3* mutants.
A, Aerial biomass of plants harvested 3 weeks after bolting under LD conditions; *n* = 11–12. Statistical tests were performed using ANOVA followed by Tukey's HSD test. DW, dry weight. **B**, Silique length was measured with a ruler at 5 weeks after bolting for each genotype (left). The silique number 1 (n.1) was defined as the fruit of the first open flower on the main shoot. Subsequent silique numbers were defined from the base of the I2 zone to the top of the main shoot. The siliques n.8 to12 and n.15 and n.30 were measured. Lighter-coloured dot represents the first silique numbers whereas the darkest brown dots represent siliques n.30, gradient colour is indicated on the right. Seeds produced by silique n.15 were counted for each genotype (right). For Col-0 and *fdp-CRP2*, n = 9; for *fd-3*, n = 8 and for *fd-3 fdp-CRP2*, *n* = 5.

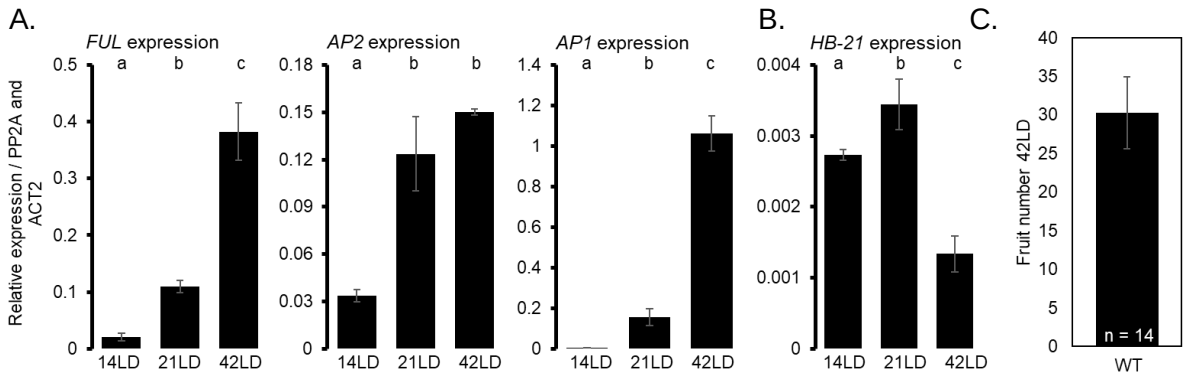

Supplementary Figure 4.2. Expression levels of genes involved in flower formation. and GPA.
A, Quantification of the expression of *FUL*, *AP2* and *AP1* mRNAs and **B**, *HB-21* mRNA by RT-qPCR in wild-type Col-0 at the indicated time points. Data represent the mean of three biological replicates ± SD and statistics were performed using ANOVA followed by Tukey's HSD test. **C**, Mean number of siliques at the main shoot of wild-type Col-0 at day 42 from samples harvested for RT-qPCR in **A**, and **B**. The number of individuals is indicated at the bottom and the error bar represents ±SD. Plants were grown in growth cabinets under LD.

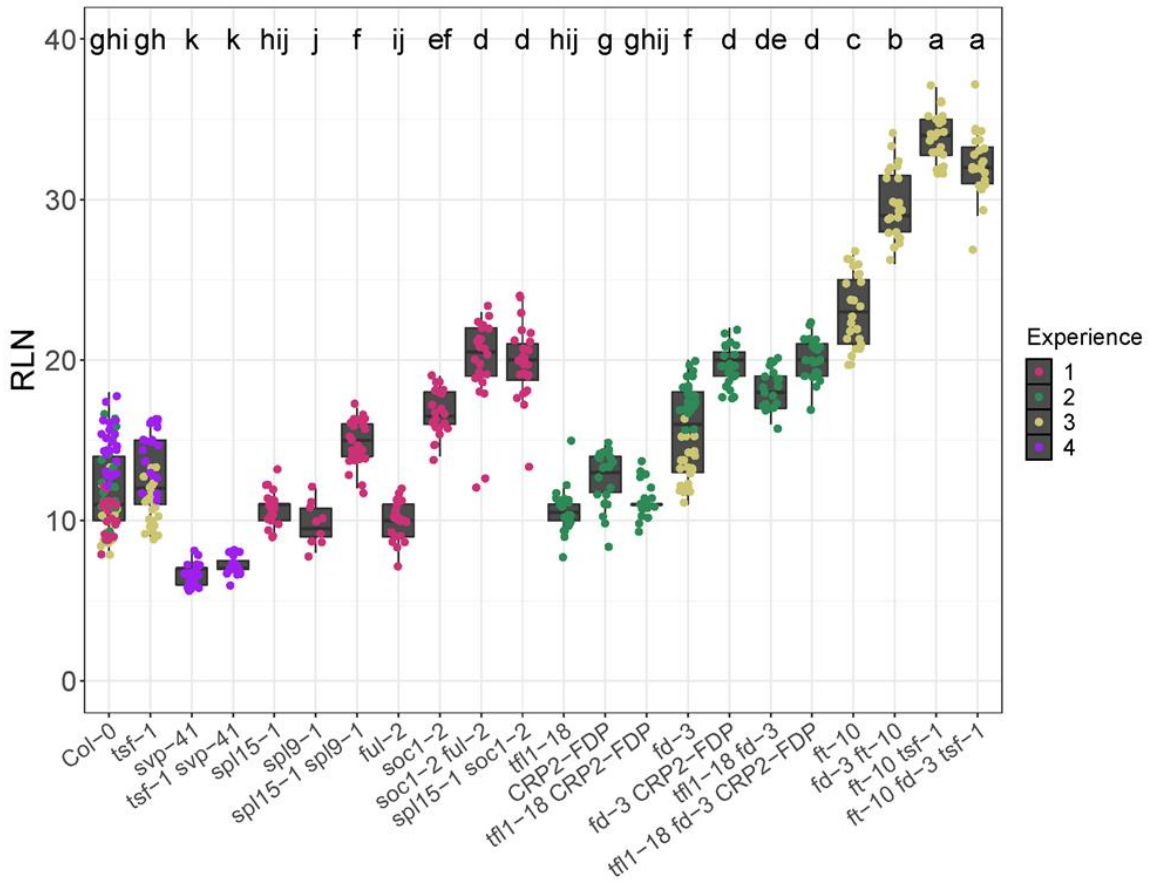

Supplementary Figure 4.3. Flowering time of mutants for genes involved in the photoperiodic and autonomous pathways.
Flowering time was scored as rosette leaf number (RLN) and plants were grown in the greenhouse under LD conditions. The data were derived from four independent experiments. Each dot represents one individual and the colours indicate the experiment number. Box-plot medians are indicated by the centre line and were analysed by ANOVA followed by Tukey's HSD test.

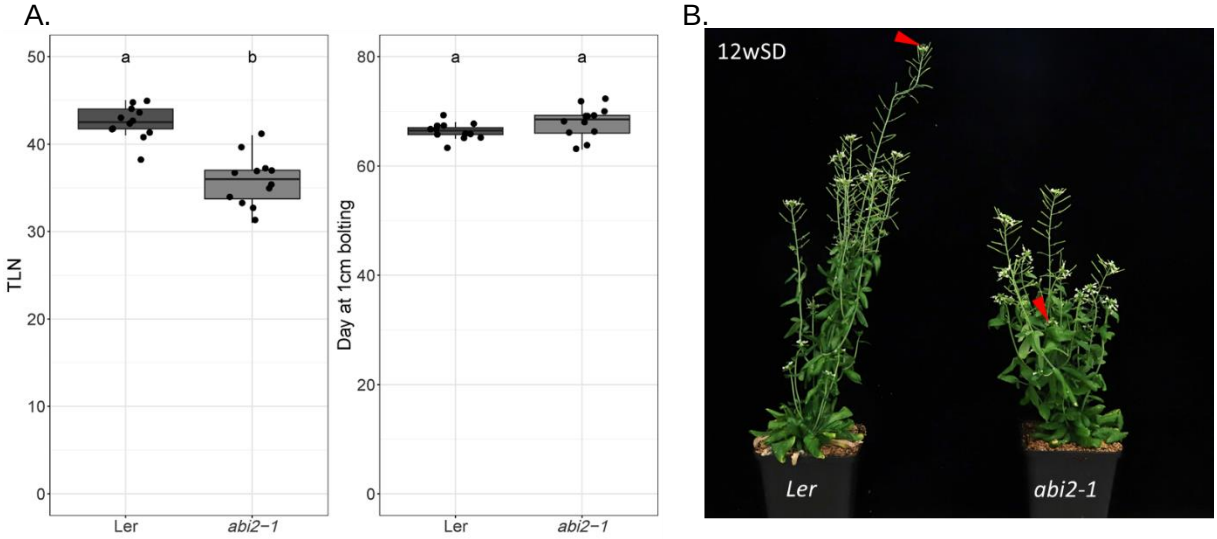

Supplementary Figure 4.4. Flowering time analysis of L*er* and *abi2-1* under SD.
A, Flowering time was scored as total leaf number (TLN) and days to bolting. The two genotypes were grown under SD conditions. To prevent water loss, the plants were covered with a plastic cover for four weeks from the day of sowing; *n* = 12. Box-plot medians are

indicated by the centre line and data were analysed with ANOVA followed by Tukey's HSD test. **B**, Image of representative 12-week-old L*er* and *abi2-1* plants. The red arrowhead indicates the primary inflorescence of the plant which stops to elongate in the *abi2-1* mutant.

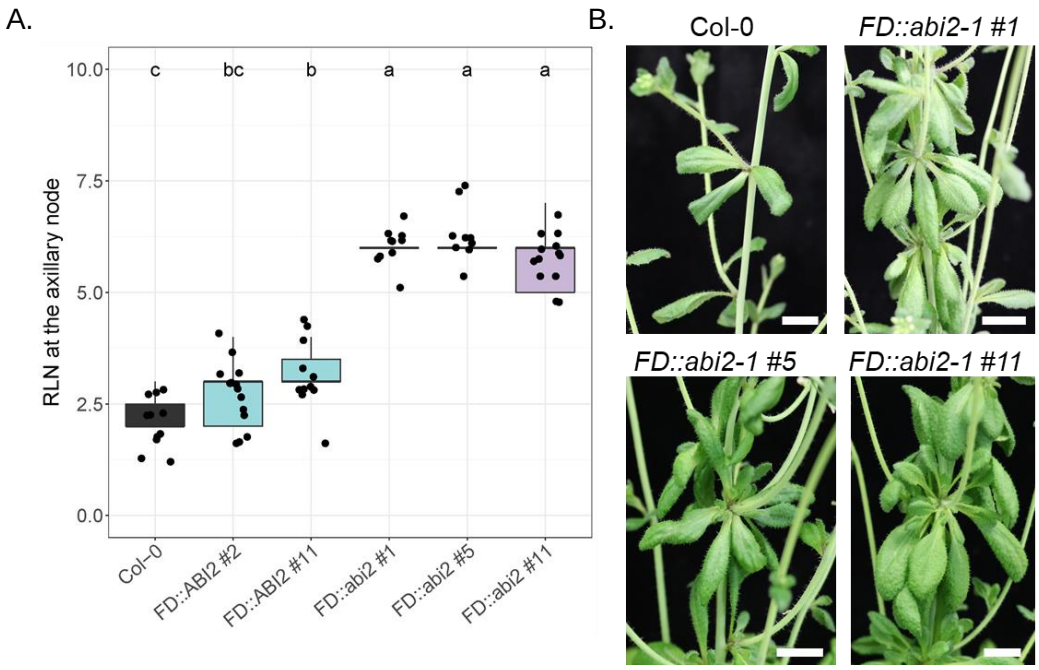

Supplementary Figure 4.5. Architectural traits along the main shoot of *FD::abi2-1* lines under short days.
A, Rosette leaf number of the third aerial rosette from the top of the main shoot was scored for each genotype 20 days after flowering; *n* = 9–14. Box-plot medians are indicated by the centre line and data were analysed by ANOVA followed by Tukey's HSD test. **B**, Image of the aerial rosette of Col-0 and *FD::abi2-1* transgenic lines *#1, #5* and *#11* under SD, 20 days after flowering. The scale bar represents 1 cm.

Chapter 5. Summary of the PhD thesis chapter conclusions and concluding remarks

The FD–(14-3-3)–FT/TSF complex promotes floral transition in Arabidopsis under LD. The role of FD in activating transcription at the SAM of downstream genes involved in the floral transition, and floral integrators in particular, has been described (Abe et al., 2005; Wigge et al., 2005; Collani et al., 2019; Romera-Branchat et al., 2020; Zhu et al., 2020). FD is strongly expressed in the SAM at all stages of development, but activates different targets in a temporal sequence: it accumulates at the SAM during seedling development before the translocation of FT and TSF from the leaves to the SAM and thus prior to floral induction, and at that stage has been implicated in ABA-mediated seedling greening (Romera-Branchat et al., 2020). Subsequently, FD promotes *FUL* transcription within the SAM, whereas *AP1* transcription is promoted later by FD, during floral primordium development. Genetic evidence supports a role for FD downstream of FT and its paralogue TSF, as *fd* mutation partially suppresses the early-flowering phenotype of 35S::*FT* plants (Abe et al., 2005; Wigge et al., 2005) and introduction of the *fd* mutation into the *ft tsf* mutant does not delay flowering further suggesting they act in the same pathway (Jang et al., 2009). This PhD project aimed to define the multiple functions of FD in the photoperiodic induction of the floral transition and to explore possible functions after floral induction during inflorescence development.

5.1 Two conserved motifs in the *FUL* promoter are bound by FD but are not essential for *FUL* transcription *in planta*

Genome-wide ChIP-seq analysis previously identified direct targets of FD and established that FD preferentially recognises G-box *cis*-elements (Collani et al., 2019; Romera-Branchat et al., 2020; Zhu et al., 2020). This analysis confirmed that FD binds to the *FUL* promoter, and I showed that the accumulation of *FUL* mRNA and the encoded FUL protein was delayed in *fd* compared to wild-type plants (Figures 3.1 and 3.4B). Using *in silico* tools, I showed that the proximal promoter region of *FUL* that was implicated in FD-binding in the ChIP-seq experiments contains two ACGT motifs that represent the core of the bZIP motif and are conserved among *Brassicaceae* species (Figures 3.3 and 3.4A). I hypothesized that mutation of these two motifs might prevent the activation of *FUL* by FD and thereby cause a slight delay in flowering similar to that reported in the *ful* mutant. Although ChIP-qPCR confirmed that FD binds to this so-called *B-FD* region, mutation of the two ACGT motifs in plants expressing *FULm1m2* did not affect flowering time under LD nor the dynamics of FUL protein accumulation at the SAM (Figures 3.4B, 3.7 and 3.8). The SPL15 transcription factor is a major positive regulator of *FUL* under SD as *FUL* expression is strongly delayed under SD in an *spl15* mutant, whereas the FD–(14-3-3)–FT/TSF complex is important for *FUL* expression under LDs because its expression is strongly delayed under these conditions in

fd and *ft tsf* mutants (Figure 3.1; Torti et al., 2012; Hyun et al., 2016). Thus, the control of *FUL* expression is considered to represent a point of intersection between the LD and SD pathways. Unexpectedly, mutation of putative SPL-binding sites in the *FUL* promoter in *FULmGTAC* transgenes, caused *FUL* expression to occur earlier and consequently the transgenic plants were early flowering under LD (A. van Driel PhD thesis, 2020). This was assumed to occur because an unidentified SPL transcription factor bound to this site during seedling development to repress *FUL* transcription. The early flowering phenotype of these plants was not affected by disruption of the putative FD binding sites in the *B-FD* region (Figures 3.7, 3.8 and 3.9). Moreover, mutagenesis of the putative FD-binding C-box in the *AP1* promoter *in planta* did not affect the *AP1* expression pattern in plants (Benlloch et al., 2011). SPL transcription factors have also been proposed to mediate FD binding to DNA (Jung et al., 2016). To reconcile the delayed expression of *FUL* in *fd* mutants, but the absence of any effect of mutating putative FD binding sites, I hypothesise that: 1) FD activates *FUL* transcription directly and indirectly by activating another transcription factor that can act redundantly with FD or 2) FD binds to other sites in the *FUL* promoter that were not detected by ChIP-seq or are used when the primary sites are mutated. In addition, mutation of the putative FD and SPL15 binding sites in the same promoter did not affect *FUL* expression, indicating that FD binding to these sites is not responsible for the early activation of *FUL* when the SPL15 binding sites are mutated and that there is no evidence for SPL15 and FD competition for DNA binding at the *FUL* promoter. Thus, the precise mechanistic role for FD in *FUL* transcriptional activation remains unknown, and a broader understanding of which regulatory proteins bind to the *FUL* promoter, particularly those that are expressed in response to FD activity, and their functions in *FUL* regulation will be required to explain how *FUL* is activated at the SAM under LD.

5.2 The timing of FD induction is crucial for floral transition

The temporal regulation of the genetic components that promote floral transition at the SAM is complex but highly conserved in plants (Meir et al., 2021). Arabidopsis plants that are transferred from SD to LD show an increase in the level of *FD* and *SOC1* mRNA before *FUL*, *AP1* and *LFY* are expressed (Torti et al., 2012). Similarly, when *FD::GFP:FD fd-2* and *fd-2* plants are transferred from SD to LD, *FD* is upregulated one day after transfer, *FUL* expression increases from the second day and the *AP1* mRNA level increases on the fifth day (Collani et al., 2019). I used a GR:FD fusion protein to induce FD activity at defined times and found that the induction of GR:FD at day 12 caused a slight reduction in the number of leaves produced by the SAM at bolting (Figure 2.4), suggesting that at this stage FD expression levels are limiting on flowering time. This early flowering was explained by morphological changes at the SAM caused by GR:FD induction and upregulation of flowering-time integrators in the induced GR:FD plants compared with the control plants.

Furthermore, RNA-seq analysis revealed that the levels of *FUL*, *AP1*, *SPL4* and *LFY* mRNA increased after FD induction and that expression of *SNZ* was downregulated two days after induction (Figure 2.7). *FUL* mRNA was detected before that of *AP1*, confirming the differential temporal activation of FD targets in response to GR:FD activation. The sequential activation of FD targets might be explained by various mechanisms. Specific targets might require an FD complex containing different components, as on the FD functions as part of large transcriptional complexes and FD-interaction partners are FT, TFL1, 14-3-3s, TCPs, SPLs or the identified putative MBF1 and BT2 cofactors (Table 2.1). The composition of these complexes is likely to be dynamic and lead to the activation of different targets. A related possibility is that post-translational modification of FD might change with time altering the activity of the protein, and leading to the activation of different genes, Notably, the phosphorylation site at the SAP motif, which has been shown to be required for FD promotion of flowering (Abe et al., 2005; Collani et al., 2019), may be dynamically regulated and determine which targets can be activated. Testing these ideas will depend on a temporal investigation of FD phosphorylation and protein partners.

FD is continuously expressed at the SAM (Figure 4.1; Romera-Branchat et al., 2020). To identify the time period during which FD is required to activate floral integrators and promote floral transition, I induced FD in *FD::GR:FD fd-3* transgenic plants at different developmental time points. I concluded that the greatest degree of complementation of the *fd* late-flowering phenotype occurs following DEX application at three-day intervals from day 7 to day 16 (Figures 2.3A, 2.4 and 4.5A). The activity of FD is required at the SAM for several days to regulate its targets supporting the idea that it is continuously required during floral induction for flowering to proceed. How this temporal activity overlaps with the expression of its interacting proteins including FT and TFL1 at the SAM has not yet been described in detail.

5.3 FD regulates shoot architecture and fruit production

The FD orthologues of the legume species *Medicago truncatula* and *Pisum sativum* are expressed in the reproductive SAM and mutation of these genes causes defects in plant architecture (Sussmilch et al., 2015; Cheng et al., 2021; Zhang et al., 2021). I showed that *fd* and *fd fdp-CRP2* Arabidopsis plants produced taller shoots with more siliques on the main shoot than wild-type plants, probably due to a delay in GPA (Figure 4.2). These phenotypes were correlated with and may be partially explained by the downregulation of *BLH1* and *HB-21* in *fd* and *fd fdp-CRP2* inflorescences (Figure 4.3). Mutation of *BLH1* and *HB-21*, both of which encode homeobox transcription factors and are discussed in more detail in the next section, affects the height of the main shoot and the number of fruits produced (Martínez-Fernández et al., 2020), and both have been implicated in ABA responses, consistent with the close relationship between FD and bZIPs involved in ABA signaling. The delayed GPA

caused by mutation of FD and FDP could not be linked to the AP2/FUL module (Martínez-Fernández et al., 2020), but further analysis is required to confirm this.

To distinguish between the regulatory functions of FD that determine floral transition and shoot architecture, I showed that induction of FD by multiple DEX treatments after the floral transition reduced the height of the main shoot and the number of fruits produced compared with wild-type plants (Figure 4.5). This illustrates that FD mediates inflorescence development after floral induction in the inflorescence meristem. The loss of function of positive regulators of the floral transition causes late flowering (Koornneef et al., 1991). I showed that the length of the vegetative phase of these mutants could not be correlated with the height of the main shoot nor the number of fruits produced on the main shoot (Figure 4.6A). However, I showed that *fd* and *fd fdp-CRP2* showed altered inflorescence architecture phenotypes, which make these genotypes useful for studying plant inflorescence development and yield-related traits.

5.4 FD regulates ABA-related genes such as *HB-21*, which contributes to inflorescence development

According to ChIP-seq datasets, FD binds to many genes related to ABA-signalling (Collani et al., 2019; Romera-Branchat et al., 2020; Zhu et al., 2020). Furthermore, FD is phylogenetically closely related to other bZIP transcription factors with central roles in ABA signalling (Jakoby et al., 2002, Dröge-Laser et al., 2018). ABA signalling regulates the phosphorylation of downstream proteins, particularly Group A bZIP transcription factors (reviewed in Cutler et al., 2010). The C-terminus of FD is also phosphorylated by at least two plant kinases (Kawamoto et al., 2015) and the interaction of FD with protein partners, as well as FD activity in the floral transition, require phosphorylation (Abe et al., 2005; Collani et al., 2019). However, the relationship between FD and ABA signalling in Arabidopsis development is poorly understood. Therefore, my goal was to study the connection between ABA signalling and FD. I showed that FD regulated the expression of *DREB2A, AITR1, HB53* and *HB-21*. These genes encode proteins involved in ABA-related responses and are bound by FD (Kim et al., 2011; Gonzalez-Grandio et al., 2017; Tian et al., 2017; Martínez-Fernández et al., 2020), but except for *HB-21*, it is unknown how the function of these genes relates to the floral transition or inflorescence development. The expression of *DREB2A* was upregulated shortly after DEX treatment in the RNA-seq experiment in vegetative meristems and its genomic region is bound by FD in one ChIP-seq dataset, suggesting that *DREB2A* is a direct target of FD (Figure 2.9; Romera-Branchat et al., 2020). However, the flowering-time of the *dreb2a* mutant in the Col-0 background was not altered under LD (Figure 2.9). Inflorescence tissues were used for the ChIP-seq experiment published by Romera-Branchat et al. (2020); therefore, the regulation of *DREB2A* by FD might be related to other

developmental responses, such as accelerated flowering as a drought-escape response, or inflorescence development.

Expression of *abi2-1* within the *FD* expression domain impaired ABA-signalling responses (Figure 4.7). However, even transgenic lines expressing high *abi2-1* mRNA levels in Col-0 background did not exhibit altered floral transition phenotypes under LD, and only slightly delayed flowering of *fd-3* (Figures 4.8 and 4.12). This suggests that FD is not phosphorylated by the ABA-signalling pathway, because mutant *FD* transgenes that cannot be phosphorylated do not promote flowering (Kawamoto et al., 2015; Collani et al., 2019). Interestingly, the *FD::abi2-1* transgene caused an increase in the number of fruits on the main shoot under LD (Figure 4.8C). In *fd-3* mutant, the increased number of fruits was attributed to GPA, a developmental process that involves ABA signaling (Figure 4.2; Wuest et al., 2016; Martínez-Fernández et al., 2020). If the *fd* GPA phenotypes are due to reduced expression of ABA-related genes, I hypothesize that *fd FD::abi2-1* plants should produce a similar number of fruits to *FD::abi2-1*.

5.5 Concluding remarks

Reproductive growth strategies involve the perception of environmental stimuli such as light and temperature. The genetic pathways in Arabidopsis that respond to exogenous and endogenous flowering signals converge at the SAM to determine the optimum time for flowering. The FD transcription factor is a component of the FD–(14-3-3)–FT/TSF complex that promotes floral transition. In addition to regulating other gene targets, FD activates *FUL* transcription in the vegetative SAM. I showed that FD is expressed in inflorescence meristems and its function contributes to stem growth and meristem arrest. To explain these phenotypes, I identified *HB-21*, to be a probable direct target of FD in inflorescence meristems. I confirmed that the temporal activation of FD is important for its function and I extended knowledge concerning its diverse functions at the SAM during plant development (Figure 5.1). The genes that are bound by FD at the SAM and how they are transcriptionally regulated may depend on the phosphorylation status and protein interaction partners of FD. Collectively, the results indicate that FD promotes floral transition, termination of shoot development and a short life cycle, which are important traits in the life history of annual plants and offer the potential to manipulate yield-related traits in crops.

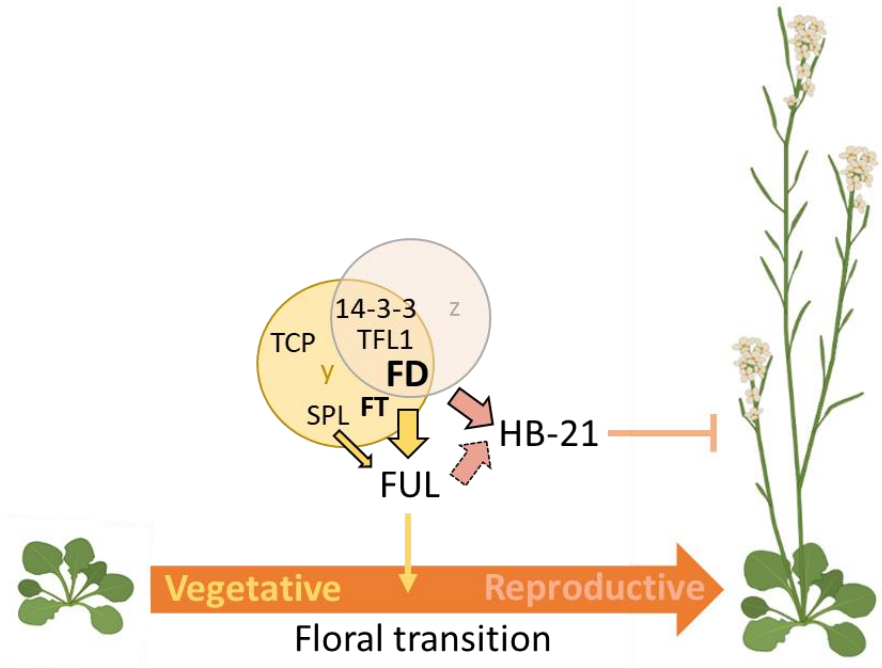

Figure 5.1. Illustration of FD action at the shoot apical meristem under LD conditions
Marked in yellow: During the vegetative growth of Arabidopsis, FD and TFL1 are expressed at the shoot apical meristem (SAM). The resulting complex FD–(14-3-3)–TFL1 represses floral induction. Several flowering pathways converge at the SAM and notably, a LD photoperiod promotes transcription of *FLOWERING LOCUS T* (*FT*) in the leaf vasculature and the FT florigen moves to the shoot apical meristem (SAM) to interact with FD. The FD–(14-3-3)–FT complex promotes floral transition at the SAM and overcomes the active repressive role of TFL1. Other FD interactors have been identified, such as the transcription factors of the SQUAMOSA PROMOTER BINDING PROTEIN-LIKE (SPL) and class II TCP families. Both these classes of proteins are reported to facilitate the binding of FD to DNA of its target loci. The floral integrator FRUITFULL (FUL) promotes flowering downstream of the FD–(14-3-3)–FT complex. SPL transcription factors also activate *FUL* transcription.
Marked in beige: During reproductive growth in the inflorescence, FD is still expressed at the SAM. Together with the 14-3-3 proteins and TFL1, the FD–(14-3-3)–TFL1 complex maintains the identity of the inflorescence meristem. Moreover, FD binds to the *HOMEOBOX PROTEIN 21* (*HB-21*) DNA locus and activates its expression. Independently, the transcription factor FUL activates the expression of *HB-21* (indirectly, dotted lines). The regulation of FUL by FD in the inflorescence meristem has not been confirmed by this work. HB-21 activation then contributes to global proliferative arrest (GPA) of the inflorescence.

The interactors of FD for the floral transition and inflorescence development are displayed within the yellow and beige circles, respectively. Many interactors remain to be identified, represented here by the letters y and z. The TFL1 and 14-3-3 proteins may be associated with FD at all developmental stages. Images are from www.biorender.com.

Erklärung zur Dissertation

Erklärung zur Dissertation
gemäß der Promotionsordnung vom 12. März 2020

Diese Erklärung muss in der Dissertation enthalten sein.
(This version must be included in the doctoral thesis)

„Hiermit versichere ich an Eides statt, dass ich die vorliegende Dissertation selbstständig und ohne die Benutzung anderer als der angegebenen Hilfsmittel und Literatur angefertigt habe. Alle Stellen, die wörtlich oder sinngemäß aus veröffentlichten und nicht veröffentlichten Werken dem Wortlaut oder dem Sinn nach entnommen wurden, sind als solche kenntlich gemacht. Ich versichere an Eides statt, dass diese Dissertation noch keiner anderen Fakultät oder Universität zur Prüfung vorgelegen hat; dass sie - abgesehen von unten angegebenen Teilpublikationen und eingebundenen Artikeln und Manuskripten - noch nicht veröffentlicht worden ist sowie, dass ich eine Veröffentlichung der Dissertation vor Abschluss der Promotion nicht ohne Genehmigung des Promotionsausschusses vornehmen werde. Die Bestimmungen dieser Ordnung sind mir bekannt. Darüber hinaus erkläre ich hiermit, dass ich die Ordnung zur Sicherung guter wissenschaftlicher Praxis und zum Umgang mit wissenschaftlichem Fehlverhalten der Universität zu Köln gelesen und sie bei der Durchführung der Dissertation zugrundeliegenden Arbeiten und der schriftlich verfassten Dissertation beachtet habe und verpflichte mich hiermit, die dort genannten Vorgaben bei allen wissenschaftlichen Tätigkeiten zu beachten und umzusetzen. Ich versichere, dass die eingereichte elektronische Fassung der eingereichten Druckfassung vollständig entspricht."

Teilpublikationen:

23.08.2021

Datum, Name und Unterschrift

24.08.2021

Chloé Pocard

Erklärung zum Gesuch um Zulassung zur Promotion

gemäß der Promotionsordnung vom 12. März 2020

1. Zugänglichkeit von Daten und Materialien

Die Dissertation beinhaltet die Gewinnung von Primärdaten oder die Analyse solcher Daten oder die Reproduzierbarkeit der in der Dissertation dargestellten Ergebnisse setzt die Verfügbarkeit von Datenanalysen, Versuchsprotokollen oder Probenmaterial voraus.

☐ Trifft nicht zu

☒ Trifft zu.
In der Dissertation ist dargelegt wie diese Daten und Materialien gesichert und zugänglich sind (entsprechend den Vorgaben des Fachgebiets beziehungsweise der Betreuerin oder des Betreuers).

2. Frühere Promotionsverfahren

Ich habe bereits einen Doktortitel erworben oder ehrenhalber verliehen bekommen.
Oder: Für mich ist an einer anderen Fakultät oder Universität ein Promotionsverfahren eröffnet worden, aber noch nicht abgeschlossen.
Oder: Ich bin in einem Promotionsverfahren gescheitert.

☒ Trifft nicht zu

☐ Zutreffend
Erläuterung:

3. Straftat

Ich bin nicht zu einer vorsätzlichen Straftat verurteilt worden, bei deren Vorbereitung oder Begehung der Status einer Doktorandin oder eines Doktoranden missbraucht wurde.

Ich versichere, alle Angaben wahrheitsgemäß gemacht zu haben.

Datum	Name	Unterschrift
21.08.2021	Chloé Pocard	Pocard

01-2021

Chapter 6. Materials and Methods

Plant materials and growth conditions

The *Arabidopsis thaliana* wild-type ecotype Columbia (Col-0) was used for almost all experiments, except in a few cases when the ecotype Landsberg *erecta* (L*er*) and the *abi2-1* mutant were used, and these are indicated in the text. All other mutants and transgenic lines were in the Col-0 background. Seeds were stratified for three days either directly in pots in the dark cold room (4°C) or in 1 mL water in Eppendorf tubes placed at 4°C in the fridge prior to sowing. Plants were grown on soil under LD (16 h light/8 h dark) or SD (8 h light/16 h dark) at 21°C in the greenhouse or in growth cabinets. The light intensity was between 150 and 180 µmol/s/m. The relative humidity in the growth cabinets was about 70%. Pots for plants grown in SD conditions were 9 × 9 cm and those for plants in LD were 7 × 7 cm. Plants grown in cabinets received fertilizer capsules and were watered with rainwater, whereas plants grown in the greenhouse were irrigated with water and nutrients.

Seed sterilisation

To select for transgenic plants carrying the *bar* gene that were resistant to phosphinothricin (PPT), approximately 150 seeds per genotype were sterilized in ethanol (EtOH) or chlorine gas. For EtOH sterilisation, the seeds were immersed in 1 mL 70% EtOH for 5 min in Eppendorf tubes and the tubes were continuously rotated. After removal of the EtOH, the step was repeated. Then, 1 mL 100% EtOH was added to each tube under a laminar flow hood. Seeds were dried for 5 min on top of a Petri-Pad™ Petri dish (ThermoFischer) to allow the ethanol to evaporate. For sterilisation with chlorine gas, a mixture of 9 parts (v/v) 12% sodium hypochlorite and 1 part (v/v) 37% HCl was prepared in a desiccator under the fume hood and seeds were exposed to the fumes for about 4–6 h. After sterilisation, the seeds were plated on Murashige and Skoog (MS) medium without sucrose that contained 12 µg/mL PPT. The plates were placed in a continuous light chamber for ten days prior to the selection of resistant plants.

Phenotypic analysis of plants grown in the greenhouse and growth cabinets

To assess flowering time, the number of rosette and cauline leaves produced by plants were counted. The number of days to bolting represented the time period from when seeds were transferred to LD or SD until the stem elongated to a height of 1 cm. At global proliferative arrest, the height of the main shoot, and the length of the I1 and I2 zones were measured with a 2-m folding ruler. If several plants from one experiment did not reach GPA, the entire experiment was discarded. The number of flowers produced and shoot height were measured every day at specific times during shoot development. The date to GPA in figure 4.2A corresponds to the arrest of both stem height growth and flower production of plants. Measurements of figure 4.2A were performed on plants analysed in figure 4.2D. For all figures with number of fruits on the main shoot, fertile and unfertile flowers were scored without

distinction, as no severe unfertile genotype was used. Plants were photographed with a Canon EOS 600D or Canon 800 camera. In some cases, the brightness of the images was adjusted.

Plant DNA extraction, genotyping and PCR

For DNA extraction, portions of young leaves were harvested from each plant. Samples were frozen at -80°C until use. DNA was extracted using a rapid extraction method (Edwards et al., 1991). Briefly, plant tissue was homogenised using the TissueLyser II system (Qiagen, #85300) for 2 min, 400 µL of Edwards' buffer was added (200 mM Tris-HCl, pH 7.5, 250 mM NaCl, 25 mM EDTA, 0.5% SDS) and the samples were processed according to (Edwards et al., 1991).

For large genotyping experiments, DNA was extracted from up to 96 samples simultaneously using the Qiagen BioSprint robot following the manufacturer's instructions of the BioSprint 96 DNA Plant Kit (Qiagen, # 941557) and the DNA was eluted in 100 µL milli-Q water.

Plants were genotyped using 2 µL freshly extracted DNA and 0.25 units (U) of GoTaq® Flexi DNA Polymerase (Promega, #M8291) in 10 µL of reaction mixture, according to the manufacturer's recommendations. The resulting amplified DNA was visualised on a 1% agarose gel. For genotyping plants carrying *fdp-CRP2*, a DNA fragment was amplified using dCAPS primers and was digested with 0.2 µL *Hpa*I (NEB, # R0105S) and 3.8 µL water for 4 h and the amplicons were electrophoresed on a 3% agarose gel. The genotyping primers are listed in Table 6.1.

PIPE-cloning technology

The polymerase incomplete primer extension (PIPE) method (Klock and Lesley, 2009) was optimised by Dr. R. Martinez Gallego (MPIPZ). This technique allows the rapid insertion of a fragment of interest into a recipient plasmid. The design of specific mismatching primers from the original template allows site-directed mutagenesis of the DNA. Independent PCR reactions amplified the PIPE-insert (PIPE-I) and linear PIPE-vector (PIPE-V). The fragments were amplified with either PrimeSTAR® GXL DNA Polymerase (TaKaRa, #R050A) or Phusion® High-Fidelity DNA Polymerase (NEB, # M0530L). PCR reactions were performed according to the manufacturer's recommendations. The amplified PIPE-I and PIPE-V were digested with the *Dpn*I (NEB, #R0176S) in CutSmart® Buffer (NEB, #B7204S) for 1 h at 37°C to target and cleave methylated bacterial remaining. The samples were purified with either the NucleoSpin™ Gel and PCR Clean-up Kit (Macherey-Nagel™, #740609.50) following the manufacturer's recommendations, or via the polyethylene glycol (PEG) method. For the PEG method, 50 µL PCR product was added to 150 µL TE buffer (pH 8.0; 10 mM Tris-HCl, pH 8.0, 1 mM EDTA) and 100 µL PEG 8000/30 mM $MgCl_2$, and the mixture was centrifuged for 30 min at 10,000 *g*. The DNA pellets were resuspended in 30 µL TE buffer. After amplification and PCR clean up,

the PIPE-I and PIPE-V fragments were mixed in a 200:20 fmol ratio and TE buffer was added to a total volume of 10 µL. Recombination between PIPE-I and PIPE-V occurred via complementary DNA ends and the recombinant plasmid was selected in *Escherichia coli* (*E. coli*) DH10B cells after transformation.

Gateway cloning

Gateway™ cloning allows recombination between the entry vector and destination vector containing the *att*L and *att*R cassettes, respectively. The reaction is catalysed by the Gateway™ LR Clonase™ II Enzyme Mix (ThermoFischer, #11791020). Approximately 45 ng/µL entry vector and 90 ng/µL destination vector were mixed with 1 µL LR Clonase® II enzyme. The samples were incubated for between 1 h to overnight at 25°C. The LR reactions were transformed into competent *E. coli* cells by the heat-shock method.

Heat-shock transformation of *Escherichia coli*

Recombinant DNA was transformed into competent *E. coli* cells by heat shock. Competent *E. coli* cells (100 µL) were stored at -80°C and were placed on ice prior to transformation. The DNA mixture was gently added to the competent cells, which were then incubated for 5 min on ice. Heat shock was performed at either 37°C for 3 min or 42°C for 45 sec and the cells were placed on ice again for 5 min. Liquid Lysogeny broth (LB) medium (450 µL) was added to the transformed cells and the tube was placed horizontally in a 37°C shaker (200 r.p.m.) for 90 min. Approximately 100–300 µL of the mixture was then plated on LB agar plates containing relevant antibiotics for plasmid selection. The plates were incubated overnight (about 16 h) with the agar-side uppermost at 37°C. Single colonies were selected and placed into liquid LB containing an appropriate bacterial selection antibiotic and were cultured overnight in a 37°C shaker (200 r.p.m.). Plasmids were purified using the NucleoSpin Plasmid QuickPure kit (Macherey-Nagel™, # 740588.50) following the manufacturer's instructions.

Verification of constructs

The size and quality of PCR amplicons were confirmed by electrophoresing 5 to 10 µL of each reaction on a 1% agarose gel containing ethidium bromide. Electrophoresis was performed for about 45 min at 100 V in TAE buffer (40 mM Tris; 20 mM acetic acid; 1 mM EDTA pH 8,0) and gels were visualised with Bio-Rad UV light.

Extracted plasmids from *E. coli* were verified by colony PCR as follows: approximately 20 bacterial colonies per plate were individually suspended in 45 µL PCR mix containing 11% (v/v) home buffer (15 mM $MgCl_2$; 500 mM KCl; 100 mM TrisHCl pH 8.5; 0,5% Tween20; 250 µg/mL BSA), 3 mM $MgCl_2$, 0.3 mM dNTPs, 0.02 U of Brown Taq enzyme and 0.2 mM each primer. PCR was used to amplify DNA by an initial denaturation for 3 min at 94°C, then 35 cycles of 94°C for 30 sec, 52°C for 30 sec and 72°C for 1 min and a final extension step at

72°C for 7 min. The resulting PCR products were visualised following electrophoresis on a 1% agarose gel containing ethidium bromide.

To test the recombination efficiency, plasmid restriction mapping was performed as follows: 200 ng plasmid DNA was digested with 10% of the appropriate buffer and 2 U of the selected restriction enzyme in a 20-µL reaction. The products were incubated 37°C for 90 min, separated on a 1% agarose gel containing ethidium bromide and visualised. Sanger sequencing (GATC Biotech) was used to verify the DNA sequence of each sample that showed the correct enzyme digestion pattern.

***Agrobacterium tumefaciens* transformation and *Arabidopsis thaliana* floral dip**

The final destination vectors were introduced into electrocompetent *Agrobacterium tumefaciens* GV3101 pSoup cells. Briefly, 50 µL of *Agrobacterium* cells were thawed and were electroporated with 100 ng of each construct, using a 2-mm cuvette with a pulse of 2.20kV. The electroporated cells were diluted in warm LB (1 volume cells:9 volumes LB) and were shaken for 6 h at 28°C. Electroporated cells (100 µL) were plated on LB medium and incubated at 28°C for 48 to 72 h. Colonies were selected on agar plates and the presence of the destination vector was selected with either kanamycin (25 µg/mL) or spectinomycin (100 µg/mL) and then gentamycin 8 µg/mL, rifampicin 50 µg/mL, tetracycline 10 µg/mL.
A single antibiotic-resistant colony of *Agrobacterium tumefaciens* was selected and transferred to 5 mL liquid LB with the appropriate antibiotic. The cells were incubated overnight at 28°C with shaking and the preculture was used to inoculate 500 mL liquid LB, which was incubated overnight at 28°C with shaking until an optical density (OD_{600}) between 0.8–1.0 was reached. The *Agrobacterium* were mixed with a solution of 20% (w/v) sucrose and 0.1% (v/v) of surfactant Silwet L-77 (Loveland Industries LTD). Inflorescences of 10 to 15 Arabidopsis plants were dipped into the *Agrobacterium* suspension (Clough and Bent, 1998). The plants were covered overnight with a plastic bag at room temperature to maintain humidity. The following day, the plants were transferred to the LD greenhouse until they set seed. For transformation of *FUL* constructs into the *ful-2* mutant background, dipping was performed twice with 20 *ful-2* plants. The T1 seeds, resulting from the dipped plants, were grown on soil and transgenic plants were selected by spraying with Basta® (glufosinate-ammonium, BASF), if not indicated otherwise. To identify homozygous lines, plants with 3 to 1 segregation ratio in T2 and T3 were selected, according to Mendel's Law.

Construction of binary vector plasmids for plant transformation

The genomic locus of *FD* was previously cloned into the pEntry pLV201 vector to generate *gFD_pLV201* (Romera-Branchat et al., 2020). The *FD* promoter and the 5′ UTR region consisted of 3,686 bp. To generate the *FD::GR:FD_pLV201* plasmid, 873 bp of *GR* sequence

was amplified from the *pBJ36-GR* plasmid (Ó'Maoiléidigh et al., 2013) by PCR amplification with PrimeSTAR® GXL DNA Polymerase and was integrated into *gFD_pLV201* using PIPE. Nucleic acid sequences after the GR-encoding region allowed the translation of one glycine and nine alanine (G9A) amino-acid residues as a linker between GR and FD. The sequence terminated with the *FD*-coding sequence and the 3′ UTR. The resulting *FD::GR:FD* fragment was introduced into the *pEarleyGate301* (Earley et al., 2006) expression vector by Gateway cloning and the final size of *FD::GR:FD_pEarlyGate301* was 15,391 bp.

The *FUL* genomic locus was amplified by Dr. A. van Driel and Dr. R. Martinez Gallego to generate *FUL::FUL:9AV_pSTB205* (A. van Driel PhD thesis, 2020). The promoter and 5′ UTR of *FUL* was 5,182-bp long in total. The genomic *FUL* CDS was followed by a linker of nine alanine residues and the *VENUS* CDS. The *B1* and *B2* ACGT motifs in the *FUL::FUL:9AV_pSTB205* were mutated simultaneously by PIPE cloning: the PIPE-V fragment was amplified with PrimeSTAR® enzyme and the PIPE-I was amplified with Phusion® Polymerase. The modified *FULm1m2::FUL:9AV_pSTB205* fragment was inserted into *pFAST-R01* (Shimada et al., 2010) by Gateway cloning to generate *FULm1m2::FUL:9AV_pFASTR01* (22,429 bp). The same procedure was used to modify *B1* and *B2* in *FULmGTAC::FUL:9AV_pSTB205*. The *FUL::FUL:9AV_pSTB205* construct generated by Dr. A. van Driel was inserted into *pDEST-Alligator*. The T1 to T3 seeds carrying the T-DNA were selected using an epifluorescence microscope and a laser wavelength suitable for RFP detection.

To generate the *ABI2* constructs, total RNA from Landsberg *erecta* (L*er*) and *abi2-1* mutant plants was extracted using the Qiagen RNeasy Plant Mini Kit (Qiagen #74904) and was reverse-transcribed to obtain the cDNAs of *ABI2* and *abi2-1* using the primers listed in Table 6.2. Both fragments were digested with *Xho*I and *Xma*I (NEB, #R0146 and #R0181) and were directly inserted into *FDpro_pGreen-0229* via compatible restriction digestion cuts (Hellens et al., 2000). The *pGreen* vector was modified and contained the *FD* promoter sequence (3,915 bp; generated by Dr. D. Ó´Maoiléidigh). The *ABI2*-coding sequence ended with six nucleotides that were used for enzyme digestion, and was followed by the OCS terminator. The *FD::ABI2_pGreen-0229* plasmid was 10,357 bp long. All plasmids generated during this PhD thesis are listed in Table 6.3.

Gene expression analysis by quantitative real-time PCR

The quantification of candidate gene mRNAs was performed in hand-dissected Arabidopsis tissues enriched for apices. Frozen samples were disrupted with the TissueLyser II system (Qiagen, #85300) at maximum speed for 90 s. Total RNA was extracted using the Qiagen RNeasy Plant Mini Kit (Qiagen #74904) following the manufacturer's instructions and was eluted in 32 µL RNA-free H_2O. Total RNA was quantified with NanoDrop (ThermoScientific, ND-1000) and 4 µg was incubated with DNaseI, which was then inactivated using the TURBO

DNA-free™ kit (Invitrogen #AM1907). Reverse transcription was performed using 1 µg purified RNA and the SuperScript IV (Invitrogen #18090050). The oligo (dT)-primer sequence is listed in Table 6.4. The cDNAs were diluted with milli-Q water in a 1:5 ratio. Quantitative PCR was performed on the BioRad CFX384 qPCR system with 8 µL PCR reaction containing iQ SYBR Green Supermix (Bio-Rad #170-8884) and 2 µL cDNA for 35 cycles of amplification. Each Supermix contained: 2.2 µL of milli-Q water, 5 µL of the iTaq™ DNA Polymerase and 0.4 µL for each 10 µM concentrated primer. qRT-PCR was performed for three technical replicates for each biological replicate. Results were analysed by the $2^{-\Delta\Delta Ct}$ method (Livak and Schmittgen, 2001) using endogenous controls. The primer efficiencies were tested. Melting curves were examined and all cDNA amplifications gave a single peak for each primer combination. All primers used in RT-PCR experiments are listed in Table 6.4 and the genes they were used to analyse are indicated.

Dexamethasone treatment of plants

To study the effect of FD induction in the *FD::GR:FD* lines, dexamethasone (DEX) was applied to plant apices. For this, a stock solution of 100 mM DEX (Sigma, #D1756) in 100% EtOH was made and a working solution of 10 µM DEX was generated by diluting the stock solution with water and 0.015% of Silwet L-77 was added. For the 10 µM mock solution, 0.01% EtOH 100% and 0.015% Silwet L-77 were mixed with water. The solutions were applied directly to the centre of seedling apices by brushing the apices with a paint brush seven times in succession. For the GPA assay in chapter 4, DEX and mock solutions were applied as a single drop of 2–5 µL, depending on the growth stage.

RNA-sequencing of *GR::FD:GR fd-3* apices

Material was harvested for three independent experiments with a one- to two-day interval between sowing for each experiment. Mock (0.01% EtOH, 0.015% Silwet L-77) and DEX 10 µM (0.01% EtOH, 0.015% Silwet L-77) treatments were performed at ZT1 on plants grown for 12 LD. The centre of the apex of each plant was then individually treated by brushing with either mock or DEX solutions and meristem-enriched tissues were harvested 8 h after the treatment and then every 24 h for 5 days. Fifteen apices were harvested for each sample. Total RNA was extracted from the samples with the RNeasy Plant Mini Kit (Qiagen). The RNA Clean & Concentrator kit (Zymo Research #R1019) was used to digest contaminating DNA and concentrate total RNA, following the manufacturer's recommendations. In total, 39 RNA samples were sent to the Genome Centre at the MPIPZ for sequencing. Sequencing was performed with an Illumina HiSeq3000 with 150-bp single reads, and 15 million reads were specified. The library type was RNA including poly(A) enrichment. The reads sequenced were then comprised between 11.5 and 17 million. The pipeline for read cleaning and merging was performed by Dr. Severing in the lab. The reads were aligned to the Arabidopsis TAIR10

genome using TopHat2. Gene expression analysis from the table of generated raw counts was performed using the DESeq2 package in Rstudio. Each time point was compared with t0 for the respective mock- or DEX-treated sample, and DEGs specific to the DEX samples were selected as DEG for a specific time point (Figure 2.7A). Cut-offs of a $\log_2$(fold change) of 1.5 and a *p*-value of 0.05 were applied. Count normalization was performed by DESeq2 using the median of ratios method, which allowed gene-count comparisons between samples. The median was calculated based on all gene counts and was corrected for outliers.

Tissue fixation and confocal imaging

Portions of leaves or meristem-enriched tissue from apices were dissected by hand and fixed in 4% (w/v) paraformaldehyde (PFA; ThermoFischer, #15713S) in 1× phosphate buffer saline (PBS, pH7.4) on ice. Samples in tubes without lids were desiccated in a vacuum on ice. Vacuum was imposed for 15 min and samples were left for a further 10 min in full vacuum. After releasing the pressure, the samples were fixed again. Fresh PFA solution was added and the samples were either kept 1 h at room temperature or overnight in a 4°C cold chamber. After 3 × 5 min washes with 1× PBS, the samples were cleared with 1 mL Clearsee for 2 to 5 days (Kurihara et al., 2015). The Clearsee reagent was prepared according to (Kurihara et al., 2015). If the samples were thick, for example meristems grown for 6 weeks in SD, fresh Clearsee was added two days after the first clearing step. Samples were then stained with fresh Clearsee and 1:1000 dilution of SCRI Renaissance 2200 about 16 to 48 h prior to imaging and samples placed in dark (Musielak et al., 2015). The samples were imaged using a Leica SP8 confocal laser scanning microscope. The laser wavelength used to detect Renaissance dye was 405 nm and the detection wavelength was 410–480 nm. A hybrid detector (HyD) was used to image the VENUS and mCherry signals with laser wavelengths of 514 and 561, respectively. The detection wavelengths were 519–539 nm and 595–620 nm, respectively. The images were subsequently analysed with FiJi. In some cases, the brightness was adjusted without affecting the expression pattern.

Chromatin Immunoprecipation (ChIP) followed by qPCR

ChIP assays were performed with 2 g of either 16 LD-tissues enriched for apices, or three-week-old inflorescences of the *FD::VENUS:FD fd-3* and *35S::GFP:YFP* lines. The procedure was described in (Romera-Branchat et al., 2020) and the protocol “CHIP using plant samples: Arabidopsis” from Abcam was followed, except that tissues were fixed with formaldehyde for 3 × 15 min. The anti-GFP antibody, (Abcam, #ab290) was used to pull down the VENUS:FD protein and the amount of pulled-down DNA was quantified with a Qubit™ 3 Fluorometer (Invitrogen, #Q33216).

The resulting input and IP DNAs were diluted with RNAse-free water in a 1:4 ratio. The iQ SYBR Green Supermix (Bio-Rad #170-8884) was used for ChIP-qPCR as described for the

RT-qPCR reaction. Samples were run with technical triplicates using the Roche LightCycler® 480 System with 40 cycles of amplification.

ABA treatment of plant apices

To analyse changes in gene expression after treatment with ABA, ABA was applied to plant apices. For this, 0.01 g ABA powder (Sigma-Aldrich, #90769) was diluted in 1 mL DMSO to give a 40-mM stock solution. 50 µL of 40 mM ABA was diluted 1,000-fold with water to make a 40 µM ABA solution and in parallel, 50 µL of DMSO was diluted 1,000-fold with water to make the mock control solution. The ABA was applied to each apex with a small paint brush seven times in succession at ZT1 and samples were harvested at ZT5. Independent experiments were performed twice and the data displayed here correspond to independent biological triplicates for each experiment.

Statistical analyses

Statistical analyses were preformed using Microscoft Excel 2019 and Rstudio. The organisation of the box plots is as follows: The line within the box shows the median of the distribution of the samples. The boxplot is delimited by the lower and upper quartiles. One-quarter of the values are below the lower quartile. The lower and upper whiskers extend to the most extreme values.

The CRAN Emmeans package was used to interpret the 2-way ANOVA in figures 4.5 and 4.7C. The model follows “Values ~ Genotype*Treatment” where “Values” corresponds to the studied trait, such as plant height of relative expression. The pairwise comparison was adjusted with the Bonferroni correction. The correlation plot figure 4.6A was performed using the Pearson correlation and true interactions were selected for *P*-value < 0.01

Name	Sequence	Purpose	Note
MR14	GGTTTTGGTTGTGGTGGTTT	wild type fragment of *FD*	Dr. M. Romera Branchat
X371	TCCAGAAATGACCGGCTAAAGTC		
MR74	ATTTTGCCGATTTCGGAAC	With MR14 for *fd-3*	
FDP-dCAPs_F	GCGAGGGTTAGAAGCAAGAAGA	dCAPs genotyping FDP-CRP2 with HpaI	Dr. M. Romera Branchat
FDP-dCAPs_R	GTTCACTTCACTACCATCGGCAAGTTAA		
CP314	GGTGGAGAAGACCTCAGGAAC	CP314 and CP315 for WT *FT*	
CP315	TTTTGGGAGACAAATTGATGC	CP315 and LBb3.1 for ft-10	
LbB3.1	ATTTTGCCGATTTCGGAAC		
X132	CACGAGGTTGGTCTCTCTTAAG	X132 and X133 for WT *TSF*	Dr. M. Romera Branchat
X133	CTGGCAGTTGAAGTAAGAG	X133 and MR74 for *tsf-1*	
CP237b	AGTTCAAGTGTGTTCCTTTATATGG		
CP428	GACCCAACAGTTTCCGGAGC	Amplify *ABI2* CDS	
CP237c	TGTGGTAGACGACCAGAGATGGA	Sequence CP237b+CP428 for *abi2-1* mutant	
CP435	ATAATAACGCTGCGGACATCTACATTTT	To sequence *dreb2a-2* mutant allele	
CP436	TACGAGCAAGAAGACTAAACACGA		
CP437	TTGCTCCTTCTGTTTCTCTTTCTC	CP437 and CP436 for WT *DREB2A*	
TFL1-ATG-Fw	ATGGAGAATATGGGAACTAGAGTGA	Amplify WT *TFL1*	Dr. V. Falavigna
tfl1_18_RB	AGTCTTGGTCATAGATAGGGGTTGA		
o8474	ATAATAACGCTGCGGACATCTACATTTT	o8478 with TFL1_ATG_Fw for *tfl1-18*	
B272	TTGGCCGAGACGTTTCACAA	Amplify *FUL* fragment	Dr. A. van Driel
B273	TTGTTGGGACTCTGAAGCGG		
B274	attagaagtttgtatgtgcgaccc	Sequence B272+B273 for *ful-2* genotyping	

Table 6.1. List of primers used for genotyping the mutants.

Name	Sequence	Purpose	Construct
CP79	tgctccacttaaatgatgacaataccagaGACCCAGCTTTCTTGTACAAAGTtGGC	Amplify PIPE-V *pLV201_gFD*	*FD::GR:FD*
CP80	cccaaaagagaaacaaggacttgtagatttcTCAAAATGGAGCTGTGGAAGACCGTTGAAG		
CP81	CTTCAACGGTCTTCCACAGCTCCATTTTGAgaaatctacaagtccttgtttctcttttggg	Amplify PIPE-I in *pBJ36-GR*	
CP82	GCCaACTTTGTACAAGAAAGCTGGGTCtctggtattgtcatcatttaagtggagca		
CP171	CCATGctagatttaagaaagaaaaaaaaggtcaacactcgattaatttga	PIPE-V in *pSTB205_FUL* and *pSTB205_FUL_SBP* Introduce mutation at *B1* and *B2* motifs in *FUL* promoter, PIPE-I	*FULm1m2::FUL:9AV*
CP172	ttttctttcttaaatctagCATGGAGAGGATACTTGAACGCTATGATCGC		
CP167	ccacaaatatcatcgtctatgtatt**CAATAT**acataccgtatttataccacatcact**CAATAT**actgtagactc		
CP168	tgatgtggtataaatacggtatgt**ATATTG**aatacatagacgatgatatttgtggaaaaaaaagaaaga		
CP60	GGGGACAAGTTTGTACAAAAAAGCAGGCTTCTTA**ATG**GACGAAGTTTCTCCTGCA	To enrich cDNA of *ABI2* from Ler	*FD::ABI2* and *FD::abi2-1*
CP61	GGGGACCACTTTGTACAAGAAAGCTGGGTC**TCA**ATTCAAGGATTTGCTCTTGA		
CP85	CGTcTCGAG**ATG**GACGAAGTTTCTCCTGC	To add digestion sites at the extermities of the CDS	
CP86	GCACCCGGG**TCA**ATTCAAGGATTTGCTCT		

Table 6.2. List of primers used for PIPE and restriction enzyme cloning.

Plasmid name	Plasmid vector	Bacterial resistance	Plant selection
gFD_pLV201	Cloning vector	Kan	
pBJ36-GR	Expression vector	Spec	Basta®/PPT
FD::GR:FD_pLV201	Cloning vector	Kan	
pEarlyGate301	Gateway vector	Kan	Basta®/PPT
FD::GR:FD_ pEarlyGate301	Expression vector	Kan	Basta®/PPT
FUL::FUL:9AV_pSTB205	Cloning vector	Kan	
FULm1m2::FUL:9AV_pSTB205	Cloning vector	Kan	
FULm1m2+mGTAC::FUL:9AV_pSTB205	Cloning vector	Kan	
pFASTR01	Gateway vector	Spec	seed coat RFP
FULm1m2::FUL:9AV_pFASTR01	Expression vector	Spec	seed coat RFP
FULm1m2+mGTAC::FUL:9AV_pFASTR01	Expression vector	Spec	seed coat RFP
FDpro_pGreen-0229	Expression vector	Kan	Basta®/PPT
FD::ABI2_pGreen-0229	Expression vector	Kan	Basta®/PPT
FD::abi2-1_pGreen-0229	Expression vector	Kan	Basta®/PPT

Table 6.3. List of plasmids used for cloning and plasmids generated.

Name	Sequence (5′ to 3′)	Target	Received from
FD	CATCAACCTTGCTTCCATCC	*FD*	Dr. M. Romera Branchat
FD	GGTTTTGGTTGTGGTGGTTT		
X123	TGGAGGAGGTTACGCAGTATTGA	*FUL*	Dr. M. Romera Branchat
X122	TGCTCCAACTCTTCTTCAGTTCTTC		
YB6F	ATGAGAGGTACTCTTACGCCGA	*AP1*	Dr. Y. Hyun
YB6R	CAAGTCTTCCCCAAGATAATGC		
CP308	AAGCAGGCTTCtaaaataagagga	*GRFD*	
CP309	cgaacaagtaacacgccaaa		
CP153	AGGAGCTGCAACAGATTGAG	*SOC1*	
CP154	GCTAGAGCTTTCTCCTTTTGC		
SR114	ACTCCAGCTGAACCCTAACC	*SEP3*	Dr. M. Romera Branchat
SR113	TCCATCTTGTTGCCCCTGAT		
CP391	TCACTTGTAAGCTTTTCACCAGTT	*HEC1*	
CP392	GTTGTGGTCGGGAGAGAAGA		
CP393	GGGTCTTGCTAAGGGGCTAA	*GolS2*	
CP394	CACAGCCTTGATCCACCAAC		
CP395	GCTCCAAGGTTTGATGGGTTAC	*AT4G28290*	
CP396	CCTCTTCTAAAGAAAATCAGAACAATGC		
CP361	CTTTATGGGCCTTAGTGTGTCTC	*DREB2A*	
CP362	CCCTCTAATCCCTAGAGAACTTCC		
MR68	GCTTCGGCTATTTTCAGCTG	*FDP*	
MR67	GTTCAAGGGCTAGGAAGCAG		
CP405	TCTAAACCACCCATTGCCTTCGTT	*HB21*	Balanzà et al., 2020
CP406	GTACCACAACAAGGAGGAGAAGCA		
CP407	TGCCTGCTCCTTCATTTCCTCCA	*BLH1*	Balanzà et al., 2020
CP408	ACTCGTAGCCAGGTGTCGAACT		
Q114	GTCACCCATCAGTTCTTCCC	*AP2*	
Q214	GTGGCTAGATCCGACTGACA		
X217	CCACTCGTATGTAGCTTTTGTG	*FUL ChIPseq*	Dr. M. Romera Branchat
X216	TGGACTTTTGTTGGGTTTCGC		
CP363	TGAGCTGCAGAGACTAAACGA	*AtHB12*	
CP364	TAGAGCCAGTCCTTGATCACC		
CP373	CAGTTTCATGCCAAAGCTCCT	*SPL3*	
CP374	TCTCTCGTTGTGTCCAGCTAA		
CP375	ATACCAAGGTGCCAAGTGGA	*SPL9*	
CP376	TGTTCGATACCAGCCACAGT		
CP381	ACTCTAGGGCGGTTTTGTGT	*ABI2*	
CP382	AGGTATCTATCGCCAATGGATCT		
CP163	TGACCACACAGTCTCTGCAA	*eIF4A*	
CP164	ACCAGGGAGACTTGTTGGAC		
CP186	GTTGCTCCGCCGTTATTCAA	*PYL4*	
CP187	TACCAACGTTATCGCCGTCT		
CP227	AAGCGGTTGTGGAGAACATGATACG	*PP2AA3*	Dr. D. Ó'Maoiléidigh
CP228	TGGAGAGCTTGATTTGCGAAATACCG		
CP229	TCCCTCAGCACATTCCAGCAGAT	*ACTIN2*	Dr. A. Pajoro
CP230	AACGATTCCTGGACCTGCCTCATC		
dT	CCTAGGCCACTGTGGCCTTTTTTTTTTTTTT	Oligo dT	Dr. M. Romera Branchat

Table 6.4. List of primer sets used for RT-PCR and ChIP-qPCR.

Acknowledgements

Most importantly, my PhD journey begun thanks to Prof. Dr. George Coupland. I am pleased about the opportunity you provided me George, to work on the flowering time regulation in your lab at the Max Planck Institute for Plant Research over the past years. I am thankful for your supervision. Mostly, I really appreciated the scientific freedom and trust you gave me. I am still amazed about your truly great scientific knowledge. And thank you for making this lab a good place to work in.

I would like to acknowledge all the Coupland group members, past and present, who also made this journey enjoyable. All members contributed to enrich my scientific knowledge. Especially Dr. Diarmuid Ó'Maoiléidigh, Dr. Atsuko Kinoshita and Dr. René Ritcher who shared materials and discussed my project. I would like to thanks Dr. Youbong Hyun and Dr. Luise Brand who first trained me during my master internship. Thank you, Dr. Alice Pajoro, for the time we worked together and the opportunity to study plant shoot architecture and for the helpful advices. I would like to thanks Dr. John Chandler for his amazing help with scientific English and for making this PhD thesis better. To the young generation of researchers: Annabel, Adrian, Enric and Yi-Chen.

I would like to thanks my two Thesis Advisory Committee (TAC) members, Dr. Maida Romera-Branchat and Dr. Ivan Acosta for all the input and guidance. Dr. Ivan Acosta always put my project back on tracks. Thank you, Dr. Stephan Wagner, PhD coordinator, for improving the life of the PhD students at the campus.

I am grateful to my PhD thesis examination committee, Prof. Dr. Ute Höcker, Prof. Dr. Maria von Korff Schmising and Prof. Dr. Stanislav Kopriva for their time and evaluation of my PhD work.

A special thanks to Denitsa Veselinova Vasileva for her work in the greenhouse, no matter the temperatures. I would like to thanks everybody who helped with my project: the great technicians of the lab, the gardeners and the genome center members.

To all my colleagues and friends at the institute, thank you for the friendship, discussions, lunches, beers at the TATA-bar and coffee breaks.

To my dear friends and the French community in Cologne, thanks for your encouragements.

To my family back in France, for their constant support. To my proud parents.

Lastly, I am thankful for the education I received, to all the teachers, mentors and family members, from the early stages of school up to my PhD.

Abbreviations

°C	Degree Celsius
9AVENUS	nine times alanine VENUS
ABA	abscisic acid
Arabidopsis	*Arabidopsis thaliana*
bp	base pair
bZIP	basic leucine zipper
cDNA	complementary DNA
CDS	coding sequence
ChIP	Chromatin immunoprecipitation
CLN	cauline leaf number
cm	centimeter
C-terminal	carboxy-terminal
d	day(s)
dCAPS	derived cleaved amplified polymorphic sequences
ddH2O	distilled, deionized water
DEG	differentially expressed genes
DEX	dexamethasone
DMSO	dimethylsulfoxide
DNA	deoxyribonucleic acid
DNase	deoxyribonuclease
dNTP	deoxynucleosidetriphosphate
DTB	day at bolting
EDTA	ethylenediaminetetraacetic acid
EMSA	Electrophoretic Mobility Shift Assay
g	gravity
GA	acid gibberellic
GFP	green fluorescent protein
GPA	global proliferation arrest
h	hour(s)
HA	hemagglutinin
HCl	Hydrochloric acid
JA	jasmonic acid
kb	kilo base(s)
kDa	kilo Dalton
L	litre
LD	long days
m	meter
MADS	MCM1 AGAMOUS DEFICIENS SRF
mg	milligram
min	minute(s)
mL	milliliter
mM	millimolar
mRNA	messenger RNA
ncRNA	non-coding RNA
ng	nanogram

nM	nanomolar
nm	nanometer
nt	nucleotide
N-terminal	amino-terminal
OD	optical density
p35S	35S promoter from Cauliflower Mosaic Virus
PCA	principal component analysis
PCR	polymerase chain reaction
pH	power of hydrogen
qRT-PCR	real-time quantitative reverse transcription PCR
r	resistant (form)
RLN	rosette leaf number
RNA	ribonucleic acid
ROS	reactive oxygen species
r.p.m	revolution per minute
RT	room temperature
s	second
SAM	shoot apical meristem
SD	short days
SDS	sodium dodecyl sulphate
seq	sequencing
t	time
T-DNA	transferred DNA
TLN	total leaf number
TSS	transcription start site
UTR	untranslated region
V	volt(s)
v/v	volume per volume
w/v	weight/volume
WT	wild-type plant, usually *Arabidopsis thaliana* Col-0
Y2H	yeast-two-hybrid
YFP	yellow fluorescent protein
µg	microgram
µL	microliter
µm	micrometer
µmol	micromolar

References

Abe M, Kobayashi Y, Yamamoto S, Daimon Y, Yamaguchi A, Ikeda Y, Ichinoki H, Notaguchi M, Goto K, Araki T (2005) FD, a bZIP protein mediating signals from the floral pathway integrator FT at the shoot apex. Science **309:** 1052-1056

Abe M, Kosaka S, Shibuta M, Nagata K, Uemura T, Nakano A, Kaya H (2019) Transient activity of the florigen complex during the floral transition in Arabidopsis thaliana. Development **146**

Aguilar-Martínez JA, Poza-Carrion C, Cubas P (2007) Arabidopsis BRANCHED1 acts as an integrator of branching signals within axillary buds. Plant Cell **19:** 458-472

Ahn JH, Miller D, Winter VJ, Banfield MJ, Lee JH, Yoo SY, Henz SR, Brady RL, Weigel D (2006) A divergent external loop confers antagonistic activity on floral regulators FT and TFL1. EMBO J **25:** 605-614

Alvarez J, Guli CL, Yu X-H, Smyth DR (1992) terminal flower: a gene affecting inflorescence development in Arabidopsis thaliana. The Plant Journal **2:** 103-116

An H, Roussot C, Suarez-Lopez P, Corbesier L, Vincent C, Pineiro M, Hepworth S, Mouradov A, Justin S, Turnbull C, Coupland G (2004) CONSTANS acts in the phloem to regulate a systemic signal that induces photoperiodic flowering of Arabidopsis. Development **131:** 3615-3626

Andres F, Porri A, Torti S, Mateos J, Romera-Branchat M, Garcia-Martinez JL, Fornara F, Gregis V, Kater MM, Coupland G (2014) SHORT VEGETATIVE PHASE reduces gibberellin biosynthesis at the Arabidopsis shoot apex to regulate the floral transition. Proc Natl Acad Sci U S A **111:** E2760-2769

Arend M, Schnitzler JP, Ehlting B, Hansch R, Lange T, Rennenberg H, Himmelbach A, Grill E, Fromm J (2009) Expression of the Arabidopsis mutant ABI1 gene alters abscisic acid sensitivity, stomatal development, and growth morphology in gray poplars. Plant Physiol **151:** 2110-2119

Aukerman MJ, Sakai H (2003) Regulation of flowering time and floral organ identity by a MicroRNA and its APETALA2-like target genes. Plant Cell **15:** 2730-2741

Ausín I, Alonso-Blanco C, Jarillo JA, Ruiz-Garcia L, Martinez-Zapater JM (2004) Regulation of flowering time by FVE, a retinoblastoma-associated protein. Nat Genet **36:** 162-166

Balanzà V, Martinez-Fernandez I, Sato S, Yanofsky MF, Ferrandiz C (2019) Inflorescence Meristem Fate Is Dependent on Seed Development and FRUITFULL in Arabidopsis thaliana. Front Plant Sci **10:** 1622

Balanzà V, Martinez-Fernandez I, Sato S, Yanofsky MF, Kaufmann K, Angenent GC, Bemer M, Ferrandiz C (2018) Genetic control of meristem arrest and life span in Arabidopsis by a FRUITFULL-APETALA2 pathway. Nat Commun **9:** 565

Balasubramanian S, Sureshkumar S, Lempe J, Weigel D (2006) Potent induction of Arabidopsis thaliana flowering by elevated growth temperature. PLoS Genet **2:** e106

Bao A, Chen H, Chen L, Chen S, Hao Q, Guo W, Qiu D, Shan Z, Yang Z, Yuan S, Zhang C, Zhang X, Liu B, Kong F, Li X, Zhou X, Tran LP, Cao D (2019) CRISPR/Cas9-mediated targeted mutagenesis of GmSPL9 genes alters plant architecture in soybean. BMC Plant Biol **19:** 131

Bartrina I, Otto E, Strnad M, Werner T, Schmulling T (2011) Cytokinin regulates the activity of reproductive meristems, flower organ size, ovule formation, and thus seed yield in Arabidopsis thaliana. Plant Cell **23:** 69-80

Bemer M, van Mourik H, Muino JM, Ferrandiz C, Kaufmann K, Angenent GC (2017) FRUITFULL controls SAUR10 expression and regulates Arabidopsis growth and architecture. J Exp Bot **68:** 3391-3403

Benlloch R, Berbel A, Serrano-Mislata A, Madueno F (2007) Floral initiation and inflorescence architecture: a comparative view. Ann Bot **100:** 659-676

Benlloch R, Kim MC, Sayou C, Thevenon E, Parcy F, Nilsson O (2011) Integrating long-day flowering signals: a LEAFY binding site is essential for proper photoperiodic activation of APETALA1. Plant J **67:** 1094-1102

Blázquez MA, Ahn JH, Weigel D (2003) A thermosensory pathway controlling flowering time in Arabidopsis thaliana. Nat Genet **33:** 168-171

Blumel M, Dally N, Jung C (2015) Flowering time regulation in crops-what did we learn from Arabidopsis? Curr Opin Biotechnol **32:** 121-129

Bowman JL, Alvarez J, Weigel D, Meyerowitz EM, Smyth DR (1993) Control of flower development in Arabidopsis thaliana by APETALA1 and interacting genes. Development **119:** 721-743

Bradley D, Ratcliffe O, Vincent C, Carpenter R, Coen E (1997) Inflorescence commitment and architecture in Arabidopsis. Science **275:** 80-83

Brand U, Fletcher JC, Hobe M, Meyerowitz EM, Simon R (2000) Dependence of stem cell fate in Arabidopsis on a feedback loop regulated by CLV3 activity. Science **289:** 617-619

Byrne ME, Barley R, Curtis M, Arroyo JM, Dunham M, Hudson A, Martienssen RA (2000) Asymmetric leaves1 mediates leaf patterning and stem cell function in Arabidopsis. Nature **408:** 967-971

Cai Z, Liu J, Wang H, Yang C, Chen Y, Li Y, Pan S, Dong R, Tang G, Barajas-Lopez Jde D, Fujii H, Wang X (2014) GSK3-like kinases positively modulate abscisic acid signaling through phosphorylating subgroup III SnRK2s in Arabidopsis. Proc Natl Acad Sci U S A **111:** 9651-9656

Cardon G, Höhmann S, Klein J, Nettesheim K, Saedler H, Huijser P (1999) Molecular characterisation of the Arabidopsis SBP-box genes. Gene **237:** 91-104

Castillejo C, Pelaz S (2008) The balance between CONSTANS and TEMPRANILLO activities determines FT expression to trigger flowering. Curr Biol **18:** 1338-1343

Chandler JW (2012) Floral meristem initiation and emergence in plants. Cell Mol Life Sci **69:** 3807-3818

Chatfield SP, Stirnberg P, Forde BG, Leyser O (2000) The hormonal regulation of axillary bud growth in Arabidopsis. Plant J **24:** 159-169

Chen X (2004) A microRNA as a translational repressor of APETALA2 in Arabidopsis flower development. Science **303:** 2022-2025

Cheng WH, Endo A, Zhou L, Penney J, Chen HC, Arroyo A, Leon P, Nambara E, Asami T, Seo M, Koshiba T, Sheen J (2002) A unique short-chain dehydrogenase/reductase in Arabidopsis glucose signaling and abscisic acid biosynthesis and functions. Plant Cell **14:** 2723-2743

Cheng X, Li G, Krom N, Tang Y, Wen J (2021) Genetic regulation of flowering time and inflorescence architecture by MtFDa and MtFTa1 in Medicago truncatula. Plant Physiol **185:** 161-178

Choi H, Hong J, Ha J, Kang J, Kim SY (2000) ABFs, a family of ABA-responsive element binding factors. J Biol Chem **275:** 1723-1730

Christmann A, Weiler EW, Steudle E, Grill E (2007) A hydraulic signal in root-to-shoot signalling of water shortage. Plant J **52:** 167-174

Clark SE, Running MP, Meyerowitz EM (1995) CLAVATA3 is a specific regulator of shoot and floral meristem development affecting the same processes as CLAVATA1. Development **121:** 2057-2067

Clough SJ, Bent AF (1998) Floral dip: a simplified method for Agrobacterium-mediated transformation of Arabidopsis thaliana. Plant J **16:** 735-743

Collani S, Neumann M, Yant L, Schmid M (2019) FT Modulates Genome-Wide DNA-Binding of the bZIP Transcription Factor FD. Plant Physiology **180:** 367-380

Conti L (2017) Hormonal control of the floral transition: Can one catch them all? Dev Biol **430:** 288-301

Conti L (2019) The A-B-A of Floral Transition: The to Do List for Perfect Escape.

Conti L, Bradley D (2007) TERMINAL FLOWER1 is a mobile signal controlling Arabidopsis architecture. Plant Cell **19:** 767-778

Corbesier L, Lejeune P, Bernier G (1998) The role of carbohydrates in the induction of flowering in Arabidopsis thaliana: comparison between the wild type and a starchless mutant. Planta **206:** 131-137

Corbesier L, Vincent C, Jang S, Fornara F, Fan Q, Searle I, Giakountis A, Farrona S, Gissot L, Turnbull C, Coupland G (2007) FT protein movement contributes to long-distance signaling in floral induction of Arabidopsis. Science **316:** 1030-1033

Craft J, Samalova M, Baroux C, Townley H, Martinez A, Jepson I, Tsiantis M, Moore I (2005) New pOp/LhG4 vectors for stringent glucocorticoid-dependent transgene expression in Arabidopsis. Plant J **41:** 899-918

Csorba T, Questa JI, Sun Q, Dean C (2014) Antisense COOLAIR mediates the coordinated switching of chromatin states at FLC during vernalization. Proc Natl Acad Sci U S A **111:** 16160-16165

Cutler SR, Rodriguez PL, Finkelstein RR, Abrams SR (2010) Abscisic acid: emergence of a core signaling network. Annu Rev Plant Biol **61:** 651-679

de Jong M, Tavares H, Pasam RK, Butler R, Ward S, George G, Melnyk CW, Challis R, Kover PX, Leyser O (2019) Natural variation in Arabidopsis shoot branching plasticity in response to nitrate supply affects fitness. PLoS Genet **15:** e1008366

De Lucia F, Crevillen P, Jones AM, Greb T, Dean C (2008) A PHD-polycomb repressive complex 2 triggers the epigenetic silencing of FLC during vernalization. Proc Natl Acad Sci U S A **105:** 16831-16836

Deng W, Ying H, Helliwell CA, Taylor JM, Peacock WJ, Dennis ES (2011) FLOWERING LOCUS C (FLC) regulates development pathways throughout the life cycle of Arabidopsis. Proc Natl Acad Sci U S A **108:** 6680-6685

Dharmasiri N, Dharmasiri S, Weijers D, Lechner E, Yamada M, Hobbie L, Ehrismann JS, Jurgens G, Estelle M (2005) Plant development is regulated by a family of auxin receptor F box proteins. Dev Cell **9:** 109-119

Dijkwel PP, Lai AG (2019) Hypothesis: Plant stem cells hold the key to extreme longevity. Translational Medicine of Aging **3:** 14-16

Dill A, Sun T (2001) Synergistic derepression of gibberellin signaling by removing RGA and GAI function in Arabidopsis thaliana. Genetics **159:** 777-785

Dong T, Park Y, Hwang I (2015) Abscisic acid: biosynthesis, inactivation, homoeostasis and signalling. Essays Biochem **58:** 29-48

Dong X, Li Y, Guan Y, Wang S, Luo H, Li X, Li H, Zhang Z (2021) Auxin-induced AUXIN RESPONSE FACTOR4 activates APETALA1 and FRUITFULL to promote flowering in woodland strawberry. Hortic Res **8:** 115

Dröge-Laser W, Snoek BL, Snel B, Weiste C (2018) The Arabidopsis bZIP transcription factor family-an update. Curr Opin Plant Biol **45:** 36-49

Earley KW, Haag JR, Pontes O, Opper K, Juehne T, Song K, Pikaard CS (2006) Gateway-compatible vectors for plant functional genomics and proteomics. Plant J **45:** 616-629

Ecker J, Wellmer F, Alves-Ferreira M, Dubois A, Riechmann JL, Meyerowitz EM (2006) Genome-Wide Analysis of Gene Expression during Early Arabidopsis Flower Development. PLoS Genetics **2**

Edwards K, Johnstone C, Thompson C (1991) A simple and rapid method for the preparation of plant genomic DNA for PCR analysis. Nucleic Acids Res **19:** 1349

Ellis CM, Nagpal P, Young JC, Hagen G, Guilfoyle TJ, Reed JW (2005) AUXIN RESPONSE FACTOR1 and AUXIN RESPONSE FACTOR2 regulate senescence and floral organ abscission in Arabidopsis thaliana. Development **132:** 4563-4574

Endrizzi K, Moussian B, Haecker A, Levin JZ, Laux T (1996) The SHOOT MERISTEMLESS gene is required for maintenance of undifferentiated cells in Arabidopsis shoot and floral meristems and acts at a different regulatory level than the meristem genes WUSCHEL and ZWILLE. Plant J **10:** 967-979

Fernández V, Takahashi Y, Le Gourrierec J, Coupland G (2016) Photoperiodic and thermosensory pathways interact through CONSTANS to promote flowering at high temperature under short days. Plant J **86:** 426-440

Ferrandiz C, Gu Q, Martienssen R, Yanofsky MF (2000) Redundant regulation of meristem identity and plant architecture by FRUITFULL, APETALA1 and CAULIFLOWER. Development **127:** 725-734

Fletcher JC (2018) The CLV-WUS Stem Cell Signaling Pathway: A Roadmap to Crop Yield Optimization. Plants (Basel) **7**

Fornara F, Panigrahi KC, Gissot L, Sauerbrunn N, Ruhl M, Jarillo JA, Coupland G (2009) Arabidopsis DOF transcription factors act redundantly to reduce CONSTANS expression and are essential for a photoperiodic flowering response. Dev Cell **17:** 75-86

Fowler S, Lee K, Onouchi H, Samach A, Richardson K, Morris B, Coupland G, Putterill J (1999) GIGANTEA: a circadian clock-controlled gene that regulates photoperiodic flowering in Arabidopsis and encodes a protein with several possible membrane-spanning domains. EMBO J **18:** 4679-4688

Foyer CH, Kerchev PI, Hancock RD (2012) The ABA-INSENSITIVE-4 (ABI4) transcription factor links redox, hormone and sugar signaling pathways. Plant Signal Behav **7:** 276-281

Frigerio M, Alabadi D, Perez-Gomez J, Garcia-Carcel L, Phillips AL, Hedden P, Blazquez MA (2006) Transcriptional regulation of gibberellin metabolism genes by auxin signaling in Arabidopsis. Plant Physiol **142:** 553-563

Fujii H, Chinnusamy V, Rodrigues A, Rubio S, Antoni R, Park SY, Cutler SR, Sheen J, Rodriguez PL, Zhu JK (2009) In vitro reconstitution of an abscisic acid signalling pathway. Nature **462:** 660-664

Fujii H, Verslues PE, Zhu JK (2007) Identification of two protein kinases required for abscisic acid regulation of seed germination, root growth, and gene expression in Arabidopsis. Plant Cell **19:** 485-494

Furihata T, Maruyama K, Fujita Y, Umezawa T, Yoshida R, Shinozaki K, Yamaguchi-Shinozaki K (2006) Abscisic acid-dependent multisite phosphorylation regulates the activity of a transcription activator AREB1. Proc Natl Acad Sci U S A **103:** 1988-1993

Gaillochet C, Daum G, Lohmann JU (2015) O cell, where art thou? The mechanisms of shoot meristem patterning. Curr Opin Plant Biol **23:** 91-97

Gaillochet C, Jamge S, van der Wal F, Angenent G, Immink R, Lohmann JU (2018) A molecular network for functional versatility of HECATE transcription factors. Plant J **95:** 57-70

Galvan-Ampudia CS, Cerutti G, Legrand J, Brunoud G, Martin-Arevalillo R, Azais R, Bayle V, Moussu S, Wenzl C, Jaillais Y, Lohmann JU, Godin C, Vernoux T (2020) Temporal integration of auxin information for the regulation of patterning. Elife **9**

Gandikota M, Birkenbihl RP, Hohmann S, Cardon GH, Saedler H, Huijser P (2007) The miRNA156/157 recognition element in the 3' UTR of the Arabidopsis SBP box gene SPL3 prevents early flowering by translational inhibition in seedlings. Plant J **49:** 683-693

Golldack D, Li C, Mohan H, Probst N (2013) Gibberellins and abscisic acid signal crosstalk: living and developing under unfavorable conditions. Plant Cell Rep **32:** 1007-1016

Gomez-Roldan V, Fermas S, Brewer PB, Puech-Pages V, Dun EA, Pillot JP, Letisse F, Matusova R, Danoun S, Portais JC, Bouwmeester H, Becard G, Beveridge CA, Rameau C, Rochange SF (2008) Strigolactone inhibition of shoot branching. Nature **455:** 189-194

Gonzalez-Grandio E, Pajoro A, Franco-Zorrilla JM, Tarancon C, Immink RG, Cubas P (2017) Abscisic acid signaling is controlled by a BRANCHED1/HD-ZIP I cascade in Arabidopsis axillary buds. Proc Natl Acad Sci U S A **114:** E245-E254

Goretti D, Silvestre M, Collani S, Langenecker T, Mendez C, Madueno F, Schmid M (2020) TERMINAL FLOWER1 Functions as a Mobile Transcriptional Cofactor in the Shoot Apical Meristem. Plant Physiol **182:** 2081-2095

Gorham SR, Weiner AI, Yamadi M, Krogan NT (2018) HISTONE DEACETYLASE 19 and the flowering time gene FD maintain reproductive meristem identity in an age-dependent manner. J Exp Bot **69:** 4757-4771

Goslin K, Zheng B, Serrano-Mislata A, Rae L, Ryan PT, Kwasniewska K, Thomson B, O'Maoileidigh DS, Madueno F, Wellmer F, Graciet E (2017) Transcription Factor Interplay between LEAFY and APETALA1/CAULIFLOWER during Floral Initiation. Plant Physiol **174:** 1097-1109

Gosti F, Beaudoin N, Serizet C, Webb AA, Vartanian N, Giraudat J (1999) ABI1 protein phosphatase 2C is a negative regulator of abscisic acid signaling. Plant Cell **11:** 1897-1910

Greb T, Clarenz O, Schafer E, Muller D, Herrero R, Schmitz G, Theres K (2003) Molecular analysis of the LATERAL SUPPRESSOR gene in Arabidopsis reveals a conserved control mechanism for axillary meristem formation. Genes Dev **17:** 1175-1187

Griffiths J, Murase K, Rieu I, Zentella R, Zhang ZL, Powers SJ, Gong F, Phillips AL, Hedden P, Sun TP, Thomas SG (2006) Genetic characterization and functional analysis of the GID1 gibberellin receptors in Arabidopsis. Plant Cell **18:** 3399-3414

Gu Q, Ferrandiz C, Yanofsky MF, Martienssen R (1998) The FRUITFULL MADS-box gene mediates cell differentiation during Arabidopsis fruit development. Development **125:** 1509-1517

Gunl M, Liew EF, David K, Putterill J (2009) Analysis of a post-translational steroid induction system for GIGANTEA in Arabidopsis. BMC Plant Biol **9:** 141

Hanano S, Goto K (2011) Arabidopsis TERMINAL FLOWER1 is involved in the regulation of flowering time and inflorescence development through transcriptional repression. Plant Cell **23:** 3172-3184

Hanzawa Y, Money T, Bradley D (2005) A single amino acid converts a repressor to an activator of flowering. Proc Natl Acad Sci U S A **102:** 7748-7753

Hartmann U, Hohmann S, Nettesheim K, Wisman E, Saedler H, Huijser P (2000) Molecular cloning of SVP: a negative regulator of the floral transition in Arabidopsis. Plant J **21:** 351-360

Hartmann U, Sagasser M, Mehrtens F, Stracke R, Weisshaar B (2005) Differential combinatorial interactions of cis-acting elements recognized by R2R3-MYB, BZIP, and BHLH factors control light-responsive and tissue-specific activation of phenylpropanoid biosynthesis genes. Plant Mol Biol **57:** 155-171

Hayama R, Sarid-Krebs L, Richter R, Fernandez V, Jang S, Coupland G (2017) PSEUDO RESPONSE REGULATORs stabilize CONSTANS protein to promote flowering in response to day length. EMBO J **36:** 904-918

He J, Xu M, Willmann MR, McCormick K, Hu T, Yang L, Starker CG, Voytas DF, Meyers BC, Poethig RS (2018) Threshold-dependent repression of SPL gene expression by miR156/miR157 controls vegetative phase change in Arabidopsis thaliana. PLoS Genet **14:** e1007337

He Y, Michaels SD, Amasino RM (2003) Regulation of flowering time by histone acetylation in Arabidopsis. Science **302:** 1751-1754

Hellens RP, Allan AC, Friel EN, Bolitho K, Grafton K, Templeton MD, Karunairetnam S, Gleave AP, Laing WA (2005) Transient expression vectors for functional genomics, quantification of promoter activity and RNA silencing in plants. Plant Methods **1:** 13

Hellens RP, Edwards EA, Leyland NR, Bean S, Mullineaux PM (2000) pGreen: a versatile and flexible binary Ti vector for Agrobacterium-mediated plant transformation. Plant Mol Biol **42:** 819-832

Helliwell CA, Wood CC, Robertson M, James Peacock W, Dennis ES (2006) The Arabidopsis FLC protein interacts directly in vivo with SOC1 and FT chromatin and is part of a high-molecular-weight protein complex. Plant J **46:** 183-192

Hensel LL, Grbic V, Baumgarten DA, Bleecker AB (1993) Developmental and age-related processes that influence the longevity and senescence of photosynthetic tissues in arabidopsis. Plant Cell **5:** 553-564

Hensel LL, Nelson MA, Richmond TA, Bleecker AB (1994) The fate of inflorescence meristems is controlled by developing fruits in Arabidopsis. Plant Physiol **106:** 863-876

Heo JB, Sung S (2011) Vernalization-mediated epigenetic silencing by a long intronic noncoding RNA. Science **331:** 76-79

Hiraoka K, Yamaguchi A, Abe M, Araki T (2013) The florigen genes FT and TSF modulate lateral shoot outgrowth in Arabidopsis thaliana. Plant Cell Physiol **54:** 352-368

Ho WW, Weigel D (2014) Structural features determining flower-promoting activity of Arabidopsis FLOWERING LOCUS T. Plant Cell **26:** 552-564

Hornyik C, Duc C, Rataj K, Terzi LC, Simpson GG (2010) Alternative polyadenylation of antisense RNAs and flowering time control. Biochem Soc Trans **38:** 1077-1081

Hwang K, Susila H, Nasim Z, Jung JY, Ahn JH (2019) Arabidopsis ABF3 and ABF4 Transcription Factors Act with the NF-YC Complex to Regulate SOC1 Expression and Mediate Drought-Accelerated Flowering. Mol Plant **12:** 489-505

Hyun Y, Richter R, Vincent C, Martinez-Gallegos R, Porri A, Coupland G (2016) Multi-layered Regulation of SPL15 and Cooperation with SOC1 Integrate Endogenous Flowering Pathways at the Arabidopsis Shoot Meristem. Dev Cell **37:** 254-266

Ibanez C, Poeschl Y, Peterson T, Bellstadt J, Denk K, Gogol-Doring A, Quint M, Delker C (2017) Ambient temperature and genotype differentially affect developmental and phenotypic plasticity in Arabidopsis thaliana. BMC Plant Biol **17:** 114

Imaizumi T, Schultz TF, Harmon FG, Ho LA, Kay SA (2005) FKF1 F-box protein mediates cyclic degradation of a repressor of CONSTANS in Arabidopsis. Science **309:** 293-297

Imaizumi T, Tran HG, Swartz TE, Briggs WR, Kay SA (2003) FKF1 is essential for photoperiodic-specific light signalling in Arabidopsis. Nature **426:** 302-306

Immink RG, Pose D, Ferrario S, Ott F, Kaufmann K, Valentim FL, de Folter S, van der Wal F, van Dijk AD, Schmid M, Angenent GC (2012) Characterization of SOC1's central role in flowering by the identification of its upstream and downstream regulators. Plant Physiol **160:** 433-449

Irish VF, Sussex IM (1990) Function of the apetala-1 gene during Arabidopsis floral development. Plant Cell **2:** 741-753

Jaeger KE, Pullen N, Lamzin S, Morris RJ, Wigge PA (2013) Interlocking feedback loops govern the dynamic behavior of the floral transition in Arabidopsis. Plant Cell **25:** 820-833

Jaeger KE, Wigge PA (2007) FT protein acts as a long-range signal in Arabidopsis. Curr Biol **17:** 1050-1054

Jakoby M, Weisshaar B, Droge-Laser W, Vicente-Carbajosa J, Tiedemann J, Kroj T, Parcy F, b ZIPRG (2002) bZIP transcription factors in Arabidopsis. Trends Plant Sci **7:** 106-111

Jang S, Marchal V, Panigrahi KC, Wenkel S, Soppe W, Deng XW, Valverde F, Coupland G (2008) Arabidopsis COP1 shapes the temporal pattern of CO accumulation conferring a photoperiodic flowering response. EMBO J **27:** 1277-1288

Jang S, Torti S, Coupland G (2009) Genetic and spatial interactions between FT, TSF and SVP during the early stages of floral induction in Arabidopsis. Plant Journal **60:** 614-625

Jaspert N, Throm C, Oecking C (2011) Arabidopsis 14-3-3 proteins: fascinating and less fascinating aspects. Front Plant Sci **2:** 96

Jerabek-Willemsen M, Wienken CJ, Braun D, Baaske P, Duhr S (2011) Molecular Interaction Studies Using Microscale Thermophoresis. Assay and Drug Development Technologies **9:** 342-353

Jiang D, Wang Y, Wang Y, He Y (2008) Repression of FLOWERING LOCUS C and FLOWERING LOCUS T by the Arabidopsis Polycomb repressive complex 2 components. PLoS One **3:** e3404

Jin R, Klasfeld S, Zhu Y, Fernandez Garcia M, Xiao J, Han SK, Konkol A, Wagner D (2021) LEAFY is a pioneer transcription factor and licenses cell reprogramming to floral fate. Nat Commun **12:** 626

Johanson U, West J, Lister C, Michaels S, Amasino R, Dean C (2000) Molecular analysis of FRIGIDA, a major determinant of natural variation in Arabidopsis flowering time. Science **290:** 344-347

Jung JH, Ju Y, Seo PJ, Lee JH, Park CM (2012) The SOC1-SPL module integrates photoperiod and gibberellic acid signals to control flowering time in Arabidopsis. Plant J **69:** 577-588

Jung JH, Lee HJ, Ryu JY, Park CM (2016) SPL3/4/5 Integrate Developmental Aging and Photoperiodic Signals into the FT-FD Module in Arabidopsis Flowering. Mol Plant **9:** 1647-1659

Kaneko-Suzuki M, Kurihara-Ishikawa R, Okushita-Terakawa C, Kojima C, Nagano-Fujiwara M, Ohki I, Tsuji H, Shimamoto K, Taoka KI (2018) TFL1-Like Proteins in Rice Antagonize Rice FT-Like Protein in Inflorescence Development by Competition for Complex Formation with 14-3-3 and FD. Plant Cell Physiol **59:** 458-468

Kania T, Russenberger D, Peng S, Apel K, Melzer S (1997) FPF1 promotes flowering in Arabidopsis. Plant Cell **9:** 1327-1338

Kaufmann K, Wellmer F, Muino JM, Ferrier T, Wuest SE, Kumar V, Serrano-Mislata A, Madueno F, Krajewski P, Meyerowitz EM, Angenent GC, Riechmann JL (2010) Orchestration of floral initiation by APETALA1. Science **328:** 85-89

Kawamoto N, Sasabe M, Endo M, Machida Y, Araki T (2015) Calcium-dependent protein kinases responsible for the phosphorylation of a bZIP transcription factor FD crucial for the florigen complex formation. Sci Rep **5:** 8341

Kebrom TH (2017) A Growing Stem Inhibits Bud Outgrowth - The Overlooked Theory of Apical Dominance. Front Plant Sci **8:** 1874

Kiefer C, Willing EM, Jiao WB, Sun H, Piednoel M, Humann U, Hartwig B, Koch MA, Schneeberger K (2019) Interspecies association mapping links reduced CG to TG substitution rates to the loss of gene-body methylation. Nat Plants **5:** 846-855

Kim D-H (2020) Current understanding of flowering pathways in plants: focusing on the vernalization pathway in Arabidopsis and several vegetable crop plants. Horticulture, Environment, and Biotechnology **61:** 209-227

Kim JS, Mizoi J, Yoshida T, Fujita Y, Nakajima J, Ohori T, Todaka D, Nakashima K, Hirayama T, Shinozaki K, Yamaguchi-Shinozaki K (2011) An ABRE promoter sequence is involved in osmotic stress-responsive expression of the DREB2A gene, which encodes a transcription factor regulating drought-inducible genes in Arabidopsis. Plant Cell Physiol **52:** 2136-2146

Kinoshita A, Richter R (2020) Genetic and molecular basis of floral induction in Arabidopsis thaliana. J Exp Bot **71:** 2490-2504

Kinoshita A, Vayssieres A, Richter R, Sang Q, Roggen A, van Driel AD, Smith RS, Coupland G (2020) Regulation of shoot meristem shape by photoperiodic signaling and phytohormones during floral induction of Arabidopsis. Elife **9**

Klock HE, Lesley SA (2009) The Polymerase Incomplete Primer Extension (PIPE) method applied to high-throughput cloning and site-directed mutagenesis. Methods Mol Biol **498:** 91-103

Kobayashi Y, Kaya H, Goto K, Iwabuchi M, Araki T (1999) A pair of related genes with antagonistic roles in mediating flowering signals. Science **286:** 1960-1962

Koorneef M, Elgersma A, Hanhart CJ, Loenen-Martinet EP, Rijn L, Zeevaart JAD (1985) A gibberellin insensitive mutant of Arabidopsis thaliana. Physiologia Plantarum **65:** 33-39

Koornneef M, Hanhart CJ, van der Veen JH (1991) A genetic and physiological analysis of late flowering mutants in Arabidopsis thaliana. Mol Gen Genet **229:** 57-66

Koornneef M, Reuling G, Karssen CM (1984) The isolation and characterization of abscisic acid-insensitive mutants of Arabidopsis thaliana. Physiologia Plantarum **61:** 377-383

Koornneef M, van der Veen JH (1980) Induction and analysis of gibberellin sensitive mutants in Arabidopsis thaliana (L.) heynh. Theor Appl Genet **58:** 257-263

Koppolu R, Schnurbusch T (2019) Developmental pathways for shaping spike inflorescence architecture in barley and wheat. J Integr Plant Biol **61:** 278-295

Krämer U (2015) Planting molecular functions in an ecological context with Arabidopsis thaliana. Elife **4**

Kumar SV, Lucyshyn D, Jaeger KE, Alos E, Alvey E, Harberd NP, Wigge PA (2012) Transcription factor PIF4 controls the thermosensory activation of flowering. Nature **484:** 242-245

Kumar SV, Wigge PA (2010) H2A.Z-containing nucleosomes mediate the thermosensory response in Arabidopsis. Cell **140:** 136-147

Kurihara D, Mizuta Y, Sato Y, Higashiyama T (2015) ClearSee: a rapid optical clearing reagent for whole-plant fluorescence imaging. Development **142:** 4168-4179

Landrein B, Refahi Y, Besnard F, Hervieux N, Mirabet V, Boudaoud A, Vernoux T, Hamant O (2015) Meristem size contributes to the robustness of phyllotaxis in Arabidopsis. J Exp Bot **66:** 1317-1324

Laubinger S, Marchal V, Le Gourrierec J, Wenkel S, Adrian J, Jang S, Kulajta C, Braun H, Coupland G, Hoecker U (2006) Arabidopsis SPA proteins regulate photoperiodic flowering and interact with the floral inducer CONSTANS to regulate its stability. Development **133:** 3213-3222

Lee JH, Ryu HS, Chung KS, Pose D, Kim S, Schmid M, Ahn JH (2013) Regulation of temperature-responsive flowering by MADS-box transcription factor repressors. Science **342:** 628-632

Lee JH, Yoo SJ, Park SH, Hwang I, Lee JS, Ahn JH (2007) Role of SVP in the control of flowering time by ambient temperature in Arabidopsis. Genes Dev **21:** 397-402

Leung J, Merlot S, Giraudat J (1997) The Arabidopsis ABSCISIC ACID-INSENSITIVE2 (ABI2) and ABI1 genes encode homologous protein phosphatases 2C involved in abscisic acid signal transduction. Plant Cell **9:** 759-771

Li D, Zhang H, Mou M, Chen Y, Xiang S, Chen L, Yu D (2019) Arabidopsis Class II TCP Transcription Factors Integrate with the FT-FD Module to Control Flowering. Plant Physiol **181:** 97-111

Li S, Liu L, Zhuang X, Yu Y, Liu X, Cui X, Ji L, Pan Z, Cao X, Mo B, Zhang F, Raikhel N, Jiang L, Chen X (2013) MicroRNAs inhibit the translation of target mRNAs on the endoplasmic reticulum in Arabidopsis. Cell **153:** 562-574

Li S, Zhu Y, Varshney RK, Zhan J, Zheng X, Shi J, Wang X, Liu G, Wang H (2020) A systematic dissection of the mechanisms underlying the natural variation of silique number in rapeseed (Brassica napus L.) germplasm. Plant Biotechnol J **18:** 568-580

Lifschitz E, Eviatar T, Rozman A, Shalit A, Goldshmidt A, Amsellem Z, Alvarez JP, Eshed Y (2006) The tomato FT ortholog triggers systemic signals that regulate growth and flowering and substitute for diverse environmental stimuli. Proceedings of the National Academy of Sciences of the United States of America **103:** 6398-6403

Lim PO, Lee IC, Kim J, Kim HJ, Ryu JS, Woo HR, Nam HG (2010) Auxin response factor 2 (ARF2) plays a major role in regulating auxin-mediated leaf longevity. Journal of Experimental Botany **61:** 1419-1430

Liu F, Quesada V, Crevillen P, Baurle I, Swiezewski S, Dean C (2007) The Arabidopsis RNA-binding protein FCA requires a lysine-specific demethylase 1 homolog to downregulate FLC. Mol Cell **28:** 398-407

Liu L, Farrona S, Klemme S, Turck FK (2014) Post-fertilization expression of FLOWERING LOCUS T suppresses reproductive reversion. Front Plant Sci **5:** 164

Liu L, Liu C, Hou X, Xi W, Shen L, Tao Z, Wang Y, Yu H (2012) FTIP1 is an essential regulator required for florigen transport. PLoS Biol **10:** e1001313

Livak KJ, Schmittgen TD (2001) Analysis of relative gene expression data using real-time quantitative PCR and the 2(-Delta Delta C(T)) Method. Methods **25:** 402-408

Llorca CM, Berendzen KW, Malik WA, Mahn S, Piepho HP, Zentgraf U (2015) The Elucidation of the Interactome of 16 Arabidopsis bZIP Factors Reveals Three Independent Functional Networks. PLoS One **10:** e0139884

Long JA, Moan EI, Medford JI, Barton MK (1996) A member of the KNOTTED class of homeodomain proteins encoded by the STM gene of Arabidopsis. Nature **379:** 66-69

Luo X, Chen T, Zeng X, He D, He Y (2019) Feedback Regulation of FLC by FLOWERING LOCUS T (FT) and FD through a 5' FLC Promoter Region in Arabidopsis. Mol Plant **12:** 285-288

Mandadi KK, Misra A, Ren S, McKnight TD (2009) BT2, a BTB protein, mediates multiple responses to nutrients, stresses, and hormones in Arabidopsis. Plant Physiol **150:** 1930-1939

Mandel MA, Gustafson-Brown C, Savidge B, Yanofsky MF (1992) Molecular characterization of the Arabidopsis floral homeotic gene APETALA1. Nature **360:** 273-277

Mandel MA, Yanofsky MF (1995) A gene triggering flower formation in Arabidopsis. Nature **377:** 522-524

Mandel MA, Yanofsky MF (1998) The Arabidopsis AGL 9 MADS box gene is expressed in young flower primordia. Sexual Plant Reproduction **11:** 22-28

Marquardt S, Raitskin O, Wu Z, Liu F, Sun Q, Dean C (2014) Functional consequences of splicing of the antisense transcript COOLAIR on FLC transcription. Mol Cell **54:** 156-165

Martignago D, Siemiatkowska B, Lombardi A, Conti L (2020) Abscisic Acid and Flowering Regulation: Many Targets, Different Places. Int J Mol Sci **21**

Martínez-Fernández I, Menezes de Moura S, Alves-Ferreira M, Ferrandiz C, Balanza V (2020) Identification of Players Controlling Meristem Arrest Downstream of the FRUITFULL-APETALA2 Pathway. Plant Physiol **184:** 945-959

Mathieu J, Warthmann N, Kuttner F, Schmid M (2007) Export of FT protein from phloem companion cells is sufficient for floral induction in Arabidopsis. Curr Biol **17:** 1055-1060

Mayer KFX, Schoof H, Haecker A, Lenhard M, Jürgens G, Laux T (1998) Role of WUSCHEL in Regulating Stem Cell Fate in the Arabidopsis Shoot Meristem. Cell **95:** 805-815

Meir Z, Aviezer I, Chongloi GL, Ben-Kiki O, Bronstein R, Mukamel Z, Keren-Shaul H, Jaitin D, Tal L, Shalev-Schlosser G, Harel TH, Tanay A, Eshed Y (2021) Dissection of floral transition by single-meristem transcriptomes at high temporal resolution. Nat Plants **7:** 800-813

Melcher K, Ng LM, Zhou XE, Soon FF, Xu Y, Suino-Powell KM, Park SY, Weiner JJ, Fujii H, Chinnusamy V, Kovach A, Li J, Wang Y, Li J, Peterson FC, Jensen DR, Yong EL, Volkman BF, Cutler SR, Zhu JK, Xu HE (2009) A gate-latch-lock mechanism for hormone signalling by abscisic acid receptors. Nature **462:** 602-608

Melzer S, Lens F, Gennen J, Vanneste S, Rohde A, Beeckman T (2008) Flowering-time genes modulate meristem determinacy and growth form in Arabidopsis thaliana. Nat Genet **40:** 1489-1492

Merlot S, Gosti F, Guerrier D, Vavasseur A, Giraudat J (2001) The ABI1 and ABI2 protein phosphatases 2C act in a negative feedback regulatory loop of the abscisic acid signalling pathway. Plant J **25:** 295-303

Michaels SD, Amasino RM (1999) FLOWERING LOCUS C encodes a novel MADS domain protein that acts as a repressor of flowering. Plant Cell **11:** 949-956

Mizoguchi T, Wright L, Fujiwara S, Cremer F, Lee K, Onouchi H, Mouradov A, Fowler S, Kamada H, Putterill J, Coupland G (2005) Distinct roles of GIGANTEA in promoting flowering and regulating circadian rhythms in Arabidopsis. Plant Cell **17:** 2255-2270

Musielak TJ, Schenkel L, Kolb M, Henschen A, Bayer M (2015) A simple and versatile cell wall staining protocol to study plant reproduction. Plant Reprod **28:** 161-169

Nakajima M, Shimada A, Takashi Y, Kim YC, Park SH, Ueguchi-Tanaka M, Suzuki H, Katoh E, Iuchi S, Kobayashi M, Maeda T, Matsuoka M, Yamaguchi I (2006) Identification and characterization of Arabidopsis gibberellin receptors. Plant J **46:** 880-889

Nishimura N, Sarkeshik A, Nito K, Park SY, Wang A, Carvalho PC, Lee S, Caddell DF, Cutler SR, Chory J, Yates JR, Schroeder JI (2010) PYR/PYL/RCAR family members are major in-vivo ABI1 protein phosphatase 2C-interacting proteins in Arabidopsis. Plant J **61:** 290-299

Ó'Maoiléidigh DS, van Driel AD, Singh A, Sang Q, Le Bec N, Vincent C, de Olalla EBG, Vayssieres A, Romera Branchat M, Severing E, Martinez Gallegos R, Coupland G (2021) Systematic analyses of the MIR172 family members of Arabidopsis define

their distinct roles in regulation of APETALA2 during floral transition. PLoS Biol **19:** e3001043

Ó'Maoiléidigh DS, Wuest SE, Rae L, Raganelli A, Ryan PT, Kwasniewska K, Das P, Lohan AJ, Loftus B, Graciet E, Wellmer F (2013) Control of reproductive floral organ identity specification in Arabidopsis by the C function regulator AGAMOUS. Plant Cell **25:** 2482-2503

Ongaro V, Leyser O (2008) Hormonal control of shoot branching. J Exp Bot **59:** 67-74

Parent B, Leclere M, Lacube S, Semenov MA, Welcker C, Martre P, Tardieu F (2018) Maize yields over Europe may increase in spite of climate change, with an appropriate use of the genetic variability of flowering time. Proc Natl Acad Sci U S A **115:** 10642-10647

Park SJ, Jiang K, Tal L, Yichie Y, Gar O, Zamir D, Eshed Y, Lippman ZB (2014) Optimization of crop productivity in tomato using induced mutations in the florigen pathway. Nat Genet **46:** 1337-1342

Park SY, Fung P, Nishimura N, Jensen DR, Fujii H, Zhao Y, Lumba S, Santiago J, Rodrigues A, Chow TF, Alfred SE, Bonetta D, Finkelstein R, Provart NJ, Desveaux D, Rodriguez PL, McCourt P, Zhu JK, Schroeder JI, Volkman BF, Cutler SR (2009) Abscisic acid inhibits type 2C protein phosphatases via the PYR/PYL family of START proteins. Science **324:** 1068-1071

Perilleux C, Lobet G, Tocquin P (2014) Inflorescence development in tomato: gene functions within a zigzag model. Front Plant Sci **5:** 121

Ponnu J, Schlereth A, Zacharaki V, Dzialo MA, Abel C, Feil R, Schmid M, Wahl V (2020) The trehalose 6-phosphate pathway impacts vegetative phase change in Arabidopsis thaliana. Plant J **104:** 768-780

Porri A, Torti S, Romera-Branchat M, Coupland G (2012) Spatially distinct regulatory roles for gibberellins in the promotion of flowering of Arabidopsis under long photoperiods. Development **139:** 2198-2209

Pouteau S, Ferret V, Gaudin V, Lefebvre D, Sabar M, Zhao G, Prunus F (2004) Extensive phenotypic variation in early flowering mutants of Arabidopsis. Plant Physiol **135:** 201-211

Qin F, Sakuma Y, Tran LS, Maruyama K, Kidokoro S, Fujita Y, Fujita M, Umezawa T, Sawano Y, Miyazono K, Tanokura M, Shinozaki K, Yamaguchi-Shinozaki K (2008) Arabidopsis DREB2A-interacting proteins function as RING E3 ligases and negatively regulate plant drought stress-responsive gene expression. Plant Cell **20:** 1693-1707

Questa JI, Song J, Geraldo N, An H, Dean C (2016) Arabidopsis transcriptional repressor VAL1 triggers Polycomb silencing at FLC during vernalization. Science **353:** 485-488

Reddy GV, Meyerowitz EM (2005) Stem-cell homeostasis and growth dynamics can be uncoupled in the Arabidopsis shoot apex. Science **310:** 663-667

Reinhardt D, Pesce ER, Stieger P, Mandel T, Baltensperger K, Bennett M, Traas J, Friml J, Kuhlemeier C (2003) Regulation of phyllotaxis by polar auxin transport. Nature **426:** 255-260

Ren S, Mandadi KK, Boedeker AL, Rathore KS, McKnight TD (2007) Regulation of telomerase in Arabidopsis by BT2, an apparent target of TELOMERASE ACTIVATOR1. Plant Cell **19:** 23-31

Riboni M, Galbiati M, Tonelli C, Conti L (2013) GIGANTEA enables drought escape response via abscisic acid-dependent activation of the florigens and SUPPRESSOR OF OVEREXPRESSION OF CONSTANS. Plant Physiol **162:** 1706-1719

Riboni M, Robustelli Test A, Galbiati M, Tonelli C, Conti L (2016) ABA-dependent control of GIGANTEA signalling enables drought escape via up-regulation of FLOWERING LOCUS T in Arabidopsis thaliana. J Exp Bot **67:** 6309-6322

Robert HS, Quint A, Brand D, Vivian-Smith A, Offringa R (2009) BTB and TAZ domain scaffold proteins perform a crucial function in Arabidopsis development. Plant J **58:** 109-121

Rodriguez PL, Benning G, Grill E (1998) ABI2, a second protein phosphatase 2C involved in abscisic acid signal transduction in Arabidopsis. FEBS Letters **421:** 185-190

Romera-Branchat M, Severing E, Pocard C, Ohr H, Vincent C, Nee G, Martinez-Gallegos R, Jang S, Andres F, Madrigal P, Coupland G (2020) Functional Divergence of the Arabidopsis Florigen-Interacting bZIP Transcription Factors FD and FDP. Cell Rep **31:** 107717

Roussin-Leveillee C, Silva-Martins G, Moffett P (2020) ARGONAUTE5 Represses Age-Dependent Induction of Flowering through Physical and Functional Interaction with miR156 in Arabidopsis. Plant Cell Physiol **61:** 957-966

Ruiz-Garcia L, Madueno F, Wilkinson M, Haughn G, Salinas J, Martinez-Zapater JM (1997) Different roles of flowering-time genes in the activation of floral initiation genes in Arabidopsis. Plant Cell **9:** 1921-1934

Sakuraba Y, Bulbul S, Piao W, Choi G, Paek NC (2017) Arabidopsis EARLY FLOWERING3 increases salt tolerance by suppressing salt stress response pathways. Plant J **92:** 1106-1120

Samach A, Onouchi H, Gold SE, Ditta GS, Schwarz-Sommer Z, Yanofsky MF, Coupland G (2000) Distinct roles of CONSTANS target genes in reproductive development of Arabidopsis. Science **288:** 1613-1616

Santuari L, Sanchez-Perez GF, Luijten M, Rutjens B, Terpstra I, Berke L, Gorte M, Prasad K, Bao D, Timmermans-Hereijgers JL, Maeo K, Nakamura K, Shimotohno A, Pencik A, Novak O, Ljung K, van Heesch S, de Bruijn E, Cuppen E, Willemsen V, Mahonen AP, Lukowitz W, Snel B, de Ridder D, Scheres B, Heidstra R (2016) The PLETHORA Gene Regulatory Network Guides Growth and Cell Differentiation in Arabidopsis Roots. Plant Cell **28:** 2937-2951

Sawa M, Nusinow DA, Kay SA, Imaizumi T (2007) FKF1 and GIGANTEA complex formation is required for day-length measurement in Arabidopsis. Science **318:** 261-265

Schmid M, Uhlenhaut NH, Godard F, Demar M, Bressan R, Weigel D, Lohmann JU (2003) Dissection of floral induction pathways using global expression analysis. Development **130:** 6001-6012

Schoof H, Lenhard M, Haecker A, Mayer KFX, Jürgens G, Laux T (2000) The Stem Cell Population of Arabidopsis Shoot Meristems Is Maintained by a Regulatory Loop between the CLAVATA and WUSCHEL Genes. Cell **100:** 635-644

Schroeder JI, Kwak JM, Allen GJ (2001) Guard cell abscisic acid signalling and engineering drought hardiness in plants. Nature **410:** 327-330

Schwab R, Palatnik JF, Riester M, Schommer C, Schmid M, Weigel D (2005) Specific effects of microRNAs on the plant transcriptome. Dev Cell **8:** 517-527

Schwarz S, Grande AV, Bujdoso N, Saedler H, Huijser P (2008) The microRNA regulated SBP-box genes SPL9 and SPL15 control shoot maturation in Arabidopsis. Plant Mol Biol **67:** 183-195

Seale M, Bennett T, Leyser O (2017) BRC1 expression regulates bud activation potential but is not necessary or sufficient for bud growth inhibition in Arabidopsis. Development **144:** 1661-1673

Searle I, He Y, Turck F, Vincent C, Fornara F, Krober S, Amasino RA, Coupland G (2006) The transcription factor FLC confers a flowering response to vernalization by repressing meristem competence and systemic signaling in Arabidopsis. Genes Dev **20:** 898-912

Serrano-Mislata A, Sablowski R (2018) The pillars of land plants: new insights into stem development. Curr Opin Plant Biol **45:** 11-17

Shalit A, Rozman A, Goldshmidt A, Alvarez JP, Bowman JL, Eshed Y, Lifschitz E (2009) The flowering hormone florigen functions as a general systemic regulator of growth and termination. Proc Natl Acad Sci U S A **106:** 8392-8397

Shannon S, Meeks-Wagner DR (1991) A Mutation in the Arabidopsis TFL1 Gene Affects Inflorescence Meristem Development. Plant Cell **3:** 877-892

Shi B, Zhang C, Tian C, Wang J, Wang Q, Xu T, Xu Y, Ohno C, Sablowski R, Heisler MG, Theres K, Wang Y, Jiao Y (2016) Two-Step Regulation of a Meristematic Cell Population Acting in Shoot Branching in Arabidopsis. PLoS Genet **12:** e1006168

Shimada TL, Shimada T, Hara-Nishimura I (2010) A rapid and non-destructive screenable marker, FAST, for identifying transformed seeds of Arabidopsis thaliana. Plant J **61:** 519-528

Shinohara N, Taylor C, Leyser O (2013) Strigolactone can promote or inhibit shoot branching by triggering rapid depletion of the auxin efflux protein PIN1 from the plasma membrane. PLoS Biol **11:** e1001474

Shu K, Chen Q, Wu Y, Liu R, Zhang H, Wang S, Tang S, Yang W, Xie Q (2016) ABSCISIC ACID-INSENSITIVE 4 negatively regulates flowering through directly promoting Arabidopsis FLOWERING LOCUS C transcription. J Exp Bot **67:** 195-205

Simon R, Igeno MI, Coupland G (1996) Activation of floral meristem identity genes in Arabidopsis. Nature **384:** 59-62

Sirichandra C, Davanture M, Turk BE, Zivy M, Valot B, Leung J, Merlot S (2010) The Arabidopsis ABA-activated kinase OST1 phosphorylates the bZIP transcription factor ABF3 and creates a 14-3-3 binding site involved in its turnover. PLoS One **5:** e13935

Sivitz AB, Reinders A, Johnson ME, Krentz AD, Grof CP, Perroux JM, Ward JM (2007) Arabidopsis sucrose transporter AtSUC9. High-affinity transport activity, intragenic control of expression, and early flowering mutant phenotype. Plant Physiol **143:** 188-198

Smith HM, Ung N, Lal S, Courtier J (2011) Specification of reproductive meristems requires the combined function of SHOOT MERISTEMLESS and floral integrators FLOWERING LOCUS T and FD during Arabidopsis inflorescence development. J Exp Bot **62:** 583-593

Son O, Hur YS, Kim YK, Lee HJ, Kim S, Kim MR, Nam KH, Lee MS, Kim BY, Park J, Park J, Lee SC, Hanada A, Yamaguchi S, Lee IJ, Kim SK, Yun DJ, Soderman E, Cheon CI (2010) ATHB12, an ABA-inducible homeodomain-leucine zipper (HD-Zip) protein of Arabidopsis, negatively regulates the growth of the inflorescence stem by decreasing the expression of a gibberellin 20-oxidase gene. Plant Cell Physiol **51:** 1537-1547

Song YH, Kubota A, Kwon MS, Covington MF, Lee N, Taagen ER, Laboy Cintron D, Hwang DY, Akiyama R, Hodge SK, Huang H, Nguyen NH, Nusinow DA, Millar AJ, Shimizu KK, Imaizumi T (2018) Molecular basis of flowering under natural long-day conditions in Arabidopsis. Nat Plants **4:** 824-835

Song YH, Yoo CM, Hong AP, Kim SH, Jeong HJ, Shin SY, Kim HJ, Yun DJ, Lim CO, Bahk JD, Lee SY, Nagao RT, Key JL, Hong JC (2008) DNA-binding study identifies C-box and hybrid C/G-box or C/A-box motifs as high-affinity binding sites for STF1 and LONG HYPOCOTYL5 proteins. Plant Physiol **146:** 1862-1877

Soon FF, Ng LM, Zhou XE, West GM, Kovach A, Tan MH, Suino-Powell KM, He Y, Xu Y, Chalmers MJ, Brunzelle JS, Zhang H, Yang H, Jiang H, Li J, Yong EL, Cutler S, Zhu JK, Griffin PR, Melcher K, Xu HE (2012) Molecular mimicry regulates ABA signaling by SnRK2 kinases and PP2C phosphatases. Science **335:** 85-88

Stirnberg P, van de Sande K, Leyser HMO (2002) MAX1 and MAX2 control shoot lateral branching in Arabidopsis. Development **129:** 1131-1141

Su YH, Zhou C, Li YJ, Yu Y, Tang LP, Zhang WJ, Yao WJ, Huang R, Laux T, Zhang XS (2020) Integration of pluripotency pathways regulates stem cell maintenance in the Arabidopsis shoot meristem. Proc Natl Acad Sci U S A **117:** 22561-22571

Suarez-Lopez P, Wheatley K, Robson F, Onouchi H, Valverde F, Coupland G (2001) CONSTANS mediates between the circadian clock and the control of flowering in Arabidopsis. Nature **410:** 1116-1120

Sun TP, Kamiya Y (1994) The Arabidopsis GA1 locus encodes the cyclase ent-kaurene synthetase A of gibberellin biosynthesis. Plant Cell **6:** 1509-1518

Sun Y, Zhou Q, Zhang W, Fu Y, Huang H (2002) ASYMMETRIC LEAVES1, an Arabidopsis gene that is involved in the control of cell differentiation in leaves. Planta **214:** 694-702

Sussmilch FC, Berbel A, Hecht V, Vander Schoor JK, Ferrandiz C, Madueno F, Weller JL (2015) Pea VEGETATIVE2 Is an FD Homolog That Is Essential for Flowering and Compound Inflorescence Development. Plant Cell **27:** 1046-1060

Suzuki N, Bajad S, Shuman J, Shulaev V, Mittler R (2008) The transcriptional co-activator MBF1c is a key regulator of thermotolerance in Arabidopsis thaliana. J Biol Chem **283:** 9269-9275

Taji T, Ohsumi C, Iuchi S, Seki M, Kasuga M, Kobayashi M, Yamaguchi-Shinozaki K, Shinozaki K (2002) Important roles of drought- and cold-inducible genes for galactinol synthase in stress tolerance in Arabidopsis thaliana. Plant J **29:** 417-426

Tao Z, Shen L, Liu C, Liu L, Yan Y, Yu H (2012) Genome-wide identification of SOC1 and SVP targets during the floral transition in Arabidopsis. Plant J **70:** 549-561

Taoka K, Ohki I, Tsuji H, Furuita K, Hayashi K, Yanase T, Yamaguchi M, Nakashima C, Purwestri YA, Tamaki S, Ogaki Y, Shimada C, Nakagawa A, Kojima C, Shimamoto K (2011) 14-3-3 proteins act as intracellular receptors for rice Hd3a florigen. Nature **476:** 332-335

Teotia S, Lamb RS (2009) The paralogous genes RADICAL-INDUCED CELL DEATH1 and SIMILAR TO RCD ONE1 have partially redundant functions during Arabidopsis development. Plant Physiol **151:** 180-198

Tian C, Zhang X, He J, Yu H, Wang Y, Shi B, Han Y, Wang G, Feng X, Zhang C, Wang J, Qi J, Yu R, Jiao Y (2014) An organ boundary-enriched gene regulatory network uncovers regulatory hierarchies underlying axillary meristem initiation. Mol Syst Biol **10:** 755

Tian H, Chen S, Yang W, Wang T, Zheng K, Wang Y, Cheng Y, Zhang N, Liu S, Li D, Liu B, Wang S (2017) A novel family of transcription factors conserved in angiosperms is required for ABA signalling. Plant Cell Environ **40:** 2958-2971

Tiwari SB, Shen Y, Chang HC, Hou Y, Harris A, Ma SF, McPartland M, Hymus GJ, Adam L, Marion C, Belachew A, Repetti PP, Reuber TL, Ratcliffe OJ (2010) The flowering time regulator CONSTANS is recruited to the FLOWERING LOCUS T promoter via a unique cis-element. New Phytol **187:** 57-66

Torti S, Fornara F, Vincent C, Andres F, Nordstrom K, Gobel U, Knoll D, Schoof H, Coupland G (2012) Analysis of the Arabidopsis shoot meristem transcriptome during floral transition identifies distinct regulatory patterns and a leucine-rich repeat protein that promotes flowering. Plant Cell **24:** 444-462

Tsuji H, Nakamura H, Taoka K, Shimamoto K (2013) Functional diversification of FD transcription factors in rice, components of florigen activation complexes. Plant Cell Physiol **54:** 385-397

Tylewicz S, Petterle A, Marttila S, Miskolczi P, Azeez A, Singh RK, Immanen J, Mahler N, Hvidsten TR, Eklund DM, Bowman JL, Helariutta Y, Bhalerao RP (2018) Photoperiodic control of seasonal growth is mediated by ABA acting on cell-cell communication. Science **360:** 212-215

Uchida N, Lee JS, Horst RJ, Lai HH, Kajita R, Kakimoto T, Tasaka M, Torii KU (2012) Regulation of inflorescence architecture by intertissue layer ligand-receptor communication between endodermis and phloem. Proc Natl Acad Sci U S A **109:** 6337-6342

Umezawa T, Nakashima K, Miyakawa T, Kuromori T, Tanokura M, Shinozaki K, Yamaguchi-Shinozaki K (2010) Molecular basis of the core regulatory network in ABA responses: sensing, signaling and transport. Plant Cell Physiol **51:** 1821-1839

Umezawa T, Sugiyama N, Mizoguchi M, Hayashi S, Myouga F, Yamaguchi-Shinozaki K, Ishihama Y, Hirayama T, Shinozaki K (2009) Type 2C protein phosphatases directly regulate abscisic acid-activated protein kinases in Arabidopsis. Proc Natl Acad Sci U S A **106:** 17588-17593

Urbanus SL, de Folter S, Shchennikova AV, Kaufmann K, Immink RG, Angenent GC (2009) In planta localisation patterns of MADS domain proteins during floral development in Arabidopsis thaliana. BMC Plant Biol **9:** 5

Valverde F, Mouradov A, Soppe W, Ravenscroft D, Samach A, Coupland G (2004) Photoreceptor regulation of CONSTANS protein in photoperiodic flowering. Science **303:** 1003-1006

Van Daele I, Gonzalez N, Vercauteren I, de Smet L, Inze D, Roldan-Ruiz I, Vuylsteke M (2012) A comparative study of seed yield parameters in Arabidopsis thaliana mutants and transgenics. Plant Biotechnol J **10:** 488-500

Vayssières A, Mishra P, Roggen A, Neumann U, Ljung K, Albani MC (2020) Vernalization shapes shoot architecture and ensures the maintenance of dormant buds in the perennial Arabis alpina. New Phytol **227:** 99-115

Vlad F, Rubio S, Rodrigues A, Sirichandra C, Belin C, Robert N, Leung J, Rodriguez PL, Lauriere C, Merlot S (2009) Protein phosphatases 2C regulate the activation of the Snf1-related kinase OST1 by abscisic acid in Arabidopsis. Plant Cell **21:** 3170-3184

Waadt R, Hitomi K, Nishimura N, Hitomi C, Adams SR, Getzoff ED, Schroeder JI (2014) FRET-based reporters for the direct visualization of abscisic acid concentration changes and distribution in Arabidopsis. Elife **3:** e01739

Wagner D, Sablowski RW, Meyerowitz EM (1999) Transcriptional activation of APETALA1 by LEAFY. Science **285:** 582-584

Wahl V, Ponnu J, Schlereth A, Arrivault S, Langenecker T, Franke A, Feil R, Lunn JE, Stitt M, Schmid M (2013) Regulation of flowering by trehalose-6-phosphate signaling in Arabidopsis thaliana. Science **339:** 704-707

Walla A, Wilma van Esse G, Kirschner GK, Guo G, Brunje A, Finkemeier I, Simon R, von Korff M (2020) An Acyl-CoA N-Acyltransferase Regulates Meristem Phase Change and Plant Architecture in Barley. Plant Physiol **183:** 1088-1109

Wang B, Smith SM, Li J (2018) Genetic Regulation of Shoot Architecture. Annu Rev Plant Biol **69:** 437-468

Wang H, Tang J, Liu J, Hu J, Liu J, Chen Y, Cai Z, Wang X (2018) Abscisic Acid Signaling Inhibits Brassinosteroid Signaling through Dampening the Dephosphorylation of BIN2 by ABI1 and ABI2. Mol Plant **11:** 315-325

Wang JW, Czech B, Weigel D (2009) miR156-regulated SPL transcription factors define an endogenous flowering pathway in Arabidopsis thaliana. Cell **138:** 738-749

Wang JW, Schwab R, Czech B, Mica E, Weigel D (2008) Dual effects of miR156-targeted SPL genes and CYP78A5/KLUH on plastochron length and organ size in Arabidopsis thaliana. Plant Cell **20:** 1231-1243

Wang L, Yamashita M, Greaves IK, Peacock WJ, Dennis ES (2020) Arabidopsis Col/Ler and Ws/Ler hybrids and Hybrid Mimics produce seed yield heterosis through increased height, inflorescence branch and silique number. Planta **252:** 40

Wang Y, Kumaishi K, Suzuki T, Ichihashi Y, Yamaguchi N, Shirakawa M, Ito T (2020) Morphological and Physiological Framework Underlying Plant Longevity in Arabidopsis thaliana. Front Plant Sci **11:** 600726

Ware A, Walker CH, Simura J, Gonzalez-Suarez P, Ljung K, Bishopp A, Wilson ZA, Bennett T (2020) Auxin export from proximal fruits drives arrest in temporally competent inflorescences. Nat Plants **6:** 699-707

Weigel D, Alvarez J, Smyth DR, Yanofsky MF, Meyerowitz EM (1992) LEAFY controls floral meristem identity in Arabidopsis. Cell **69:** 843-859

Wigge PA, Kim MC, Jaeger KE, Busch W, Schmid M, Lohmann JU, Weigel D (2005) Integration of spatial and temporal information during floral induction in Arabidopsis. Science **309:** 1056-1059

William DA, Su Y, Smith MR, Lu M, Baldwin DA, Wagner D (2004) Genomic identification of direct target genes of LEAFY. Proc Natl Acad Sci U S A **101:** 1775-1780

Wilson RN, Heckman JW, Somerville CR (1992) Gibberellin Is Required for Flowering in Arabidopsis thaliana under Short Days. Plant Physiol **100:** 403-408

Wu G, Poethig RS (2006) Temporal regulation of shoot development in Arabidopsis thaliana by miR156 and its target SPL3. Development **133:** 3539-3547

Wu Z, Fang X, Zhu D, Dean C (2020) Autonomous Pathway: FLOWERING LOCUS C Repression through an Antisense-Mediated Chromatin-Silencing Mechanism. Plant Physiol **182:** 27-37

Wuest SE, Philipp MA, Guthorl D, Schmid B, Grossniklaus U (2016) Seed Production Affects Maternal Growth and Senescence in Arabidopsis. Plant Physiol **171:** 392-404

Xin W, Wang Z, Liang Y, Wang Y, Hu Y (2017) Dynamic expression reveals a two-step patterning of WUS and CLV3 during axillary shoot meristem formation in Arabidopsis. J Plant Physiol **214:** 1-6

Xu M, Hu T, Zhao J, Park MY, Earley KW, Wu G, Yang L, Poethig RS (2016) Developmental Functions of miR156-Regulated SQUAMOSA PROMOTER BINDING PROTEIN-LIKE (SPL) Genes in Arabidopsis thaliana. PLoS Genet **12:** e1006263

Xue Z, Liu L, Zhang C (2020) Regulation of Shoot Apical Meristem and Axillary Meristem Development in Plants. Int J Mol Sci **21**

Yadav RK, Perales M, Gruel J, Girke T, Jonsson H, Reddy GV (2011) WUSCHEL protein movement mediates stem cell homeostasis in the Arabidopsis shoot apex. Genes Dev **25:** 2025-2030

Yadav UP, Ivakov A, Feil R, Duan GY, Walther D, Giavalisco P, Piques M, Carillo P, Hubberten HM, Stitt M, Lunn JE (2014) The sucrose-trehalose 6-phosphate (Tre6P) nexus: specificity and mechanisms of sucrose signalling by Tre6P. J Exp Bot **65:** 1051-1068

Yamaguchi-Shinozaki K, Shinozaki K (1994) A novel cis-acting element in an Arabidopsis gene is involved in responsiveness to drought, low-temperature, or high-salt stress. Plant Cell **6:** 251-264

Yamaguchi A, Kobayashi Y, Goto K, Abe M, Araki T (2005) TWIN SISTER OF FT (TSF) acts as a floral pathway integrator redundantly with FT. Plant and Cell Physiology **46:** 1175-1189

Yamaguchi A, Wu MF, Yang L, Wu G, Poethig RS, Wagner D (2009) The microRNA-regulated SBP-Box transcription factor SPL3 is a direct upstream activator of LEAFY, FRUITFULL, and APETALA1. Dev Cell **17:** 268-278

Yamaguchi N, Winter CM, Wellmer F, Wagner D (2015) Identification of direct targets of plant transcription factors using the GR fusion technique. Methods Mol Biol **1284:** 123-138

Yamaguchi N, Winter CM, Wu MF, Kanno Y, Yamaguchi A, Seo M, Wagner D (2014) Gibberellin acts positively then negatively to control onset of flower formation in Arabidopsis. Science **344:** 638-641

Yan Y, Shen L, Chen Y, Bao S, Thong Z, Yu H (2014) A MYB-domain protein EFM mediates flowering responses to environmental cues in Arabidopsis. Dev Cell **30:** 437-448

Yant L, Mathieu J, Dinh TT, Ott F, Lanz C, Wollmann H, Chen X, Schmid M (2010) Orchestration of the floral transition and floral development in Arabidopsis by the bifunctional transcription factor APETALA2. Plant Cell **22:** 2156-2170

Yao C, Finlayson SA (2015) Abscisic Acid Is a General Negative Regulator of Arabidopsis Axillary Bud Growth. Plant Physiol **169:** 611-626

Yoshida T, Fujita Y, Maruyama K, Mogami J, Todaka D, Shinozaki K, Yamaguchi-Shinozaki K (2015) Four Arabidopsis AREB/ABF transcription factors function predominantly in gene expression downstream of SnRK2 kinases in abscisic acid signalling in response to osmotic stress. Plant Cell Environ **38:** 35-49

Yoshida T, Fujita Y, Sayama H, Kidokoro S, Maruyama K, Mizoi J, Shinozaki K, Yamaguchi-Shinozaki K (2010) AREB1, AREB2, and ABF3 are master transcription factors that cooperatively regulate ABRE-dependent ABA signaling involved in drought stress tolerance and require ABA for full activation. Plant J **61:** 672-685

Yoshida T, Nishimura N, Kitahata N, Kuromori T, Ito T, Asami T, Shinozaki K, Hirayama T (2006) ABA-hypersensitive germination3 encodes a protein phosphatase 2C (AtPP2CA) that strongly regulates abscisic acid signaling during germination among Arabidopsis protein phosphatase 2Cs. Plant Physiol **140:** 115-126

Zhang P, Liu H, Mysore KS, Wen J, Meng Y, Lin H, Niu L (2021) MtFDa is essential for flowering control and inflorescence development in Medicago truncatula. J Plant Physiol **260:** 153412

Zhang W, Qin C, Zhao J, Wang X (2004) Phospholipase D alpha 1-derived phosphatidic acid interacts with ABI1 phosphatase 2C and regulates abscisic acid signaling. Proc Natl Acad Sci U S A **101:** 9508-9513

Zhao F, Chen W, Sechet J, Martin M, Bovio S, Lionnet C, Long Y, Battu V, Mouille G, Moneger F, Traas J (2019) Xyloglucans and Microtubules Synergistically Maintain Meristem Geometry and Phyllotaxis. Plant Physiol **181:** 1191-1206

Zhu Y, Klasfeld S, Jeong CW, Jin R, Goto K, Yamaguchi N, Wagner D (2020) TERMINAL FLOWER 1-FD complex target genes and competition with FLOWERING LOCUS T. Nat Commun **11:** 5118

Zhu Y, Liu L, Shen L, Yu H (2016) NaKR1 regulates long-distance movement of FLOWERING LOCUS T in Arabidopsis. Nat Plants **2:** 16075

Zuo X, Wang S, Xiang W, Yang H, Tahir MM, Zheng S, An N, Han M, Zhao C, Zhang D (2021) Genome-wide identification of the 14-3-3 gene family and its participation in floral transition by interacting with TFL1/FT in apple. BMC Genomics **22:** 41